Natural stone sludge as secondary raw materials: towards a new sustainable recovery process

Doctoral Dissertation
Doctoral Program in Environmental Engineering (31th Cycle)

# Natural stone sludge as secondary raw materials: towards a new sustainable recovery process

by

**Lorena Zichella**

* * * * * *

**Supervisor:**

Prof. Paola Marini

**Doctoral Examination Committee:**

Researcher PhD Nicola Careddu, University of Cagliari, Cagliari (Italy)

Researcher PhD Maria Heloisa Barros de Oliveira Frascá, Centro de Tecnologia Mineral (CETEM), Rio de Janeiro (Brazil)

Prof. PhD Silvia Serranti, University of Roma, Roma (Italy)

Prof. PhD Alessandra Bonoli, University of Bologna, Bologna (Italy)

Prof. PhD Mariachiara Zanetti, Polytechnic of Turin, Turin (Italy)

Politecnico di Torino
2019

# DECLARATION

I hereby declare that, the contents and organization of this dissertation constitute my own original work and does not compromise in any way the rights of third parties, including those relating to the security of personal data.

.

Lorena Zichella
Turin, 2019

*Garbage is a great resource in the wrong place lacking someone's imagination to recycle it into everyone's benefit.*

*Mark Victor Hansen*

# Abstract

The problem related to the reuse of sludge deriving from the cutting of ornamental stone is a relevant topic at National and International level. According to the European Commission's Thematic Strategy on the Prevention and Recycling of Waste (EC raw materials strategies), proper management of sawing sludge by means of its characterization is essential to predict its future recovery. The sawing sludge is classified, according to the Italian framework in force (Legislative Decree 152/2006) as inert waste codified with the CER code 010413, produced by the processing of ornamental stone, in particular by volume treatments and destined to disposal operations. The volume treatments considered derive from the stone block sawing into slabs through the three technologies: gangsaw, diamond blade and diamond wire.

The main challenges to deal with for their correct management are:

- huge volume produced in quite limited areas.

- very fine particle size distribution.

- chemical properties of waste due to the presence of heavy metal content, sometimes over the threshold values, which can polluted the water and the soil if the residual sludge is not properly managed.

The aim of the PhD research project is the development of a guideline for the correct management of this waste by means of its characterization, to provide a specific recovery based on chemical characteristics.

The first step of the thesis consists in quantifying the amount of material that can be recovered as a by-product for other processes. A comparison between the data obtained from the Piedmont Institute (ARPA and IRES) and the empirically calculated data on the three different cutting technologies (band saws, diamond blade and diamond wire) was carried out. In particular for the diamond wire a study on the wear of the cutting tools based on the rocks workability classification was performed. Topics discussed for the European EASE R3 Project and deepened during the PhD research.

The second step of the study involves the characterization of 10 different sawing sludge, deriving from the cutting of silicate stones in the Piedmont districts of Turin, Cuneo and Verbania. The following characterization analyzes have been carried out: distribution particle size, chemical analysis, leaching test, specific density, wet magnetic separation, SEM analysis, XRPD and image analysis.

The third step of the project involves the choice of the type of recovery, based on sludge properties and in particular in its heavy metals content. For this purpose the magnetic separation, the SEM analysis, the XRPD and the image analysis by means of Image J software, were useful to understand the nature and quantity of the metallic elements present. Two applications have been foreseen, using materials in their as it is state:

- Control Low Strength Material (CLSM): performed with sludge characterized by a high metals concentration.

- Thermal eco-mortar for application of light macropore plasters: with sludge characterized by low concentration of metals.

The sludge used for the application as CLSM comes from two plants located in the Verbano District, where different rocks are cutting by means of different technologies. This two sludge have different physical and chemical properties. The cement mortar required for the filling of road substrates must meet certain requirements, such as self-leveling capacity, adequate fluidity, and a high and constant thermal conductivity. These properties are fundamental considering the presence of cables for the transmission of electricity. The material must be able to dissipate the heat produced by the cables throughout their life. The choice of using quartzite aggregates and sludge with a high percentage of metals, for the composition of the mix design, has been carried out as they increase the thermal conductivity of the concrete conglomerate. Four mixes have been prepared, whit two different sludge and dosage of the components. Laboratory tests, thermal conductivity and triaxial cell, were performed to validate the required requisites.

The sludge used for the application as plaster instead, must satisfy requirements related to thermal insulation, resistance to moisture, mechanical resistance and good injection. For this purpose low-content metals sludge was used for the composition of the mix design. The laboratory tests carried out on finished product, in accordance with European standards, are as follows: water absorption, specific density, flexural and compressive strength resistance before and after freeze and thaw cycles, pull out, salt crystallization cycle resistance and thermal conductivity.

In both applications the chemical and leaching test were carried out to verify the possible release of heavy metals into the environment after installation. The quality of the products obtained has been demonstrated as the cement mortars incorporate the metals and do not allow their release in nature.

A sludge recovery in unaltered state is provided, to reduce any costs connected to a pre-treatment and to make the recovery economically advantageous for companies. In the case of sludge with high heavy metal contents, which exceed the Law threshold limits, a magnetic separation can be provided downstream of the cut, as a pre-treatment. In this way obtaining two distinct by-products, of which the amagnetic fraction can be used as an application for plaster, and the magnetic fraction can be disposed in specialized landfill. In this way, the quantities and costs related to disposal would be reduced.

The circular economy approach, with the decrease in costs related to disposal, the improvement of environmental conditions and the retrieval of still exploitable secondary raw materials, must be necessary in an era in which the quantity of waste increases considerably. A collaboration between entities that produce waste and administrations that provide guidelines to recover it is necessary to make what is now a unidirectional system, a circular system.

# Acknowledgment

I would like to thank my tutor Paola Marini, who supported me throughout the PhD period. I would also like to thank all the companies that have provided materials and data and for their availability to provide all the information requested.

In particular I would like to thank Dr. Paolo Marone of the IS.I.M. (International Marble Institute of Italy) and Mr. Pasquale Buonanno of the company TEK.SP.ED srl (Naples) for the preparation and installation of plaster using sawing sludge.

As regards recovery as a CLSM I would like to thank Dr. PierPaolo Riviera and Eldho Choorackal Avirachan for supporting me in the laboratory tests and in data interpretation.

# Contents

# List of Tables

# List of Figure

# Chapter 1

# 1. Introduction

The problem related to the reuse of sludge deriving from the cutting of ornamental stone is a relevant topic at National and International level. The amount of material that can be recovered as a by-product for other processes is high and would be a considerable economic and environmental advantage.

The sawing sludge considered in this Thesis are coming from stone blocks cutting into slabs by means of three different cutting technologies: gangsaw, diamond blade and diamond wire. A study on quantity production of sludge from the three technologies was carried out, comparing official data with experimental data evaluation. A cutting processes optimization by means of rocks workability classification in case of cut with diamond wire technology was performed.

The potential recovery of sawing sludge must be in line with the circular economy approach, which can lead, on the one side, to the decrement of costs for its disposal in dumps, and, on the other side, to the quality improvement of the material (and of its environmental characteristics).The choice of the type of recovery was carried out on the basis of sludge characterization and in particular in heavy metal content. Two applications were foreseen for sawing sludge:

- Control Low Strength Material (CLSM) application: performed with sludge characterized by an high metals concentration (>2%).
- Thermal Eco- Mortar for macroporous light plaster application: with sludge characterized by low metals concentration (<2%).

A sludge recovery in unaltered state is provided, to reduce any costs connected to a pre-treatment and to make the recovery economically advantageous for companies. In ***Figure 1*** is shown a flowchart that summarizes all the steps followed for the research.

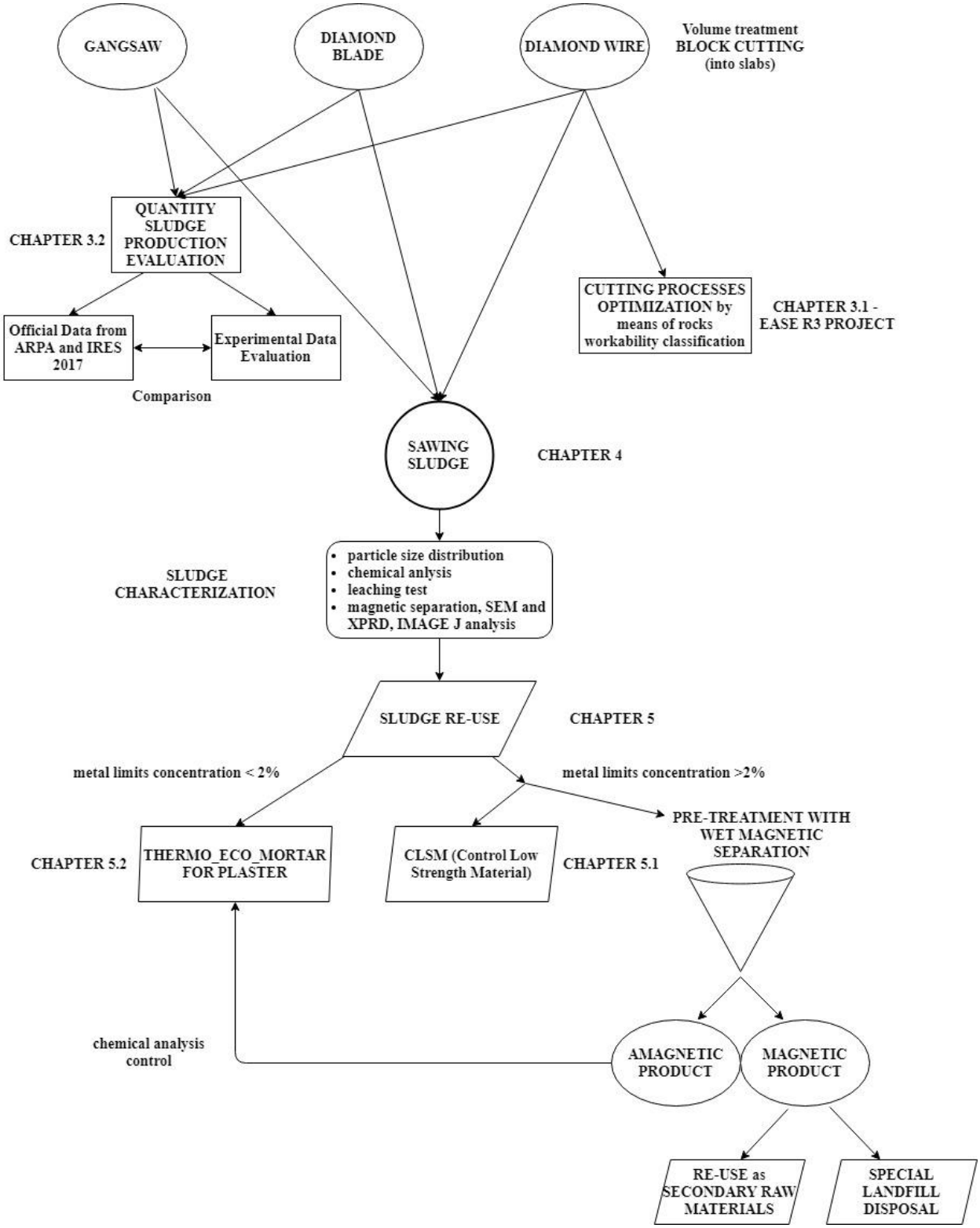


*Figure 1: Sawing sludge characterization and re-use flowchart.*

# 1.1 European legislative framework in the mining sector

One of the largest waste streams in the European Union is that deriving from mining operations and processing of mineral resources. The ambitious goal of the European Union is to turn these waste into recyclable resources, avoiding waste and minimizing the extraction of additional natural resources.

The concept of waste is defined for the first time in Directive 75/442/EEC (Art.1), with the aim of ensuring the correct disposal of waste. With the Directive 91/156/EEC the field of application was extended from waste disposal to recovery, as recycling and re-use. On 21 December 2005 the European Commission publishes the "Thematic Strategy on Waste" (COM 2005), where it provides clarifications on when a waste ceases to be a waste. The definition of waste is now embedded in the Directive 2008/98/EC (Waste Framework Directive) in the Art.3 which define waste as: *"…any substance or object which the holder discards or intends or is required to discard…*". In the same Directive the definition of by-products and End-Of-Waste criteria were explained.

Waste management is based on its hierarchy. It establishes a priority order of what constitutes the best environmental option. Respecting the hierarchy, measures must be adopted to encourage the options that guarantee the best overall result, taking into account the health, social and economic impacts, including technical feasibility and economic viability. The five step hierarchy option are shown in ***Figure 2***.

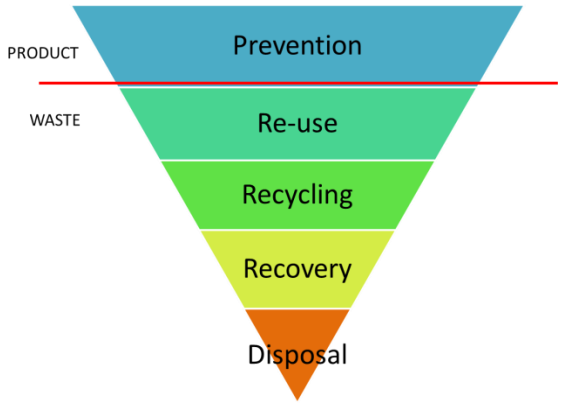


*Figure 2: Waste management priority order actions hierarchy defined by Directive 2008/98 EC.*

Prevention measures are aimed at reducing the amount of waste, through the reuse of products or the extension of their products life cycle (End-Of-Waste), reducing the content of hazardous materials and the negative environment and human health impacts. The re-use, recycling and recovery of "waste" are all operations aimed at resource efficiency, for reducing environmental impacts.

The European Commission on 19th January 2011(COM 2011) introduced the

concept of End-Of-Waste with the "Report on the Thematic Strategy on waste prevention and recycling", in which it proposed to specify the criteria when waste might cease to be waste, as part of the review of the Waste Framework Directive (Art. 6, Directive 2008/98 / EC). The strategic goal of the End-Of-Waste concept is to promote recycling by ensuring a high level of environmental protection by reducing the consumption of critical raw materials and the amount of waste destined for disposal. For the European Commission one of the important issues was the distinction between waste and by-product. The Art. 5 of the Directive 2008/98/EC defines as a by-product a substance or an object that can be used directly without any further treatment different from “normal industrial practice” and which lays down specific requirements for the protection of health and the environment and which will not lead to overall negative impacts on the environment or human health, furthermore, a future use of the substance or object must be certain. The definition of treatment different from “normal industrial practice” is an important concept. It is defined by the European Directive as a treatment to change the size or shape by mechanical treatment, which does not prevent the production residues from being considered by-products. On the other hand treatment techniques that bring additional contaminants with components that are dangerous or not useful, would prevent classification as non-waste.

Thus, normal industrial practice may include filtration, drying, cleaning, addition of other materials for further use, or simple quality control. Some of these treatment activities may be carried out by the same manufacturer of the residue, some by the end user who will use it and some by intermediaries, provided they satisfy the criterion of being “produced as an integral part of a production process”(Falkenberg K., 2012). However, it must be considered that a by-product could no longer be considered a by-product if it is subjected to further treatments once the establishment it has generated has been left. Therefore it is necessary that the treatments of normal industrial practice are an integral part of the production process. Only in this way the residues can be considered a by-product.

Raw materials for the manufacturing industry are of strategic importance, especially those raw materials that are at risk of supply. The European Commission with the COM (2017) 490 final, defines the 2017 list of Critical Raw Materials (CRMs) essential for the EU. The fundamental purpose of the list is to help stimulate the production of CRMs in Europe by strengthening recycling activities and facilitating the start-up of new mining activities. CRMs are part of a priority action plan for circular economy. From a study carried out by the JRC (Joint Research Center) of the European Community, the main parameters for characterizing critical raw materials have been established. These parameters are the economic importance and the supply risk (dependence on imports and export restrictions) (***Figure 3***). 27 CRMs were defined, listed in ***Table 1***.

| 2017 CRMs (27) | | | |
|---|---|---|---|
| Antimony | Fluorspar | LREEs | Phosphorus |
| Baryte | Gallium | Magnesium | Scandium |
| Beryllium | Germanium | Natural graphite | Silicon metal |
| Bismuth | Hafnium | Natural Rubber | Tantalum |
| Borate | Helium | Niobium | Tungsten |
| Cobalt | HREEs* | PGMs | Vanadium |
| Coking coal | Indium | Phosphate rock | |

*Table 1: List of CRMs (2017) created by EU and JRC. *HREEs=heavy rare earth elements, LREEs=light rare earth elements, PGMs=platinum group metals. (Source: http://rmis.jrc.ec.europa.eu/?page=crm-list-2017-09abb4)*

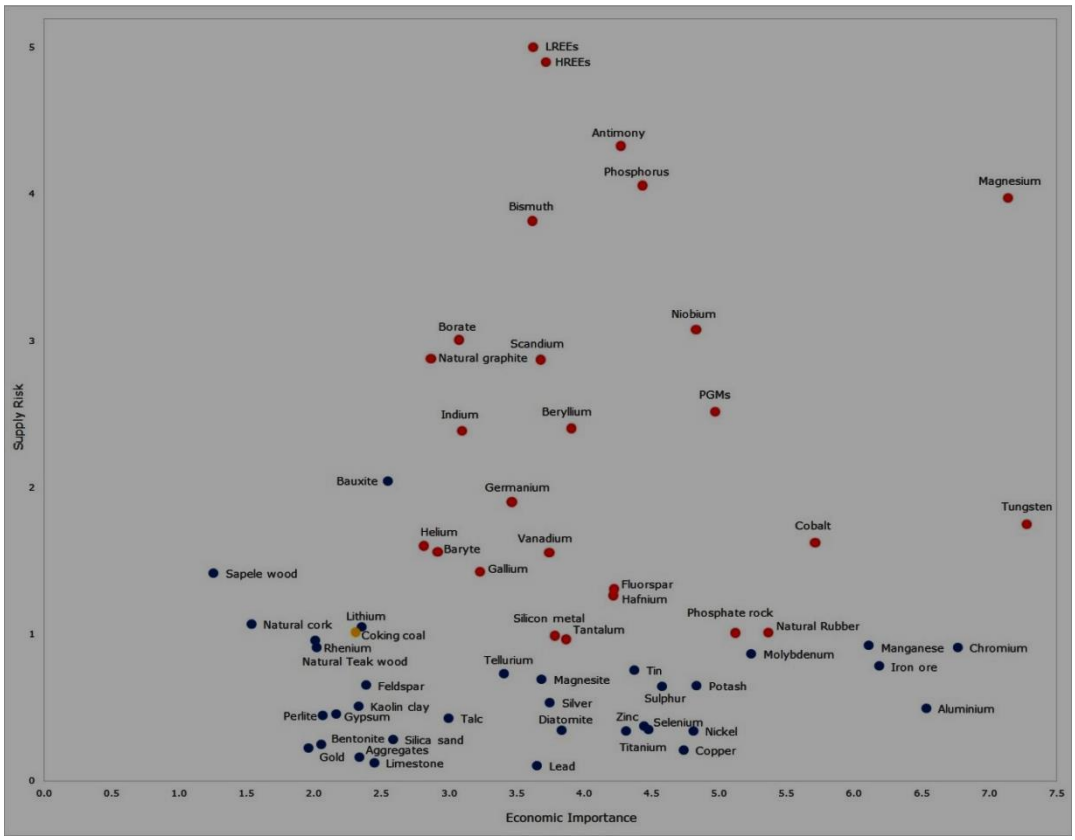


*Figure 3: CRMs identified according to the two parameters economic importance and supply risk. In red the CRMs identified in 2017, in blue CMRs identified in 2014 but not confirmed in 2017.(Source: http://rmis.jrc.ec.europa.eu/?page=crm-list-2017-09abb4).*

The Directive 2006/21/EC presents procedures, measures and guidelines to prevent and/or reduce the environmental risks deriving from the waste generated by the mining industry. The primary objectives of the European Directive are to minimize the production of waste and encourage the recovery of waste through recycling, reuse or recovery operations.

The concept of circular economy is therefore introduced. The circular

economy is an economic system designed to regenerate itself, where waste and the use of resources are reduced to a minimum and when a product reaches the end of its life, it is reused to create further value. This aspect can generate economic benefits, contribution to innovation, growth and job creation.

The objectives that the Directive 2006/21/EC aims to achieve are those related to the identification of best practices for the recovery of critical raw materials, for aspects related to the circular economy (***Figure 4***).

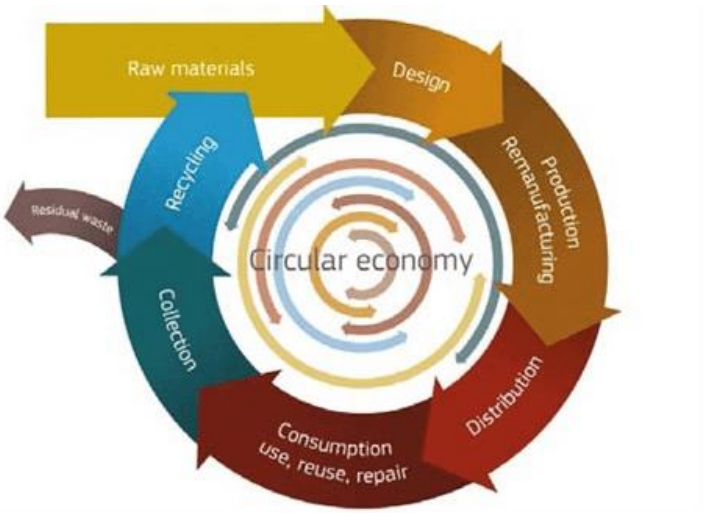


*Figure 4: Circular economy for the management of life cycles of natural resources, for which nothing is wasted. (source: http://rmis.jrc.ec.europa.eu/?page=circular-economy-be990b).*

Directive 1999/31/EC on the landfill of waste presents operational and technical requirements to prevent possible negative effects on the environment and the information that must contain applications for permission to land a waste. The subsequent Decision 2003/33/EC establishes the criteria and procedures for the acceptance of waste in landfills, ie the technical requirements that must have hazardous waste to be accepted in the landfill dedicated to them, the criteria and long-term security assessments for the storage of waste.

With regard to the decisions on recyclability and statistical purposes of waste management, it is important to assign a reference nomenclature which provides a common terminology throughout the Community with a view to improving the efficiency of waste management activities. The European Community through the Commission Decision 2000/532/EC, provides a waste list (LoW) with the relevant CER codes. The CER code consists of 6 numbers that define the type of waste. The first two numbers identify the chapter of the source that generates the waste, the next two numbers indicate the production process from which they derive. For the case study of this thesis the CER reference code is shown in ***Table 2***.

| CER CODE | DESCRIPTION |
|---|---|
| 01 | Waste resulting from exploration, mining, quarrying, and physical and chemical treatment of minerals. |
| 01 04 | Wastes from physical and chemical processing of non-metalliferous minerals |
| **01 04 13** | Waste from stone cutting and sawing other than those mentioned in 01 04 07 |

*Table 2: CER CODE reference for waste from stone cutting and sawing. (Extract from Commission Decision 2000/532/EC).*

Moreover, for a statistical-economic classification of the activities the European Union has created the NACE codes (nomenclature of the economic activities of the European Community). In ***Table 3*** are reported the codes of the mining sector.

| NACE CODE | DESCRIPTION |
|---|---|
| **B** | Mining and quarrying |
| **B8** | Other mining and quarrying |
| **B8.1.1** | Quarrying of ornamental and building stone, limestone, gypsum, chalk and slate |

*Table 3: NACE codes for Statistical classification of economic activities in the European Community (source: http://ec.europa.eu/competition/mergers/cases/index/nace_all.html).*

The legislation of the European Union has widely regulated the management of mining waste, but the problem remains of the interpretation and implementation of the European Directives at national level by the Member States. Scannell Y. (2012) has addressed this topic in an article, stating that the National Directives are often nebulous and interpret the European Directives in an incorrect way. This aspect makes the real application of a circular economy model difficult. In the chapter 1.3 the Italian transpositions of the European Directives will be analyzed.

# 1.2 WeCare Commitment as European Innovation Partnership on Raw Materials

The European community in 2012 with the communication COM (2012) 82 final, proposes the European partnership for innovation on raw materials (EIP).

The EIP brings together different figures: industries, academies, public services and non-governmental associations to provide innovative approaches to the issues of raw materials. The EIP's task may be to provide and propose objectives, methodologies, strategies and priority areas of intervention, which can be concretely used by stakeholders and industries, through knowledge, competence and international cooperation. The main objectives are:

- improve the supply of resources, such as recycling, by finding alternative raw materials;

- mitigate social, environmental and economic impacts.

All data and information sent by the EIPs are monitored and evaluated by the JRC (Joint Research Center), which creates a SIP (Strategic Implementation Plan) implementation document of strategic assessment report.

The European Union has also undertook the EIT raw materials (European Institute of Innovation and Technology), a consortium that is a source of funds to develop and promote the competitiveness, growth and attractiveness of the European raw materials sector, supporting the creation of businesses . The EIT brings together over 120 partners (industries, universities and research institutes) from over 20 EU countries (https://eitrawmaterials.eu/).

This Doctoral thesis is part of WeCare Commitment. WeCare is the acronym of Wastes from Construction industry As a Resource and is a Commitment for European Innovation Partnership (EIP) on Raw Materials, sector waste.

The aims is to propose a solution for waste generation and access to raw materials.

WeCare is focused on the development of sustainable technologies for the production of secondary raw materials from waste and by-products generated in the construction industry, mainly focusing on Natural Stone Industry.

The objectives of the commitment are the follows:

• Development of clean and sustainable technologies for the production of secondary raw materials from wastes and byproducts in the construction industry, focusing on wastes from natural stones machining and construction demolition.

• Strategic, Environmental and Technical specific objectives will be achieved addressing the long term sustainability of European Critical Raw Materials production, supply and recycling, implementing more ambitious environmental standards in waste management and reuse and improving competitiveness of the European Production of Secondary Raw Materials.

• New Secondary Raw Materials for Construction-Composite Materials (inert part) and Metallurgical Industry (heavy metal part).

• A complete characterization of wastes coming from three pilot areas/use cases.

• New market opportunities and employment

• Trust of the society in products containing sustainable secondary raw materials.

WeCARE commitment aims to exploit wastes coming from cutting of natural stones and from deconstruction processes as a sustainable source for the production of secondary raw materials and Critical Raw Materials (CRMs). These wastes are generally contaminated with heavy metals such as cobalt and tungsten, which are toxic, responsible of high environmental impacts and critical supply risk. Clarification of sludge and reuse of metal and mineral fractions into industrial processes will improve their environmental and social sustainability. In ***Figure 5*** is shown a flowchart of the processes for the recovery of soft stones, granite and hard stones and demolition waste.

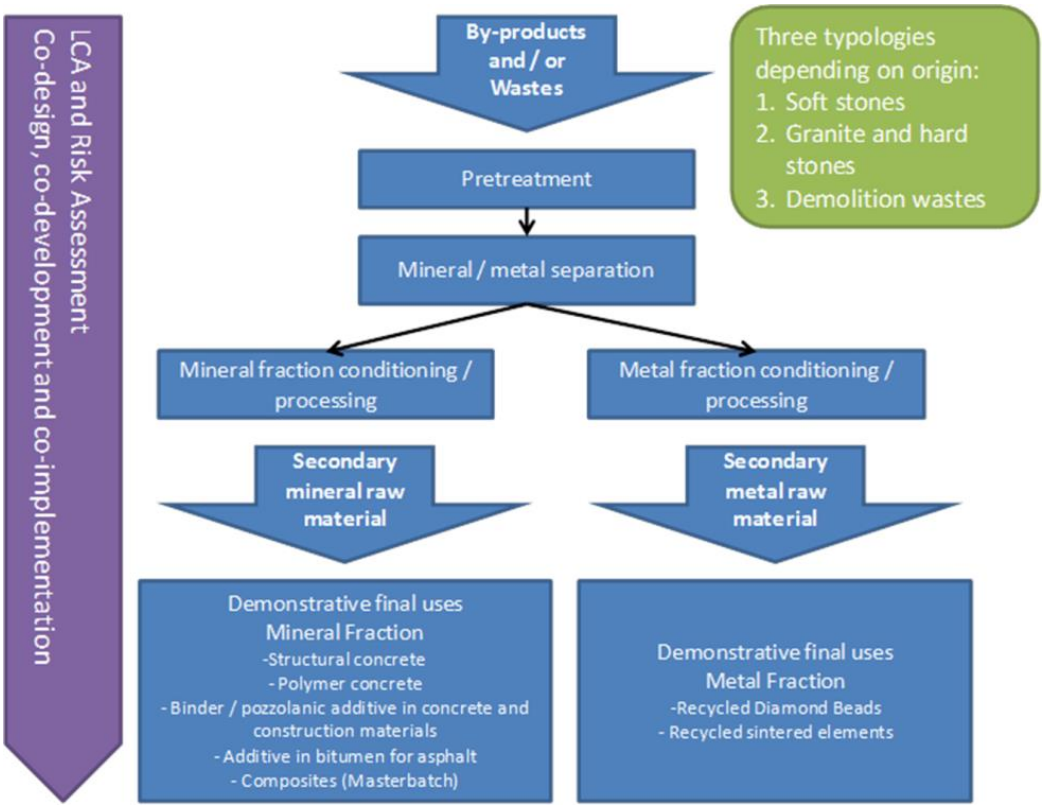


*Figure 5: Resumen of the activity of WeCare Commitment.*

Politecnic of Turin with DIATI (Department of Environmental Territory and Infrastructure Engeneering) focus is study on the recovery of soft stones, granite and hard stones.

# 1.3 Italian policy on waste management

Extractive activities have significant economic importance in Italy, such as the valorization, recycling and reuse of raw materials, based on the circular economy criteria. The majority of the Member States[1] of the European Union have implemented a national raw materials policy, adapting their specific environmental, economic and social needs to the development of objectives set out at Community level. Italy still does not have a well-defined national policy, due to its strong fragmentation of administrative competences between the State, Regions, Local Administrations and Territory. There is basically a lack of coordination between industrial needs and environmental protection requirements. However, Italy actively participates in the European raw materials policy, with ministerial representations, regions, industry and research. The individual Italian Regions are not coordinated with common objectives especially for productive needs linked to the availability of resources for the business system.

The regulation of mining activities in Italy is still regulated by the Royal Decree of 29 July 1927 No. 1443. Since 1927 there has been no national regulatory intervention that would determine unique criteria for Italy. With the DPR 616/1977 the administrative functions related to the quarry activities were transferred to the Regions with Regional Regulations that regulate the sector.

From 2000 onwards, following new decrees imposed by the European Union for the adoption of strict measures on the management of waste derived from mining, it was mandatory for the Member States and therefore for Italy to draw up a waste management plan for the minimization, the treatment, recovery and disposal of the extraction waste, respecting the principle sustainable development. The intention is clearly to push the sector towards innovation, thus leading to a strong recovery of the quarry material as well as the increasingly massive use, in particular for aggregates, of recycled material.

The Italian implementation of European directives takes place through various legislative decrees summarized in the ***Figure 6***.

The Italian implementation of the European Directive 2006/21/EC is the Legislative Decree n° 117 of 30 May 2008 concerning the management of waste from the extractive industries. This decree provides the definitions of waste, hazardous waste and treatment and the guidelines for the management of the same. Legislative Decree n.152/2006 is related to waste management and environmental regulations, outlining prevention (Article 180) and reducing the production of hazardous waste and encouraging the reduction of energy consumption through recycling operations (art. 181); it also defines guidelines for disposal (Article 182), landfilling and incineration. Furthermore establishes qualitative and quantitative criteria (art. 184-bis) in order to considered by-

[1] Austria, Belgium, Bulgaria, Cyprus, Croatia, Denmark, Estonia, Finland, France, Germany, Greece, Ireland, Italy, Latvia, Lithuania, Luxembourg, Malta, Netherlands, Poland, Portugal, United Kingdom, Czech Republic, Romania, Slovakia , Slovenia, Spain, Sweden, Hungary.

products specific categories of substances or objects. Legislative Decree n. 205/2010 (implementation of the directive 2008/98/CE) modifies part IV of the D.Lgs. 152/2006, providing a new definition of by-product (art.12).

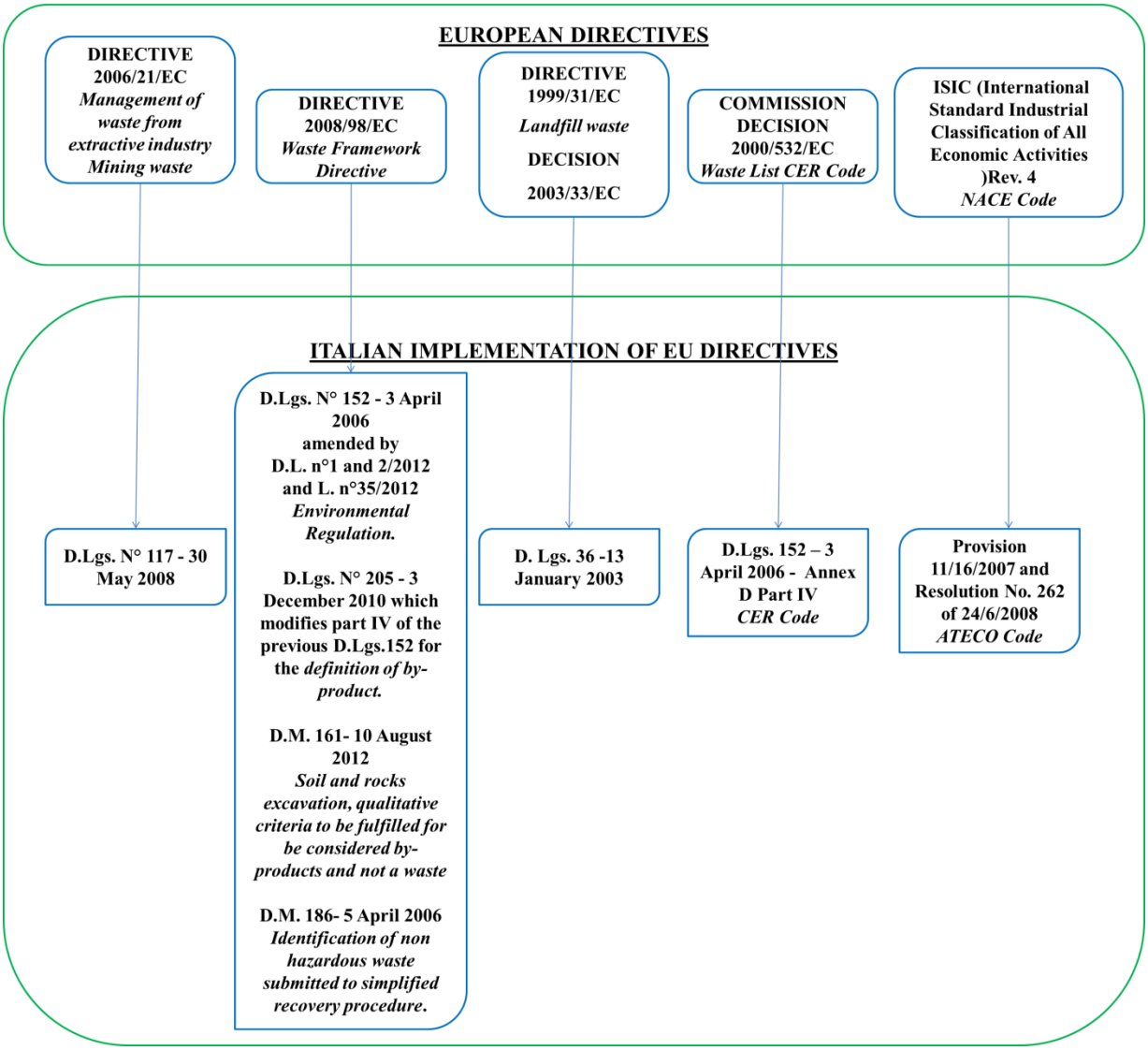


*Figure 6: Italian implementation of EU Directives in mining waste sector.*

This Decree in art. 4 identifies the hierarchy criteria presented by the European Directive 2008/98/EC. Below the definitions provides by legislation of by-product.

Any substance or object is a by-product and not a waste if it comes from a production process, of which it is an integral part, if it is certain that they will be used directly without further treatment other than "normal industrial practice" and if its use fulfils the protection of health and the environment not having negative impacts. So a waste ceases to be such, when it has been subjected to a recovery operation, including recycling and preparation for re-use, if there is a market for the object or substance, if it fulfils the technical requirements and will not have negative impacts to environment and human health.

The technical requirements that the substance or object must fulfils in order to

be considered by-products, in Italy are specified by Ministerial Decree 161 of 10 August 2012 and Ministerial Decree 186 of 5 April 2006. The D.M. 186/2006 identifies the procedures and the methods for recovery and recycling, identifying those non-hazardous waste that can be subjected to simplified procedures. For this reason already in Annex 5, Title V, Part IV of Legislative Decree 152/06, and also in the D.M. 186/2006, limits were introduced for the concentration of hazardous metals to which the materials must undergo in order to be reused.

In Annex 5, Title V, Part IV of Legislative Decree 152/06 a reference table is provided for chemical analyzes (***Table 4***), performed according to standardized methods, EPA 3051A 2007 and EPA 6020A 2007 , and is carried out by the owner of the plant where the material is produced before recovery and every two years, however each time the production process changes. The limits change according to the site reuse, green areas or industrial areas. In case of use for industrial areas the concentration limits are greater.

| Parameter | Column A sites private use and residential public green [mg/kg ss] | Column B sites commercial and industrial use [mg/kg ss] |
|---|---|---|
| **Arsenic** | 20 | 50 |
| **Cadmium** | 2 | 15 |
| **Cobalt** | 20 | 250 |
| **Nickel** | 120 | 500 |
| **Lead** | 100 | 1000 |
| **Copper** | 120 | 600 |
| **Zinc** | 150 | 1500 |
| **Mercury** | 1 | 5 |
| **Hydrocarbons C> 12** | 50 | 750 |
| **Total chrome** | 150 | 800 |
| **Chromium VI** | 2 | 15 |
| **Asbestos** | 1000 | 1000 |

*Table 4: Chemical analysis in unaltered state concentration limit (source: D.Lgs. 152 Annex 5 part IV)*

In the D.M. 186/2006 instead, the table (***Table 5***) of heavy metal concentration in the eluate for the leaching test is reported. In this case there is no distinction based on the site of reuse of the material. The leaching test is carried out at least at the beginning of each activity and subsequently every twelve months, unless otherwise specified by the competent authority. The standard used to perform the test are UNI 10802 and UNI EN 12457- 2.

| Parameter | Unit of measure | Limit Concentration |
|---|---|---|
| **Nitrate NO3** | mg/l | 50 |
| **Fluorides F** | mg/l | 1.5 |
| **Sulfates SO4** | mg/l | 250 |
| **Chloride Cl** | mg/l | 100 |
| **Cyanides Cn** | µg/l | 50 |
| **Bario Ba** | mg/l | 1 |
| **Copper Cu** | mg/l | 0.05 |
| **Zinc Zn** | mg/l | 3 |
| **Berillio Be** | µg/l | 10 |
| **Cobalt Co** | µg/l | 250 |
| **Nickel Ni** | µg/l | 10 |
| **Arsenic As** | µg/l | 50 |
| **Vanadium V** | µg/l | 250 |
| **Cadmium Cd** | µg/l | 5 |
| **Chromium Total Cr** | µg/l | 50 |
| **Lead Pb** | µg/l | 50 |
| **Selenium Se** | µg/l | 10 |
| **Mercury Hg** | µg/l | 1 |
| **Asbestos** | mg/l | 30 |
| **COD** | mg/l | 30 |
| **Ph** | | 5.5<>12.0 |

*Table 5: Leaching test on eluate, concentration limit (source: D.M. 186/2006)*

All waste is identified by a six-digit code (CER code), which classifies each waste based on the source that generates it. In Italy, Legislative Decree 152/2006 identifies the CER codes. For this study he reference CER code is 010413 "waste produced by the processing of the stone". The same European identification code (***Table 2***).

The Italian ATECO Code, correspond to the European NACE Code. ATECO Code are identify with the Provision 11/16/2007 and Resolution n° 262 of 24/6/2008. In ***Table 6*** are reported the ATECO Code that correspond at NACE Code.

| **ATECO CODE** | DESCRIPTION |
|---|---|
| 23 | Manufacture of other products of the processing of non metallified minerals. |
| 23.70 | Cutting, modelling and finishing of stones. |
| 23.70.10 | Sawing and processing of stones and marble. |

*Table 6: ATECO Code (Source: ISTAT – National Statistic Institute).*

The ATECO codes and the CER codes are important for the statistical study on the amount of material that is currently landfilled, rather than being re-used. It also gives economic-financial information on the Italian situation regarding the mining sector respect Europe situation.

## 1.3.1 Piedmont waste management

As mentioned in the previous chapter, through the DPR 616/1977 the administrative functions to the quarry activities have been transferred to the Regions, and gradually they have been approved Regional Normative to regulate the sector. Unfortunately, not all Italian Regions still have their own regulatory plan for quarrying.

The legislation of the different Regions on mining activities is heterogeneous and shows an absence of adequate planning in various areas of the country that instead should define clear rules for a very delicate sector considering the environmental problems related to it.

Many areas of the country do not have a Quarry Plan, such as the province of Bolzano, but also Piedmont has issued a planning document that should be followed by the provincial plans, which at the moment have been adopted only by the Province of Novara.

The Italian situation related to Quarry Plan is shown in the ***Table 7***.

| Italy Regions | **Provinces** | Approved Quarry Plan |
|---|---|---|
| **Abruzzo** | | NO |
| **Basilicata** | | NO |
| **Pr. Bolzano** | | NO |
| **Calabria** | | NO |
| **Campania** | | YES |
| **Emilia-Romagna** | | PROVINCIAL PLANS |
| | Modena | YES |
| | Piacenza | YES |
| | Parma | YES |
| | Reggio Emilia | YES |
| | Bologna | YES |
| | Forlì-Cesena | YES |
| | Ferrara | YES |
| | Ravenna | YES |
| | Rimini | YES |
| **Friuli Venezia Giulia** | | NO |
| **Lazio** | | YES |
| **Liguria** | | YES |
| **Lombardia** | | PROVINCIAL PLAN (PPAE) |
| | Bergamo | YES |
| | Brescia | YES |
| | Como | YES |
| | Cremona | YES |
| | Sondrio | YES |
| | Pavia | YES |
| | Mantova | YES |
| | Milano | YES |
| | Lodi | YES |
| | Lecco | YES |

| | | |
|---|---|---|
| | Varese | YES |
| **Marche** | | PROVINCIAL PLAN |
| | Ascoli Piceno | YES |
| | Ancona | YES |
| | Pesaro-Urbino | YES |
| | Macerata | YES |
| **Molise** | | NO |
| **Piemonte** | | PROVINCIAL PLAN |
| | Alessandria | NO |
| | Asti | NO |
| | Biella | NO |
| | Cuneo | NO |
| | Novara | YES |
| | Torino | NO |
| | Verbania | NO |
| | Vercelli | NO |
| **Puglia** | | YES |
| **Sardegna** | | NO |
| **Sicilia** | | YES |
| **Toscana** | | PROVINCIAL PLAN |
| | Firenze | YES |
| | Prato | NO |
| | Pistoia | NO |
| | Lucca | NO |
| | Massa Carrara | NO |
| | Pisa | YES |
| | Livorno | YES |
| | Grosseto | YES |
| | Siena | YES |
| | Arezzo | YES |
| **Pr. Trento** | | YES |
| **Umbria** | | YES |
| **Valle D'Aosta** | | YES– 3Plans(inert-marble-stone) |
| **Veneto** | | NO |

*Table 7: Framework of the Rules in the Italian Regions (source: Legambiente 2017)*

In Piedmont the Regional Law of 26 April 2000, n. 44 providing functions and administrative tasks of the State to the Regions and local authorities. According to Art.28 and 35 of L.r. n ° 44/2000, the Region has the administrative and monitoring function of the quarries, as well as coordinating interventions and research in the territorial, environmental, energy and prevention and forecasting of natural hazards, ensuring technical support for the planning. While the Provinces contribute to the definition of regional planning in the territorial and environmental field and ensure the specification and implementation at provincial level of the same ensuring the achievement of a suitable level of protection of the provincial environmental system, through the coordinated adoption of plans and programs (Art.36). Municipalities perform the functions in an integrated manner in order to guarantee an adequate level of protection of the environmental system

within their territory (Art.37). Furthermore, the Region, the Provinces and the Municipalities, single or associated, perform the functions in the environmental field through technical-scientific support, technical assistance, monitoring of environmental resources and pressure factors of the Regional Agency for Environmental Protection ( ARPA) (Art.38). In Piedmont, the regional plan that regulates mining activities is being drafted. When is approved, the Province of Novara will also have to adopt the new Regional plan.

The Regional Law n. 23 of 17 November 2016, with article 2, provides that the Region regulates the planning and operation of quarrying activities, as well as the protection and preservation of deposits through ecofriendly methods of cultivation and an adequate use of resources of the quarries according to their natural characteristics. The goals of the Region are the following:

- strike a balance between industrial production and environmental recovery, valorizing and retraining contaminated sites;

- reduce soil degradation, through the recycling of quarry waste, inert aggregates from construction and demolition recovery and the use of alternative materials for quarry products;

- enhance the abandoned mining heritage;

- promote preventive actions in order to improve safety in quarries.

Article 3 of Regional Law n.23/2016, asserts that the planning of extractive activities is carried out through the Regional Plan of Extractive Activities (PRAE). The PRAE is approved by the Region, which promotes its sharing at local level, and constitutes the single reference framework for mining activities, as well as the priority criterion for issuing permits (art. 4 of Regional Law n.23/2016).

The PRAE is divided into the following three extractive compartments:

1) aggregates for buildings and infrastructures;

2) ornamental stones;

3) industrial minerals.

The PRAE defines the technical and regulatory aspects related to mining activities, drafting of the Planning Document, and contains the details necessary for its Strategic Environmental Assessment (VAS). The Planning Document, following adoption by the Regional Council, is transmitted to the entities involved for the acquisition of contributions and observations (neighboring Regions, Metropolitan City of Turin and Provinces, Municipalities and their association forms, competent subjects).

The Planning Document defines:

• the strategic and operational guidelines of the PRAE;

• the methodology to follow for the clarification of strategic and operational guidelines in the drafting phase of the PRAE.

The Planning Document is placed in a framework of strict consistency with what is defined by Regional Law n. 23/2016 concerning both the general

guidelines of the PRAE and its specific contents. The index of the Plan programmatic document, in particular, is drawn up starting from the 10 general objectives that the Regional Law. n. 23/2016 assigns to the PRAE.

The purpose of the Planning Document is to draw up a sufficiently comprehensive description of the planning intentions taking into account the dynamics in terms of criticality and opportunity, and with reference to the prospective visions (field, economic, environmental, territorial, etc.). The plan programmatic document is originates from the contributions of the experts of the restricted plan table (TRP) and the extended technical table (TTA) (coordinated by Ires Piemonte), with the contribution of the inter-directional institutional table (TII) (coordinated by the Sector) Mining Police, Quarries and Mines of the Piedmont Region). It aims to clarify the framework of problematic issues and opportunities for planning extraction activities. For each of the objectives that the law assigns to the PRAE, the Planning Document specifies the lines of interpretation to be followed during the drafting of the Plan Document.

The Planning Document is divided into three parts:

1) first part of the document is aimed at illustrating the current location of the mining activities in the territory of the Piedmont Region and illustrating the main characteristics / dynamics of the sector, as they emerge from the analysis of the data available. The main sources for the work of statistical classification are the data of the BDAE (Extractive Activity Database) and those of the ISTAT.

2) second part illustrates the process of the plan and, in more detail, the working method followed for the drafting of the planning document. This section deals with the guidelines of the law and the general objectives of the PRAE.

3) third part contains the description of the specific objectives and actions that can be envisaged for each of the ten general objectives that the Regional Law. n. 23/2016 attributes to the PRAE, as well as the indication of the investigations deemed necessary for the preparation phase of the PRAE.

Therefore, the PRAE will have the value of an instrument of a higher level than local urban planning in relation to the identification of the extraction poles and their developments, as well as the forecasts concerning the existing extraction sites and their extensions. The region has commissioned IRES to update data on the location of mining activities in Piedmont

The sectors 2 and 3, ornamental stones and industrial minerals, present smaller quantities than the aggregates of construction and infrastructure, but are more export-oriented. For ornamental stones, for example, 23% of the useful material used has a destination outside the Region, 65% is directly extracted in Piedmont, while 35% is imported from outside the Region (Source: Quarry Report IRES 2017).

The IRES Research Institute of the Piedmont Region (2017) carried out a study on material flows in Italy and in Piedmont, which showed a total material requirement in 1 year of 47.4 tons/cap in Piedmont compared to 40.7 tons/cap in

Italy, while direct material inputs, ie the resources used, are 18.96 tons/cap in Piedmont compared to 18.91 tons/cap in Italy. The difference between the values of total material requirements and direct material input consists of primary waste (extraction), secondary waste (processing) and material and indirect (energy and consumption machinery). It can therefore be concluded that the resources used by the mining sector represent around 30% while the waste is 18.5%. In the European context we talk about the valorization of waste materials and the creation of synergistic programs between mining and infrastructure. The percentage of waste with respect to the material used must therefore be reduced.

In the context of the following thesis it is important to analyze the situation of section 2, concerning ornamental stones. ***Figure 7*** shows the distribution by provinces of the number of quarries operating for all three sectors. (source: http://www.regione.piemonte.it/attivitaProduttive/web/attivita-estrattive/cave).

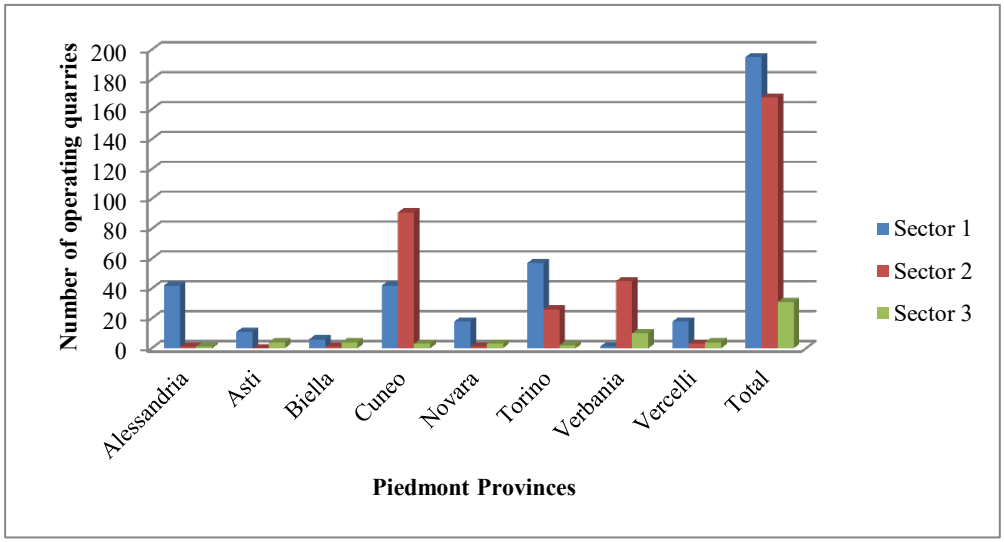


*Figure 7: Number of operating quarries in different Provinces of Piedmont Region for the three sector. Where: Sector 1: aggregates for buildings and infrastructures; Sector 2: ornamental stones; Sector 3: industrial minerals (Source: Quarry report IRES 2017)..*

The most represented quarries in terms of numbers and volumes are those of the first sector (more than 200) and present considerable dispersion at the regional level. Aggregates are distributed in all the provinces and prevalently in the Cuneo, Alessandria and Torino area, according to the main regional river. The quarries of the third sector (industrial materials) are also widespread, but lower in number (almost 40). While the quarries of the second sector (ornamental stone) present a fragmented organization on many small units concentrated from the spatial point of view: almost all the quarries of the sector is limited to well defined areas of the Province of VCO (for the Valdossola stones) and the area between Torino and Cuneo (for the Luserna stone), which emerge as mainly district systems. ( ***Figure 7*** and ***Figure 8***).

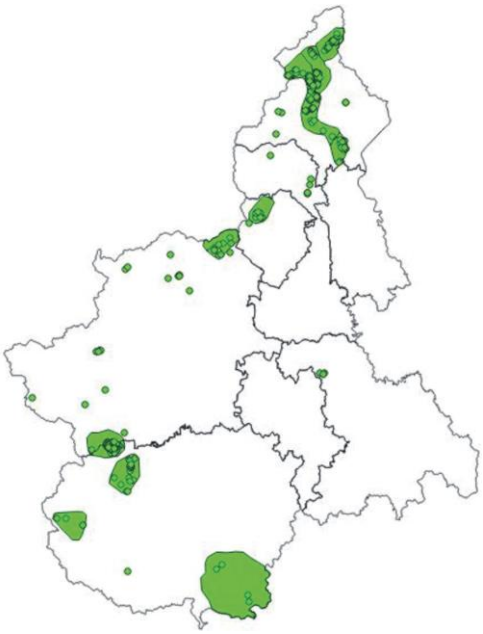

*Figure 8: Distribution of the quarries (points) and basins of the sector 2 of the PRAE.(source: Report IRES 2017)*

The BDAE (Extractive Activity Data Base) indicates that 75% of the total Piedmont ornamental stone consists of Gneiss, while 5-7% of granites, quartzites and marbles and only 1-2% of diorites and syenites (***Figure 9***). The districts of Cuneo, Torino extract mainly Luserna stone, while the Verbano area mainly extracts Serizzo, Beola, Granite and Gneiss. Most of the Piedmont rocks is of silicate origin.

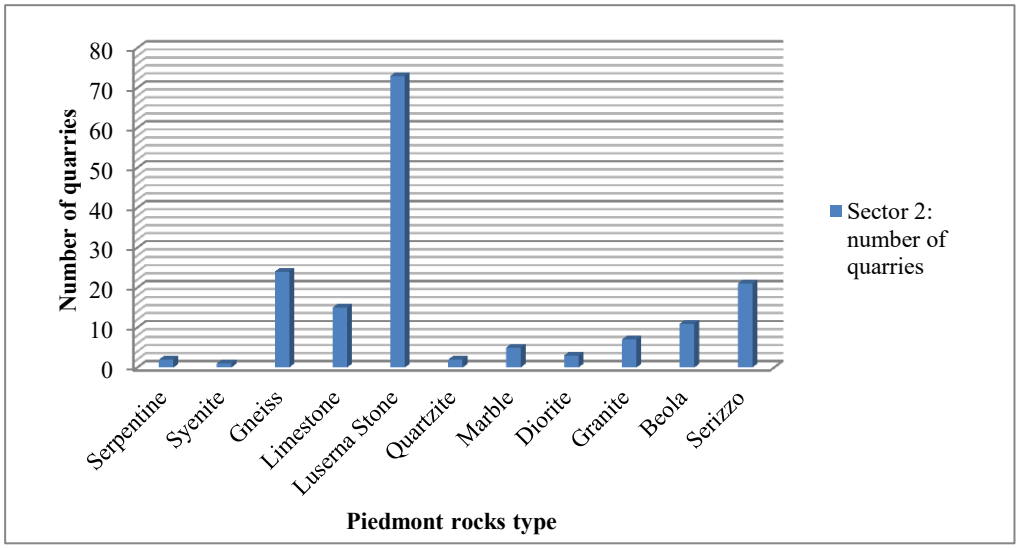


*Figure 9: Types of ornamental rocks mainly extracted in Piedmont (Source: Report IRES 2017).*

Following the statistics on the most extracted and treated materials in Piedmont, it was decided to focus the research on the 3 districts of Turin, Verbano and Cuneo. Most of Piedmont silicate ornamental stone are cut in these districts, and therefore more quantities of sludge destined for landfill are present.

# Chapter 2

# 2. Production cycle of ornamental stones

The production cycle of ornamental stones begins from the extraction process in the quarry with the realization of commercial blocks satisfying certain volumetric, dimensional and aesthetic requirements. The block volume size is generally of the order of 2.5 $m^3$ up to 9 $m^3$. The block can be obtained both from large portions of rock, called bank, having the shape of a large, more or less elongated parallelepiped and a volume of the order of hundreds or thousands of cubic meters, both directly from the quarry front. One or the other choice is due by practicality and cost factor, the cost cutting unit is a function of the material extracted.

The subsequent processes after excavation are, the sawing of blocks in slabs through different technologies, chosen according to the type of rock, and the surface treatment, such as polishing, sandblasting, bush-hammering. Sawing is the first processing step in plant and is a volume treatment, while the second phase is a surface treatment.

***Figure 10*** shows a generic pattern of production cycle of ornamental stones, in case of slabs production.

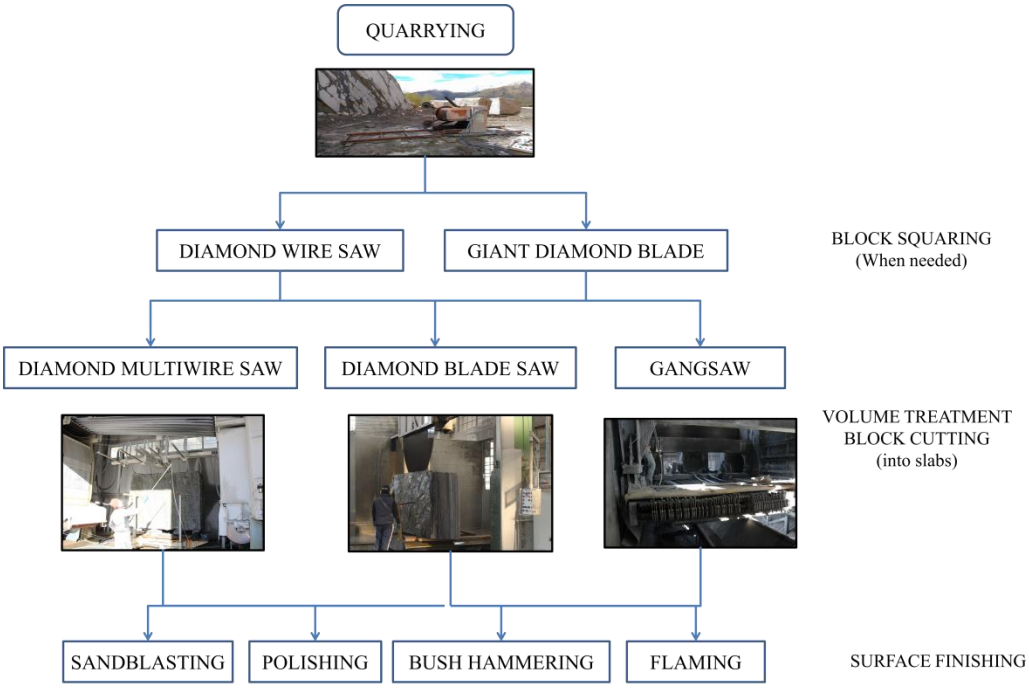


*Figure 10: Production cycle of ornamental stones, for slabs production.*

Object of the following research thesis is the sludge produced by the first phase of volumetric processing.

The sawing takes place mainly through three different technologies. The gangsaw technology is the classic one, the other two are diamond technologies such as the diamond blade and the diamond wire. In the following paragraphs, each cutting technique is analyzed in detail. For technical and commercial convenience, the cutting technologies used are different according to the composition of the stones to be sawn (silicate or marble). The characteristics of tools, and parameters of the machine are different due to the stones characteristic.

# 2.1 Gangsaw technology

The multi-blade gangsaw is the most common and traditional technology, consisting of a large and heavy frame, a blade carrier frame and a set of blades which are moved back and forward alternatively along the cutting surface, with programmed cutting speed and feed rate. A heavy flywheel rotation controls the alternative movements of the blade holder frame. The length of the cutting movements, transmitted to the blade holder frame by two rods, is generated from two cranks connected to the flywheel axis extremities. In ***Figure 11*** is showed the principal operating scheme.

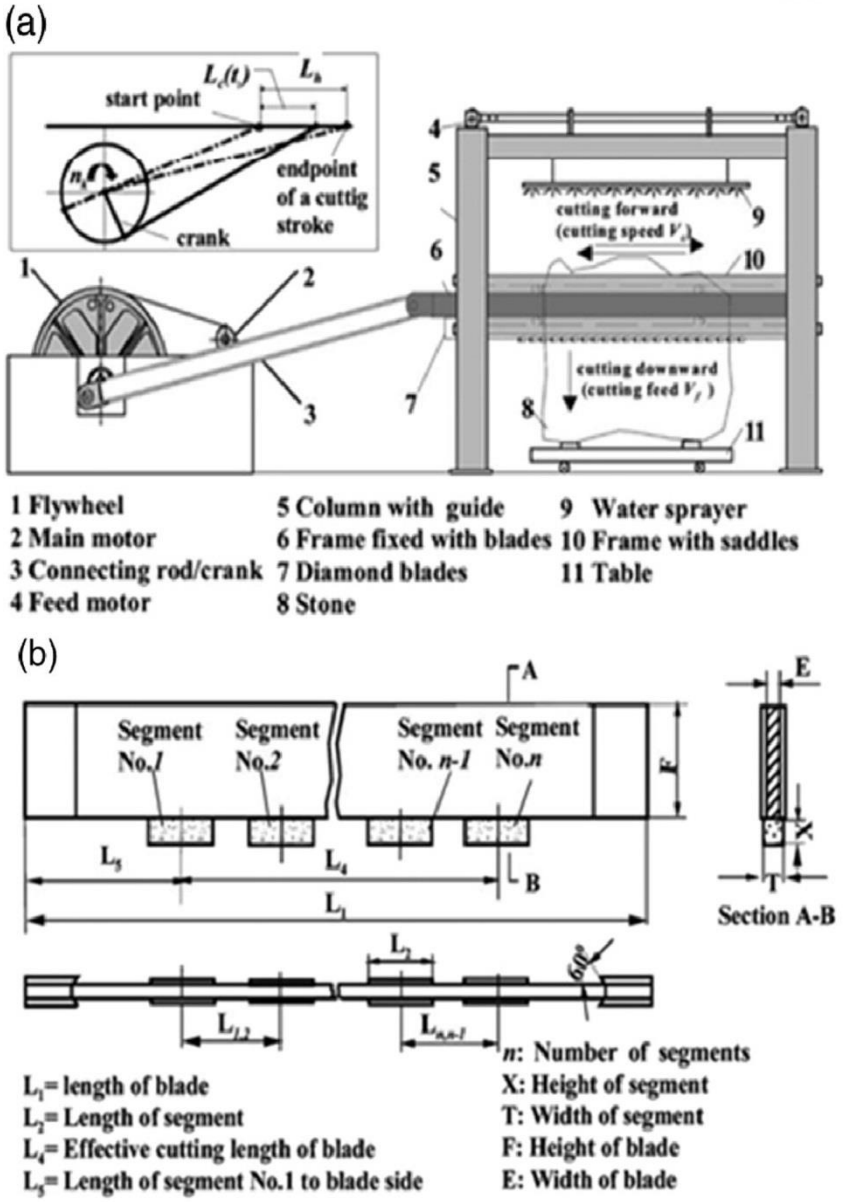


*Figure 11: a) technical scheme of the gangsaw machine b) scheme of the blades used in gangsaw. (source: H. Zhang et al, 2016).*

There are two major types of gangsaw: the diamond blade to saw marble and other soft stones and the grit gangsaw used for granite and hard stones (***Figure 12***).

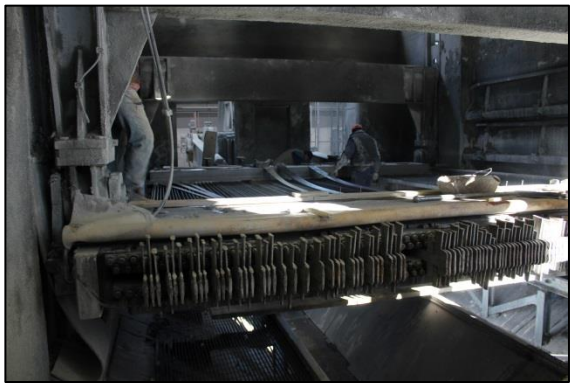

*Figure 12: Gangsaw machine for hard cutting stones.*

Following several studies to improve the mechanical system of the gangsaw and its tools allowed the use also for cutting granite and harder stones. H. Zhang et al. in 2016 they investigated, through a series of cutting tests and simulations, a new gangsaw prototype (***Figure 13*** - ***Figure 14***) that uses an eccentric hinge guide mechanism, rather than a rectilinear one, so the contact between the blade and the granite is less and thus allows a less wear of the blades, greater flatness of the slabs and therefore better cutting efficiency.

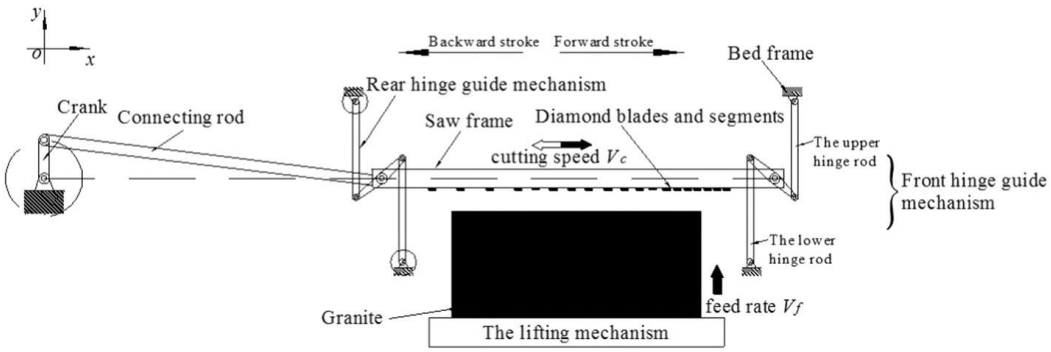


*Figure 13: Scheme of the gangsaw kinematic, new prototype of H. Zhang et al (2016)*

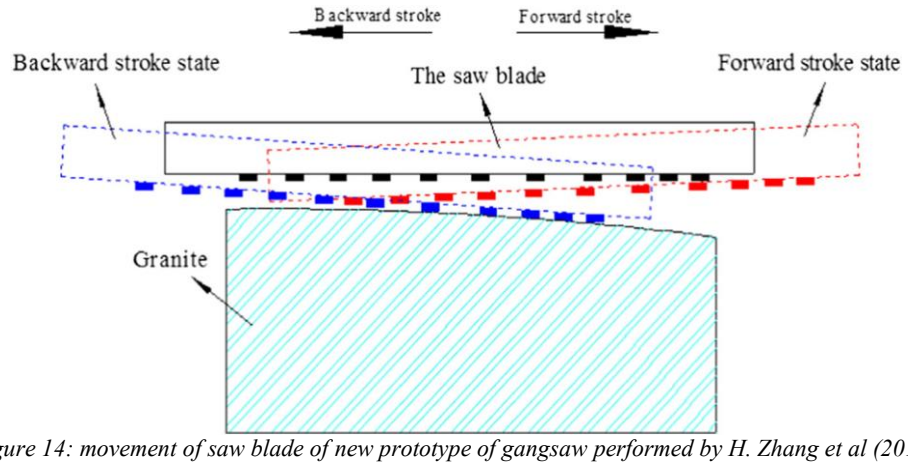


*Figure 14: movement of saw blade of new prototype of gangsaw performed by H. Zhang et al (2016).*

On the market there are gangsaw which apply three different blade

movement: the horizontal movement gangsaw (described above), pendular movement gangsaw that hit the surface of the block at each passage of the blade holder structure (used for granite and hard rocks), and the gangsaw that combine the two techniques.

In the case of the cutting of hard silicate rocks, the cut of the block in slabs is obtained through the friction created by the combined action of the pendular movement of blades and by an abrasive slurry composed of water, lime and metallic grit.

*Figure 15:Metal grit for gangsaw*

This abrasive slurry is sprayed through nozzles, placed over the blades, continuously. The exhausted grit is normally passed through a hydrocyclone, which selects the still reusable grit, to re-insert it in the cutting process (***Figure 16***).

*Figure 16: abrasive slurry before selection of reusable grit.*

The choice of metal grit is important and is carried out on the basis of the hardness of the cut stone, of the type of gangsaw available and of the production (that is the "feed rate") needed. There are three different types of metal grit:

- steel grit: spherical and angular extremely hard and durable;

- cast iron grit: spherical and angular, of considerable hardness and abrasiveness;

- mixtures of steel and cast-iron grit: combines the characteristics of the previous two types.

The particle size distribution of the grit ranges from 0.2mm to 3mm, but the most used for hard rocks cutting are 0.4mm, 0.6mm and 0.8mm. It is possible to combine different shapes and sizes suitable for cutting needs. The life of the grit varies from 400 to 600 cycles, for this reason the plants provide the recovery of the grit by means of a hydrocyclone which selects the still-usable grit size. The dosage during the cutting process is also important, since an overdose can cause a greater wear of both the blade and the grit and an irregularly accumulation of the grit in the cut can cause a deviation of the blades; while an underdosing may cause the breakage of the segments of the blade and a reduction in production ("feed rate"). The grit feed for the cutting cycle must be measured by weight and not by volume to obtain a constant density mixture.

The lifetime of the blades and the quality of cut depends on the correct quantity and distribution of the cooling water. Correctly filtered water must be used, particularly when working with materials that produce abrasive or sludge residues.

It is also important to program the process according to the cutted stones characteristics.

When the same stones are processed it is possible to establish and maintain an optimal cutting speed. This is not possible when different materials must be cut. In this case, it will be necessary not only to adapt the feed rate of the blade to the characteristics of the material, but also to alternate the cut material. It is therefore important to program the alternation of the blocks in the best way to ensure longer blade life (https://www.diamant-boart.com/en-GB/product/processing-tools/gang-saw-blades/).

When cutting different kind of materials on the same gangsaw machine, the same blades are used even if normally different tools should be provided. To use only one type of blades, optimizing them, it is important to classify the cutting stones on the basis of theirs hardness and abrasiveness. The feed rate must be adapted according to the blocks characteristics by alternating hard materials and abrasive materials.

## 2.1.1 Metal composition of gangsaw tools

For the purposes of the following study it is important to understand the metal composition of the machinery tools. The sludge produced during the cutting has, in addition to the rock fraction, also a metal fraction obtained from the wear of the tools and in the case of the gangsaw also from metal grit.

The composition of metallic grit varies according to the manufacturer and type of grit (cast iron or steel). ***Table 8*** shows examples of the grit metal composition.

| metallic grit type | FAST BLAST-Chilled Iron Shots | PANACUT-Granite cutting grit | PANASHOT – Steel shot | PANAGRIT – Steel grit | SATINBLAST-Stainless steel shot |
|---|---|---|---|---|---|
| **Martensite matrix** | >90% | >85% | + Bainite - >95% | + Austenite - >95% | >60% |
| **C** | 2.50-3% | 0.8-1.2% | 0.8-1.2% | 0.8-1.2% | <0.25% |
| **Si** | 1.4-1.8% | 0.4-1.2% | 0.4÷1.2% | 0.4-1.2% | <3% |
| **Mn** | 0.3-0.5% | 0.5-1.2% | 0.5-1.2% | 0.5-1.2% | <2% |
| **Cr** | | | | | 16-20% |
| **Ni** | | | | | 12-14% |
| **S** | 0.14-0.2% | <0.05% | <0.05% | <0.05% | |
| **P** | 0.5-1% | <0.05% | <0.05% | <0.05% | |
| **Rockwell hardness** | 62 HRC | 63÷67 HRC | 62 HRC | 60 HRC | 300 HV |
| **Bulk Density (kg/m$^3$)** | 4250 | 3700 | 4450 | 3700 | 4500 |

*Table 8: Grit metal composition of different manufacturer, Rockwell hardness and bulk dennsity. (source: PAN abrasives)*

Gangsaw blades are made up of steel which yields highest level of performance with long life. The chemical composition of the blades also varies according to the manufacturer and the performances to be achieved. The ***Table 9*** shows examples of chemical composition as percentage by weight (sources: http://purvainternational.com/en_US/gangsaw-blades/, http://stelcolimited.com/gang-saw-steel/ and Hard strips (India) http://www.hardstrips.com/steel-grades-gang-saw/).

| Steel type | 75Ni8 | 75Cr25 | 75Cr1 | C65 | C75 | C80 |
|---|---|---|---|---|---|---|
| **Martensite matrix** | >95% | >97% | >97% | >98% | >97% | >96% |
| **Fe C** | 0.75% | 0.70-0.78% | 0.70-0.80% | 0.65% | 0.75% | 0.80% |
| **Si** | 0.25% | max0.35% | 0.15-0.35% | 0.35% | 0.35% | 0.35% |
| **Mn** | 0.40% | 0.60-0.90% | 0.60-0.80% | 0.60-0.90% | 0.60-0.90% | 0.60-0.90% |
| **P** | ≤0.025% | 0.04% | 0.03% | 0.035% | 0.035% | 0.035% |
| **S** | ≤0.020% | 0.03% | 0.03% | 0.025% | 0.025% | 0.025% |
| **Ni** | 2% | | | | | |
| **Cr** | max 0.15% | 0.15-0.27% | 0.30-0.40% | | | |
| **Mo** | max 0.1% | | | | | |

*Table 9: Gangsaw blades composition for different manufacturer.*

The advantages of the presence of Ni in the composition are: minimum

rusting, longer life, improved tensioning, better relaxation resistance, minimum sawing variation, smooth sawing, constant tensile strength. C65, C75 and C80 are carbon steel for standard application; when more hardness and wear resistance is required Nickel and Chromium steel alloy are used.

When cutting marble and soft rock material diamond segments are applied to the gangsaw blades and the use of metallic grit is not foreseen. The diamond segments consist of powders of Cu, Sn, Fe, Ag, Co, Ni, WC, Mo, graphite, etc. The exact composition is reported in paragraph 2.2.1, ***Table 12***, of this Chapter. The powders, whose percentage changes from manufacturer, are mixed with bonding materials and loaded into molds , hot pressed or cold-pressed, sintered and ground.

# 2.2 Giant diamond saw blade

The giant blade cutting machine is composed of a robust frame and of a longitudinal beam where a large diameter diamond blade is installed (***Figure 17***). The diameter of the disk can be of different sizes depending on the height of the block to be cut. The giant disks have diameters ranging from 2500 mm to 3500 mm. With disk diameters of 2500 mm, blocks with a maximum height of 1100 mm can be cut, while blocks with a maximum height of 1600 mm can be cut with a 3500 mm diameter disk. The diameter of the internal hole of the disk must be equal to the diameter of the spindle (1/10mm) so as to avoid incorrect movement of the disk. The thickness of the disk changes according to its diameter, as it show in ***Table 10***.

| Disk diameter | Disk thickness |
|---|---|
| **2500 mm** | 12 mm |
| **3000 mm** | 13.2 mm |
| **3500 mm** | 14.2 mm |

*Table 10:Disk thickness according to its diameter (Source data: Pulitor Spa Company).*

Compared to the other two technologies of cutting, gangsaw and diamond wire, the diamond saw blade has as limitation the cutting height of the block. Furthermore, only one cut can be performed at a time. There are also multi-diamond disks on the market, used mostly for blocks of smaller heights to produce tiles. This technology uses cooling water to prevent overheating of the tool. The water supply must be carried out correctly, remembering that the tool must be refrigerated in all its depth of cut. The positioning of the disk is very important, in order to avoid the flag waving of the flange and its support surface and therefore any inaccuracies in the cutting of the slabs. To make the most linear cuts possible, the disk must be flanged at least 1/3 of its diameter. The optimization of the positioning is in any case obtained by means of an optical device (encoder). Also the tensioning of the disk is a parameter which, if incorrect, can cause vibrating effects on the disk and therefore a non-flatness of the slabs.

In order to correctly deal cutting processing with diamond disks, the following elements must be considered:

- the cutting material and its workability class (hardness, compactness, abrasiveness, structure, etc.)
- the parameters of the machine (a correct feed rate and power machine)
- the disk (chosen according to the type of material to be cut, to offer maximum capacity for cutting).

*Figure 17: Giant diamond blade saw.*

Diamond disks (***Figure 18***) are essentially composed of:

- central bore;
- steel core;
- segments (connected to the steel core by laser welding);
- gullet between segments.

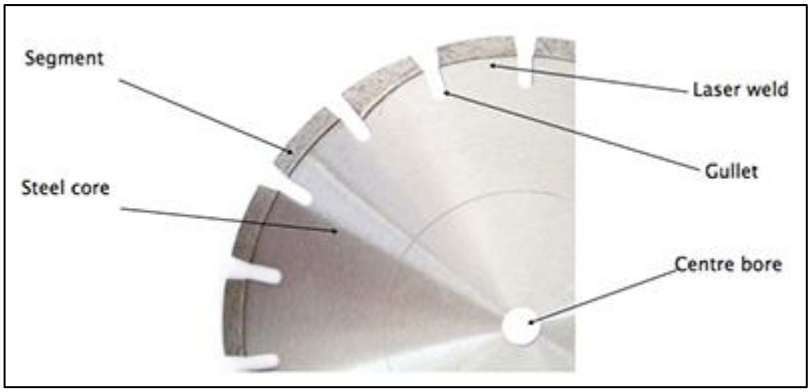


*Figure 18: anatomy of a diamond blade (source: http://www.pulvex.co.uk/technical-information/a-buyers-guide-to-diamond-blades/)*

The core of the disk is made of heat-treated high-alloy laminated steel. For cutting very hard materials it may contain holes that are used to cool the tool.

They are also used in case the disk doesn't present gullet but continuous rim blade, that do not allow cooling and may therefore be subject to overheating which can lead to loss of tension in the steel core. Gullet improve air flow but also remove sludge from the cut. Sludge has a wearing effect on the blade, therefore its

removing is better for the blade life.

Saw blades could have some different periphery configuration based on the type of cutting rock. In ***Figure 19*** are reported the typical possible configuration.

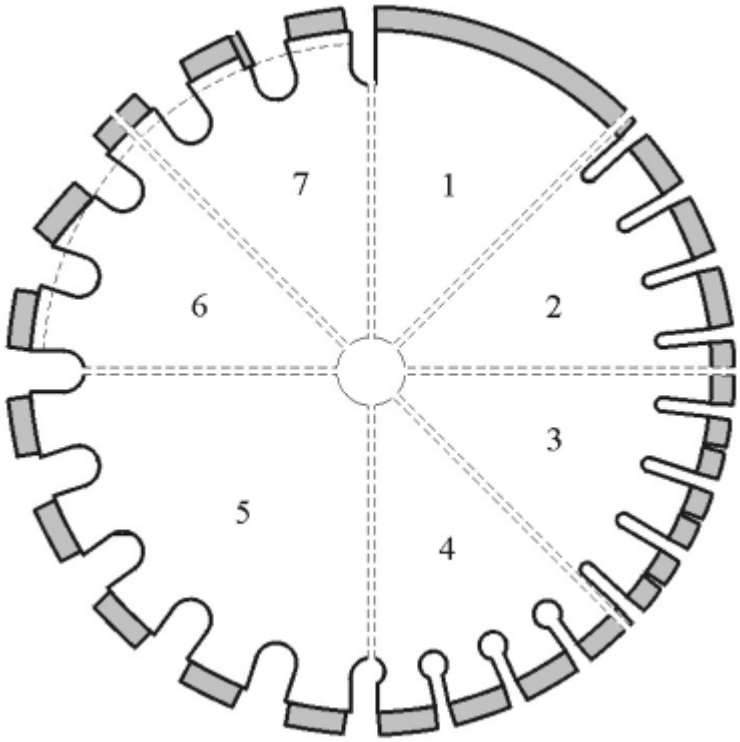


*Figure 19: Configuration of saw blade segment. Type 1:continuos rim balde; Type 2: blade with narrow slot; Type 3: long segment substitution with two short segment; Type 4: keyhole shaped slot; Type 5: wide slot; Type 6 and 7: blade periphery incorporation of wear protective segment. (source: J. Konstanty, 2006).*

The first configuration is use for hard and dense ceramic and glass. The second one is use for igneous rocks. The third configuration help to decrease the abrasive action of sludge produced during cutting, due to the possibility of directing more coolant into the cutting area. Configuration 4 and 5, are provided with holes between the segments which have a beneficial effect on the tool life, especially in the case of giant disks. which exhibit high fatigue stresses. Type 5 in particular is use for very abrasive materials. Configuration 6 and 7 prevent the loss of segment due to a wear protective layer.

The segments consist of a mixture of diamond grit and metal powders that form the bond that retains the grain of the diamond. They can have a different depth, from 5 mm to 17 mm. However, the depth of the segment is not an indicator of a good quality of the segment because the diamond concentration could be higher on less deep segments.

The diamonds used in the tools are synthetic, due to theirs stronger and more uniform characteristics. The quality and strength of a segment is determined by the diamond concentration, its distribution size and its shape. When the blade worn, the diamond sand breaks or falls from the bond and the same bond reveals the next layers of diamond. The metal bond is a mixture of metal powders that create a bond of varying hardness that will determine the wear rate of the segment.

## 2.2.1 Metal composition of diamond saw blade

The tools consist of the steel core which carries the diamond segments. The diamond segments can be attached to the steel centre using two basic methods:

- brazing (segment attached to the core by brazing with silver solder), used on standard blades for wet cutting;

- laser-welding (segment are welded to the centre using laser beam), strongest bond possible between steel centre and segment suitable for wet and dry cutting application.

***Table 11*** shows an example of composition of the disk steel core. The chrome is used in alloy to obtain special high strength and stainless steels.

| | **tool-steel 75Cr 1** |
|---|---|
| **Martensite matrix** | >97% |
| **Fe C** | 0.70÷0.80 % |
| **Si** | 0.25÷0.50 % |
| **Mn** | 0.50÷0.70 % |
| **Cr** | 0.30÷0.40 % |
| **hardness Rockwell** | 46 |

*Table 11: saw disk steel core material composition in weight %*

The segments are composed by diamonds and metal matrix. The metal matrix has two basic function: hold the diamond tight, but at the same time allow it to be detached if it breaks. The key factors for choosing the powder to use to bind the diamond grain are:

- the chemical composition and the degree of binding,

- the granulometric distribution of the grains

- the type and content of impurities.

The right combination of these properties allows diamond to not degrade but consolidate itself to the matrix and to have a good resistance to wear.

Cobalt, W-Co and Cobalt based alloys are the most used as a matrix for impregnating the diamond.

Konstanty J. (2006) in his study, reported the chemical composition of some commercial matrix of the segments (***Table 12***).

| | **Cobaltite 601** | **Cobaltite HDR** | **Cobaltite CNF** | **Next 100** | **Next 200** | **Next 300** | **Next 900** | **Cu-Fe-Co matrix** |
|---|---|---|---|---|---|---|---|---|
| **Fe** | 70% | 66 | 68·4 | 26 | 15 | 72 | 80 | 45÷55 |
| **Cu** | 20 | 7 | 26 | 50 | 62 | 3 | 20 | 34÷38 |
| **Co** | 10 | 27 | | 24 | 23 | 25 | | |
| **Co-Cr** | | | | | | | | 5÷8 |
| **Sn** | | | 3W-$2Y_2O_3$: 0·6 | | | | | 1÷3 |
| **Ni** | | | | | | | | 5÷10 |

*Table 12: Some type of commercial matrix for the segments. (source: Konstanty J. , 2006).*

The synthetic diamonds in some cases are covered with Ti that protects the diamond from the possible graphitization effect. When the steel is subjected to temperatures above 800 ° C, the phenomenon of graphitization can take place, ie the formation of free carbon (graphite). This phenomenon causes areas of weakness on the affected steel component (S. Spriano et al., 2015).

# 2.3 Diamond wire

In the field of diamond cutting tools, diamond wire is the latest innovation in constant growth. The diamond wire is used both for the extraction process in the quarry, and for the cutting of slabs, and the squaring of marble and granite. Purpose of this thesis is specific for diamond wire machine for cutting blocks in slabs. Considering the number of wires, the diamond wire machines are of two types: monowire (***Figure 20***) and multiwires (***Figure 21***). The machine can be stationary or mobile ***(Figure 20***). The characteristics of the diamond wires change according to the type of cutting stone.

The advantages of this type of machine are different:

- minimum space and resources consuming
- absence of vibrations
- low noises
- greater precision
- higher cutting speed
- maximum cutting efficiency
- good quality/cost ratio (slab production, water supply, machine power)
- less sludge production (due to the absence of the lime-steel shot grit mixture).

Moreover, with this type of technology, it is possible to produce, at the same time, slabs of different sizes (2cm, 3cm, 4cm, 5cm, and multiples).

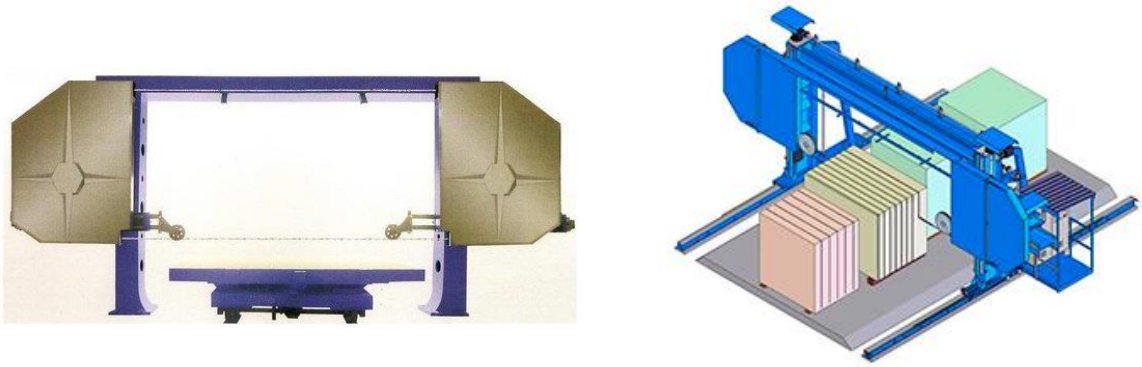

*Figure 20: Monowire machines. Left: stationary type; Right: mobile type. (source: http://www.minorsa.com/machines_55a.html and https://www.ec21.com/product-details/Monowire-Slab-Cutting-Machine--5005898.html).*

The monowire machine is preferred for block squaring. It can work marble and granite.

The cutting diamond multiwire application is addressed to cut blocks into slabs using multiple diamond wires instead of blade gangsaw. This technology represents the overtaking of traditional gangsaw. Careddu and Cai (2014), studied the main features of block sawing methods, traditional and more advanced technology, production in term of cost and performance. The diamond multiwire is an efficient machine in terms of durability and productive yield. Its structure is similar to the monowire plat, but with independent flywheels. The wires speed is adjustable using an inverter, and the entire system operation is completely automatic managed. It can be used to cut granite and marble by simply changing the configuration and type of wire. It can also produce different thicknesses at the same time, optimizing the cutting production.

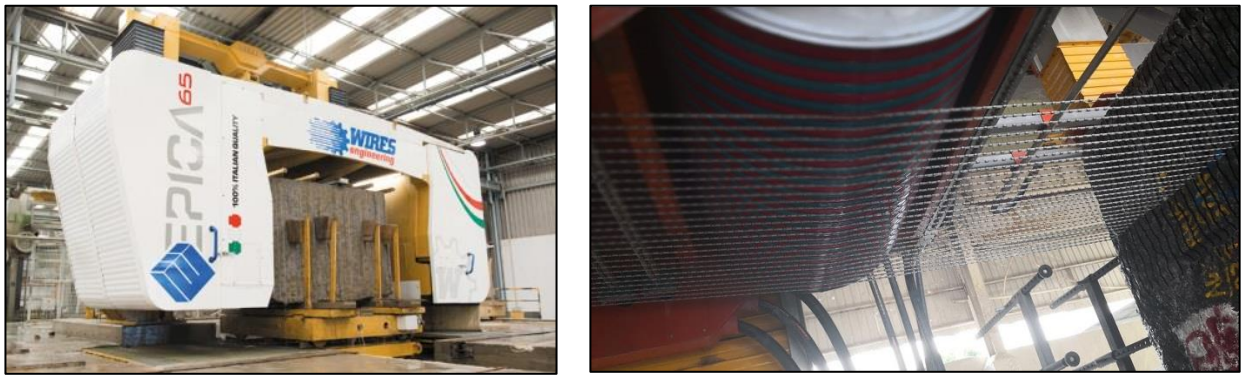


*Figure 21:Diamond multiwire. On Left: Co.Fi.Plast multiwire machine. On Right: multiwire tools.*

The machine consists of a pair of pneumatic cylinders that guarantee symmetrical operation of the structure and tensioning of the diamond wires. It is

also made up of two symmetrical tensioning pulleys, which allow the tension to be evenly distributed along the whole diamond wire. Wire tensioning is an important parameter both for good quality of slabs production and to minimize tool wear.

The wire length and overall tensioning stroke varies by manufacturers. In this context Co.Fi.Plast Wires Company is taken as an example. The length of the wire varies from 15.10 m to 65 m for long multi-wire machines. The total tensile strenght varies from 500 mm to 1000 mm. Cutting speeds range from 15 m/s to 33 m/ s. The cutting speed must be chosen according to the type of stone to be cut, for hard stone is better use a low speed respect with a marble or a soft stone. The number of wires placed in parallel can be 8, 20, 30, 40, 65 wires.

Diamond wire consists in a stainless steel cable on which the effective cutting parts and all other elements of the diamond wire are mounted. The cable absorbs static and dynamic stresses. The diamond pearls (beads) are the effective cutting parts. The diamond grains are electroplated or sintered (***Figure 22***) on an annular (ring shaped) steel frame. The spacers are steel, flexible rings that ensure correct arrangement of the pearls and keep the proper distances between the pearls on the wire. The joint clambs link sections of the wire. The stops are metal rings, solidly pressure-fitted to the wire.

*Figure 22: Diamond beads for diamond wire machine. Left: electroplated diamond grains; Right: sintered diamond grains. (Source: Tyrolit Company.)*

***Figure 22*** on left show electroplated pearls. The diamond grains are deposited by electrolysis on a ring-shaped steel frame. A layer of metal bonding agent holds the grains of diamond deposited on them until they are worn out during rock cutting process. The electroplated diamond wire has a remarkable coherence of the diamond grains and high rock-cutting capacity. It is more effectively used in sawing soft stones, or for small cuts and for squaring small blocks. It has higher initial cutting speed compared to the sintered diamond wire and needs a relatively small amount of cooling water that varies from 10 l/min minimum to 20 l/min maximum.

***Figure 22*** on right show sintered diamond grains. The diamond grains, in this case, are mixed with the bonding material according to a specified method. This mixture placed in matrix is heated and compressed under predetermined and carefully controlled. After sintering, the diamond pearls are removed from the matrix and brazing. The technical features and mostly the abrasion resistance of the alloy that hosts the diamonds grains are of high importance. So, if the alloy is of very high abrasion resistance, new diamond cutting surfaces do not effectively appear and the cutting speed decreases. Contrarily, if the hosting material is very

soft and easily abraded the diamond grains are taken off, even before they used and the productivity of the wire is minimized.

The sintered or impregnated diamond pearls wire can be effectively used in all type of stone, even the most hard and abrasive ones. The life time of the impregnated diamond wire is usually twice as long compared to that of the electroplated diamond wire. The cutting speed of the sintered diamond wire requires a minimum power and a normal amount of cooling water, from 7 l/min up to 8 l/min (Careddu et al., 2019) depending mainly upon the cut area.

The diameter of the cable and diamond beads varies by manufacturers and by cutting materials. For Co.Fi.Plast Wires the diameters of the beads can be 6.3 mm, 7.3 mm, 8.3 mm, 9.3 mm, 10.3 mm, 11.3 mm whit number of beads per wire from 36 to 40. This choice is important on the quality of the cut. Some type of diamond wire are plasticated wire (***Figure 23***), springs and spacers are replaced by sheath of thermoplastic resins injected at high pressure. In other type rubber replaces the plastic resins. This plasticated wires increase the life time of the diamond wire parts and improving safety conditions. For cutting granite and hard rocks the type of wires used are plasticated.

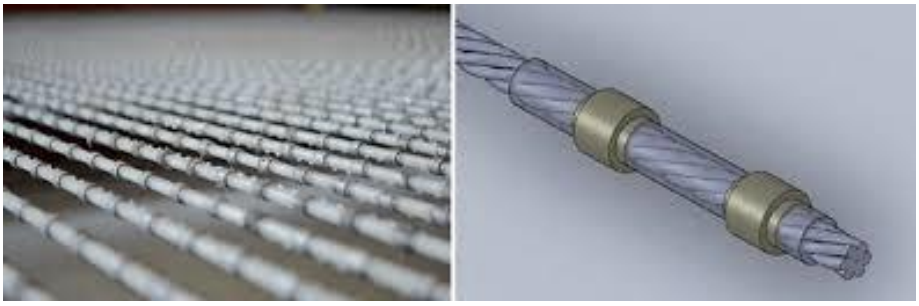

*Figure 23:Plasticated diamond wire. (Source: Co.Fi.Plast Wires).*

## 2.3.1 Metal composition of diamond wire

The metal composition of the diamond wire segments varies by manufacturer. The spacers between the diamond segments can be made of steel, copper or plastic, depending on the abrasiveness of the sawn material. What most interests this study is the composition of the segments, then the metal matrix in which the synthetic diamonds are immersed.

According to the study of M. Filgueira and D. G. Pinatti in 2003, the selection of the metal matrix is mainly based on the abrasion of the cut material. Therefore, for very abrasive materials such as gneiss, alloys SiC, Si3N4, Al2O3, and tungsten will be used. Co-based alloys are used for abrasive materials such as granite. Bronze and cobalt alloys are instead used for less abrasive rocks and marble. L.J. De Oliveira et al.(2007), claims that WC (tungsten carbide) in the percentage of 0.5 - 2% and with a size of 5 microns increases the wear resistance of the matrix, thus controlling the metal mass loss of the matrix due to abrasion;

while the Si if added in the matrix to about 2%, leads to an increase in the adhesion of the metal bond (matrix) with the diamond crystals as well with consequent increase of the retention of the diamond, avoiding the premature diamond pull out. Currently, most diamond cutting tools employ Co in the matrix, but due to the high cost it is often replaced by Ni.

In ***Table 13*** are reported some of the compositions of the metal matrix of the diamond wires.

| matrix composition [%] | Ni | Cu | Fe | Sn | Co | FeCr | C | O | N | Ta | W | Mo | Ti | Ag |
|---|---|---|---|---|---|---|---|---|---|---|---|---|---|---|
| **Niobium [wt%]** | | | 2.78 | | | | 10.52 | 6.31 | 5.26 | 57.8 | 10.5 | 4.73 | 2.1 | |
| **Copper [wt%]** | | | 22.3 | | | | 22.2 | 22.2 | | | | | | 33.3 |
| **Bronze [wt%]** | | | 0.18 | 99.1 | | | 0.27 | 0.36 | 0.09 | | | | | |
| **Ni Cu Fe** | 59 | 35 | 6 | | | | | | | | | | | |
| **Ni Cu Sn Fe** | 55 | 33 | 5.5 | 6.5 | | | | | | | | | | |
| **Cu Co Fe** | | 61 | 19 | | 20 | | | | | | | | | |
| **Cu Co Fe Sn** | | 55 | 17 | 10 | 18 | | | | | | | | | |
| **Co Sn** | | | | 11 | 89 | | | | | | | | | |
| **Fe FeCr** | | | 77 | | | 23 | | | | | | | | |
| **Fe FeCr Sn** | | | 68 | 12 | | 20 | | | | | | | | |

*Table 13: Chemical compositions of some of the metal matrices used for diamond tools. (sources: M.Filgueira and D.G. Pinatti, 2003; J. Kenda and J. Kopac, 2009; L.J. De Oliveira et al., 2007).*

The commercial metal matrix with Co and WC are more resistance from wear. The matrix with addition of SiC particles have a good resistance form wear but present problem of graphitization due to the iron attack. A coating with Ti protects the diamond from this phenomena and improves adhesion with metal matrix.

# 2.4 Sludge production and management

The European Community's policy (Directive 2006/21/CE of 15 March 2006) regarding the management of waste from stone processing is to minimize waste generated by optimizing the stone processes, reducing potential soil contamination, preventing the transport of hazardous waste, reducing the energy consumed and reducing the costs of management related to waste products.

The main problems related to the management of sawing sludge depends on the chemical-physical characteristics of this waste. The two main characteristics that are considered for the disposal of the sawing sludge are the presence of heavy metals and the very fine particle size distribution. These aspects involves in high costs for manufacturing companies, but also environmental disadvantages related to both temporary storage and landfilling. The landfill is a cost that depends both on the purchase and management costs of the filter press, on the transport of the material and on the quantity of the same.

Most companies that produce this waste currently use the filter press, to

recycle the water needed to cool the tools and to obtain a sludge with a maximum of 20-30% of humidity in order to transport it more easily to the landfill.

## 2.4.1 Filterpress system

The filter press is an automatic cycle machine for the dehydration of sludge coming from the marble and granite sawmills. The sludge filtration system allows to obtain cakes of filtered material of considerable compactness, easily removable and storable. The cycle, shown in ***Figure 24***, takes place in the follows steps:

1. The sludge pump raises the turbid waters affluent from the sawmill (***Figure 24*** - A) and carries them to the static type settler (***Figure 24*** - C). During this process the turbid water receives a dosage of flocculant solution appropriately prepared in the tank (***Figure 24*** - B).

2. depending on the water flow, the metering pump injects the flocculant amount needed for the flocculation process. The flocculants normally used are polyacrylamide, cationic type, low charge density, high molecular weight, recommended concentration 4g / l, to be injected into the turbid water sent to the decanter. They do not present environmental problems, as they are flocculants used also for the treatment of drinking water

3. the waste water enters the settler through the internal cylindrical channel. The sludge settles on the bottom cone, while the clear water goes up the cylindrical body and overflows into the weir, from which recirculated to the sawmill (***Figure 24*** - G).

4. the sludge is extracted by gravity in a discontinuous way by means of the automatic discharge valve (***Figure 24*** - D). The sludge is collected into the filter for dehydration by means of the pump (***Figure 24*** - E and F).

The waters are mostly recovered and re-introduced in the cutting cycle (***Figure 24*** - G).

At the end of the dehydration cycle, the sludge is about 30% humidity (***Figure 24*** - F).

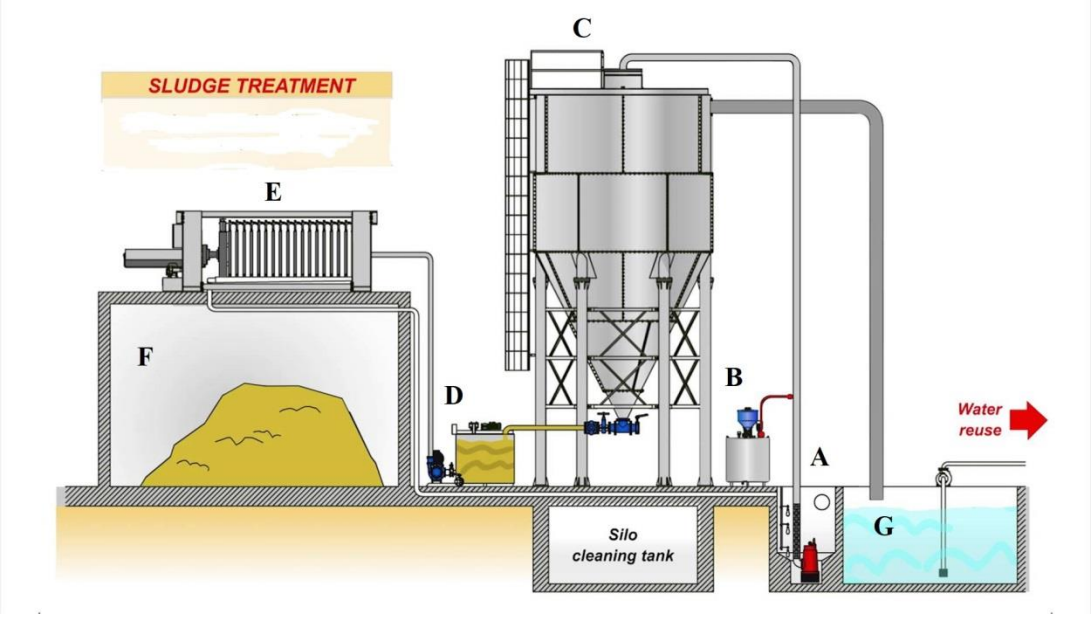


*Figure 24: Filterpress cycle for sludge dehydratation and water recovery. A) filling of turbid water well; B) flocculant station pump; C) static settling tank for clarification water; D) discharge valves and tank filling; E) filterpress; F) sludge storage with 30% of umidity; G) tank for clear water reuse. (source: Omec depurazione)*

*Figure 25: Internal view of a tank for a filter press system*

The advantages of this procedure are the less cost for sludge disposal due to less volume to treat, recovery of water up to 98% and sludge dehydration up to 85%.

# Chapter 3

# 3. Quality and quantity sludge production study.

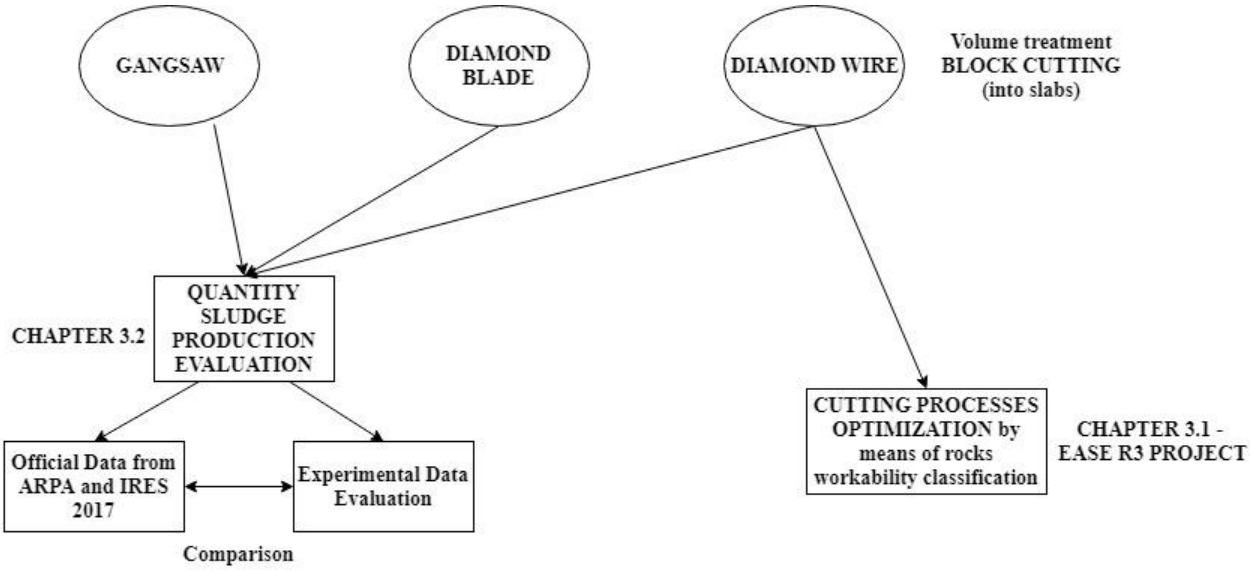


*Figure 26: Sawing sludge quantification and workability classification flowchart.*

# 3.1 Rocks workability classification for cutting optimization (EASE R3 European Project)

This research has been developed within the European Project EASE - R3 under the Seventh Framework Programme with grant agreement no. 608771. It's aimed at developing a novel integrated framework for a cost-effective and easy Repair, Renovation and Re-use of machine tools in modern factories , oriented towards both SME and OEM/end-users, and covering the entire life cycle of the system, from the design stage through the operative life (Bellopede et al., 2015).

This chapter is a deepening of the stone-cutting tools interaction, mainly diamond wires. The prediction stone – diamond wire interaction is important for mining sector both to avoid dangerous and expensive endeavours of cutting when

an unknown stone has to be introduced in the plant, and to predict tools wear. Optimize the cut for obtaining sawing sludge with a minimum metal concentration is an important issue. This work has focused only on one of the cutting technologies, diamond wire, but can also be extended to other technologies. Appropriate use of cutting technologies increases tool life, consequently reducing working time, substitution costs and improving the quality of waste obtained.

Nowadays, there are many studies on the efficiency of diamond wire cutting of soft rocks. Yilmazkaya and Ozcelik (2015) determined the optimum working conditions for a marble sample in terms of cutting performance parameters including unit wear and cutting rate and the development of cuttability charts with respect to cutting performance parameters. It is fundamental to identify the parameters that most affect cutting operations. These parameters refer one to the stone properties (petrographic and mineralogical composition, grain size, water content, weathering, discontinuities/anisotropy and hardness), others to the diamond wire (size and number of beads, cutting speed, feed rate and specific energy.

Yurdakul et al. (2014) studied the prediction of specific energy in natural stone cutting processes by a neuro-fuzzy methodology, on the base of deep of cut, feed rate and uniaxial compressive strength measurements.

Tuğrul and Zarif (1999) revealed the significant influence of textural features on the engineering properties, such as the type of contact between grains and the mineral shape and size, based on mineralogical analysis. According to Ersoy and Atici (2005), the cuttability of rocks cannot be defined adequately by a single index or a single test. They found a correlation between the textural, physical and mechanical properties of rocks and the specific cutting energy of the saw. In order to predict the workability mechanism of a rock, it must be considered in which parameters are connected with the diamond wire work. The diamond thread tension creates a reaction on the surface, which in turn causes abrasive actions between the bead and the stone material. The cutting mechanism is due to the dragging of the wire and to the force pressing the diamond beads onto the stone surface. In a recent study on the wear performance of saw blades in the processing of granitic rocks, Aydin et al. (2013) claimed that micro-hardness to be the dominant property affecting wear and that higher percentages of quartz and alkali feldspar make cutting more difficult and increase saw blade wear. However, until now the only classification used for stone cutting classes refers only to the commercial name of the rock (Confindustria Marmomacchine, 2014), not based on their petrographic characteristics. A method to use before the cutting should be useful to optimize the cutting operation with the connected problems of diamond wire wear.

The aim of this study is to find an inexpensive and simple method to predict cuttability prior to cutting, and to predict the wear of tools and consequent production of sludge with less content of metals.

For the research EASE $R^3$ Project, we choose 7 different silicate stones, to

better understand the different behavior of the cutting tools. All the stones studied are Piedmont silicate rocks and granite cutted in Piedmont but of Sardinia origin.

The following investigations were carried out:

- Petrographic analysis of the mineralogical composition, crystal size, fabric and texture;
- Determination of the physical and mechanical properties by means of micro-hardness tests with the Knoop method and ultrasonic pulse velocity measurements in situ on the block and in lab on slabs.

The decision to use the Knoop hardness test is based on its accuracy: the simply identification of hardness by means of Mohs scale, for example, does not indicate the exact hardness. Other scratch tests, however, are not suitable for this purpose because they do not consider and assess the properties of the rock, but they evaluate the wear of the tool used to cut, which is not the aim of the research. The Knoop method represents the real estimation of the material hardness and can thus provide better characterization of the rock. Ultrasonic techniques can be applied for qualitative and quantitative evaluation of the physical and elastic properties of materials.

## 3.1.1 Methodologies for determining stone characteristics

### 3.1.1.1 Petrographic study

The petrographic features (mineralogical and textural characteristics of the stone tested) were determined by thin section observation by optical microscope. The ***Table 14*** shows the mineralogical petrographic characteristics of the stones considered in the study.

| Stone trade name, macroscopic and microscopic photo photo | Rock type description | Petrographic classification | Acronym | Mineralogical composition | Grain size |
|---|---|---|---|---|---|
| **SERIZZO ANTIGORIO**  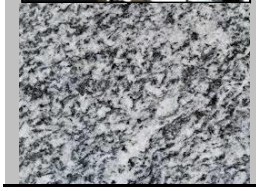 | Paragneiss with a homogeneous medium grain and dark grey colour due to the presence of a considerable quantity of mica biotite. Evident foliation | Gneiss | SER | Quartz: 30%; Plagioclase:25%Ortoclase: 26%; Biotite: 10%; Muscovite: 5%; Epidote: 3%; Accessory: 1%. | 0.5-2mm |

| | | | | | |
|---|---|---|---|---|---|
| **MONTORFANO** 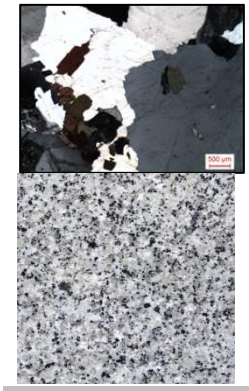 | Granite medium to large grained homogeneous, of uniform light colour due to the white colour of the feldspars and the scarcity of biotite. | Granite | MON | Quartz: 40%; Plagioclase:20%Orthoclase: 35%Biotite: 5%. | 0.5 - 3 mm |
| **LUSERNA** 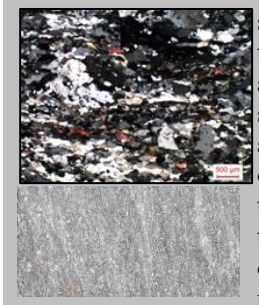 | Gneiss characterized by a flat-schistose texture and by a heteroblastic structure with a micro-occhiadine tendency due to the presence of millimetric micro-porphyroblasts . | Gneiss | LUS | Quartz: 50%; Plagioclase:15%; Alkaline Feldspar: 20%; White mica: 5%; Chlorite: 5%; Epidote: 5%. | 0.03-3 mm |
| **WHITE BEOLA** 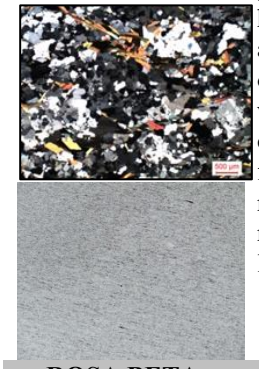 | Very fine grained, homogeneous aplitic orthogneiss, white in colour; evident foliation and moderate mineralogical lineation. | Gneiss | BEO | Quartz: 30%; Plagioclase:15%Alkaline Feldspar: 34%; Biotite: 5%; Muscovite:14%; Accessory: 2%. | 0.02-1 mm |
| **ROSA BETA** 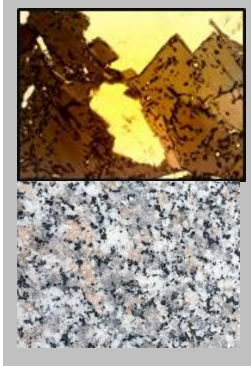 | Granite - holocrystalline rock, with a medium grain centimetric crystals of quartz, plagioclase (milky white) and K-feldspar; associated with crystals of much smaller size biotite (black polished). | Granite | RBE | Plagioclase 25%Feldspar 30%Quartz 35% | 0.05 - 12 mm |

| | | | | | |
|---|---|---|---|---|---|
| **SIENITE** 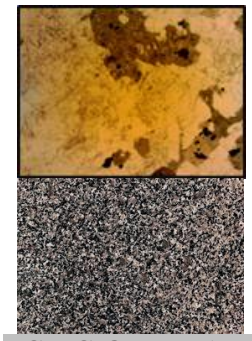 | Medium-fine grained quartz syenite, grey purplish-brown coloured isotropic fabric | Sienite | SIE | K-feldspar 50% Quartz 10% Hornblende 25% Biotite-pyroxene 5% Opaque and accessory minerals 10% | 0.03 - 2 mm |
| **GRIGIO PERLA** 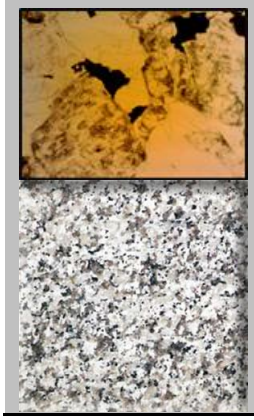 | Granite-holocrystalline rock, with a medium grain centimetric crystals of plagioclase (milky white), and quartz; associated with crystals of much smaller size biotite (black polished). | Granite | GRP | K- Feldspar + Plagioclase 65%Quartz 30%biotie + pyroxene 5% | 0.1 - 12 mm |

*Table 14: Petrographic and mineralogic description of the stone processed in Piedmont Region.*

### 3.1.1.2 Knoop Microhardness

The definition of hardness of a material can be defined also as its resistance to the superficial penetration of an identifier. It is possible to assert the hardness is one of the main mechanical parameters normally measured in the materials. The inelastic deformation process is intrinsically related to the resistance of a material to such deformation. Microhardness is the dominant property affecting wear of cutting tools, the use of this measurements has been discussed in several literatures work (Cardu et al. (1996), Amaral et al. (1999), Ersoy and Atici (2005), Aydin et al. (2013), and Agus et al. (2003).).

Microhardness of the tested stone materials was perfomed using a Leiz Knoop microdurimeter, consisting of a table for specimens, an interchangeable indenter with a mechanism for the gradual application of the load and hoisting penetration and by a microscope with a micrometer to measure the indentation.

Among the different types of microhardness indenter, the Knoop type, developed by the National Bureau of Standards in 1939 for tests on glass and ceramics, is considered the most suitable for rocks, because it produces sharper indentations in materials with fragile behaviour and provides a footprint, that is easier to read and to measure than those obtained with other indenters (Vickers, Brinell etc.). This methodology was standardized in the EN 14205: 2003 “Natural stone test methods - Determination of Knoop hardness” (now withdrawn) and in the ASTM E384: 2011 “Standard Test Method for Knoop and Vickers Hardness

of Materials".

The Knoop indenter produces a rhombic elongated indentation (***Figure 27***), which is measured along the longest diagonal.

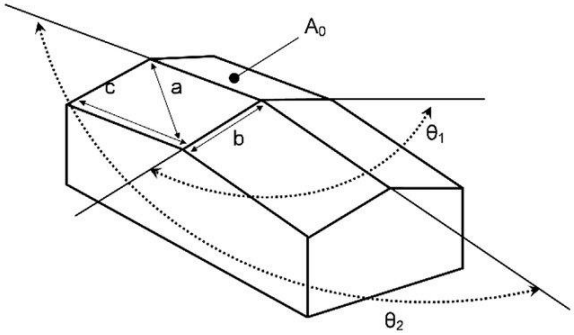


*Figure 27: Geometry of Knoop indenter. (Source: Ghorbal, G. B et al., 2017).*

During this test, a pyramidal diamond point is pressed into the polished surface of the test material with a known load, for a specified dwell time (40 s) and the resulting indentation is measured using a microscope. The (Hardness Knoop) HK index is given by equation [1]:

$$HK = \frac{P}{Cp\ L^2} \qquad [1]$$

where:

L = length of indentation along its long axis (mm);

Cp = correction factor related to the shape of the indenter, which is ideally 0.070279;

P = load (1,961 N as specified by standard EN 14205).

Knoop test was performed on three samples for each material and for each sample the cumulative frequency curve of 40 micro-hardness Knoop measurements was plotted and the mean value and quartile percentage on the diagram were calculated (***Figure 28***).

The hardness values are arranged in increasing order and are plotted against the order of rank. The y scale is graduated in percentages and it gives the diagram of the cumulative frequency of the micro-hardness values of the stone (hardness distribution diagram). The test results are expressed through the characteristic values of the diagram, that is, those corresponding to the values of 25% (HK25, lower quartile), 50% (HK50, median value) and 75% (HK75, upper quartile) cumulative frequencies, shown an example in ***Figure 28***). The HK75 / HK25 ratio is considered as the inhomogeneity value of the rock (Zichella et al. 2017).

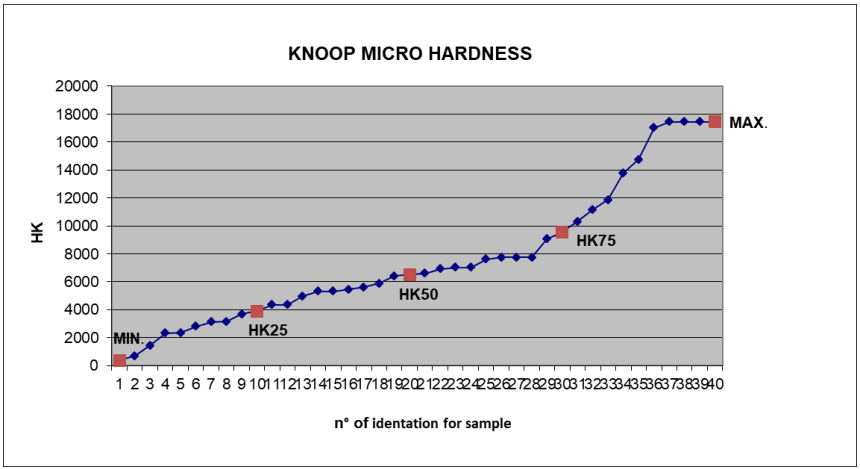


*Figure 28: Example of the micro-hardness Knoop measurements*

Many studies in literature recognize the presence of quartz and feldspars as the dominant factor that most influences the cut. Buyuksagis, in 2007, stated that the quartz most influences the wear of cutting tools. In 2002 and 2011 Ozcelik et al., in an experimental work with multiple linear regression analysis, indicated the flexural strength and the plagioclase percentage of granites as the most dominant rock properties that influenced the cutting process. An assessment of the workability can be derived from the rock hardness diagram (***Figure 28***). For this purpose, it is necessary to establish the characteristic values: HK25, HK50 and HK75 of the hardness diagrams, which can be considered as workability indicators.

However, micro-hardness alone is not enough to evaluate the workability of the rock. This is the reason why we chose to combine this analysis with ultrasound pulse velocity.

### 3.1.1.3 Ultrasound pulse velocity

The ultrasound pulse velocity passing through a solid material is directly correlated to the physical-mechanical properties of the material, density and elastic properties. Goodman, in 1989 and Tugrul et al. in 1999, observed that the speed of the ultrasonic waves increases as the mechanical strength, density and elastic modulus of the materials increase. Vasanelli et al in 2015, used the ultrasound speed velocity for evaluate stone building degradation. They asserted that the UPV is well correlated with the compressive strenght.

The ultrasonic pulse velocity (UPV) can be used to indicate the quality of the rocks and to determine its elastic properties and detect its anisotropy, important factor that affect and influence the cutting process.

UPV was determined using a Portable Ultrasonic Nondestructive Digital Indicating Tester (PUNDIT PL-200 of PROCEQ), with transducer of 33 kHz. Measurements were made using the indirect method by placing transmitter transducer in a fixed point and the receiver one at progressive distances on the same specimen surface. The measurements in lab on slabs were carried out at

25mm, 50mm, 75mm, 90mm transducers distance, up to 175mm (in the seventh point). In ***Figure 29*** is shown the methodology used in lab. In ***Figure 30*** and ***Figure 31*** is shown the measure methodology used in situ on the block. The measurements in this case are carried out in two direction, perpendicular to each other. The choice of punctual transducers was made to have a good coupling with stone surface. This method is influenced by the superficial finish of the material. The surface of the sample must be clean, polished and sufficiently flat.

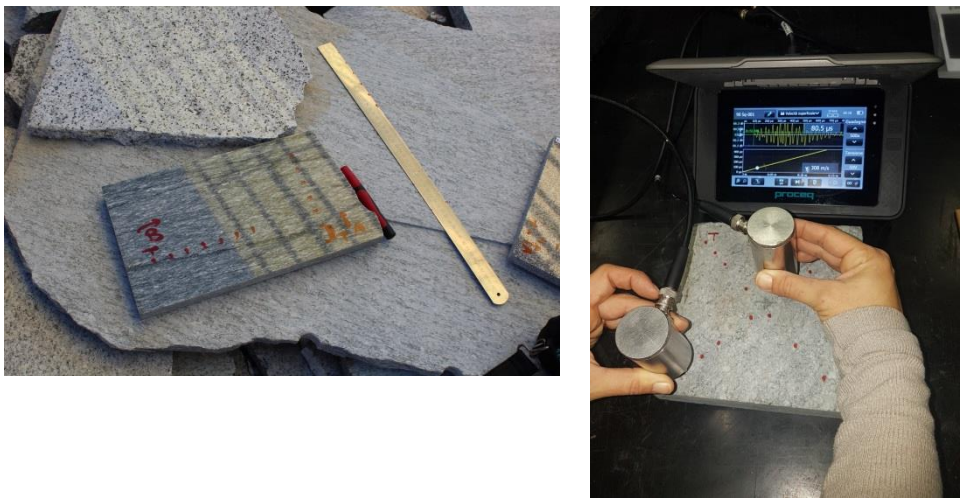

*Figure 29: Ultrasound Pulse Velocity measurements in lab on slabs.*


*Figure 30: Ultrasound Pulse Velocity measurements in situ on blocks.*

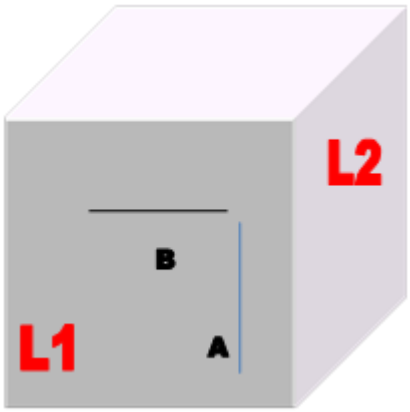


Legend:

L1: Face parallel to the drill holes

L2: Face perpendicular to the drill holes

A and B: Lines followed for UPV

*Figure 31: General scheme of the measurements carried out on the blocks.(source: Bellopede et al., 2015)*

On the transducers is applied water based gel in order to avoid the interposition of air and to improve the contact among transducers and stone surface. The indirect method has been chosen for its possible repeatability directly in the front of quarry. The direct method was also tested both in the field and in the laboratory, but not good results are obtained. The waves transmitted by the transmitting transducer cannot be received by the receiving transducer. The choice of the type of transducers (33 kHz) was carried out because on the quarry front the material is never perfectly flat and therefore the measurements with the flat transducers would have been influenced by this factor.

## 3.1.2 Assessment of the sludge quality through the stone cutting classification

One of the main purposes of this part of the work is to confirm and evaluate the mechanical properties of the stones both to increase the productivity and efficiency of work in the quarry and in the plant, and to quantify the production and quality of the waste sludge produced. The current economic needs of the companies that produce and use the tools, have strengthened the importance of performing new methodologies of materials characterization capable of interpreting the workability of the cutting stones. Currently this stone workability classification is determined by the users of the cutting machines, according to their experience. In Zichella et al. 2016 work was presented on 18 different types of stone, on which good workability correlations were provided with the industrial classification. The following paragraphs show the results of some of these analyzed stones (cut in the plants taken into account in this study), of interest for this PhD thesis.

### 3.1.2.1 Determination of Knoop Micro-Hardness

In this section the results of the Knoop microhardness test for each stone analyzed are reported (***Table 15***).

As already mentioned in paragraph 3.1.1.2, 3 polished sections were carried out per sample and the measures taken were 40 measures per polish section. The average results obtained on the 3 samples are shown in the *Table **15***.

| Rock Acronym | Knoop HK25 | Knoop HK50 | Knoop HK75 | Knoop HK75/HK25 |
|---|---|---|---|---|
| **SER** | 2109 | 4358 | 6704 | 3.2 |
| **MON** | 2789 | 4358 | 6917 | 2.5 |
| **LUS** | 4358 | 6601 | 7747 | 1.8 |
| **BEO** | 3521 | 4358 | 6735 | 1.9 |
| **RBE** | 4049 | 6032 | 7747 | 1,9 |
| **SIE** | 3602 | 4829 | 6032 | 1,7 |
| **RGP** | 5234 | 6501 | 9744 | 1,9 |

*Table 15: Knoop Micro-hardness results on seven stones tested.*

All the characteristic values of Knoop (HK25, HK50, HK75, HK75 / 25) were calculated for all stones, but only the HK25 indicator showed a good correlation (R = 0.6834) with the Industrial Workability Classification (IWC). IWC is an empirical classification, used by process stone plants, that takes into account the ease of stone cutting. The ***Table 16*** shows the industrial classification of the stones investigated and the ***Figure 32*** shows the correlation between IWC and Knoop value.

| Rock acronym | IWC classes |
|---|---|
| **SER** | 2 |
| **MON** | 3 |
| **LUS** | 3 |
| **BEO** | 3 |
| **RBE** | 4 |
| **SIE** | 3 |
| **RGP** | 4 |

*Table 16: Industrial Workability Classification (IWC) of the seven stones tested. (source: Confindustria Marmomacchine, 2014).*

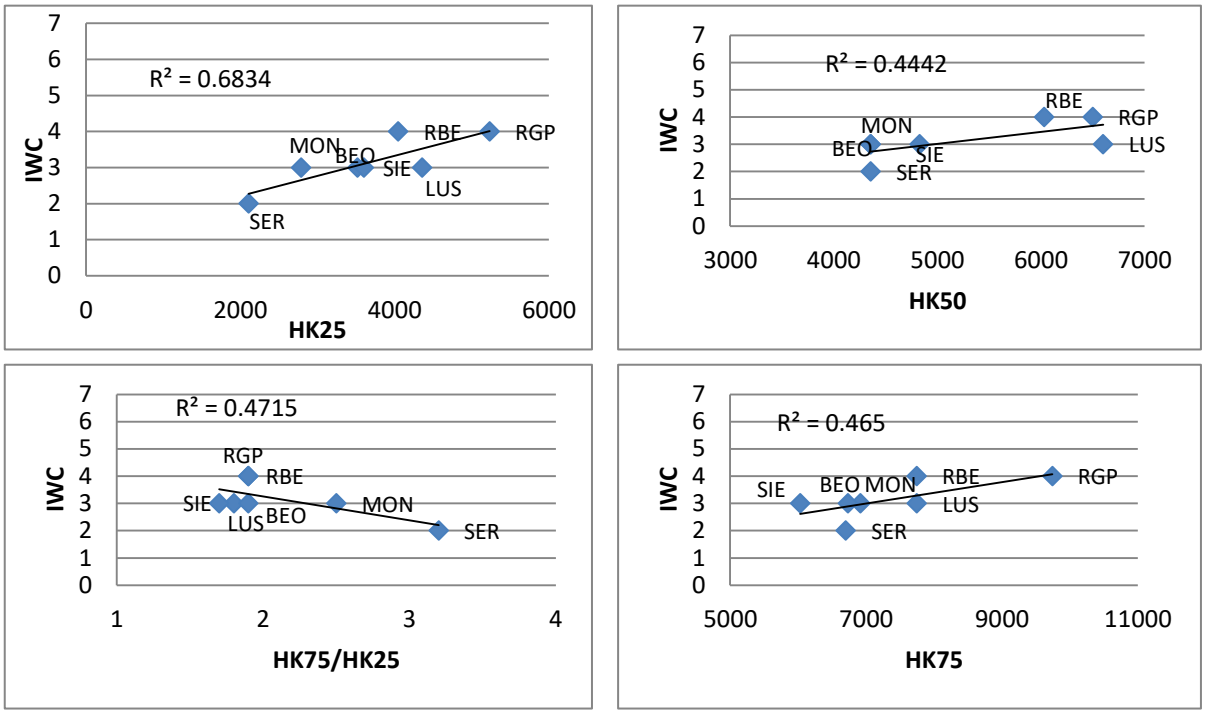


*Figure 32: Correlation between Knoop value and IWC. HK25 show the best correlation with IWC classes with R=0.8266.*

The micro-hardness data well represent the abrasion resistance of the minerals in contact with the cutting tools. The HK 25 represents the hardness of softer and medium minerals, that influence more the workability of the rock, as points of weakness during the cutting step.

### 3.1.2.2 Determination of Ultrasound Pulse Velocity

The ultrasound pulse velocity is a test method strictly connected with the physical-mechanical properties of the stones. In literature there are several studies on the evaluation of the physical-mechanical properties of stones through UPV test. Concu et al. 2014, Vasconcelos et al. 2008 and Selçuk & Nar 2015 have found a direct correlation between the UPV results and porosity, compressive strength and flexural strength of the stones. As specified in paragraph 3.1.1.3, the test was performed in both directions parallel and perpendicular to the stone scistosity using the indirect method. It was also performed both in laboratory on slabs and in situ on blocks. The results obtained are shown in the ***Table 17***.

| Rock Acronym | UPV indirect method on block direction B | UPV indirect method on block direction A | UPV indirect method on slab direction B | UPV indirect method on slab direction A |
|---|---|---|---|---|
| **SER** | 1801 | 1801 | 1927 | 1737 |
| **MON** | 1714 | 1752 | 1628 | 1704 |
| **LUS** | 2024 | 2154 | 2230 | 1756 |
| **BEO** | 2257 | 2314 | 2269 | 2321 |
| **RBE** | 2387 | 2310 | 2754 | 2430 |
| **SIE** | 2482 | 2172 | 2449 | 2299 |
| **RGP** | 2601 | 2510 | 2785 | 2780 |

*Table 17: UPV measures in indirect method on slabs and block in two direction parallel and perpendicular to the scistosity.*

In ***Figure 33*** the correlation found between IWC and UPV value (as an average of the values obtained from lab and in-situ tests in both directions) is shown.

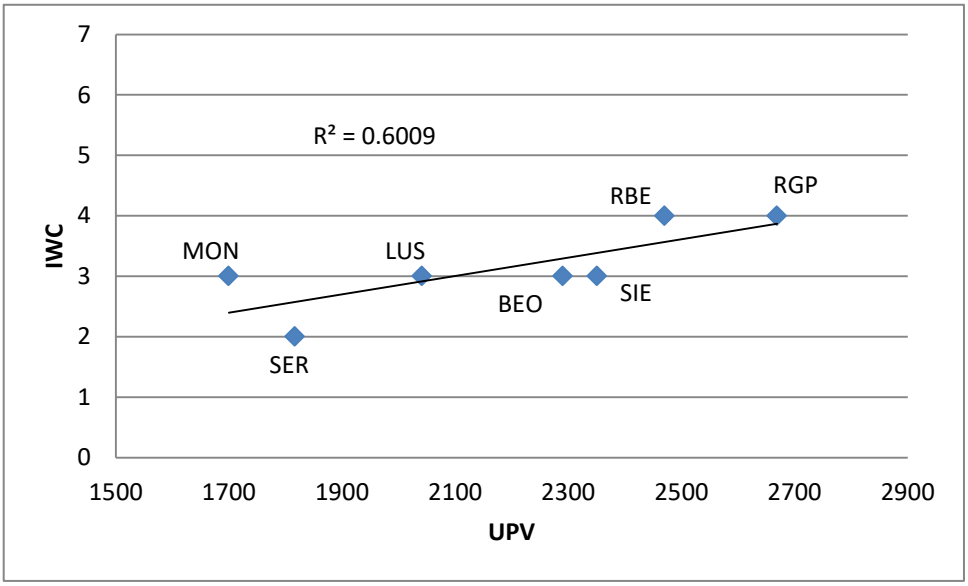


*Figure 33:Correlation between UPV measures and IWC.*

## 3.1.2.3 Stone Workability Classification

From a study conducted by Spriano et al. 2015, it was found that the interaction between stone and diamond tools depends and is a function of the stone hardness class. It has also been found that the presence of rocks with a high concentration of iron-based minerals react with the diamond tool, causing premature wear compared to other types of stones, due to the adhesion phenomenon. It is therefore important both the mineralogical aspect and the fabric

and texture of the cutting rock to understand the quality of sludge obtained (more or less concentration metals in the sludge obtained due to the wear of the cutting tools used).

In a previous study (Zichella et al., 2017) conducted on 18 different stones, comparing the quartz content with the IWC classification, it was assert that the wear mechanism of the diamond tools is not only influenced by the content of quartz. For this reason, we consider both the compactness of the material, evaluated by the UPV and the presence of grains/soft elements, to greatly influence the workability of the material. As stated by Agus et al. (2003), also the grain size play an important role in the workability of material, aspect considered with UPV test.

In order to predict stone workability, seven classes were drawn along the correlation line between UPV and HK25 measurements of the different types of stone (from 1 (easier to cut rocks) to 7 (harder to cut rocks)), according to a previous study of Zichella et al, 2017.

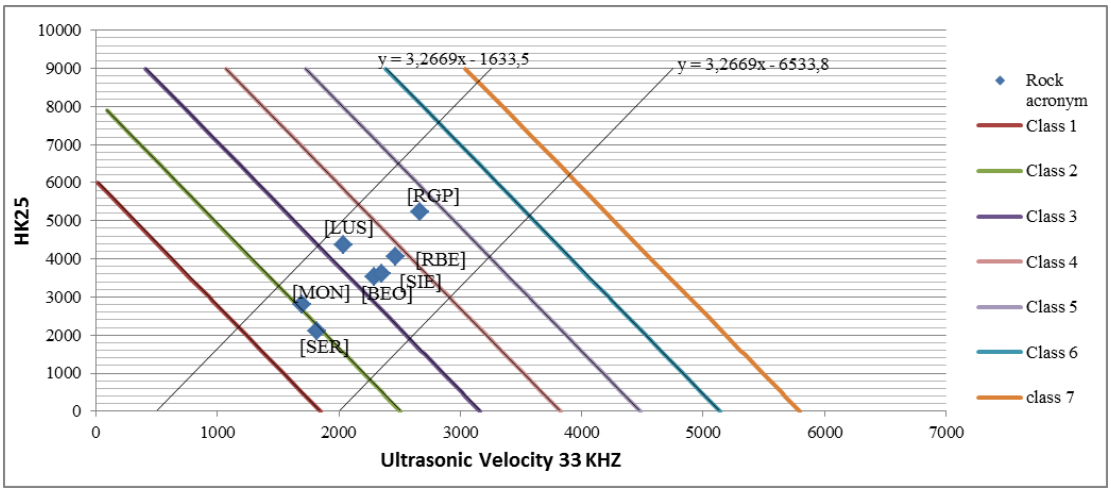


*Figure 34: Rock classification with UPV and HK25.According to Zichella et al., 2017 classification on 18 stones.*

***Figure 34*** show the classification of the seven stones tested, according to the graph construction of the previous study (Zichella et al. 2017).

The equation of rocks trend line, based on 18 different stones is [2]:

$$Y = 3.2669 * X - 4095.7 \text{ [2]}$$

Taking into account the minimum and maximum UPV and HK25 values from experimental results two lines that define the maximum HK25-UPV areas were traced with a distance between them of about 2450 (***Figure 34***). The construction of these lines demarcating the classes of workability was carried out on lines perpendicular to the trend line and separated from the same step. The ***Table 18*** shows the range of HK25 value in relation to the UPV measured on site and the minimum threshold lines for each class workability.

HK 25 range

| UPV VALUE (m/s) | CLASS 1 | CLASS 2 | CLASS 3 | CLASS 4 | CLASS 5 | CLASS 6 | CLASS 7 |
|---|---|---|---|---|---|---|---|
| 1500 | <3270 | n.p. | n.p. | n.p. | n.p. | n.p. | n.p. |
| 1830 | <1890 | >1890<4355 | n.p. | n.p. | n.p. | n.p. | n.p. |
| 2250 | =830 | >830 <3000 | >3000 <5700 | n.p. | n.p. | n.p. | n.p. |
| 2580 | n.p. | =1900 | >1900 <4340 | >4340 <7600 | n.p. | n.p. | n.p. |
| 2900 | n.p. | n.p. | =3000 | >3000 <5380 | >5380 <7840 | n.p. | n.p. |
| 3240 | n.p. | n.p. | n.p. | =4050 | >4050 <6490 | >6490 <8950 | n.p. |
| 3570 | n.p. | n.p. | n.p. | n.p. | =5130 | >5130 <7570 | >7570 |
| 3900 | n.p. | n.p. | n.p. | n.p. | n.p. | =6200 | >6200 |

*Table 18: HK25 range and UPV value. (source: Zichella et al., 2017).*

Below are shown the minimum threshold equation for classes [3][4][5][6][7][8][9]:

Eq. CLASS 1: $Y = -3{,}2669X + 6043{,}8$ [3]

Eq. CLASS 2: $Y = -3{,}2669X + 8193{,}4$ [4]

Eq. CLASS 3: $Y = -3{,}2669X + 10343$ [5]

Eq. CLASS 4: $Y = -3{,}2669X + 12493$ [6]

Eq. CLASS 5: $Y = -3{,}2669X + 14642$ [7]

Eq. CLASS 6: $Y = -3{,}2669X + 16792$ [8]

Eq. CLASS 7: $Y = -3{,}2669X + 18941$ [9]

Lines with a reverse slope respect the linear correlation between UPV and HK25, with the same distance each other, define 7 classes. In particular, while the IWC is characterized by nine classes, with the new technical classification the classes decrease to 7, reducing cases of overlapping and uncertainty due the intrinsic variability of the materials.

| ROCK ACRONYM | IWC | OBTAINED CLASS |
|---|---|---|
| **SER** | 2 | 1/2 |
| **MON** | 3 | 2 |
| **LUS** | 3 | 3 |
| **BEO** | 3 | 3 |
| **RBE** | 3 | 3 |
| **SIE** | 3 | 3 |
| **RGP** | 4 | 4 |

*Table 19: Comparison between IWC classification and the classes obtained by means of the scientific approach.*

In ***Table 19*** a comparison between IWC classification and the obtained class is reported. The results show a good classification with these two inexpensive and simple test to be performed before cutting to find a mechanism for cuttability prediction of the new stone and a prediction of the quality of sludge produced during processing stones. This method could be a good way to avoid dangerous and expensive endeavors of cutting when an unknown stone is introduced to a plant and to improve the management of sludge and related costs connected to a possible disposal or recovery.

# 3.2 Quantity sludge production study

The amount of sludge obtained from the processing of ornamental stones is important for the purposes of the following study. The feasibility of possible recoveries depend on the quantity of secondary raw materials involved.

Through statistic studies conducted by ARPA[2] and ISTAT[3] we are able to know which are the annual productions of quarried stone material and the annual quantities of sludge produced by the plants that processing stones. Data of the amount of sludge produced refer specifically to ISTAT 23701 code (sawing and processing of stones and marble), which is a sub-group of the CER code 010413. Data provided by ARPA of waste with CER codes 010413 includes other ISTAT codes, not taken into account in this study (08 other mining extraction activities from quarries and mines, 099 support activities for extraction from quarries and mines of other minerals, 23702 artistic processing of marble and other related stones , works in mosaic).

Data are related to a triennial period since 2014 to 2016. ***Figure 35*** shown the decreasing trend of active quarries on the territory, even if not so high, due to the economic sector crisis.

[2] Piedmont ARPA: Regional Agency for Environmental Protection.
[3] ISTAT: National Institute of Statistics

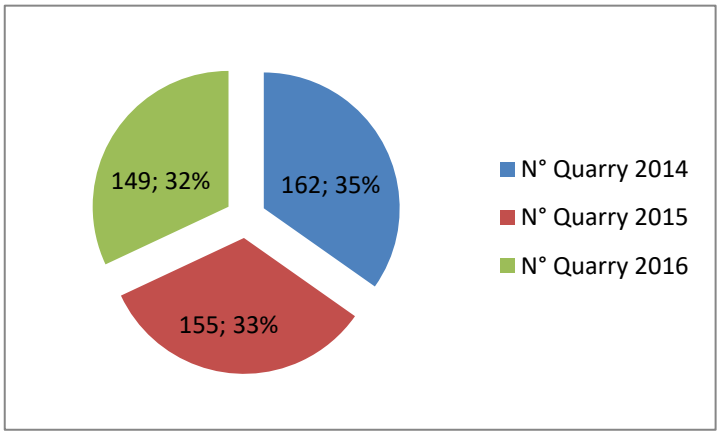


*Figure 35: Total number of active quarries from 2014 to 2016 in Piedmont Region. (Source: ARPA Piedmont).*

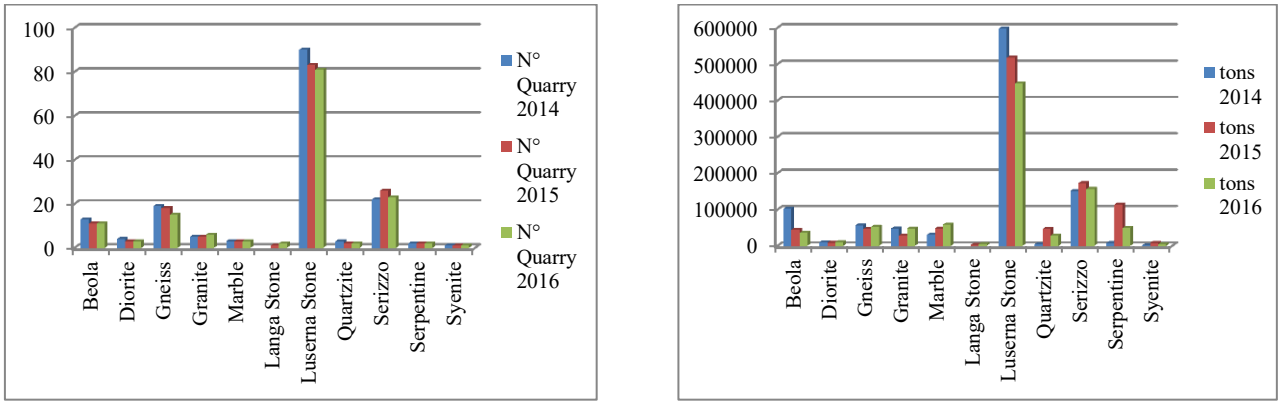


*Figure 36:Statistic on ornamental stone extraction for years 2014, 2015 and 2016 in Piedmont. Left: number of quarry for lithotype; Right: tons of extracted materials for lithotype. (Source: Piedmont ARPA)*

Considering the different lithotypes, it is possible to observe how the number of active quarries remains unchanged over the years from 2014 to 2016, except for Gneiss and Luserna stones which have a significant decrease and the Serizzo which sees an increase in the number of quarries in 2015, but then again a decrease in 2016 (***Figure 36*** *on left*). There is the same trend considering the tons extracted (***Figure 36*** *on right*).

As already mentioned in the first chapter most of the stones quarried and processed in Piedmont are Luserna, Gneiss, Beola and Serizzo, stones extracted in districts of Verbano, Cuneo and Torino. ***Figure 37*** shows the percentage of quarries in the Verbano (VB), Cuneo (CN) and Turin (TO) districts, compared to the other Piedmont districts in the years since 2014 to 2016. Minimum decrease of active quarries in the Cuneo and Turin districts (linked to the extraction of Luserna stone), and a small increase in active quarries in the Verbano district (linked to the extraction mainly of Serizzo and Beola) is shown.

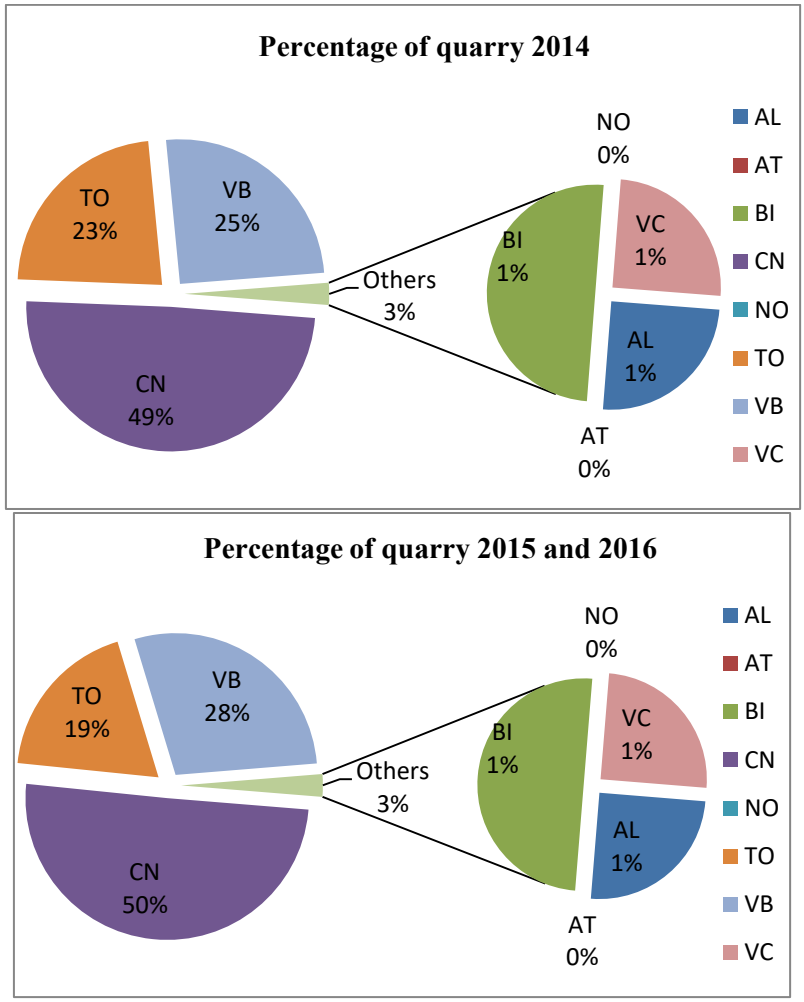


*Figure 37: Number of active quarry in each Piedmont districts. Above: Year 2014; Under: years 2015 and 2016. (Source: Piedmont ARPA)*

Analyzing in particular the individual districts, an increase in Luserna stone extraction can be observed, in Cuneo district, over the three year period (***Figure 38***). The extraction percentage of Luserna stone compared to other stones is significant.

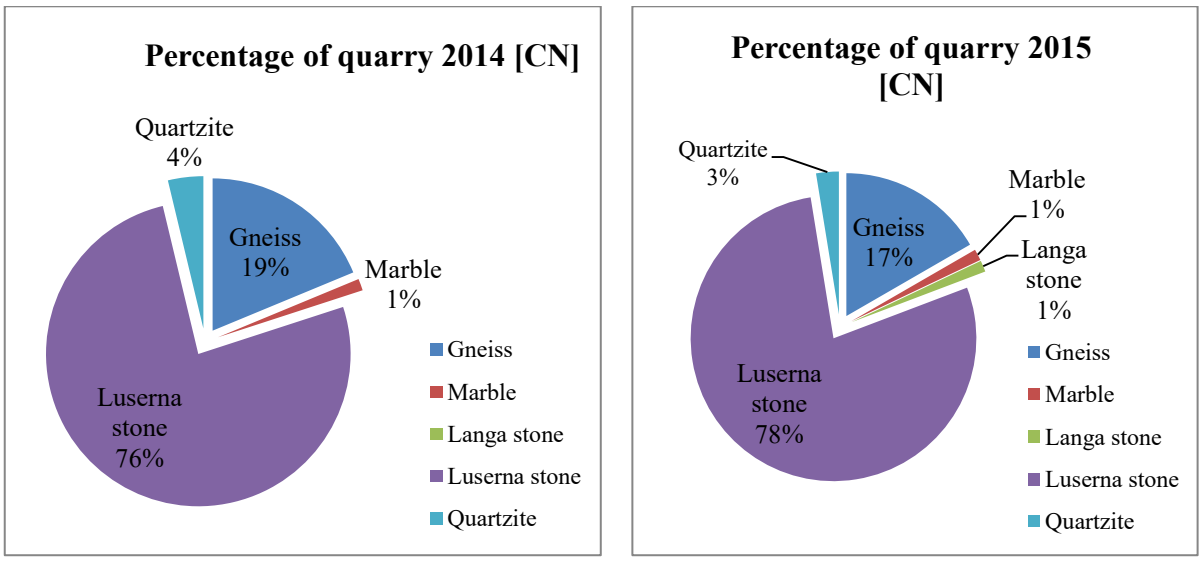

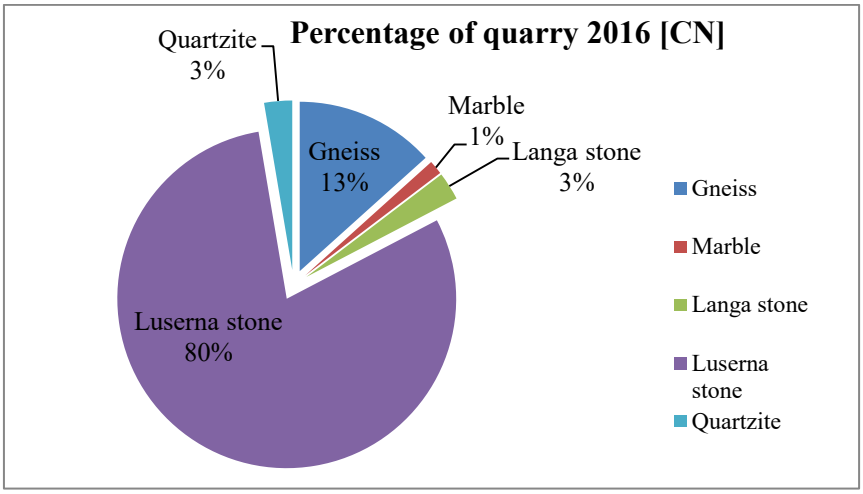


*Figure 38: Number of active quarries, divided for lithotype, in Cuneo district. Above: years 2014 and 2015; Under: year 2016. (Source: Piedmont ARPA).*

Torino district shows an inverse trend compared to Cuneo, with a decrease in the Luserna stone extraction (***Figure 39***). As for the district of Cuneo, Turin has a significant percentage of Luserna stone extraction compared to other types of stones.

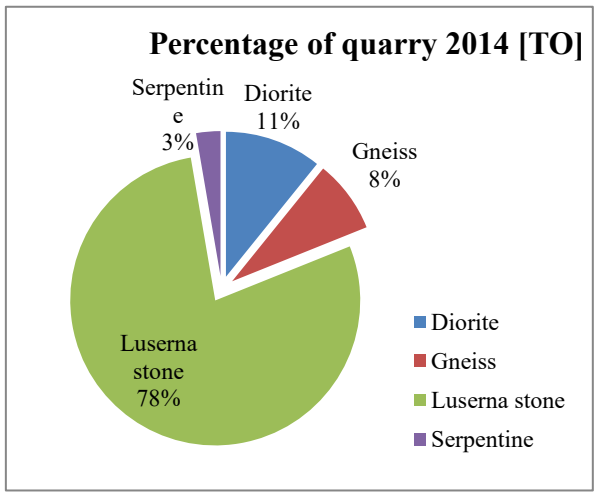


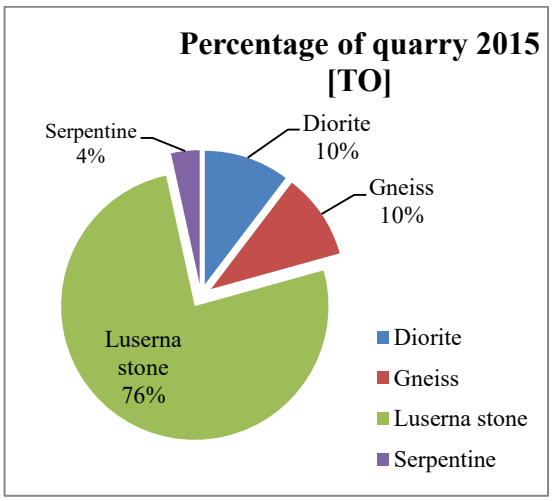

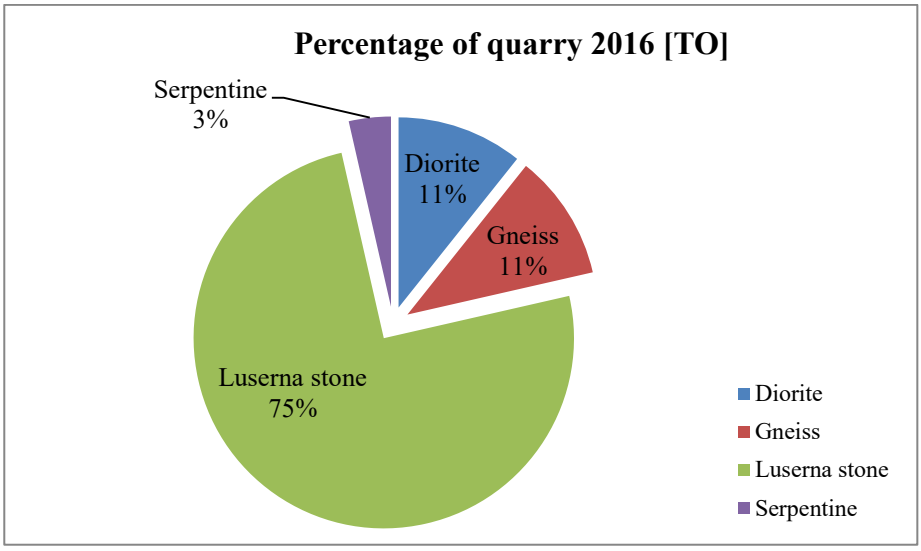


*Figure 39: Number of active quarries, divided for lithotype, in Torino district. Above: years 2014 and 2015; Under: year 2016. (Source: Piedmont ARPA).*

Verbano district show an increase of extraction in 2015 respect 2014, but a little decrease in 2016. Serizzo and Beola are the most extracted stones in this district (***Figure 40***).

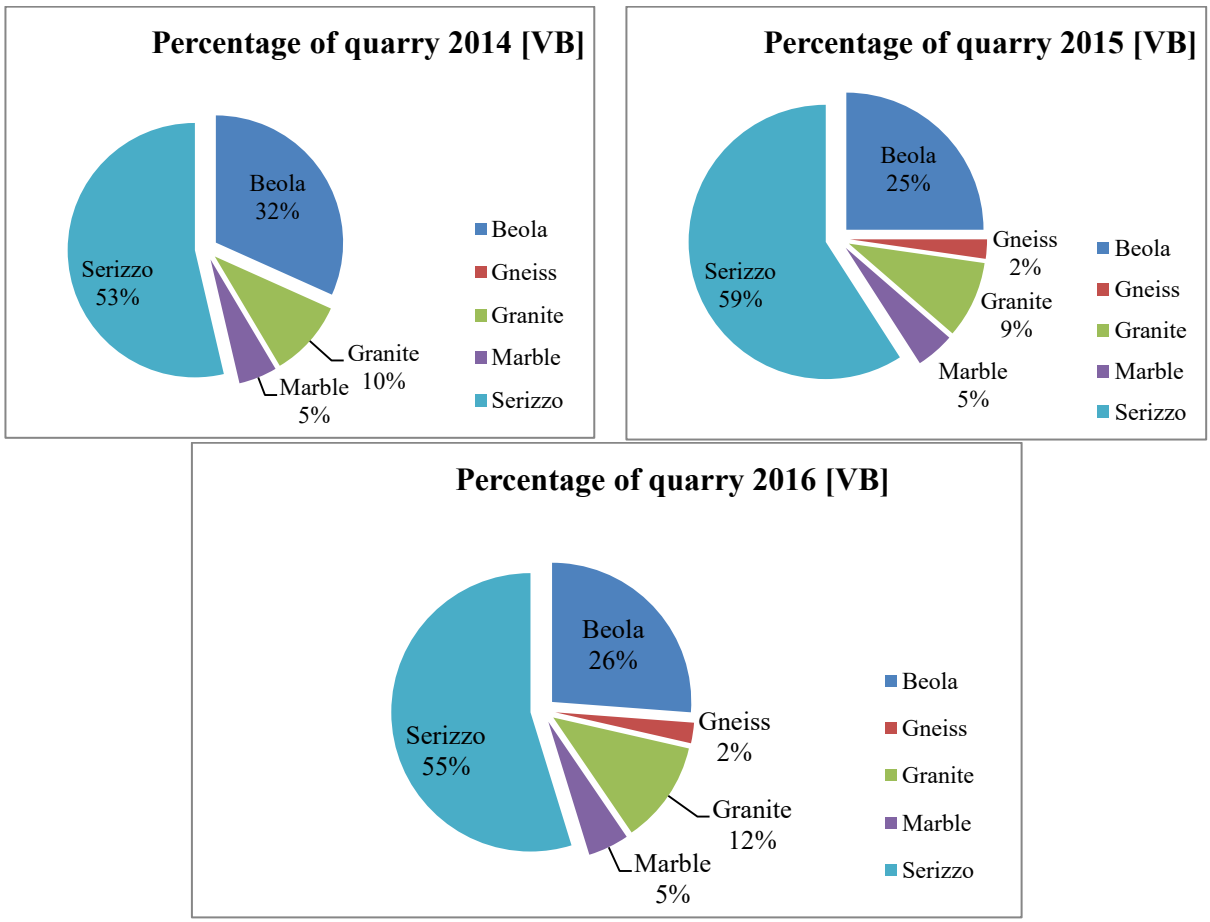


*Figure 40: Number of active quarries, divided for lithotype, in Verbano district. Above: years 2014 and 2015; Under: year 2016. (Source: Piedmont ARPA).*

The trends of the individual districts reflect the data obtained from the statistical analysis of the lithotypes of the Piedmont Region.

The plants processing and extracting ornamental stones produces processing waste. These processing waste are declared by MUD (Single Environmental Declaration Model)[4] to the Chamber of Commerce. In this context we want to compare the material extracted in each Piedmont district and the relative declared waste. ***Table 20*** shows tons of ornamental stone extracted and tons of sludge declared in each Piedmont district. The type of sludge considered in this case is only the waste with ISTAT 23701 code (sawing and processing of stones and marble).

| District | 2014 | | | 2015 | | | 2016 | | |
|---|---|---|---|---|---|---|---|---|---|
| | n° quarry | extracted tons | sludge tons | n° quarry | extracted tons | sludge tons | n° quarry | extracted tons | sludge tons |
| **AL** | 1 | 8,000 | 233.31 | 1 | 30,180 | 208.73 | 1 | 19,000 | 182.31 |
| **AT** | 0 | 0 | 0 | 0 | 0 | 0 | 0 | 0 | 0 |
| **BI** | 2 | 1,526 | 203 | 2 | 8,018 | 30.00 | 2 | 4,623.00 | 0.00 |
| **CN** | 80 | 470,262.09 | 3,870.34 | 78 | 429,093.03 | 3,979.66 | 75 | 413,373.90 | 2,850.82 |
| **NO** | 0 | 0 | 1,440.25 | 0 | 0 | 1,611.78 | 0 | 0 | 14.14 |
| **TO** | 37 | 198,624.88 | 2,260.80 | 29 | 278,005.02 | 2,056.97 | 28 | 159,115.59 | 1,901.05 |
| **VB** | 41 | 328,709.34 | 28,587.51 | 44 | 291,057.59 | 24,820.99 | 42 | 290,979.51 | 17,760.44 |
| **VC** | 1 | 1,999.20 | 241.92 | 1 | 0 | 252.90 | 1 | 7,924.53 | 47,.5 |
| **Piedmont Region** | 162 | 1,009,121.51 | 36,837.13 | 155 | 1,036,353.63 | 32,961.02 | 149 | 895,016.53 | 22,756.30 |

*Table 20: Number of quarry, extracted tons and sludge tons declared in each district and in Piedmont, for the three year period 2014 to 2016. (Source: Piedmont ARPA).*

Even if the amount of extracted materials, for some districts, increase between the years 2014 and 2016, the amount of sludge declared decrease. This anomaly may be due to an increase of direct sale of block compared to the sale after processing stones. Other districts, on the other hand, of which no extracted material is found, declare some quantity of produced sludge. This may be due to any material processed for third parties.

***Table 21*** shows the percentage sludge production per ton in the period from 2014 to 2016. With * the anomalous values due to third parties are indicated.

As can be seen the percentages of produced sludge compared to the extracted materials are very low.

To verify the amount of sludge actually produced, calculations were carried out according to the cutting method used.

[4] D.Lgs. N.152 / 2006 art.188,189,190 and 193 provide the correct management of the waste with the obligation of traceability of waste (SISTRI). In particular, Article 185 requires that anyone carrying out activities of transport, collection of waste, companies and initial producers of hazardous waste and companies and initial producers of non-hazardous waste, communicate annually to Chambers of Commerce, industry, crafts and agriculture territorially competent, in the manner provided by law January 25, 1994, n. 70, the quantity and quality characteristics of the waste covered by the aforementioned activities.

| | 2014 | 2015 | 2016 |
|---|---|---|---|
| | percentage of sludge per tons | | |
| **AL** | 2,92 | 0,69 | 0,96 |
| **AT** | 0 | 0 | 0 |
| **BI** | 13,30 | 0,37 | 0 |
| **CN** | 0,82 | 0,93 | 0,69 |
| **NO** | 0 | 0 | * |
| **TO** | 1,14 | 0,74 | 1,19 |
| **VB** | 8,70 | 8,53 | 6,10 |
| **VC** | 12,10 | * | 0,60 |
| **Piedmont Region** | 3,65 | 3,18 | 2,54 |

*Table 21: Percentage of sludge per tons for tons of extracted materials. * probable processing for third parties.*

## 3.2.1 Estimation of the amount of produced sludge according to the cutting machine used.

The production of sludge during cutting with different technologies is a function of the thickness of the slabs and of the diamond tools used. Taking into account a block dimension of 1.5m*2m*3m (9$m^3$ of block), a specific weight material of 2.7 t/$m^3$ and considering slab thickness of 2cm, 3cm, and 4cm, the percentage and ton of lost material (sludge) and the number and $m^2$ of slabs produced was calculated. ***Table 22*** shows the starting data for the calculation.

| | | | |
|---|---|---|---|
| **Block dimension [m]** | | 1.5*3*2 | |
| **Block length [m]** | | 2 | |
| **Rock specific weight [t/$m^3$]** | | 2.7 | |
| **$m^2$ for one slab [$m^2$]** | | 4.5 | |
| **Slab thickness [cm]** | 2 | 3 | 4 |
| **Slab volume [$m^3$]** | 0.09 | 0.135 | 0.18 |
| **Slab weight [t]** | 0.243 | 0.364 | 0.486 |

*Table 22: Starting data considered for the calculation of lost materials.*

Each type of cutting machine has its technical characteristics, tool size and any metal grit. The starting data used in the calculation, for each cutting technology, are given in the following tables.

As specified in chapter 2, the gangsaw in addition to the blades also uses metal grit to facilitate cutting. The calculation of the cutting width and the distance between the blades have been carried out according to formulas [10] [11] proposed by Mannella P. in 2012:

$$Cutting\ Width\ (mm) = Blade\ Thickness + (2 * Grit\ Diameter) + 1 \quad [10]$$

$$Distance\ between\ Blades\ (mm) = Slab\ Thickness\ + \ (2 * Grit\ Diameter) + 1 \quad [11]$$

In ***Table 23*** are reported the distance between blades according to the different slabs thickness and metal grit diameter.

| GANGSAW DISTANCE BETWEEN BLADE | | | | | | |
|---|---|---|---|---|---|---|
| **slab thickness [cm]** | 2 | | 3 | | 4 | |
| **grit diameter [mm]** | 0.4 | 0.8 | 0.4 | 0.8 | 0.4 | 0.8 |
| **blade distance [mm]** | 21.8 | 22.6 | 31.8 | 32.6 | 41.8 | 42.6 |

*Table 23: Distance between blades calculated according to formula [11].*

The data of blade segment thickness and metal grit diameter used have been chosen according to Dellas Spa and Pometon Spa technical specifications. In ***Table 24*** are reported starting data for gangsaw calculation.

| GANGSAW TECHNICAL SPECIFICATION | | | | | | | | |
|---|---|---|---|---|---|---|---|---|
| **blade segment thickness [mm]** | 3.5 | | 4.1 | | 4.8 | | 5.2 | |
| **grit diameter [mm]** | 0.4 | 0.8 | 0.4 | 0.8 | 0.4 | 0.8 | 0.4 | 0.8 |
| **cutting width [mm]** | 5.3 | 6.1 | 5.9 | 6.7 | 6.6 | 7.4 | 7 | 7.8 |

*Table 24: Technical characteristics of the gangsaw taken into account for the calculation. (Source: Dellas Spa and Pometon Spa.). Last line: Cutting width calculated according to formula [10].*

Regarding diamond blade, taking into account a block dimension of 1.5x2x3m, the giant blade with 3500 mm of diameter and segment thickness of 14.2 mm was chosen for the calculation of the loss of material. This thickness is to avoid possible deviation effect of the trajectory. ***Table 25*** shows the technical data used for the calculation. The cutting width was calculated with the following formula [12], according to plant operators experience:

$$Cutting\ width\ [mm] = segment\ thickness + 1 \qquad [12]$$

| GIANT DIAMOND BLADE TECHNICAL SPECIFICATION | |
|---|---|
| **disk diameter [mm]** | 3500 |
| **segment thickness [mm]** | 14.2 |
| **cutting width [mm]** | 15.2 |

*Table 25: Technical characteristics of the giant diamond blade taken into account for the calculation. (Source: Pulitor diamond tools.). Last line: cutting width calculated according to formula [12].*

The diamond wire taken into account is produced by Co.Fi.Plast Wires company. It is a plastic sintered diamond wire with beads for cutting all type of granite, with layers of sintering 2.20mm. Three different diameter beads were chosen. ***Table 26*** shows the technical data used for calculation. The cutting width was calculated with the following formula [13], according to plant operators experience:

$$Cutting\ width\ [mm] = beads\ diameter + 1 \qquad [13]$$

| DIAMOND WIRE TECHNICAL SPECIFICATION | | | |
|---|---|---|---|
| **beads diameter [mm]** | 7.3 | 8.3 | 9 |
| **cutting width [mm]** | 8.3 | 9.3 | 10 |

*Table 26: Technical characteristics of the diamond wire taken into account for the calculation. (Source: Co.Fi.Plast wires). Last line: cutting width calculated according to formula [13].*

### 3.2.1.1 Results of the estimation of amount sludge produced during cutting process

*Gangsaw amount of lost material*:

The calculation of the material lost during the gangsaw cutting was performed taking into account both the thickness of the blades and the size of the metal grit. The tables below shown the results obtained, both in terms of production (number of slabs produced for blocks and $m^2$ of slabs produced for blocks) and in terms of waste produced (tons of waste material and percentage of waste for a block), for different slabs thicknesses 2 cm (***Table 27***), 3 cm (***Table 28***) and 4 cm (***Table 29***).

| GANGSAW - SLABS 2 cm | | | | | | | | |
|---|---|---|---|---|---|---|---|---|
| **blade segment thickness [mm]** | 3.5 | | 4.1 | | 4.8 | | 5.2 | |
| **grit diameter [mm]** | 0.4 | 0.8 | 0.4 | 0.8 | 0.4 | 0.8 | 0.4 | 0.8 |
| **cutting width + blade distance[mm]** | 27.1 | 28.7 | 27.7 | 29.3 | 28.4 | 30 | 28.8 | 30.4 |
| **number of slabs for block** | 74 | 70 | 72 | 68 | 70 | 67 | 69 | 66 |
| **slabs for block [$m^2$]** | 332 | 314 | 325 | 307 | 317 | 300 | 313 | 296 |
| **lost material [ton]** | 6.37 | 7.37 | 6.75 | 7.71 | 7.19 | 8.10 | 7.43 | 8.31 |
| **lost material [%]** | **26** | **30** | **28** | **32** | **30** | **33** | **31** | **34** |

*Table 27: Results obtained with gangsaw technology for slab thickness 2 cm.*

| GANGSAW - SLABS 3 cm | | | | | | | | |
|---|---|---|---|---|---|---|---|---|
| **blade segment thickness [mm]** | 3.5 | | 4.1 | | 4.8 | | 5.2 | |
| **grit diameter [mm]** | 0.4 | 0.8 | 0.4 | 0.8 | 0.4 | 0.8 | 0.4 | 0.8 |
| **cutting width + blade distance[mm]** | 37.1 | 38.7 | 37.7 | 39.3 | 38.4 | 40 | 38.8 | 40.4 |
| **number of slabs for block** | 54 | 52 | 53 | 51 | 52 | 50 | 52 | 50 |
| **slabs for block [$m^2$]** | 243 | 233 | 239 | 229 | 234 | 225 | 232 | 223 |
| **lost material [ton]** | 4.65 | 5.46 | 4.96 | 5.75 | 5.32 | 6.08 | 5.51 | 6.26 |
| **lost material [%]** | **19** | **22** | **20** | **24** | **22** | **25** | **23** | **26** |

*Table 28: Results obtained with gangsaw technology for slab thickness 3 cm.*

| GANGSAW - SLABS 4 cm | | | | | | | | |
|---|---|---|---|---|---|---|---|---|
| **blade segment thickness [mm]** | 3.5 | | 4.1 | | 4.8 | | 5.2 | |
| **grit diameter [mm]** | 0.4 | 0.8 | 0.4 | 0.8 | 0.4 | 0.8 | 0.4 | 0.8 |
| **cutting width + blade distance[mm]** | 47.1 | 48.7 | 47.7 | 49.3 | 48.4 | 50 | 48.8 | 50.4 |
| **number of slabs for block** | 42 | 41 | 42 | 41 | 41 | 40 | 41 | 40 |
| **slabs for block [$m^2$]** | 191 | 185 | 189 | 183 | 186 | 180 | 184 | 179 |
| **lost material [ton]** | 3.66 | 4.34 | 3.92 | 4.58 | 4.22 | 4.86 | 4.38 | 5.01 |
| **lost material [%]** | **15** | **18** | **16** | **19** | **17** | **20** | **18** | **21** |

*Table 29: Results obtained with gangsaw technology for slab thickness 4 cm.*

Considering ***Table 27*** (thickness slab of 2 cm), it can be observed that an increase of the thickness of the blades correspond an increase of lost material during cutting process. Using the same thickness of blades but different diameter of metal grit, an increase in the lost material with bigger diameter of metal grit is observed.

The same trend takes place for thicknesses slab of 3 cm and 4 cm.

According to Mannella P. (2012), it is necessary consider the deviation effect of the blade in the case of smaller thicknesses. This deviation effect induce more waste production and a premature wear of the blade. Citran G. in 2000, calculated the deviation of gangsaw blade with the following formula [14]:

$$D = K * \frac{L^3}{S^3} \text{.....[14]}$$

Where:

D = blade deviation (mm)

K = proportionality constant, depends on the blade height

L = blade length (mm)

S = blade thickness (mm).

The following results are obtained from formula [14]:

| **blade thickness S (mm)** | **3.5** | **4.1** | **4.8** | **5.2** |
|---|---|---|---|---|
| **deviation D (mm)** | 22.4 | 14 | 8.7 | 6.8 |

*Table 30: Deviation of the gangsaw blade for different blade thickness. (Source: Citran G., 2000)*

From ***Table 30*** it can be stated that in order to obtain faster and safer cuts, it is necessary to use thicker blades (Citran G, 2000). However, as can be observed from ***Table 27***, ***Table 28*** and ***Table 29*** with thicker blades, greater cutting widths are obtained and therefore less number of slabs per block. An appropriate balance between the choice of the correct thickness blade is necessary. To reduce the waste and optimize the exploitation of the block instead of acting on the thickness of the blades, is better act on the size of the metal grit. The use of fine metal grit with medium blades thicknesses could be the right solution.

*Giant blade amount of lost material:*

Compared to the previous cutting technology the diamond blade is faster, but cut only one slab at a time. In addition, the disk core plays a very important role because is the only component responsible for the absorption of vibrations and noise reduction.

The giant disk considered in this study has a diameter of 3500 mm and a thickness of 14.2 mm. The deviation effect may be overcome by this high blade

thickness. Due to the high thickness of the disk, the material lost during cutting phase is greater than the gangsaw technology. The results are reported in ***Table 31***, ***Table 32*** and ***Table 33***.

| GIANT DIAMOND BLADE - SLABS 2 cm | |
|---|---|
| **disk diameter [mm]** | 3500 |
| **segment thickness [mm]** | 14.2 |
| **cutting width + slab thickness[mm]** | 35.2 |
| **number of slabs for block** | 57 |
| **slabs for block [m2]** | 256 |
| **lost material [ton]** | 10.49 |
| **lost material [%]** | **43** |

*Table 31: Results obtained with giant diamond blade technology for slab thickness 2 cm*

| GIANT DIAMOND BLADE - SLABS 3 cm | |
|---|---|
| **disk diameter [mm]** | 3500 |
| **segment thickness [mm]** | 14.2 |
| **cutting width + slab thickness[mm]** | 45.2 |
| **number of slabs for block** | 44 |
| **slabs for block [m2]** | 199 |
| **lost material [ton]** | 8.17 |
| **lost material [%]** | **34** |

*Table 32: Results obtained with giant diamond blade technology for slab thickness 3cm*

| GIANT DIAMOND BLADE - SLABS 4 cm | |
|---|---|
| **disk diameter [mm]** | 3500 |
| **segment thickness [mm]** | 14.2 |
| **cutting width + slab thickness[mm]** | 55.2 |
| **number of slabs for block** | 36 |
| **slabs for block [m2]** | 163 |
| **lost material [ton]** | 6.69 |
| **lost material [%]** | **28** |

*Table 33: Results obtained with giant diamond blade technology for slab thickness 4cm*

Due to the deviation effect and due to the diamond blade cut takes place in steps (a single-blade is used), this type of technology is normally used for cutting small blocks or for squaring big blocks and not for big production.

*Diamond wire amount of lost material*:

The calculation of the material lost during the cutting with the diamond wire, considers the same parameters of the other two types of cut: beads diameter and cutting width. In ***Table 34***, ***Table 35*** *and* ***Table 36*** are reported the results obtained.

| DIAMOND WIRE – SLABS 2 cm | | | |
|---|---|---|---|
| **beads diameter [mm]** | 7.3 | 8.3 | 9 |
| **cutting width + slabs thickness[mm]** | 28.3 | 29.3 | 30 |
| **number of slabs for block** | 71 | 68 | 67 |
| **slabs for block [m2]** | 318 | 307 | 300 |
| **lost material [ton]** | 7.13 | 7.71 | 8.10 |
| **lost material [%]** | **29** | **32** | **33** |

*Table 34: Results obtained with diamond wire technology for slab thickness 2cm.*

| DIAMOND WIRE – SLABS 3 cm | | | |
|---|---|---|---|
| **beads diameter [mm]** | 7.3 | 8.3 | 9 |
| **cutting width + slabs thickness[mm]** | 38.3 | 39.3 | 40 |
| **number of slabs for block** | 52 | 51 | 50 |
| **slabs for block [m2]** | 235 | 229 | 225 |
| **lost material [ton]** | 5.27 | 5.75 | 6.08 |
| **lost material [%]** | **22** | **24** | **25** |

*Table 35: Results obtained with diamond wire technology for slab thickness 3cm*

| DIAMOND WIRE – SLABS 4 cm | | | |
|---|---|---|---|
| **beads diameter [mm]** | 7.3 | 8.3 | 9 |
| **cutting width + slabs thickness[mm]** | 48.3 | 49.3 | 50 |
| **number of slabs for block** | 41 | 41 | 40 |
| **slabs for block [m2]** | 186 | 183 | 180 |
| **lost material [ton]** | 4.18 | 4.58 | 4.86 |
| **lost material [%]** | **17** | **19** | **20** |

*Table 36: Results obtained with diamond wire technology for slab thickness 4cm*

As can be observed from the ***Table 34***, ***Table 35*** *and* ***Table 36***, the diamond wire produces an amount of waste, similar to the gangsaw technology. However, diamond wire technology offers many advantages compared to gangsaw. One of the advantages of multiwire respect gangsaw is the down feed speed. Multiwire speed is more than four times compared to gangsaw speed. This aspect is linked to a higher production of slabs for the diamond wire. Furthermore, this type of technology uses tools that are more wear resistant than gangsaw.

# Chapter 4

# 4. Sludge characterization

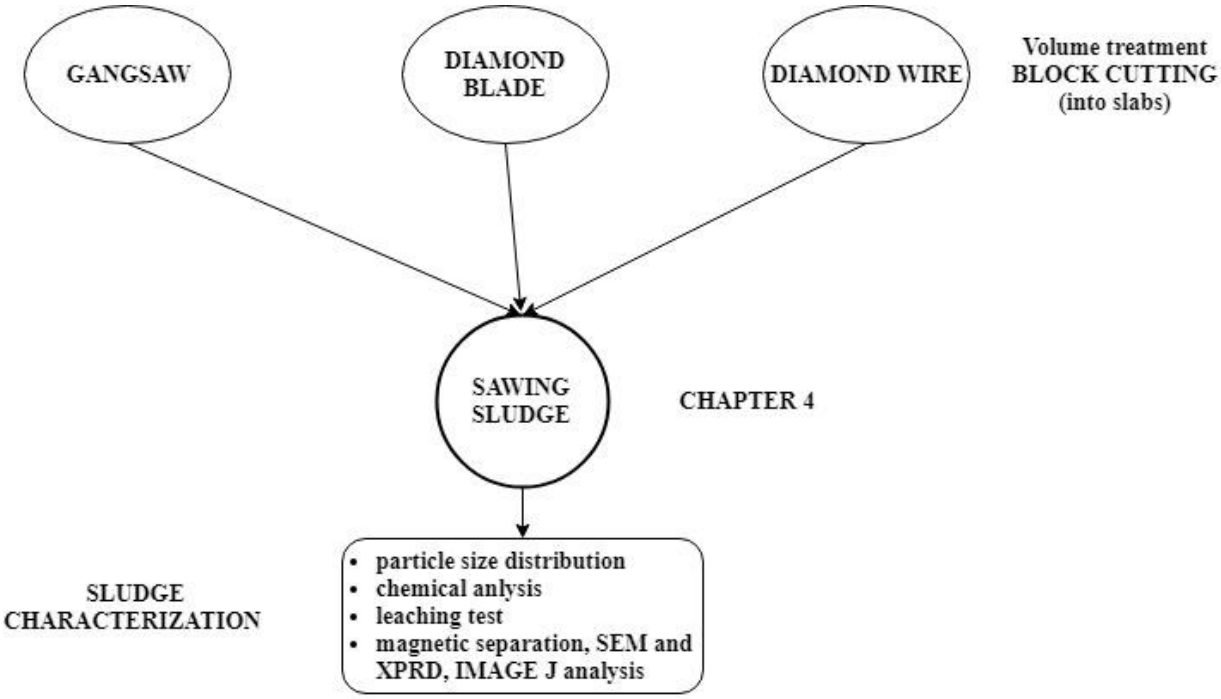


[5]

*Figure 41: Sludge characterization flowchart.*

As described in Chapter 1, the aim of European Union strategy is the end-of-waste concept. The Waste Management Plan "promotes the recovery of sludge through recycling, reuse or reclamation, if there is not environment risks involved." The Plan, therefore, aims to enhance and use waste from extraction and processing activities for other purposes, when the characteristics allow it, thus avoiding indiscriminate and dangerous disposal for human health and the environment. Article 3 of the European Directive 2006/21/EC (mining waste directive), provides the definition of waste as: "*any substance or object which the holder discards or intends or is required to discard*." Directive 2008/98/EC provides the definition of end-of-waste as: "the substance or object is commonly used for specific purposes; the existence of a market or a demand for the substance or object; the substance or object meets the technical requirements for the specific purposes and respects the existing legislation and the laws applied to the products; and use will not lead to overall negative impacts on the environment

[5] It is specified that for the SEM, XRPD and image analysis tests not all the samples considered in the study were analyzed but only the representative ones. The samples analyzed for each test are listed below:
- SEM: MVG, CTD, TTW, GVM;
- XRPD: MVG, TTW, MCD;
- Image analysis: MVG, DVM, TVD, CVW, TTW, MCG, MCD

or human health. This concept presupposes the presence of a waste, but provides for a recovery operation. The objective of the "end-of-waste" concept is to facilitate recycling, avoiding management costs and ensuring safe and high quality materials. The same Directive defines the concept as a by-product: "*The Substance or the object originated by a production process, of which it is an integral part, and whose primary purpose is not the production of this substance or object*". Article 3 (point 1) considered the substance or object not a waste but a by-product only if the following conditions are met: "(a) *certainty that the substance or object will be used / or (b) the substance or object may be used / or directly without any further treatment other than normal industrial practice c) the substance or object is produced / or an integral part of a production process and further use is legal, ie the substance or object satisfies , for the specific use, all relevant requirements concerning products and protection of health and the environment and will not lead to overall negative impacts on the environment or human health.*" The same definitions are provided by the Italian implementation in Legislative Decree 152/2006 and its amendment Lgs.D. 205/2010.

The characterization of the sludge deriving from the cutting of ornamental stones is therefore necessary to understand if what is currently considered a waste could become a by-product for other production processes, optimizing the cutting methods.

Many problems related to sawing sludge, such as very fine particle size distribution, chemical properties and costs of management and disposal, become the main challenges for the management of what is now a waste.

Allam et al. in 2014 carried out a study on re-use of granite sludge in the production of green concrete. Gencel et al., in 2012, carried out a study on the re-use of marble sludge in the production of concrete paving blocks. Many researches are based in this field. Careddu and Dino in 2016 have compared the reuse of sludge resulting from the cutting of silicate rocks with those resulting from the cutting of carbonate rocks. Zichella et al., in 2017, investigated sawing sludge deriving from different kind of cutting methods for a future recovery. However, unclear national legislation and local authorities do not consider that a simple eco-compatible treatment could transform a waste into a by-product, and has not adopted guidelines for the correct behaviour regarding the possible recovery of this material.

Piedmont districts object of this study are Torino, Cuneo and Verbania. The lithotypes considered are silicate rocks, in particular Luserna stone, Serizzi, Beole, Diorite, Sienite, Granites and Gneiss. ***Table 37*** shows the sample codes with the cutting stone type and the cutting machine used. The sample code consists of three letters XXX: the first identifies the name of the plant, the second identifies the district where the plant is located (V for Verbania district, T for Torino district and C for Cuneo district) , the third identifies the cutting technology used (G for gangsaw, D for diamond blade, W for diamond wire and M for mix technologies).

| Samples code | Districts | Stones type | Main minerals composition | Cutting methodologies |
|---|---|---|---|---|
| **MVG** | Verbania | Serizzo | Quartz, Plagioclase, Ortoclase; Biotite; Muscovite; Epidote. | Gangsaw |
| **DVM** | Verbania | Beola, Serizzo, Granite | Quartz; Plagioclase, Ortoclase, Alkaline Feldspar; Biotite; Muscovite, Piroxen. | Gangsaw – Diamond blade – Diamond wire |
| **TVD** | Verbania | Serizzo, marble | Quartz, Plagioclase, Ortoclase; Biotite; Muscovite; Epidote; calcium carbonate. | Diamond blade |
| **CVW** | Verbania | Serizzo | Quartz, Plagioclase, Ortoclase; Biotite; Muscovite; Epidote | Diamond wire |
| **GVM** | Verbania | Beola, Granite, Serizzo, Luserna, Sienite | Quartz; Plagioclase, Ortoclase, Alkaline Feldspar; Biotite; Muscovite, Piroxen, White mica; Chlorite | Gangsaw - Diamond blade - Diamond wire |
| **PTD** | Torino | Gneiss | Quartz; Plagioclase; Alkaline Feldspar; White mica; Chlorite; Epidote | Diamond blade |
| **CTD** | Torino | Granite | Quartz; Plagioclase, Orthoclase, Biotite. | Diamond blade |
| **TTW** | Torino | Diorite, Sienite, Granite, Luserna, Serizzo, Beola | Quartz; Plagioclase, Ortoclase, Alkaline Feldspar; Biotite; Muscovite, Piroxen, White mica; Chlorite | Diamond wire |
| **MCG** | Cuneo | Luserna stone | Quartz; Plagioclase; Alkaline Feldspar; White mica; Chlorite; Epidote. | Gangsaw |
| **MCD** | Cuneo | Luserna stone | Quartz; Plagioclase; Alkaline Feldspar; White mica; Chlorite; Epidote | Diamond blade |

*Table 37: List of samples tested with districts area and related cutting stone and cutting machine for each plants. Main minerals composition are reported, for detail description refers to Table 14.*

The analyses carried out on sludge samples are the following: particle size distribution, electron scanning microscope (SEM) and X-ray powder diffraction (XRD), chemical analysis, leaching test, specific gravity, wet magnetic separation, image J analysis. The petrographic and mineralogical description of principal stones cut by plants is reported in ***Table 14*** in Chapter 3.1.1.1.. In Annex 1 are reported some photos of sludge sampling.

# 4.1 Particle size distribution

The particle size is the most important physical property of a sample. Measuring the particle size distribution and understanding how it affects the products or processes is important for the characterization of the sludge.. In the case of possible re-use, it is important to know this data because the particle size distribution affects the mechanical and physical characteristics of any possible by-product obtained from the sludge. From the geomechanical point of view, the fine particle size material, if compacted, behaves as a silt-clay soil with low permeability; for the purposes of geotechnical stability, such characteristics can have a negative connotation (ARPA Puglia, 2016). This analysis is necessary to understand which particle size class presents a greater concentration of metals so as to choose the best separation method and/or the best re-use.

In this case, the particle size analysis was performed in the wet condition, according to UNI EN 933 Part 1 reference standard, using four sieves (0.038 mm, 0.063 mm, 0.106 mm and 0.212 mm), in order to obtain five classes (***Figure 42***).


*Figure 42: sieves column used for the particle size distribution of sludge.*

Wet condition was preferred to dry ones to avoid dispersions of finer material and to reduce the packaging effect. The material retained on each sieve was filtered, dried and weighed.

### 4.1.1 Particle size distribution results

Particle size distribution test was performed on three representative samples of each sludge. The average results of three sample, were graphically expressed as passing cumulative frequency (%).

As can be seen all sludge have a trend similar to a silt clay. In the ***Figure 43***, ***Figure 44***, ***Figure 45*** and ***Figure 46*** particle size distribution analyses, divided for cutting technologies, are shown.

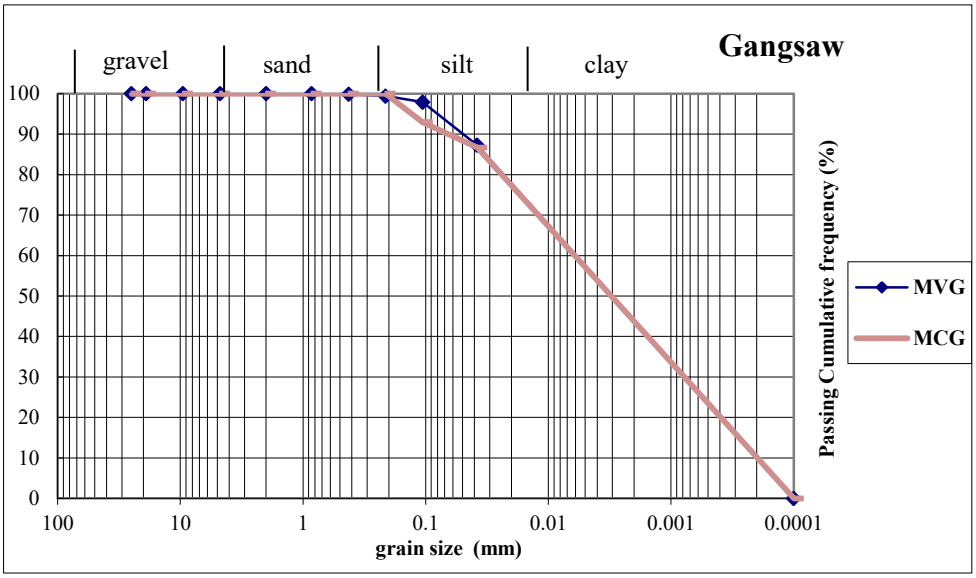


*Figure 43: Particle size distribution results of sludge deriving from gangsaw cutting.*

***Figure 43*** shows the results of particle size distribution on the two tested sludge deriving from the cutting with gangsaw technology. The trend are the same for both sample. The cut stones of these plants are Serizzo (MVG) and Luserna stone (MCG). These two type of stone show an evident foliation and more or less the same fabric characteristics.

***Figure 44*** shows the particle size distribution relating to diamond blade cutting technology. The sludge MCD and PTD that deriving from the cutting of Luserna stone and Gneiss respectively show the same trend, due to the same characteristic of both stone. The sludge TVD and CTD that cut Serizzo and marble and Granites respectively, show a slightly coarser particle size distribution than the other two samples. Probably because granite and Serizzo do not show anisotropy and because the original rocks present higher grain size.

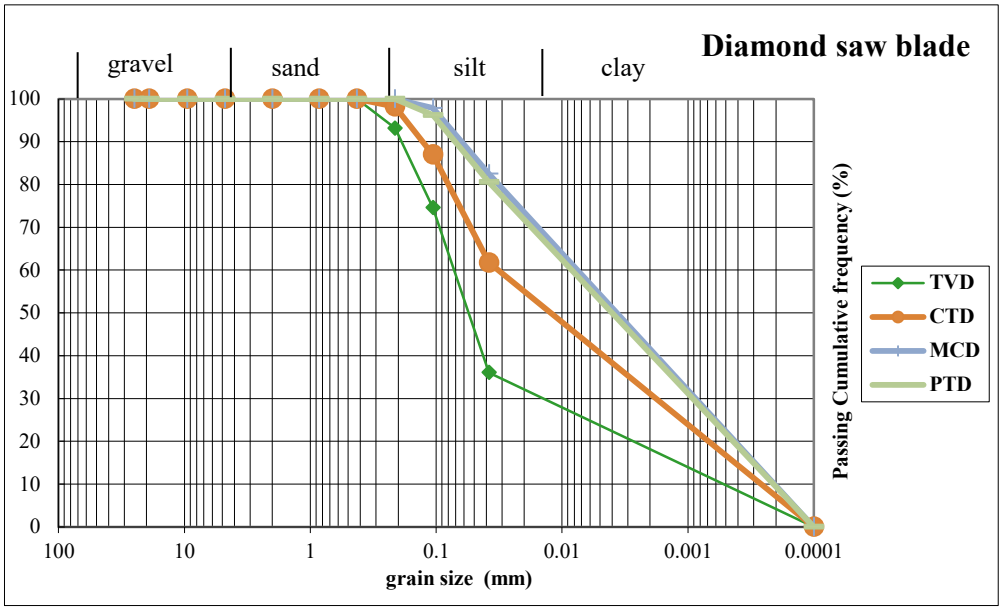


*Figure 44: Particle size distribution results of sludge deriving from diamond saw blade cutting.*

***Figure 45*** show the particle size distribution of sludge deriving from cutting with diamond wire technology. TTW cuts stones classified in chapter 3 as cuttability class 3 and 4, therefore difficult to cut respect stone cutted in plant CVW. CVW cuts Serizzo that is classified in chapter 3 as in cuttability class 1/2, therefore easy to cut. In the ***Figure 45*** it is shown how the cutting of stones classified in lower class of cuttability produced finer sludge compared to the cutting of harder stones.

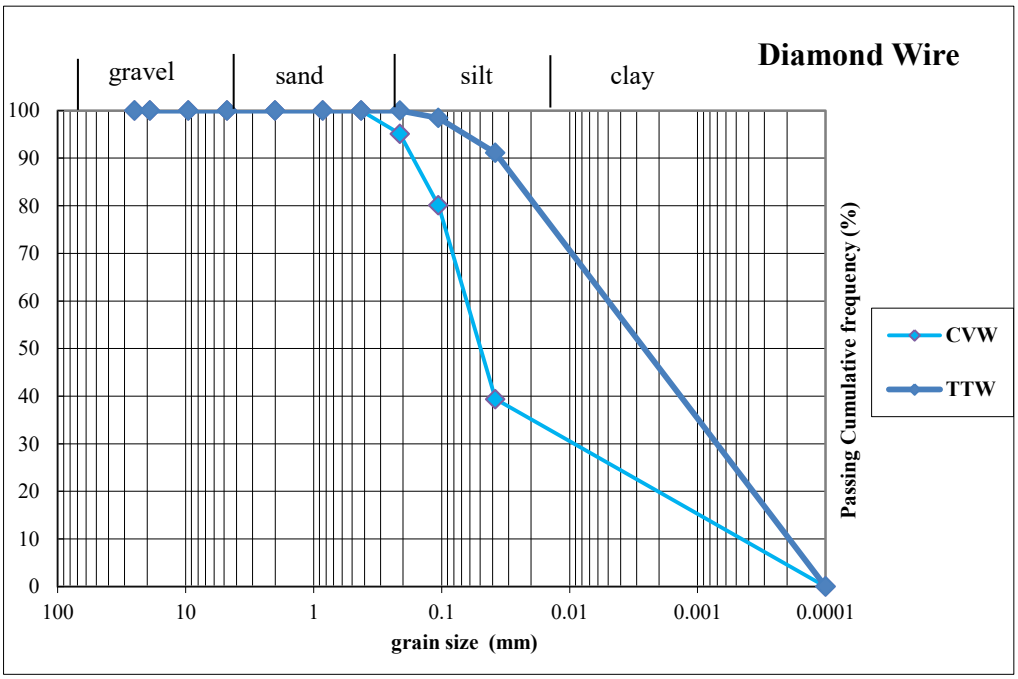


*Figure 45: Particle size distribution results of sludge deriving from diamond wire cutting.*

***Figure 46*** show the particle size distribution of sludge deriving from cutting with all the technologies and different type of stone. The trend is more or less the same.

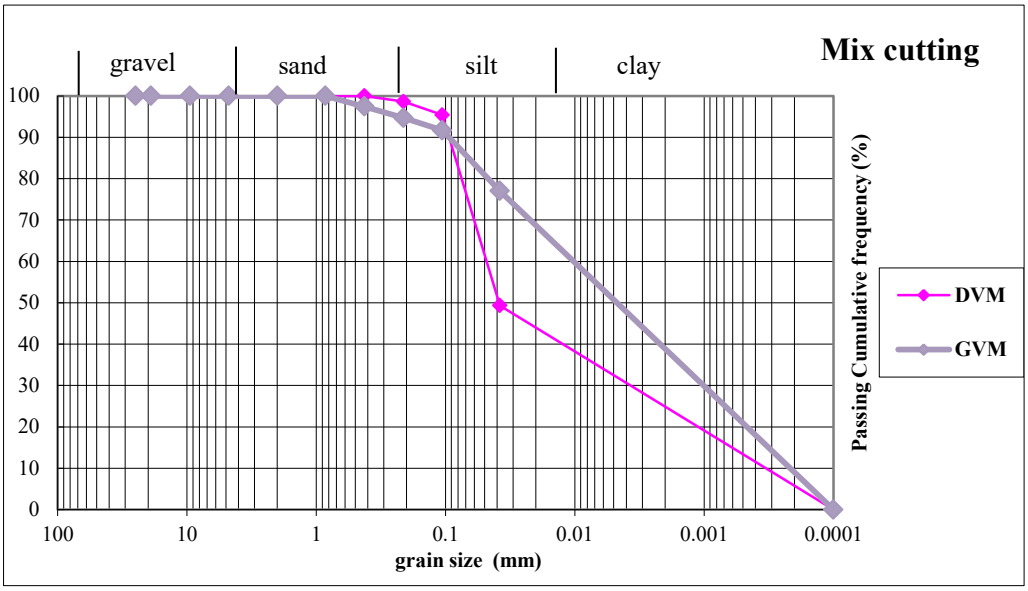


*Figure 46: Particle size distribution results of sludge deriving from mix cutting.*

In general great distribution size differences are not found among the all cutting technologies. All sludge are similar to a silt clay.

# 4.2 Chemical analysis

One of the most important technical requirements that sludge must comply in order to be recovered (whether in public green areas or industrial areas or if it goes to landfill) is the chemical composition. Sludge are subject to certain limits of concentration of heavy metals, as reported by Italian law D.Lgs. 152/2006 Annex 5, title V, part IV. The reference table, with limits concentration is reported in Chapter 1.

The sampling of the sludge, according to Art. 8 of the D.M. 05/02/1998, is carried out on the sludge in unaltered state, to obtain a representative sample. The analysis of the samples is carried out according to standardized methods that are valid or recognized at national or international level. The sampling and chemical analyses are carried out by the owner of the plant where the sludge is produced, before the recovery and every 2 years, and in any case whenever changes are made in the production process.

The procedure for the determination of the metals concentration in sludge foresees a sample mineralization and an acid dissolution, for the solubilization process, after drying. The mineralization is carried out with a Fkv Ethos Easy microwave mineralizer, which allows to maintained at controlled pressure and temperatures the acidified sludge. Microwave radiation speeds up the solubilization reactions of metals and degradation of the organic matrix. The acids used depend on the heavy metals to be investigated, for example: for Zn, Fe and Cu, 1: 1 nitric acid is used with the water, while for Ni and Co alloys, nitric acid + hydrochloric acid + fluorine is used in a 7: 3: 1 ratio. After mineralization process, the samples are examined with the ICP-Mass analyzer. ICP-MS provides an analytical technique based on the use of mass spectrometry combined with inductively coupled plasma. The ICP allows to determine the concentrations of inorganic and non-metallic substances, using a plasma torch to produce the ionization of a mass spectrometer for the separation and detection of the produced ions. The results are expressed in mg/kg, as reported to the total weight of the analyzed sample.

## 4.2.1 Chemical analysis results

Chemical analysis is necessary to define the destination of sawing sludge. If the sawing sludge falling inside the limits of concentration, required in accordance with ***Table 4*** column A (shown in chapter 1), the sludge can be reused as secondary raw material in green areas; if it is inside the limits of concentration required in according with the column B of ***Table 4*** (shown in chapter 1), it can be reused as secondary raw material in commercial or industrial areas. The results

obtained from the chemical analysis are shown below in the ***Table 38***.

| Sludge code | Ba | Cu | Zn | Be | Co | Ni | V | As | Cd | Total Cr | Cr VI | Pb | Se | Hg | Fe |
|---|---|---|---|---|---|---|---|---|---|---|---|---|---|---|---|
| | mg/kg | mg/kg | mg/kg | mg/kg | mg/kg | mg/kg | mg/kg | mg/kg | mg/kg | mg/kg | mg/kg | mg/kg | mg/kg | mg/kg | mg/kg |
| **MVG** | 68 | 186 | 54.5 | <1 | 10.4 | 86.5 | 25.6 | <1 | <1 | 130 | < 5 | 4.7 | <1 | <0.1 | 34286 |
| **DVM** | 70 | 180 | 60.2 | <1 | 7.8 | 32.7 | 27.7 | 10.3 | <0.1 | 66.9 | 22.1 | 3.7 | <1 | <0.01 | 10432 |
| **TVD** | <1 | 116.9 | 56.5 | <1 | 53.5 | 16.8 | 30.3 | 4.8 | <0.1 | 12.7 | 3.7 | 10.5 | <1 | 0.7 | 5200 |
| **CVW** | <0.1 | 35.7 | 22.3 | <1 | 30.7 | 11.4 | <1 | <0.1 | <0.1 | 24.9 | <1 | 8.4 | <1 | <0.01 | 2430 |
| **GVM** | 72 | 108 | 125 | <1 | 102 | 15 | 22 | 1 | <1 | 1836 | < 5 | 26 | <1 | <0.01 | 11840 |
| **PTD** | 1.13 | 107.88 | 109.13 | <1 | 31.66 | 17.68 | <1 | <0.1 | <0.1 | 8.66 | <1 | 19.26 | <1 | <0.01 | 24100 |
| **CTD** | <1 | 243.01 | 50.29 | <1 | 64.48 | 14.14 | 28.3 | <1 | <1 | 122.56 | <5 | / | <1 | <0.01 | 5600 |
| **TTW** | <0.1 | 41.89 | 24.82 | <1 | 26.15 | <0.01 | <1 | <1 | <0.1 | 18.21 | <1 | / | <1 | <0.01 | 27500 |
| **MCG** | / | 180.65 | 25.52 | <1 | 5.43 | 133.07 | <0.1 | <0.1 | <0.1 | 250 | <5 | 52.5 | <0.1 | <0.01 | 32580 |
| **MCD** | < 5 | 41.89 | 24.82 | <1 | 26.15 | <0.01 | <1 | <0.1 | <0.1 | 18.21 | < 5 | 23 | <1 | <0.01 | 4340 |
| **concentration limit column A** | / | **120** | **150** | / | **20** | **120** | / | **20** | **2** | **150** | **2** | **100** | / | **1** | / |
| **concentration limit column B** | / | **600** | **1500** | / | **250** | **500** | / | **50** | **15** | **800** | **15** | **1000** | / | **5** | / |

*Table 38:Results obtained from chemical analysis on ten sludge tested, in unaltered state. (according to D.Lgs. 152/2006 Annex 5, title V, part IV and Art. 8 of the D.M. 05/02/1998).Last two row indicate the limit of concentration of green area (column A) and commercial area (column B). In yellow the results over the limits of column A, In red the results over the limits of column B.*

The results of the chemical analysis on sludge reflects the alloys constituent of cutting tools, abrasives and steels. Total chromium, hexavalent chromium and copper are mainly found in the sludge deriving from the gangsaw and mixed cutting. Cobalt is found particularly in the sludge resulting from cutting with diamond wire, diamond blade and mixed. No differences in metal concentration are observed based on the different type of cutting stone.

All tested sludge can be used in industrial and commercial areas, but not in green areas, as they respect concentration limits only in column B. The GVM sample, on the other hand, is also outside the limits of column A, due to the too high total chromium concentration.

# 4.3 Leaching test

The leaching tests on the samples obtained for the purposes of the characterization of the eluate is carried out at least at the beginning of each activity and thereafter each year, unless otherwise provided by the competent authority, and in any case whenever changes are made in the recovery process (Art. 9 and Annex 3 of D.M. 05_02_1998).

For the determination of the leaching test, appendix A of UNI 10802 standard is applies, according to the method established by the UNI EN 12457-2 standard. For very fine particle size, as sawing sludge, analysis foresees a centrifugation of the material, with an ultracentrifuge (20000 G), of at least 10 minutes, instead of a natural sedimentation. Only after this process was carried out a filtration phase, according to UNI EN 12457-2 standard point 5.2.2. The sample is diluted in water considering a 1/10 ratio. Placed in an agitator for about 24 hours and the filtrated at 0.45 micron. Finally the eluate sample is analyzed by ICP-Mass analyzer. Nitrates, Sulphates, Fluorides and Chlorides are analyzed using the chromatography method. The results are expressed in µg/l, except Ba, Cu, Zn, Nitrates, Sulphates, Fluorides and Chlorides, which are expressed in mg/l.

## 4.3.1 Leaching test results

The leaching test, as the chemical test, is necessary to define the destination of the sawing sludge. If the sludge exceeds the concentration limits established by regulations (***Table 5*** – Chapter 1), it is considered a special non-hazardous waste, therefore it must be destined for special landfill disposal. Otherwise it can be reused as a secondary raw material. In ***Table 39*** are shown the leaching test results.

| Sludge code | pH | Ba | Cu | Zn | Be | Co | Ni | V | As | Cd | Total Cr | Cr VI | Pb | Se | Hg | Fe | NO3 | F | SO4 | Cl |
|---|---|---|---|---|---|---|---|---|---|---|---|---|---|---|---|---|---|---|---|---|
| | | mg/l | mg/l | mg/l | µg/l | µg/l | µg/l | µg/l | µg/l | µg/l | µg/l | µg/l | µg/l | µg/l | µg/l | mg/l | mg/l | mg/l | mg/l | mg/l |
| **MVG** | 7.8 | 0.02 | 0.01 | 0.01 | <0.001 | <1 | 10 | 3.36 | 1.3 | <1 | 2.45 | <0.01 | <1 | <1 | <0.1 | 4.48 | 1.39 | 0.025 | 27.92 | 2.81 |
| **DVM** | 7.62 | 0.02 | 0.06 | 0.27 | <0.001 | 0 | 20 | 60 | 10 | <1 | 130 | <0.01 | <1 | <1 | <0.1 | 13.3 | 1.02 | 0.023 | 21.11 | 2.84 |
| **TVD** | 7.2 | <0.1 | 0.12 | 0.14 | <0.001 | 40 | <1 | 10 | 10 | <1 | <1 | <0.01 | 30 | <0.1 | <0.01 | 1.27 | / | / | / | / |
| **CVW** | 7.3 | 0.03 | 0.01 | 0.03 | <0.001 | 330 | <1 | <1 | 1.6 | <1 | <1 | <0.01 | <1 | <0.1 | <0.01 | 0.27 | / | / | / | / |
| **GVM** | 7.6 | <0.1 | <0.001 | <0.001 | <0.001 | 4.99 | <1 | 5.48 | <1 | <1 | <1 | <0.01 | <1 | <1 | <0.1 | 0.03 | 1.13 | 0.018 | 6.62 | 3.51 |
| **PTD** | 7.41 | <0.1 | 17.96 | 0.73 | <10 | <10 | <10 | <1 | 15.47 | <0.1 | <1 | <0.01 | <1 | <1 | <0.1 | 0.5 | 13.56 | <0.1 | 68.34 | 73.15 |
| **CTD** | 7.25 | <0.1 | 248.6 | 2.47 | <1 | 28.52 | 10.25 | 6.05 | 8.21 | 0.049 | 0.10 | <0.01 | <1 | <1 | <0.1 | 0.2 | 7.8 | <0.1 | 45.8 | 51 |
| **TTW** | 7.2 | <0.1 | 22.47 | 0.43 | <1 | 1.41 | 0 | 3.11 | 8.28 | 0 | 0.12 | <0.01 | <1 | <1 | <0.1 | 0.53 | / | / | / | / |
| **MCG** | 7.75 | <0.1 | <0.05 | 0.01 | <0.001 | <1 | <1 | <1 | 2.5 | <0.1 | 6.25 | 0.01 | <1 | <0.025 | <0.05 | 3.5 | 6.35 | 0.38 | 42.5 | 39 |
| **MCD** | 7.4 | <0.1 | <0.031 | <0.01 | <1 | <10 | <1 | <1 | <0.1 | <0.1 | <1 | <0.01 | <1 | <1 | <0.1 | 1.3 | 1.86 | 0.024 | 10.68 | 3.32 |
| **concentration limit** | **5,5<>12** | **1** | **0,05** | **3** | **10** | **250** | **10** | **250** | **50** | **5** | **50** | **/** | **50** | **10** | **1** | **/** | **50** | **1.5** | **250** | **100** |

*Table 39: Results of the leaching test performed according to D.M. 05_02_1998, appendix A of UNI 10802 standard and UNI EN 12457-2 standard. Last row: threshold limit of metal concentration, by Italian regulation. In red: value over the threshold limit of concentration.*

On 10 samples examined with the leaching test, only 4 show all metal concentrations below the Regulation threshold concentration limits. Copper is the metal that is released more. But even cobalt, nickel and total chromium have some high value.

# 4.4 Magnetic separation

The magnetic separation has been provided both to characterize the material for a correct future recovery and as a pretreatment for those sludge that exceed the limits of metal concentration. In ***Figure 47*** is shown the flowchart followed for the magnetic separation test, in forecast of recovery or/and pre- treatment of sawing sludge.

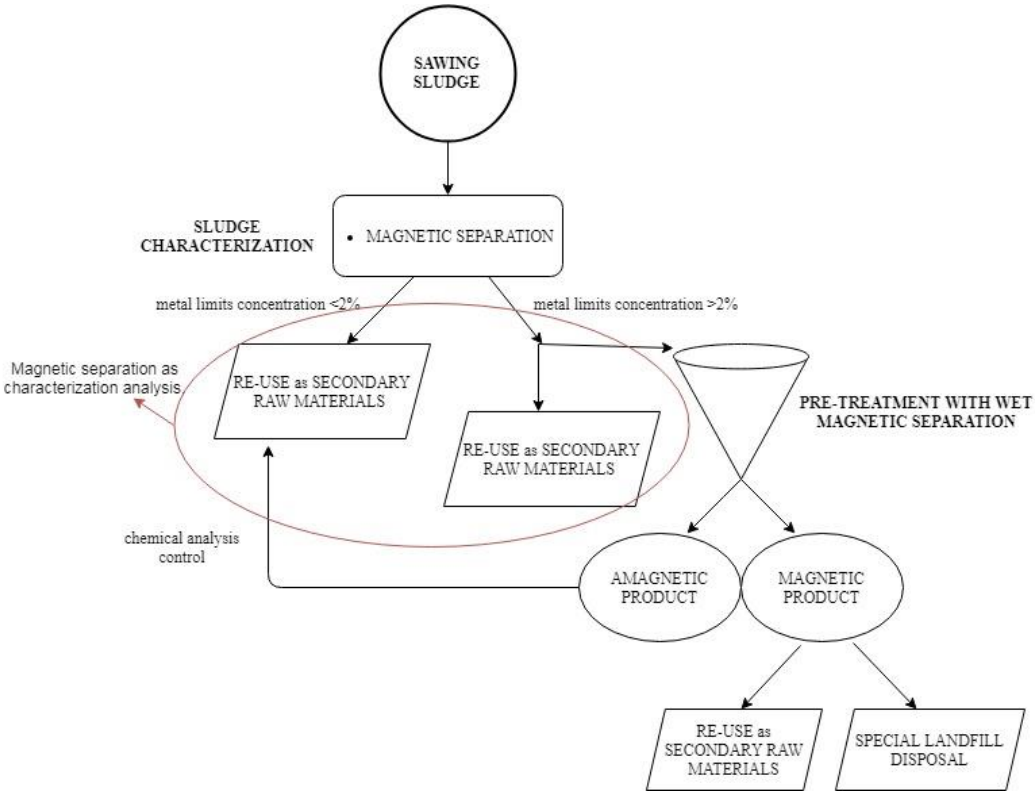


*Figure 47: Flowchart for the characterization and pre-treatment of sawing sludge in forecast of a future recovery as secondary raw material.*

Magnetic separation is a physical separation, which does not change the structure and physical-chemical constitution of the material. It can be considered as a sort of material selection. In many factories where the cutting process is done with gangsaw, this kind of separation is already used, in order to recover the metal grit to be reinserted in the cutting cycle. This practice could therefore be part of

normal industrial practice, but the legislation (in Article 184 bis1 of Legislative Decree 152/2006) is not very clear.

The components of the sawing sludge, metals fraction and rocks fraction show different magnetic characteristics and different densities. These forces act differently according to the characteristics of each component.

The sludge is split by the magnetic separator into two products: the magnetic fraction and amagnetic fraction.

Three are the tractive magnetic forces that come into play during separation:

- Gravitational force;
- Friction or inertial force;
- Attractive or repulsive interparticle forces.

The magnetic and competing gravitational, friction, hydrodynamic, or inertial forces tend to separate the particles; by contrast, attractive interparticle forces tend to reduce the degree of separation. For this reason non-magnetic particles may be found even in the magnetic fractions.

The separation efficiency can be evaluated in two ways:

1) as a recovery (quantity evaluation): the total amount of magnetic fraction with respect to the feed material;

2) as a grade (quality evaluation): the amount of magnetic material actually present in the magnetic fraction. The latter is assessed through the SEM and DRX analysis.

These two independent measures of the separation effectiveness depend on the relative magnitude of the forces described above.

The magnetic separator used is a Kolm-type high gradient magnetic separator, manufactured by Eriez Magnetics. The device is shown schematically in ***Figure 48***.

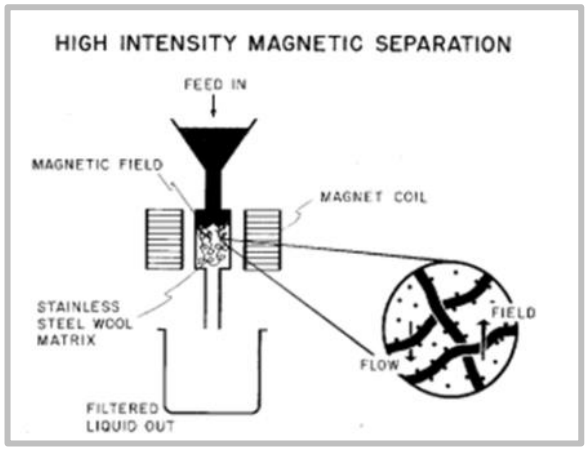


*Figure 48: Kolm-type high gradient magnetic separator (Source: Oberteuffer, 1974).*

This type of device operates with a discontinuous cycle. Magnetized coils produce a strong magnetic field. A canister is placed between the coils, inside which ferromagnetic grids of different mesh sizes are inserted (***Figure 49***).

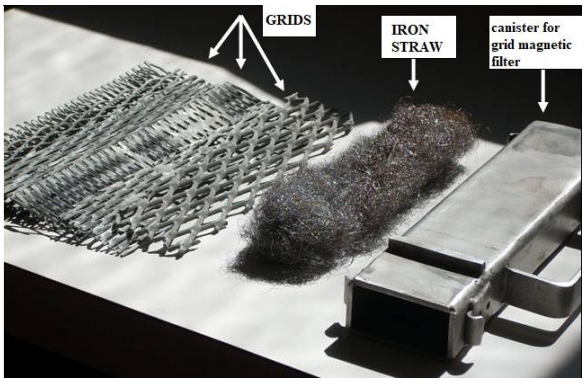


*Figure 49: Grids and canister of Eriez Separator, used for magnetic separation.*

The grids are chosen based on the size of the feed particles in order to optimize the magnetic forces. Strong magnetic forces produced by the high field gradients at the edges of the filaments are effective in capturing very fine particles (<100 microns) of even weakly magnetic substances. Sawing sludge in a fluid slurry is fed from the top of the device through a funnel and pass through canister and grids among the magnetized coils. The magnetic particles are trapped and the amagnetic fraction ends up in a container. In a second step the trapped magnetic particles are easily washed out when the applied field is reduced to zero.

In order to better separate the two fractions, it is necessary to perform multiple steps for both fractions (magnetic and amagnetic). In this experimental study it was verified, by means of different test, that only 3 steps are needed.

The performance of the separator depends both on the nature of the tested material (particle size distribution and physical properties), but also on the parameters of the separation device (magnetic field and process rate). According to Oberteuffer (1974), for separators that processed very fine particles, such as sawing sludge, the resistance that predominates is hydrodynamic. The interparticle forces, those between magnetic and non-magnetic particles, determine how pure the products of the magnetic separation will be. If the forces between the particles are larger than the magnetic and competing forces, then many non-magnetic particles may be trapped along with the magnetic particles. Conversely, many magnetic particles may be carried along with non-magnetic particles and fail to be trapped. In wet systems for very small particles, surface-chemical double-layer forces between particles will generally be an important factor.

In literature many studies are conducted to improve the performance of magnetic separation. Newns and Pascoe in 2002 verified that, lengthening the path with the filamentous iron matrix in which pass the material and decreasing the speed of passage and at the same time increasing the magnetic field, improved the separation system. Luzheng Chen, in 2011 and 2012, studied a pilot pulsating HGMS separator. This separator combines a mechanism that makes the ring vibrate during its rotation for continuous separation, and a feed vibrating mechanism that makes the material pass evenly through the separating matrix, in a

very thin layer and without blockage. Junca et al., in 2015, studied the iron recovery from waste generated during cutting of granite using two different separation methods: magnetic separation (wet high-intensity magnetic separator, Jones type) and cycloning. Through this study he had demonstrated that the best results are given by the magnetic separation.

## 4.4.1 Magnetic separation results

Magnetic susceptibility (k) is the measure of how susceptible a material is to become magnetized. The diamagnetic materials have k <0, the paramagnetic materials have k> 0, while the ferromagnetic materials have a k >> 0. The rocks interested by the following study are all igneous or metamorphic rocks with minerals that contain iron. Minerals like biotite and amphiboles contain iron and are paramagnetic. Feldspars and muscovite are paramagnetic if rich in iron. All the Piedmont rocks contain feldspars, biotite, muscovite and amphiboles. This aspect is important for the purposes of magnetic separation, as many of these minerals can be found in the magnetic product after separation, as they are attracted by the ferromagnetic metals deriving from tool wear.

Chemical analysis shows that among the metals deriving from the wear of cutting tools, Co, Ni, Cr and Cu are the ones with the highest concentration. Among the metals present in the cutting tools, however, not all have magnetic properties. For example, Zn, and Cu are diamagnetic, while Co, Ni, Fe and Cr are magnetic. Other metals such as Zn, V, Pb, Hg, Cd, Mo and W are superconductors. During magnetic separation, then we will find most of the metals deriving from the tools in the magnetic product, but there will be the probability of finding some of them as Cu and Zn in the non-magnetic product.

The set parameters of the separator device have been chosen following different experimental tests. The optimal values for this type of materials are: magnetic field 260 mT, 10A and 140V, slow material passage (not measurable since the feeding is manual), 3 steps. The product that has been passed 3 times it is the non-magnetic, as it is the product which is expected to be reused and of greater quantity. The magnetic separation was carried out both on the material as it is and on each distribution size classes. The ***Table 40*** shows the results of the test carried out on materials as it is.

| Sludge code | Magnetic fraction [%] | Amagnetic fraction [%] |
|---|---|---|
| **MVG** | 2.96 | 97.04 |
| **DVM** | 2.7 | 97.3 |
| **TVD** | 1.5 | 98.5 |
| **CVW** | 0.22 | 99.78 |
| **GVM** | 2.46 | 97.54 |
| **PTD** | 2.5 | 97.5 |
| **CTD** | 3.15 | 96.85 |
| **TTW** | 1.15 | 98.85 |
| **MCG** | 6.3 | 93.7 |
| **MCD** | 1.95 | 98.05 |

*Table 40: Results of magnetic separation on materials as it is.*

From the results obtained, it can be observed that the sludge deriving from the cutting with the gangsaw have a greater magnetic percentage compared to the diamond wire technology. On the other hand, the diamond blade technology has an high percentage of metals concentration in the sludge. By comparing the two sludge deriving from gangsaw cutting, MVG and MCG, it can be seen that MCG has an higher percentage of magnetic fraction. The type of stone cut and its workability affects the wear of the tools and therefore the concentration of metals in the sludge. Indeed MVG cuts Serizzo which is in workability class 1/2 while MCG cuts Luserna stone which is in workability class 3. Comparing the samples deriving from the cutting with diamond wire CVW and TTW we can observe the same difference: the first (CVW) cuts only Serizzo which is in class 1/2 while TTW cuts a mix of stones with a prevalent workability class 3. The percentage of concentration of metals present in the sludge also in this case is higher in the case of stones more difficultly workable.

If we consider instead the PTD, TVD and MCD samples it can be observed that the percentage of magnetic fraction is almost the same for PTD and MCD which cutting stones with the same workability class (3), while TVD which cuts Serizzo in workability class 1/2 has obtained a lower percentage of magnetic fraction.

To understand in which particle size distribution class the metals are most concentrated, the magnetic separation was carried out on each classes (lesser than 0.212 mm). The results are shown in ***Table 41***.

| Distribution size classes [mm] | MVG | DVM | TVD | CVW | GVM | PTD | CTD | TTW | MCG | MCD |
|---|---|---|---|---|---|---|---|---|---|---|
| **Magnetic fraction [%]** | | | | | | | | | | |
| **>0.106** | 0.97 | 1.02 | 1 | 0.05 | 1.21 | 0.89 | 1.24 | 0.5 | 1.15 | 0 |
| **[0.106÷0.063]** | 0.49 | 0.28 | 0.2 | 0.065 | 1.05 | 0.64 | 0.51 | 0.2 | 2.1 | 1.4 |
| **[0.063÷0.038]** | 1.34 | 1.08 | 0.25 | 0.1 | 0.2 | 0.74 | 0.9 | 0.4 | 2.05 | 0.48 |
| **<0.038** | 0.17 | 0.32 | 0.05 | 0.005 | 0 | 0.23 | 0.5 | 0.05 | 1 | 0.07 |

*Table 41: Magnetic separation results divided by distribution size classes.*

The distribution trend of magnetic fraction in the different particle size distribution for gangsaw and mix technologies (***Figure 50***) foresees the higher concentration of metals in the class ranges [0.106÷0.063] and [0.063÷0.038].

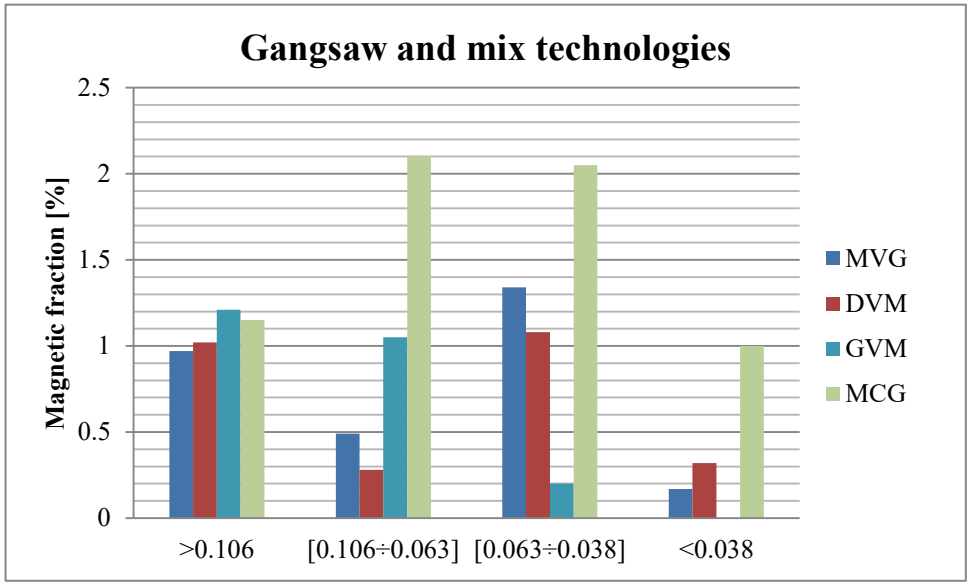


*Figure 50:Distribution of magnetic fraction in the different particle size distribution. Gangsaw and mix cutting technologies.*

In case of diamond blade technology (***Figure 51***), foresees that the higher concentration of metals is distributed on the classes >0.106mm, between 0.106 and 0.063 mm, and between 0.063 and 0.038 mm.

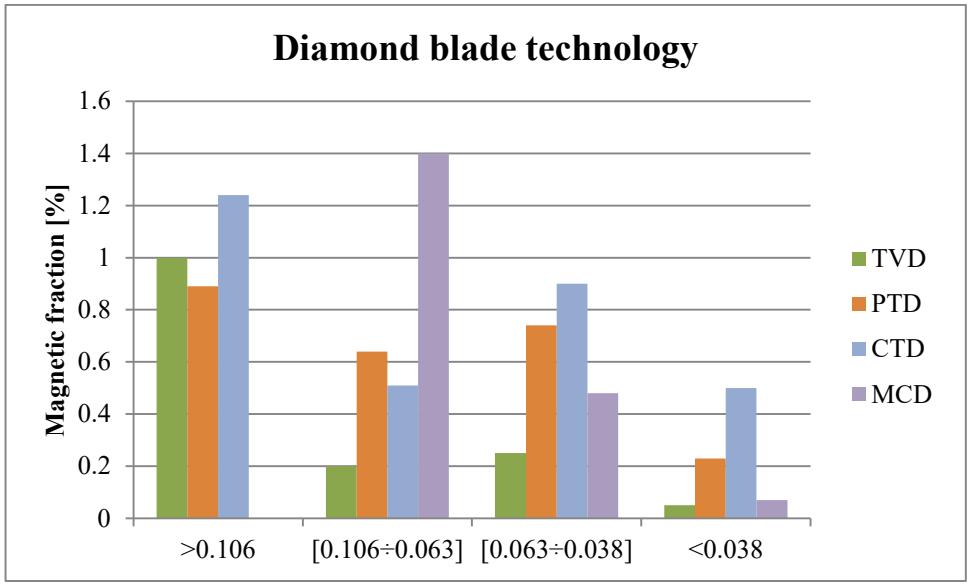


*Figure 51: Distribution of magnetic fraction in the different particle size distribution. Diamond blade cutting technology*

The same trend of diamond blade is shown for diamond wire technology (***Figure 52***).

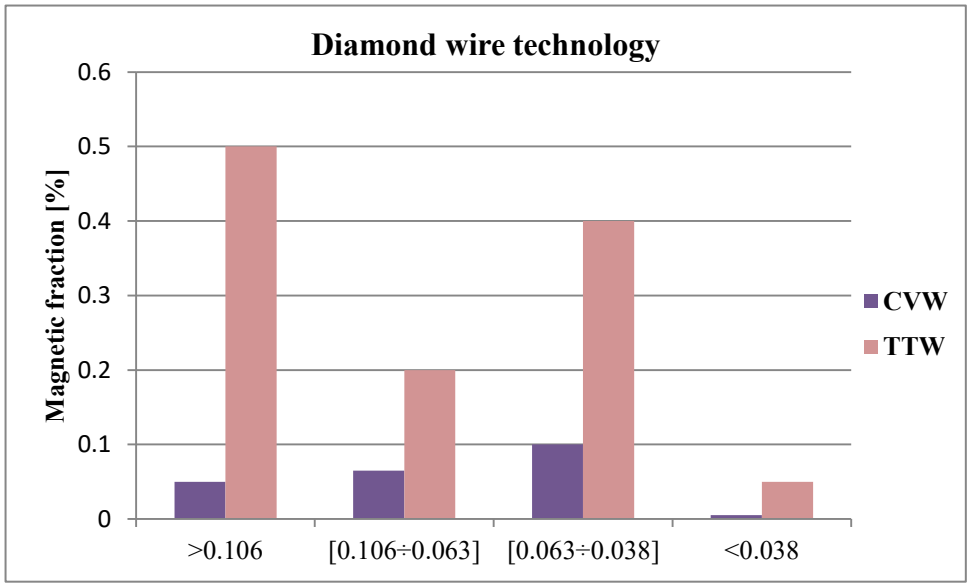


*Figure 52: Distribution of magnetic fraction in the different particle size distribution. Diamond wire cutting technology*

The lowest class of 0.038 mm fortunately, for all technologies, it is the class with the lowest concentration of magnetic fraction, in some cases absent. In case of pre-treatment with this separation, it could have a good efficiency, since the particle size class that could create more problems in the separation is just the smaller one of 0.038 due to the packing effect for the too fine material.

# 4.5 Image analysis

Image analysis was performed by means of the free ImageJ software to evaluate and verify the presence of metals in sawing sludge, comparing it with the magnetic separation results. Image J is a digital image processing software that allows the selection of the elements based on their color. This type of software has been chosen because the metals present in the sludge under the optical microscope assume a black color compared to the other mineral constituents which assume a white to gray color.

Following a previous work Zichella et al., 2017 for each distribution particle size lower than 0.106 mm, three slides were prepared for microscopic observations, and for each slide three areas were analyzed. The optical microscope used to make the photos to be analyzed with the ImageJ software is the Leika DMLP for petrography. all the slides were prepared using eugenol oil with a refractive index equal to 1,550 for a better identification of the elements to be counted. Seven of the starting sludge are analyzed (MVG, DVM, TVD, CVW, TTW, MCG and MCD).

The steps for image analysis were as follows:

- one photo with the parallel polarized light (***Figure 53*-A**) and one in cross polarized light (***Figure 53*-B**).

- the two photos were overlapped (***Figure 53*-C**) for easier identification of the metal particles. The metals and opaques are black and without regular contours in both images.

- the quantitative analysis of the metal particles selected using the RGB thresholding of ImageJ software (***Figure 53*-D-F**). One thresholding for the metal fraction and one for the other minerals fraction (***Figure 53*-E**) were chosen. After the selection of the metal grains, the software allows their size and area to be found and for these measures to be exported. To estimate the size of non-metallic elements, a second thresholding is performed so as to determine the bottom of the image not covered by grains: knowing the image area, the bottom area and the area of the metal are obtained by subtracting the area of the non-metallic grains.

- evaluation of the grain volume: it was necessary to approximate the grains to parallelepipeds and estimate the average thickness of the grain. The metal fraction is estimated to have a thickness of 5 micron, 20 micron and 30 micron respectively for the classes <0.038, from 0.063 to 0.038 mm and from 0.106 to 0.063 mm. Knowing the density of metal and rock, the mass of the different materials is obtained.

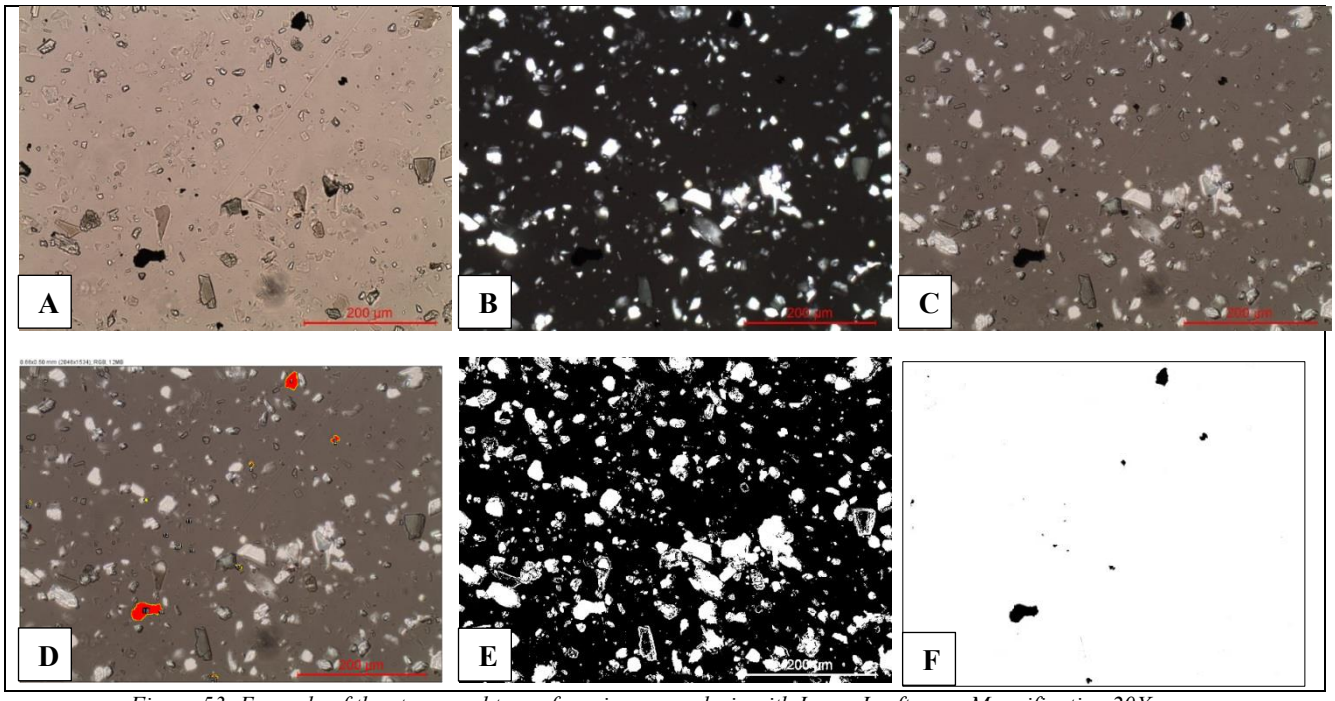


*Figure 53: Example of the steps used to perform image analysis with ImageJ software. Magnification 20X. (A) Parallel Polarized light image; (B) Cross polarized light image; (C) Overlapped image; (D) Selection of metal fraction with RGB thresholding; (E) Selection of grain with RGB thresholding; (F) Selection mask of metal fraction.*

## 4.5.1 Image J analysis results

With Image J software calculates the area occupied by the minerals and the area occupied by the metals, obtaining the volumes and the weight in percent for each distribution size. *Annex 2* shows some examples of image processing by means of Image J software. The results obtained are summarize in the ***Table 42***.

| | IMAGE J ANALYSIS | | | | | | |
|---|---|---|---|---|---|---|---|
| | **MVG** | **DVM** | **TVD** | **CVW** | **TTW** | **MCG** | **MCD** |
| **Distribution size classes** | Magnetic fraction [w%] | | | | | | |
| **[0.106÷0.063]** | 1 | 0.3 | 0.28 | 0.03 | 0.9 | 1.2 | 0.68 |
| **[0.063÷0.038]** | 1.19 | 1.29 | 0.38 | 0.13 | 1.3 | 2.99 | 1.31 |
| **<0.038** | 0.69 | 0.38 | 0.09 | 0.05 | 0.1 | 1.87 | 0.01 |
| **Total count** | **2.88** | **1.97** | **0.75** | **0.21** | **2.3** | **6.06** | **2** |
| | **WET MAGNETIC SEPARATION** | | | | | | |
| | **MVG** | **DVM** | **TVD** | **CVW** | **TTW** | **MCG** | **MCD** |
| **Distribution size classes** | Magnetic fraction [w%] | | | | | | |
| **[0.106÷0.063]** | 0.49 | 0.28 | 0.2 | 0.065 | 0.2 | 2.1 | 1.4 |
| **[0.063÷0.038]** | 1.34 | 1.08 | 0.25 | 0.1 | 0.4 | 2.05 | 0.48 |
| **<0.038** | 0.17 | 0.32 | 0.05 | 0.005 | 0.05 | 1 | 0.07 |
| **total count** | **2** | **1.68** | **0.5** | **0.17** | **0.65** | **5.15** | **1.95** |

*Table 42:Comparison of results on magnetic concentration, obtained by means of Image J analysis (over) and wet magnetic separation (under). The magnetic fraction of particle size distribution >0.106 mm are excluded from the comparison.*

From the results obtained, it can be observed that the total concentration of metals present in the sludge obtained with the magnetic separation is lower than the percentage (w%) obtained with the image analysis. The reason may be due to the presence in the sludge of metals that are not magnetic (as Zn and Cu) and therefore are not captured during the magnetic separation, while they are counted with the image analysis. Although in the magnetic separation are captured together with metals, mineral elements such as biotite and feldspars, which have a lower density than metals and therefore in the total percentage (w%) are not influent.

# 4.6 XRPD and SEM analysis

The XRPD and SEM were performed, as a qualitative analysis of the sludge, to identify the type of heavy metals present in unaltered state. Furthermore, the same investigations were carried out on the samples after magnetic separation, in particular on the magnetic fraction, to identify which metals are eliminated during this phase and the efficiency of the separation method.

## 4.6.1. XRPD analysis

Established by the particle size distribution analysis, that the sawing sludge is like a silt-clay, he diffractometric technique used is a X-ray Powder Diffraction (XRPD). The X-ray powder diffractometer is a Rigaku model Geigerflex. The analyzed material was finely ground, homogenized, and the average bulk composition was determined.

A monocrystalline sample provides very accurate and precisely localized information of the position of the signals. Each reflection is measured individually and its intensity can be used to derive the structure factor of that reflection.

If we have a polycrystalline sample, we lose the possibility of locating each node of the mutual lattice. The "three-dimensional" information of the single crystal is reduced to a one-dimensional function (the diffraction angle, θ), making obtaining information on the crystal lattice much more complex. This is the case of sawing sludge, composed of many crystalline phases deriving both from the minerals constituting the rock and from the metals deriving from the wear of the tools. For this reason a diffraction with Bragg-Brentano geometry (***Figure 54***) is used on polycrystalline samples. With this geometry, the sample is always in a precise "focused" position, which is preserved by simultaneously changing the incident angle and that of revelation (θ-θ, with mobile source and fixed sample or vice versa).

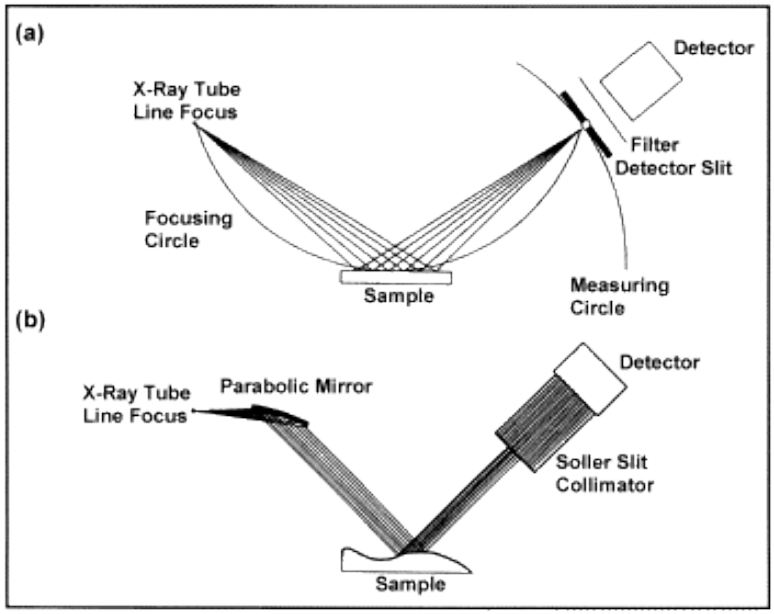


*Figure 54: Comparison between the classic Bragg-Brentano focusing geometry (a) and the parallel beam geometry with Göbel's mirrors (b). (Source: https://digilander.libero.it/elan1972/cap6/images/fig6.htm).*

The powder diffractogram (***Figure 55***) measures the diffracted intensities only for radial distances, according with the Bragg Law [15]:

$$d_{hkl} = 2\sin\theta / \lambda \qquad [15]$$

Where: d= distance between two crystalline planes belonging to the same "family";

θ = angle of incidence;

λ = monochromatic wavelength of the incident beam of X-rays with the surface of the solid sample.

All equivalent reflections by symmetry overlap completely. The main limitation of the powder method in the structural analysis derives from the need to geometrically reconstruct the mutual network three-dimensional from one-dimensional data.

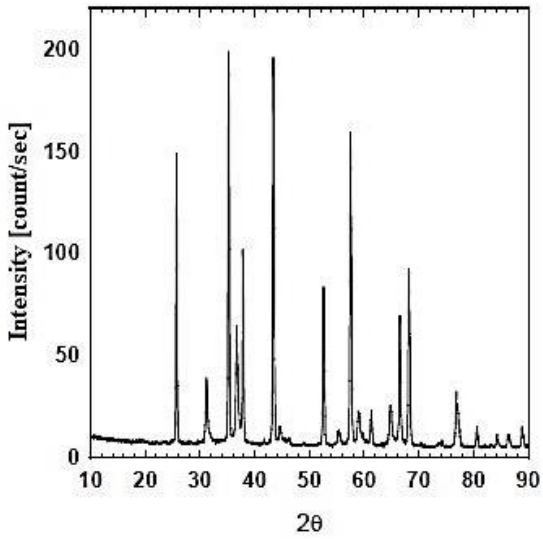


*Figure 55: Example of XRPD diagram results.*

The quantities observable from the diagram are:

- position of the peaks;
- peak intensity;
- shape of the peaks;
- bottom underlying the peaks (or noise).

The qualitative analysis is the identification of phases present in mixtures or the recognition of single component phases. In case of a polycrystalline sample, like sawing sludge, where there is the presence of more phases, the diffraction from powders will contain peaks corresponding to interplanar distances of all phases (***Figure 56***). The identification of single picks of an element is more difficult.

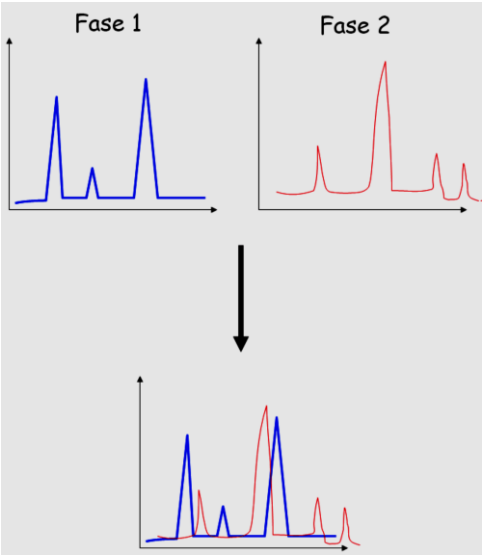


*Figure 56: overlapping of picks in case of polycrystalline phases.*

Each element has its characteristic peak Kα, characteristic radiation, and a radiation Kβ. The radiation of Kα has energy and intensity that is always greater than Kβ. The wavelength of the radiation produced depends on the Atomic Number of the target metal. Through a filter, a monochromator crystal, Kβ radiation can be completely eliminated.

### 4.6.1.1. XRPD results

The preparation to perform the analysis involves grinding, through a pestle, the sludge to obtain a fine ground. This procedure is necessary to improve the homogeneity of the material.

The first step is to characterize the material as it is. Therefore, 3 sludge samples were analyzed, each deriving from a different cutting technology. The ***Table 43*** shows the samples analyzed. The second step provide the analysis of the same sample after the magnetic separation, on magnetic fraction. This choice due to the difficult in the interpretation of the results. The sample are composed from several minerals and several metals for this reason the peaks are overlapped. Whit magnetic separation there is an elimination of some minerals phases, so the metals peaks are more evident. A comparison of spectrum for samples as it is and with the only magnetic fraction is shown, while each single spectrum with element identification is reported in *Annex 3*

| SAMPLE CODE | CUTTING TECHNOLGY | CUTTING ROCK TYPE |
|---|---|---|
| **MVG** | Gangsaw | Serizzo |
| **TTW** | Diamond Wire | Diorite, Sienite, Granite, Luserna, Serizzo, Beola |
| **MCD** | Diamond Blade | Luserna Stone |

*Table 43: Sample in unaltered state analyzed with XRPD.*

The MVG sample derives from gangsaw cutting. We would expect to find metals that belong both to the metallic grit used and to the wear of the blades. From the magnetic separation it has been found that this cutting method releases in the sludge a quite high percentage of metals, compared to the other two diamond technologies. The spectrum of sample as it is, shows peaks related to the mineral fraction deriving from Serizzo stone.

Analyzing only the magnetic fraction obtained after separation, we observe a concentration decrease of quartz and a concentration increase of micas and feldspar. As regards the identification of metals, peaks related to metal elements constituting the grit and steel of the blades are observed.

Iron Carbide ($Fe_3C$) constituent of the steel core of the blades is found. Moreover, there are Ferrite (Fe-Cr) and Silicon Chromium Iron ($CrFe_8Si$) which

are constituents of the metal grit used during cutting. ***Figure 57*** show the comparison between the results of MVG sample before and after magnetic separation.

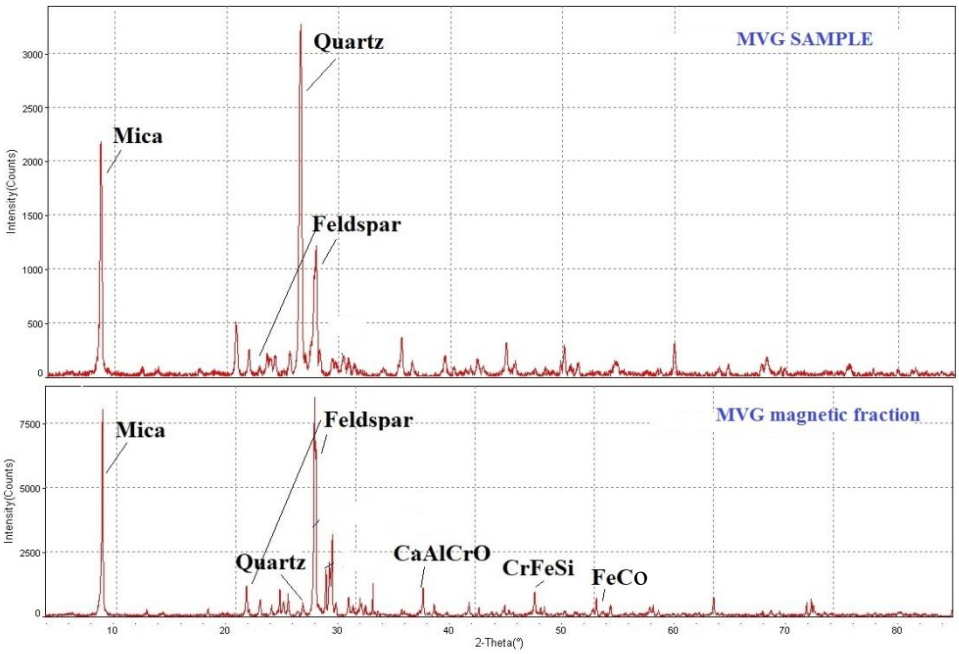


*Figure 57: XRPD – Comparison between the MVG sample spectrum (over) and after magnetic separation (under).*

Calcium Aluminum Chromium Oxide ($Ca_6Al_4Cr_2O_{15}$) can be attributed to pyrite (mineral fraction). Two other metallic elements had the same peaks of Silicon Chromium Iron, i.e. Tungsten Oxide ($WO_2$) and Cobalt Iron (FeCo), but Silicon Chromium Iron was chosen as identifier of the metal grit.

It can be asserted that during the magnetic separation, iron-based minerals such as mica, feldspars and pyrite, which are paramagnetic, are also captured together with metals.

The TTW sample come from Diorite diamond wire cutting. TTW sample show concentration of minerals such as mica and feldspar. There are many peaks due to metals, especially a high peak of Iron Oxide ($Fe_3O_4$). Other peaks can be attributed to metals coming from the wear of metal matrix diamond segment tools, as Chromite ($Fe+2Cr_2O_4$), Nickel Manganese Oxide ($NiMn_2O_4$), Nickel Zinc Titanium Oxide ($NiZnTiO_4$) and Vanadium Tungsten Carbide ($V_4WC_5$).

In the magnetic fraction, after separation, we can observe a decrease of peaks intensity related to mica and feldspar, and the presence of Chlorite. There is no presence of Quartz because Diorite does not contain it.

In ***Figure 58*** the two results obtained, before and after magnetic separation, are compared. In magnetic fraction a peak of Cobalt Tantalum Sulfide element (CoTaS), which compose some metal matrix of the diamond segments, is

identified.

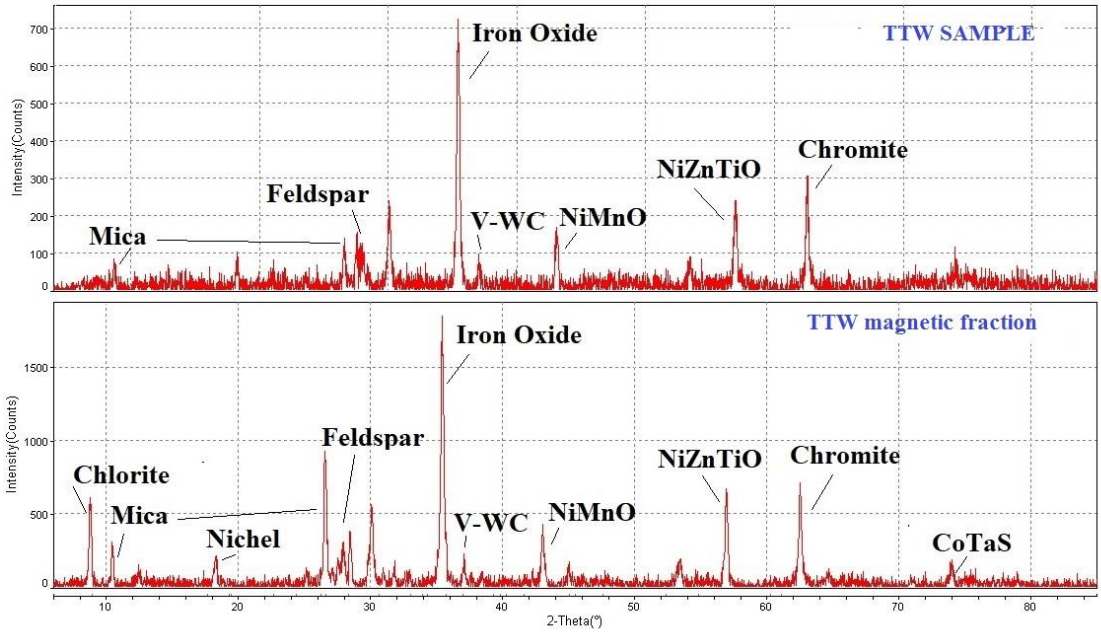


*Figure 58: Comparison between the TTW sample spectrum (over) and after magnetic separation (under).*

The MCD sample, deriving from the cutting with a diamond blade on Luserna stone, shows minerals like Quartz, Feldspar and Mica, and some peaks of metals that compose both the steel core of the disc and the matrix of the diamond segments. The metals identified are: Cobalt Molybdenum Oxide ($CoMoO_3$), Aluminum Nickel ($Al_3Ni$), Nickel Phosphide (NiP) and Nickel Chromium Oxide ($NiCrO_3$).

In the analysis performed on magnetic fraction we can be observed a peak related to the Chlorite and other metals that were not identified in sample analysis before magnetic separation. CuS, Cobalt Iron ($Co_3Fe_7$), Nickel Molybdenum Phosphide ($NiMoP_2$) and Silicon Carbide (SiC) have been identified. All elements contained in high-speed tool steels. ***Figure 59*** show the comparison between the two spectra obtained by analyzing the MCD sample, before and after magnetic separation.

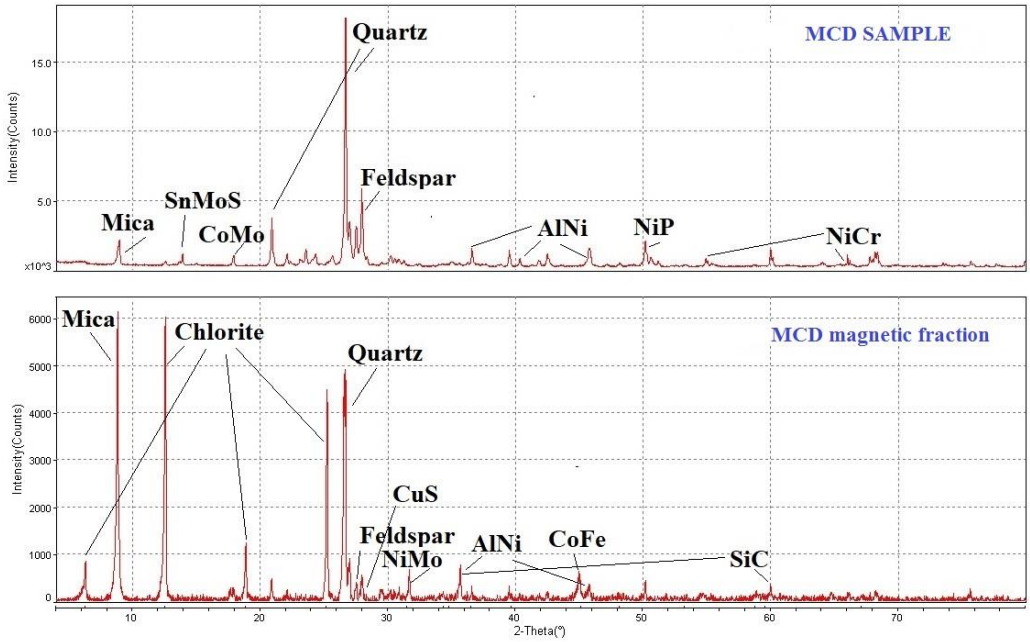


*Figure 59: Comparison between the MCD sample spectrum (over) and after magnetic separation (under).*

The analysis with the XRPD shows differences in composition between the different cutting technologies, which reflect the compositions found in literature. However, since the samples are composed of many minerals and metallic phases, the identification of the peaks is a bit complex. SEM analysis was performed to verify the results obtained with XRPD method.

## 4.6.2. SEM EDS analysis

Scanning Electron Microscope (SEM) uses a beam of primary electrons focused to hit the sample. The instrumentation used to perform this analysis is the SEM FEI model Quanta Inspect 200 LV with energy dispersive X-ray spectroscopy (EDS) using EDAX Genesis with the SUTW detector (***Figure 60***).


*Figure 60: SEM FEI model Quanta Inspect 200 LV with energy dispersive X-ray spectroscopy (EDS) using EDAX Genesis with the SUTW detector, in use in Laboratory of DIATI Department in Polytechnic of Turin.*

A scanning electron microscope consists of:

- an electron source composed of a tungsten filament;
- a focus system with electromagnetic lenses, which allow collimating the beam that hits the sample;
- a sample alignment system with the beam;
- a beam displacement system, which allows the sample to be scanned line by line on a specific area by a detector.

These elements constituting a SEM are placed in a column that ends in a chamber, where the sample to be analyzed is placed, and kept in a vacuum to ensuring that the air could disturb the creation of the electron beam (***Figure 61***).

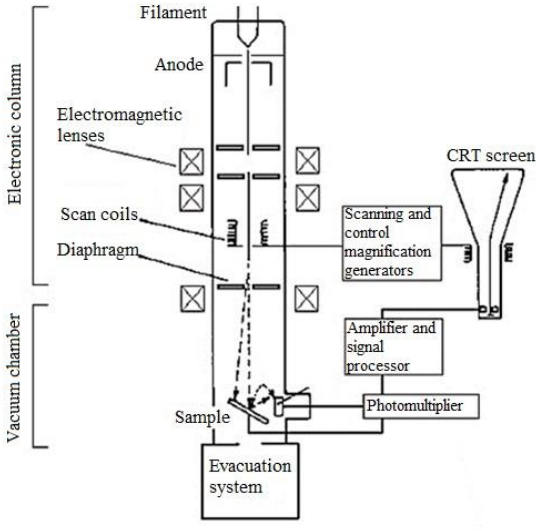


*Figure 61: Scheme of SEM function.*

The sample hits, produces different emissions. So the interaction between the electrons and the material to be analyzed can give different forms of response:

• backscattering or emission of diffuse retro electrons: the trajectory of the primary electron, which hits the sample, interacts with the electronic cloud of the atom, which has the tendency to reject them.;

• emission of a secondary electron;

• emission of an X ray: an electron of a more external orbital goes to occupy the vacuum formed by the emission of the secondary electron, generating an X ray.

The atomic number of the element plays an important role in the amount of backscattering electrons emitted from the sample. This amount is greater in lighter materials, less in heavier materials. Therefore, different gray shades are obtained based on the atomic weight of the substance. elements with higher atomic weight will assume lighter colors, while elements with lower atomic weight will take on darker colors.

For SEM observation the samples are fixed on a support, called stub, through a conductive tape. The samples prepared are placed in a metallizer to be covered with a thin layer of gold, to make the sample more conductive. The SEM provides a punctual analysis of the sample. The results obtained is a chart with the peaks of the elements that compose the object.

### 4.6.2.1 SEM EDS results

SEM analysis was performed on the tools of the three different cutting methodologies, for the recognition of the main metals that compose them. The following sample were analyzed: two different diamond beads tools of diamond wire technology, one sample of metal grit, two different diamond segment disc; all used in the plants taken into account in this research. All the spectrum correlated at the photos, of tools analysis are shown in *Annex 4A*. Then the ten sludge samples were analyzed, after the magnetic separation, to verify the separation efficiency, only four of this (representative of three technologies and mix technology) are reported here, the others in *Annex4B*

*Diamond wire tools analysis:*

*CVW beads*:

***Figure 62*** shows the diamond segment used in the CVW plant. the SEM analysis was carried out both on the underlying segment and on the matrix that holds the diamonds. A composition based on Fe and Ni can be observed for the segment. The Fe / C group is part of steel called Martensite which makes up most of the steel used for the tools. However, there is a cover based on Ni and $Al_2O_3$ and SiC metal alloys, used for cutting tools for abrasive materials. The same

alloys are found in the bead matrix, but there is the presence of Co instead of Ni.

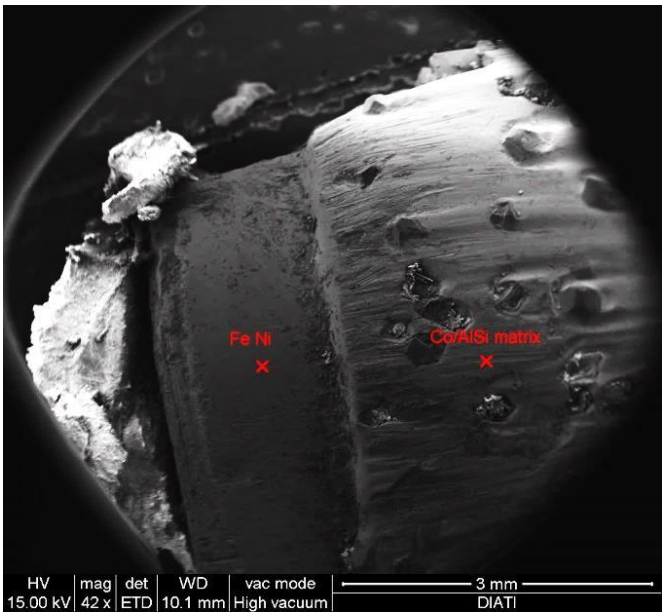


*Figure 62: SEM EDS analysis of diamond wire bead used in plant CVW. Magnification 42X. Left: FeNi composition of steel core of the bead. Right: Co-Al-Si metal matrix composition of the bead.*

***Figure 63*** and ***Figure 64*** shows the diamond analysis and the matrix that composes this tool at higher magnifications (500X). The spectrum of the diamond is composed only by the element C. While the spectrum related to the matrix sees the same composition found in the matrix found in ***Figure 62***, that is $Al_2O_3$, SiC and Co.

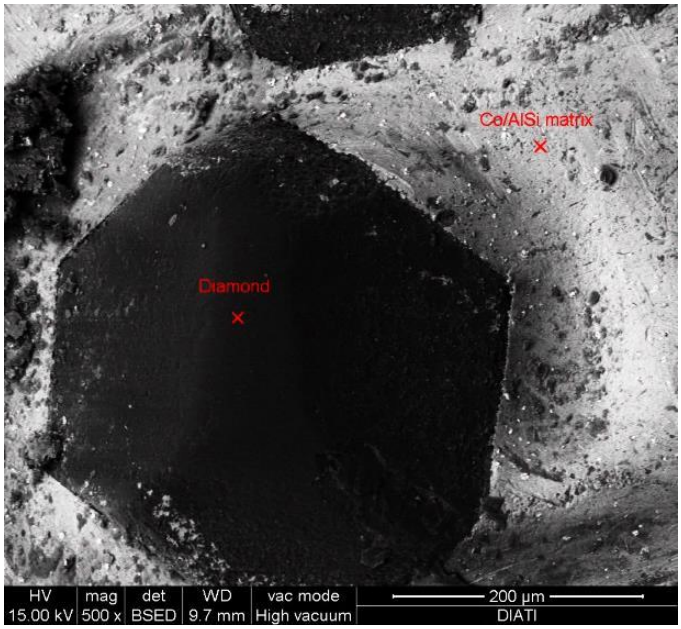


*Figure 63: SEM EDS analysis of diamond wire bead used in plant CVW. Magnification 500X. Left: Diamond. Right: Co-Al-Si metal matrix composition of the bead.*

In ***Figure 64***, instead, from diamond bead new elements are found, ie WC (tungsten carbide) and a Ti cover, used in some tools to protect the diamond from the graphitization phenomena and to improve its adhesion to the matrix.

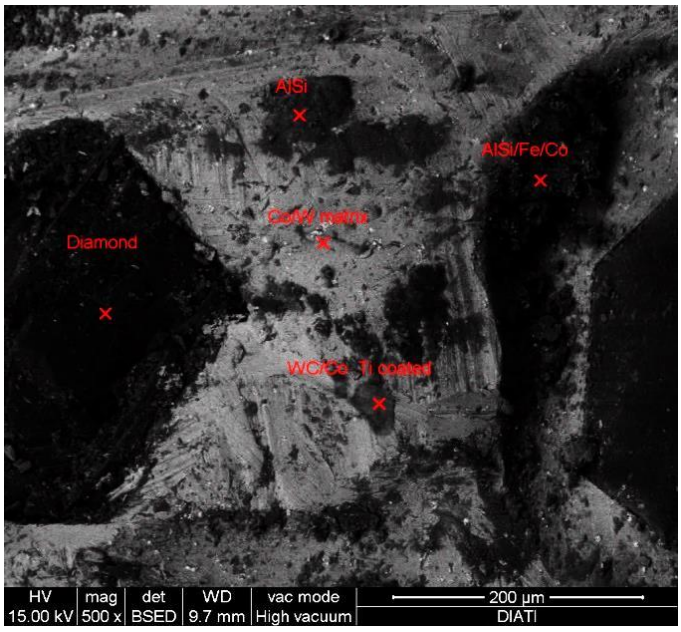


*Figure 64: SEM EDS analysis of diamond wire bead used in plant CVW. Magnification 500X. Left: Diamond. Centre upper: Al-Si metal matrix composition of the bead. Centre: CoW metal matrix; Centre-over: WC-Co metal matrix; Right: AlSi-Fe-Co metal matrix.*

***Figure 65*** is shown a hole left by the diamond removal. an analysis was carried out on the underlying elements and the presence of rock residues was found probably an amphibole, due to the presence of Na Mg Ca and K elements.

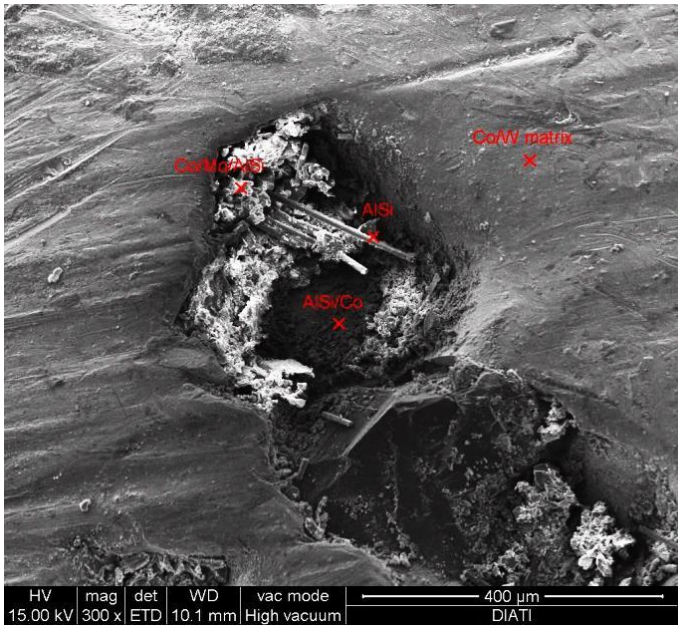


*Figure 65: SEM EDS analysis of diamond wire bead used in plant CVW. Magnification 300X. Centre: Diamond scaled;Centre upper: Co-Mo-Al-Si alloy. Centre: AlSi alloy; Centre-over: AlSi-Co alloy; Right: Co-W metal matrix.*

The analysis on the bead confirms what has been found in the chemical analysis and leaching test on the CVW sample. Cobalt is the main element constituting the beads used in this plant. From chemical analysis results, Cobalt is in higher concentration respect the other elements: 30.7 mg/kg and even in the

leaching test with 330 µg/l. It is an element outside the Regulation limits in the leaching test and outside the Regulation limits of Column A for the chemical test (Reference: **Table 38** and **Table 39**).

*TTW beads*:

The bead used in the TTW plant is different from the previous one. The SEM analysis was performed both on the diamond and on the bead matrix (***Figure 66***). The results obtained showed the presence of a matrix composed of Ni. This confirms what was found with the XRPD analysis performed on the TTW sludge sample.

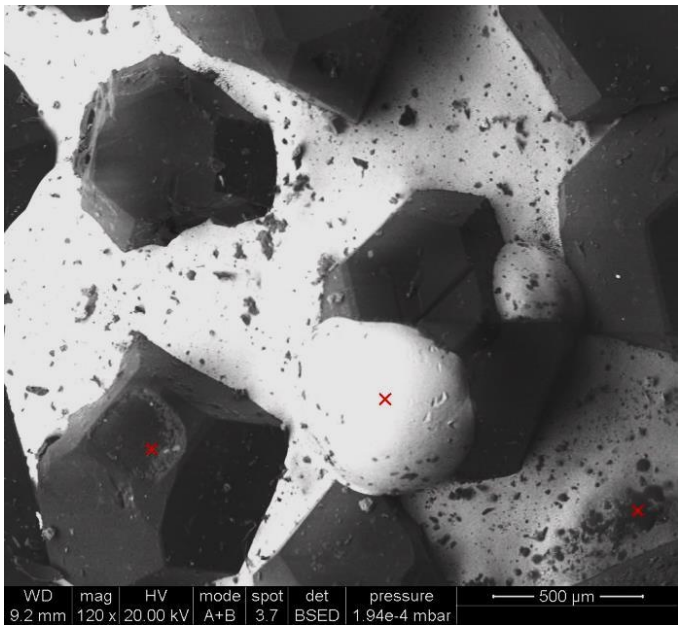


*Figure 66: SEM EDS analysis of diamond wire bead used in plant TTW. Magnification 120X. Left: Diamond; Centre and Right: Ni metal matrix.*

Analyzing the segment (***Figure 67***), the presence of the Fe/C group identified by Martensite steel was found, with some traces of Ni and Co. In the XRPD analysis, peaks of Iron oxide and Co in addition to Ni were found. This assert that despite the difficulties in recognizing so many phases, the analysis has been successful.


*Figure 67: SEM EDS analysis of diamond wire bead used in plant TTW. Magnification 44X. Composition of steel core bead.*

*Gangsaw metal grit analysis:*

*MVG metal grit:*

Regarding the gangsaw cutting technology, since a part of the blade could not be analyzed, the analysis was carried out only on the metallic grit used in the MVG plant. ***Figure 68*** shows the sphere of analyzed metal grit. The spectrum reported Fe Cr Ni Al Si O peaks. These elements correspond to those found during the XRPD analysis, ie Ferrite (Fe-Cr) and Silicon Chromium Iron ($CrFe_8Si$). The other elements, such as Ca and K could be residuals of mineral fraction remaining attached to the grit (Calcium Aluminum Chromium Oxide ($Ca_6Al_4Cr_2O_{15}$))(Reference: ***Figure 57***).

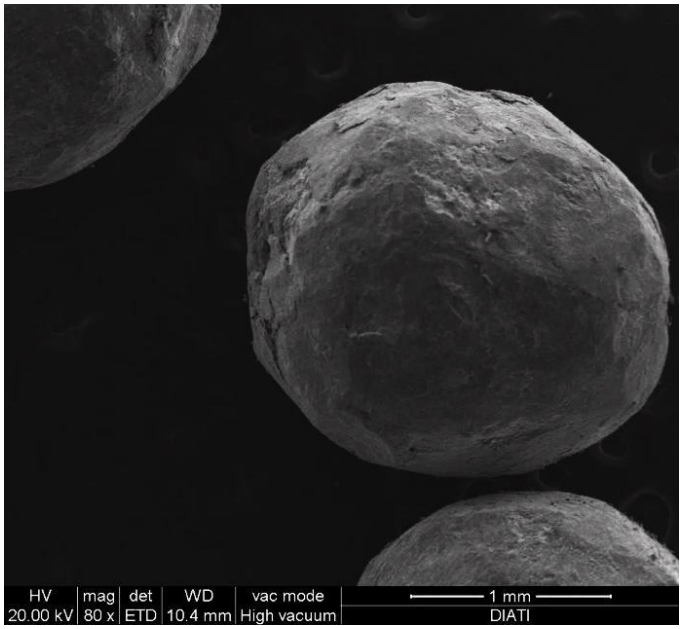


*Figure 68: SEM EDS analysis of metal grit used in gangsaw plant MVG. Magnification 80X. Composition of metal grit.*

From the chemical analyzes carried out on the sample MVG, a high concentration of total Cr (130 mg/kg) and Ni (86.5 mg/kg) was found; in agreement with the data of the SEM analysis; while in the leaching test there was a high concentration of Ni (10 µg/l), of total Cr (2.45 µg/l) and of V (10 µg/l) (Reference: ***Table 38*** and ***Table 39***). These elements are however in concentration lower than the Regulation threshold limit.

*Diamond blade segment analysis:*

*MCD blade segment:*

The first diamond disk segment analyzed refers to the one used in the MCD plant. The analysis was carried out on the matrix of the segment (***Figure 69*** and ***Figure 71***), from which the presence of the following elements has been found: SiC, Cu, CoMo, SnMoS, CoFe and elements referable to potassium feldspar as Na and K. Analyzing in particular in a hole left by scaled diamond the presence of the same metallic elements was found, but the presence of residues of feldspathic minerals was also found (***Figure 70***). This analysis reflects the analysis performed at XRPD except for the presence of Ni, not found neither at SEM nor in chemical analysis on sludge.

From chemical analysis an high concentrations of Cu (41.89 mg/kg), Zn (24.82 mg/kg), total Cr (18.21 mg/kg) and Co (26.15 mg/kg) was found. However, only the Co is outside the Regulation threshold limit of column A (Reference: ***Table 38***).

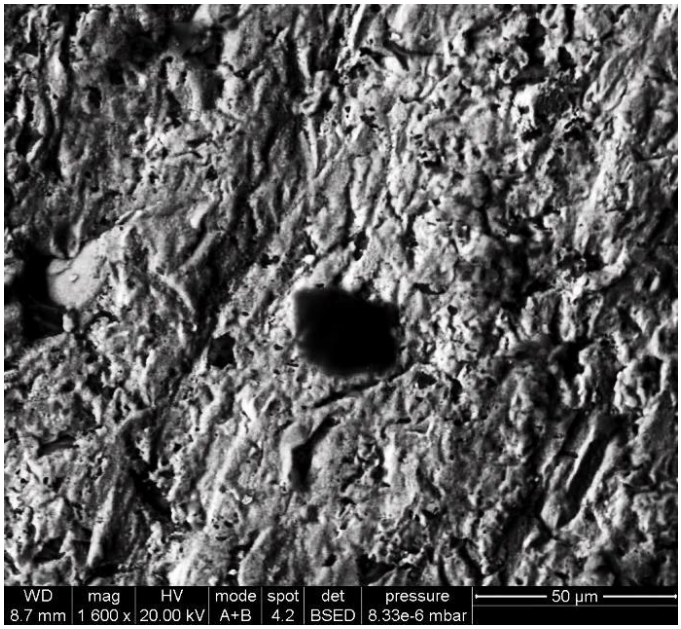


*Figure 69: SEM EDS analysis of diamond blade segment matrix used in plant MCD. Magnification 1600X.*

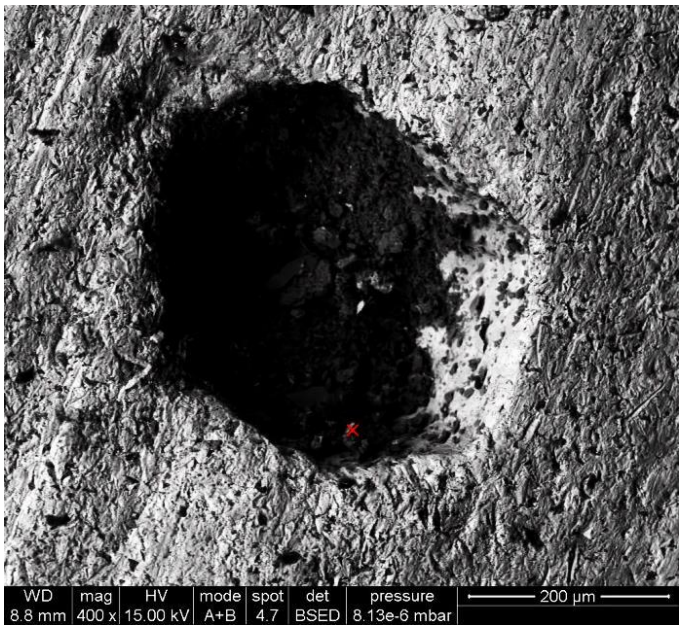


*Figure 70: SEM EDS analysis of diamond blade segment matrix used in plant MCD. Magnification 400X. Scaled diamond.*

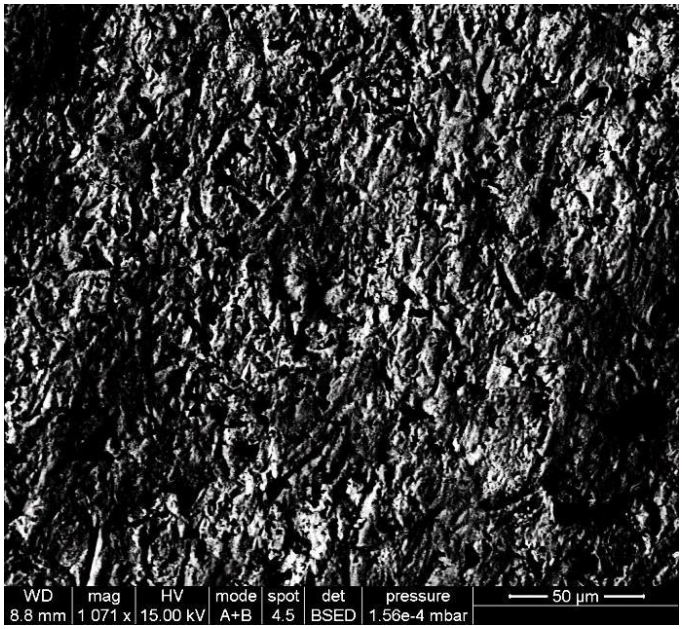


*Figure 71: SEM EDS analysis of diamond blade segment matrix used in plant MCD. Magnification 1070X. Metal Matrix.*

*PTD blade segment:*

The second diamond segment of the disc analyzed refers to the tool used in the plant PTD. ***Figure 72*** shows a generic picture of the diamond segment where the matrix wear comets can be observed.


*Figure 72: SEM EDS analysis of diamond blade segment used in plant PTD. Magnification 50X. General vision of segment – wear of segment.*

In ***Figure 73*** and ***Figure 74*** can be observed the matrix in particular where the spectra of metallic elements such as Cu, Sn, Ti, Fe and Co have been found.

Other elements such as Mg, K can be related to parts of mineral residues. From the chemical analyzes can be confirmed the presence of Cu (107.88 mg / kg) and Co (31.66 mg/kg), that have high concentrations, even if only the Cobalt is out of the threshold limits of column A (Reference: ***Table 38***) . From the leaching test, on the other hand, there is only a high concentration of Cu (17.96 mg/l) in this case outside the Regulation threshold limits (Reference: ***Table 39***).

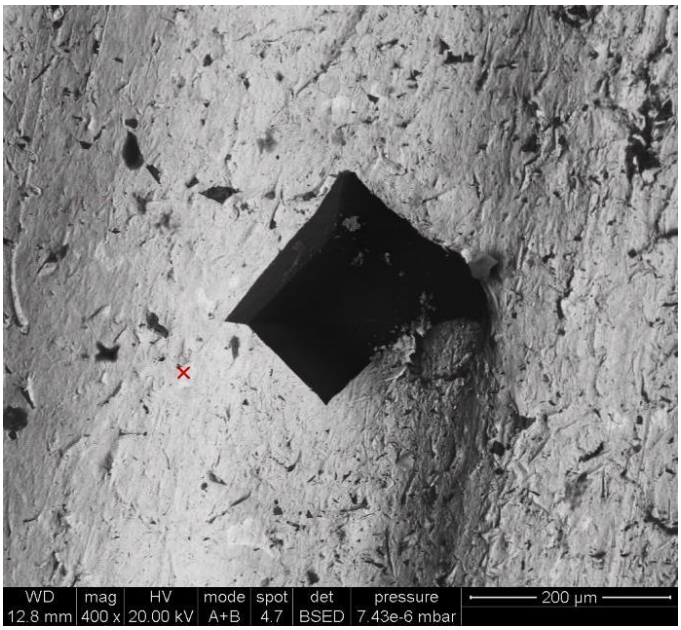


*Figure 73: SEM EDS analysis of diamond blade segment used in plant PTD. Magnification 400X. Metal matrix analysis.*

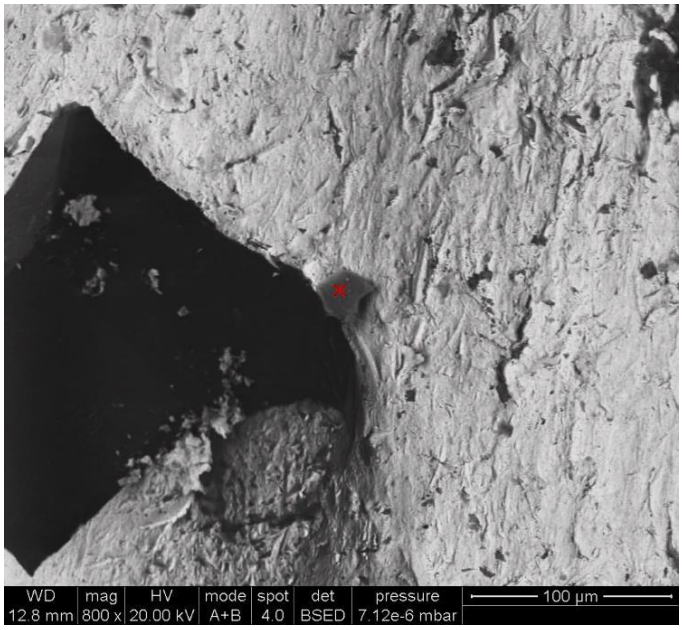


*Figure 74: SEM EDS analysis of diamond blade segment used in plant PTD. Magnification 800X. Metal matrix analysis.*

*SEM sludge analysis after magnetic separation:*

*MVG sample:*

SEM analysis performed on magnetic fraction of MVG sample show grain of metals related to metal grit part and an higher concentration of Biotite and Feldspar, due to the packing effect caused to very fine distribution particle size.

***Figure 75*** show the analysis performed on two grain. The grain at right side is a feldspar probably covered by metal parts. The spectrum show the presence of element that compose feldspar mineral and element, Fe and Co, that compose metal grit. The grain at left show a peak of Iron.

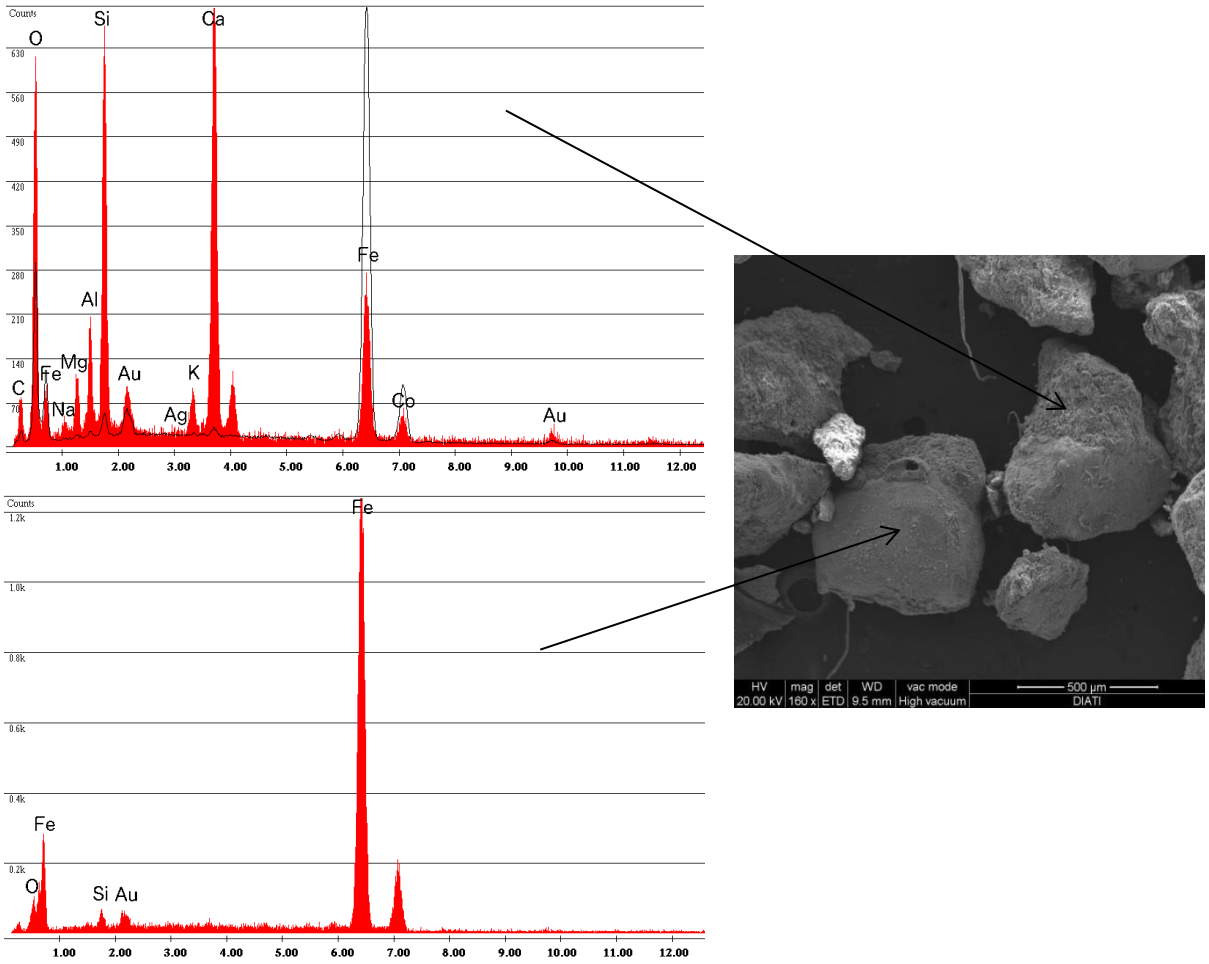


*Figure 75: MVG magnetic fraction sample – SEM analysis. Left upper: Spectrum of fledspar grain covered by metal part. Left below: Spectrum of iron grain. Right: SEM photo of the two selected grain.*

During the SEM test, MVG sample show many fine grains aggregated to form a bigger grain. This phenomenon involves in a difficult separation of the mineral and the metallic phase. An example is shown in the ***Figure 76***, where grains of feldspars are visibly incorporated in a ferrous matrix.

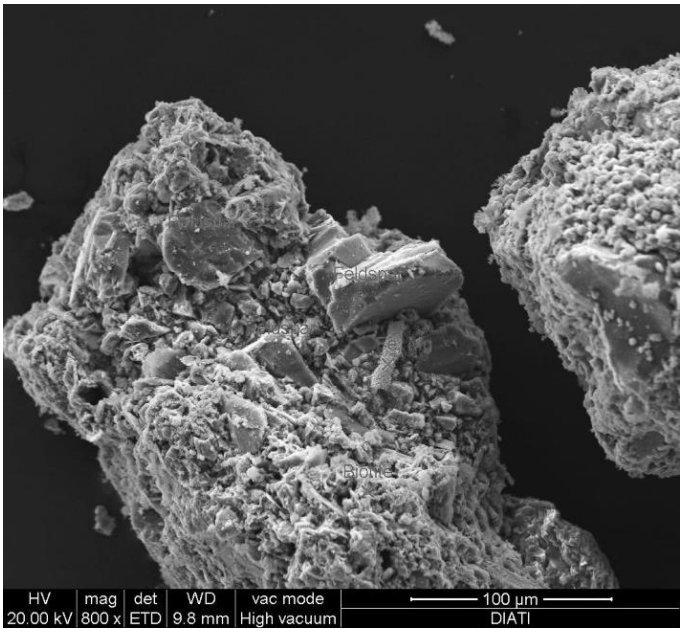


*Figure 76: SEM photo of MVG magnetic fraction sample. Aggregation of mineral and metal part.*

Biotite minerals which are paramagnetic minerals have been captured during the separation with the magnetic part deriving from the wear of the tools. An example is shown in the ***Figure 77***.

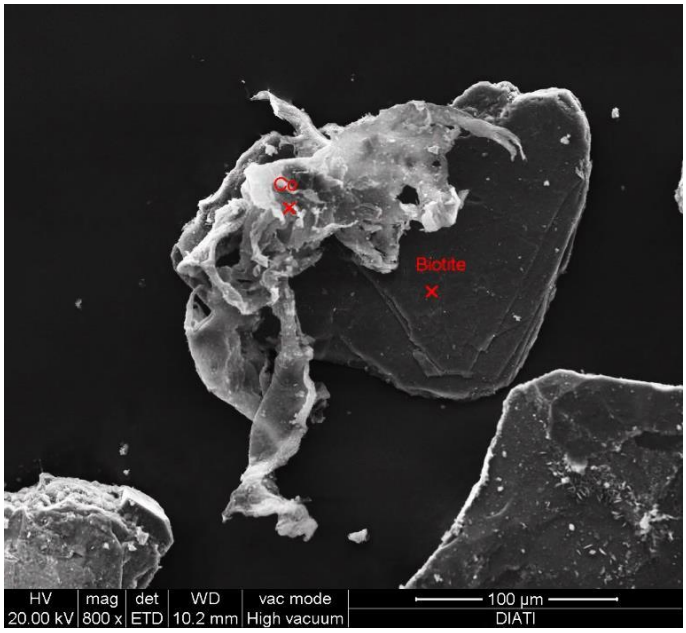


*Figure 77: SEM photo of MVG magnetic fraction sample. Biotite covered by cobalt metal part.*

*CTD sample:*

The CTD sample, as the samples deriving from the cutting with a diamond disc, show the presence of elements deriving from the wear of the diamond tool segment, that are: Ni, Fe, Cu, Cr, Mo, Co. The ***Figure 78*** and ***Figure 79*** show the photos and the spectrum found through SEM analysis.

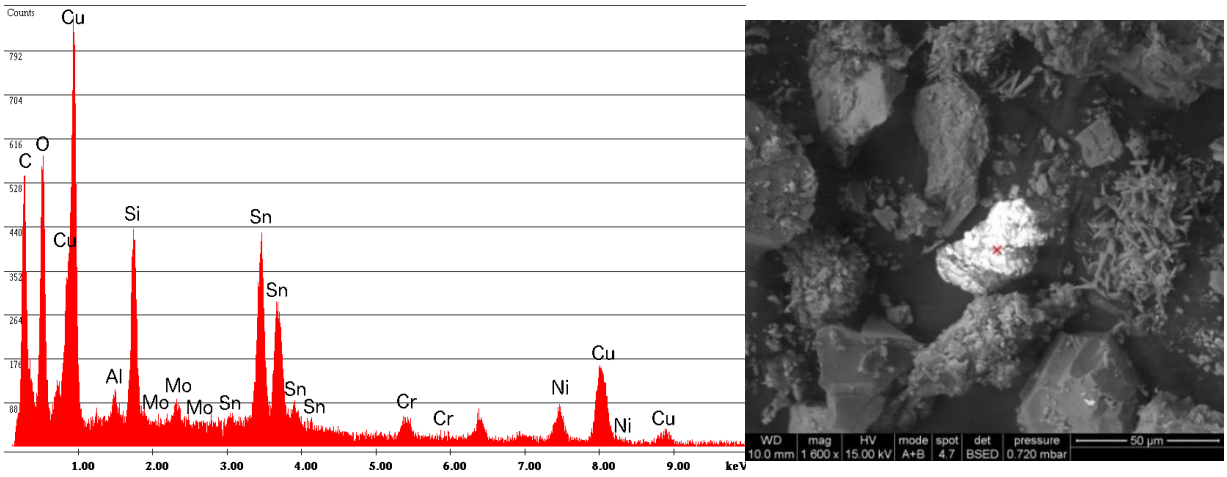


*Figure 78: SEM analysis of CTD magnetic fraction sample. Metal steel grain composed of Cr, Ni, Mo - constituent of diamond segment of diamond disc.*

The elements Cr, Ni and Mo are constituents of steels with the best mechanical characteristics. Steel composition, in addition to Fe and C, present percentages of Ni, Cr and Mo. The Ni promote hardenability[6] and toughness[7] properties; the Cr confers hardenability; Mo confers more breakage resistance. A grain of this alloy can be observed in ***Figure 78***.

In ***Figure 79***, instead, a metal chip composed of Fe, Co, Ni and Cu can be observed. These metal elements confer more ductility[8] to the alloy than Cr and Mo.

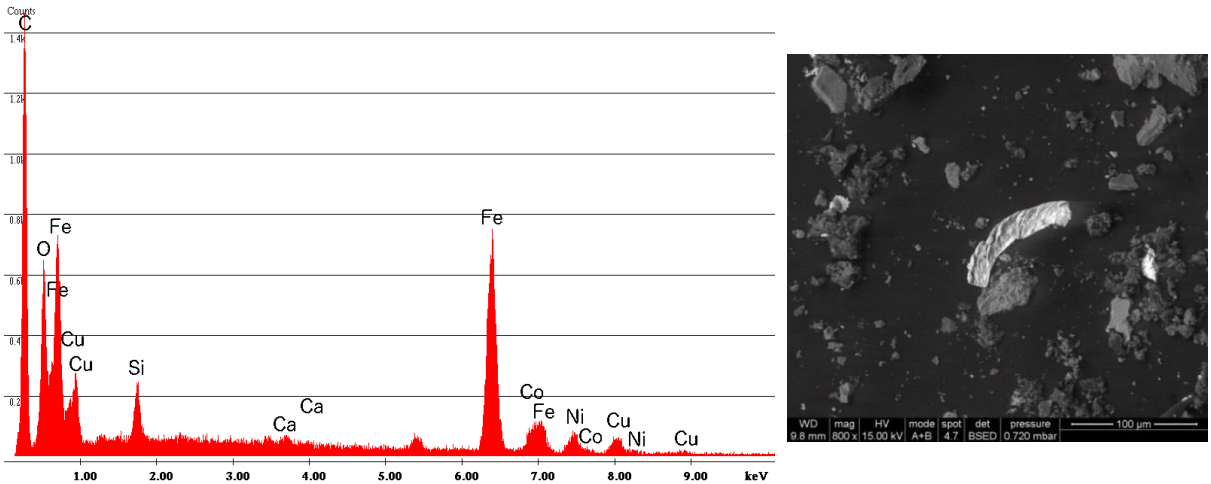


*Figure 79: SEM analysis of CTD magnetic fraction sample. Metal steel chip composed of Fe, Co, Ni, Cu - constituent of diamond segment of diamond disc.*

[6] ability of metals and metal alloys to change their structure following hardening treatment. Thanks to the hardening a material can be more harden or more soften.
[7] ability to absorb energy and to deform plastically before breaking.
[8] the aptitude of a material to be transformed into thin threads.

*TTW sample:*

The sample resulting from the cutting with diamond wire sees the presence of WC (tungsten carbide). The W gives greater hardness to the metal alloy, such as the Mo element. W and Mo in fact belong, together with the Cr, to the same group of the periodic table and have similar chemical characteristics. The shaving created during tool wear and its spectrum is visible in the ***Figure 80***.

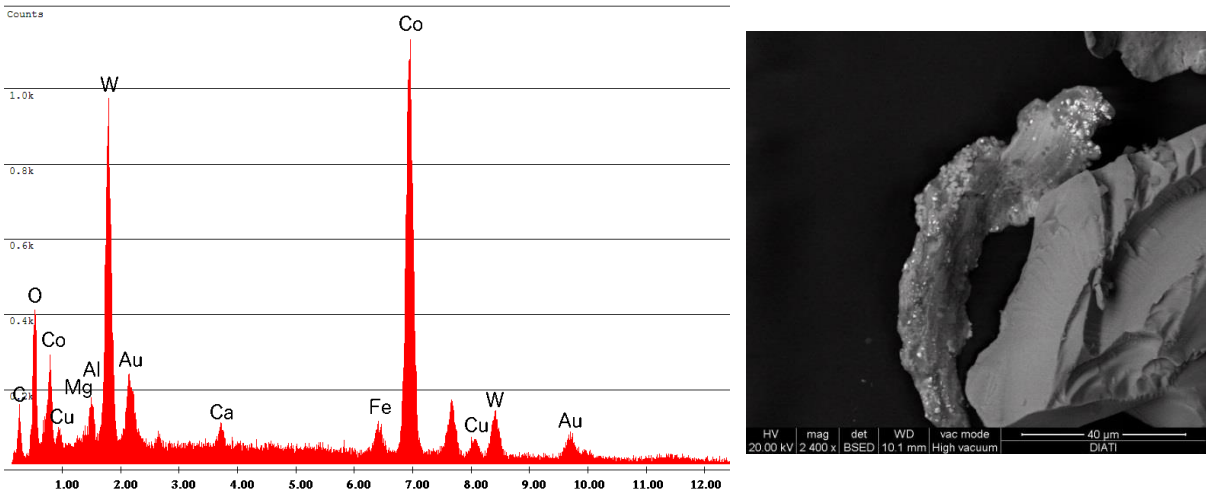


*Figure 80: SEM analysis of TTW magnetic fraction sample. Metal shaving fraction of diamond wire segment.*

In ***Figure 81***, the different form of tool residues is observed in which there is only the presence of Fe and Cr with Al and Si. They are formed as chip sheets, while residues of only Fe form more cubic grains.

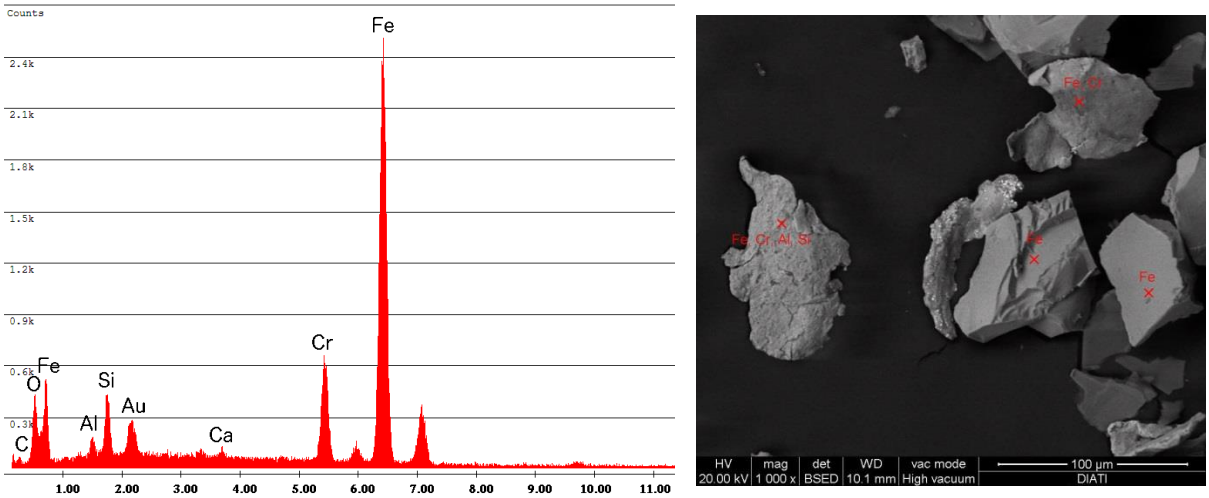


*Figure 81: SEM analysis of TTW magnetic fraction sample. Metal chips fraction of diamond wire segment and grain composed by Iron.*

*GVM sample:*

The GVM sample comes from a mixed cutting technology. In the magnetic

fraction there were whole spheres of metallic grit deriving from the cut with the gangsaw (***Figure 82***). In plants where the cutting technology is the gangsaw, normally, there is a separation by means of hydrocyclone, upstream of the sludge decantation tank, for the recovery of the metal grit to be reused during the cutting phase. In this case of cutting with mixed technology, probably, the separation system did not happen successfully, leaving metal grit spheres in the sludge. The spectrum shown in the ***Figure 82*** shows the classic Fe and Cr peaks belonging to the metal shot, with peaks of feldspar mineral.

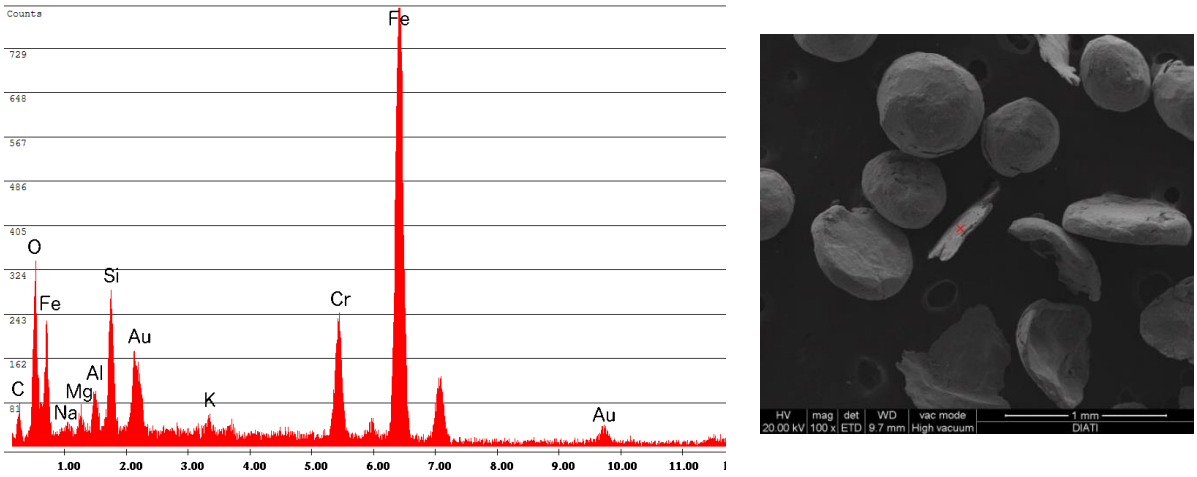


*Figure 82: SEM analysis of GVM magnetic fraction sample. Metal grit spheres of gangsaw cutting technology.*

In ***Figure 83*** and ***Figure 84*** are shown spectrum with elements of Ti and V, often used as a protects coating to improve adhesion of diamond with metal matrix.

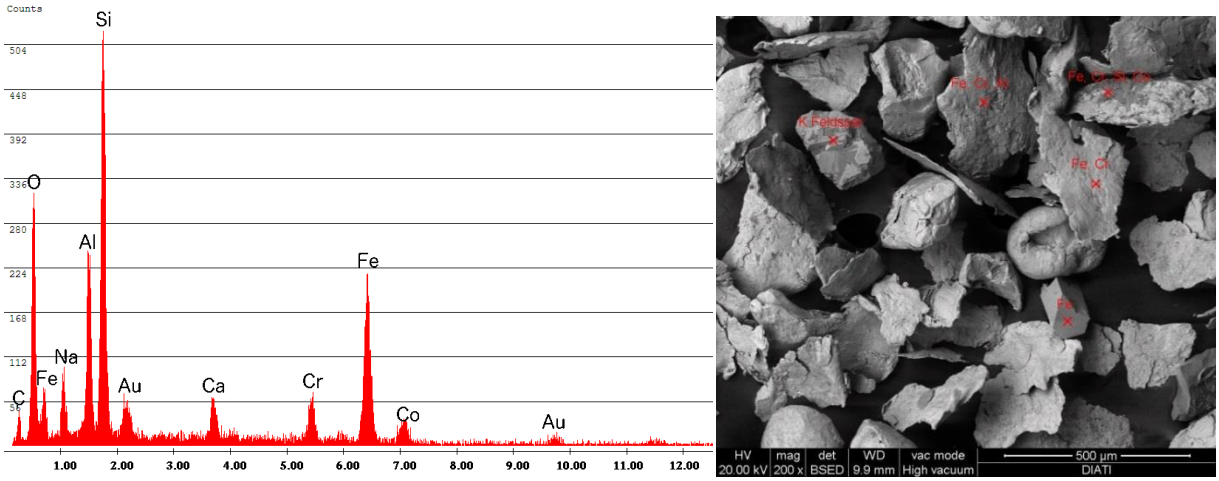

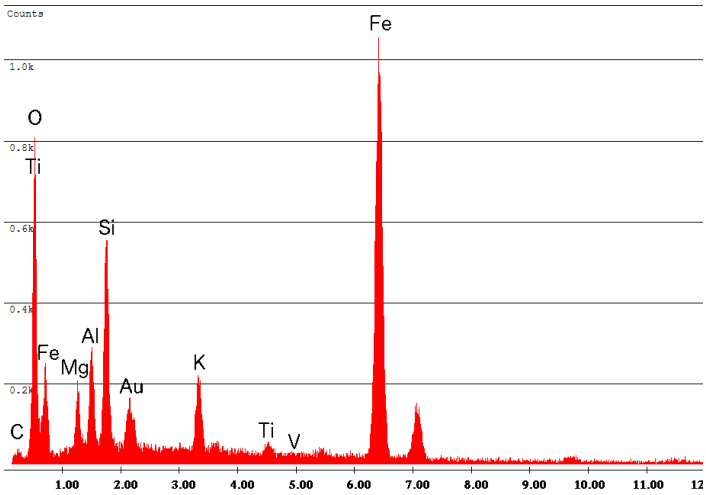


*Figure 83: SEM analysis of GVM magnetic fraction sample. Metal chips fraction and grain composed by Iron.*

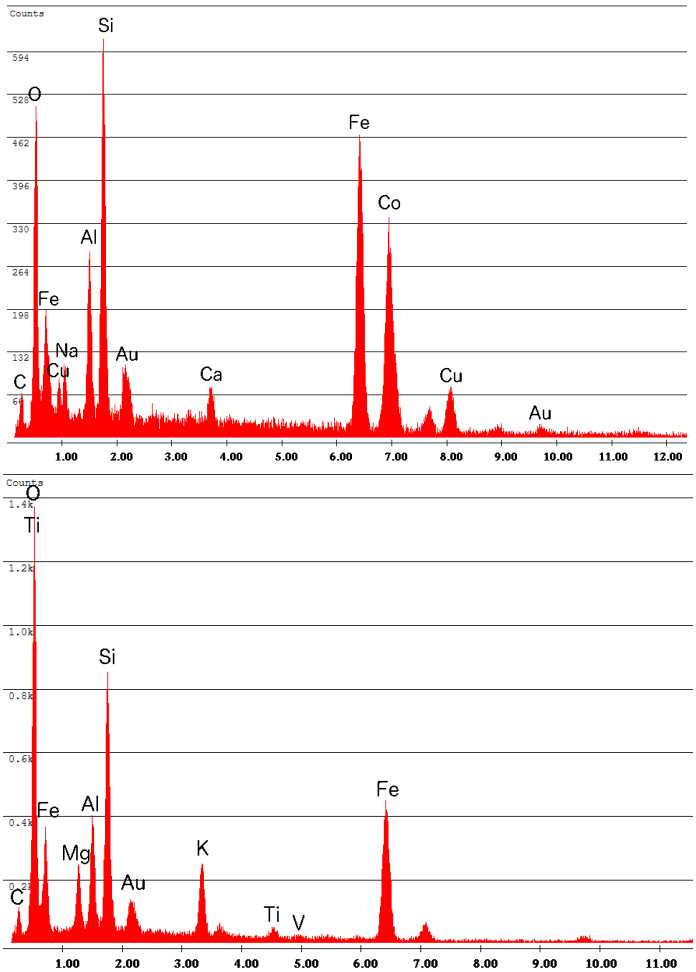


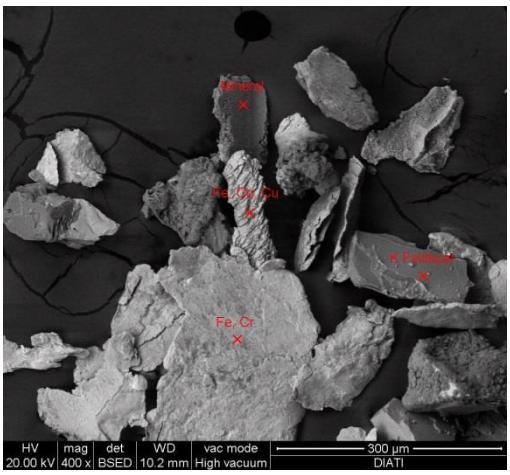


*Figure 84: SEM analysis of GVM magnetic fraction sample. Metal chips fraction and shaving composed of Ti, and V protects coating.*

***Figure 85*** shows a metal chip with a composition of WC, Fe, and Co, classic of the matrices of the segments of the diamond wire.

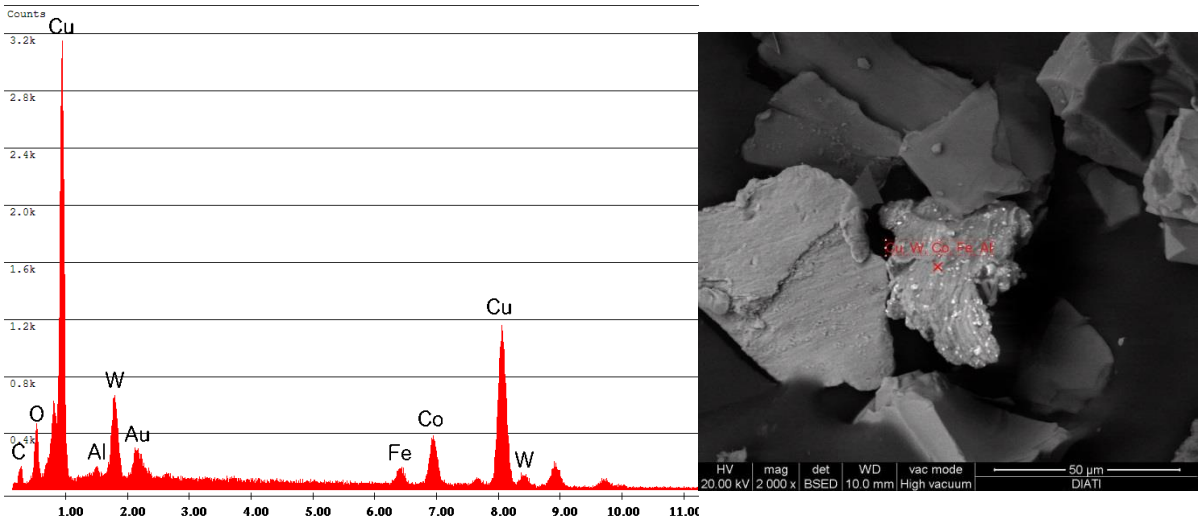


*Figure 85: SEM analysis of GVM magnetic fraction sample. Metal shaving composed by WC, Fe and Co of diamond wire tools.*

In ***Figure 86***, instead, a cubic grain of Molybdenum is represented. The difference in shape can be observed between the chips made of WC, Fe and Co respect to the cubic shape of Molybdenum. The Mo gives hardness properties to the alloy and therefore during the wear phase it is not reduced to shaving or chips as other alloys.

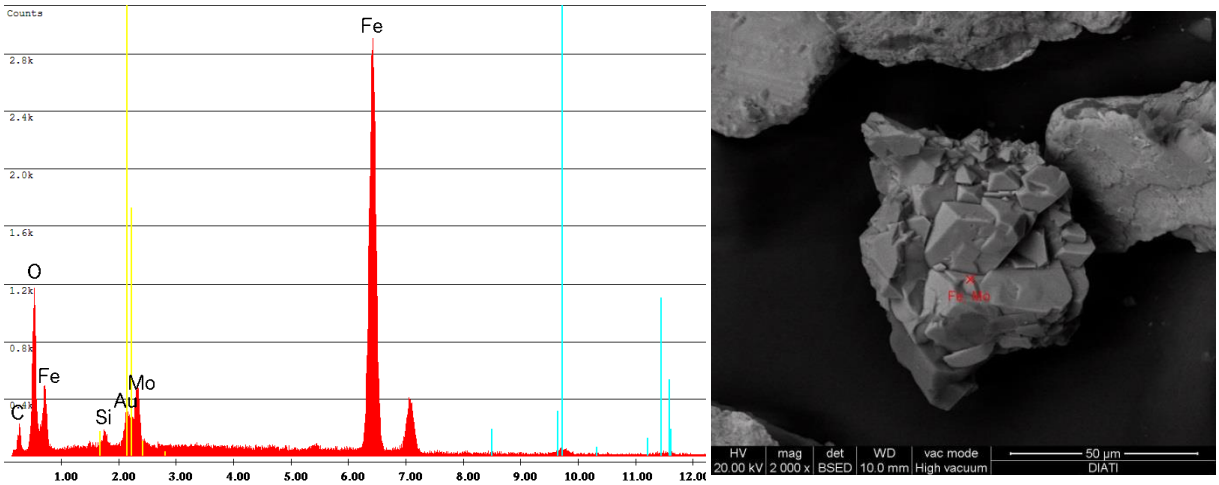


*Figure 86: SEM analysis of GVM magnetic fraction sample. Metal cubic grain of Molibdenum.*

# Chapter 5

# 5. Sawing sludge recovery

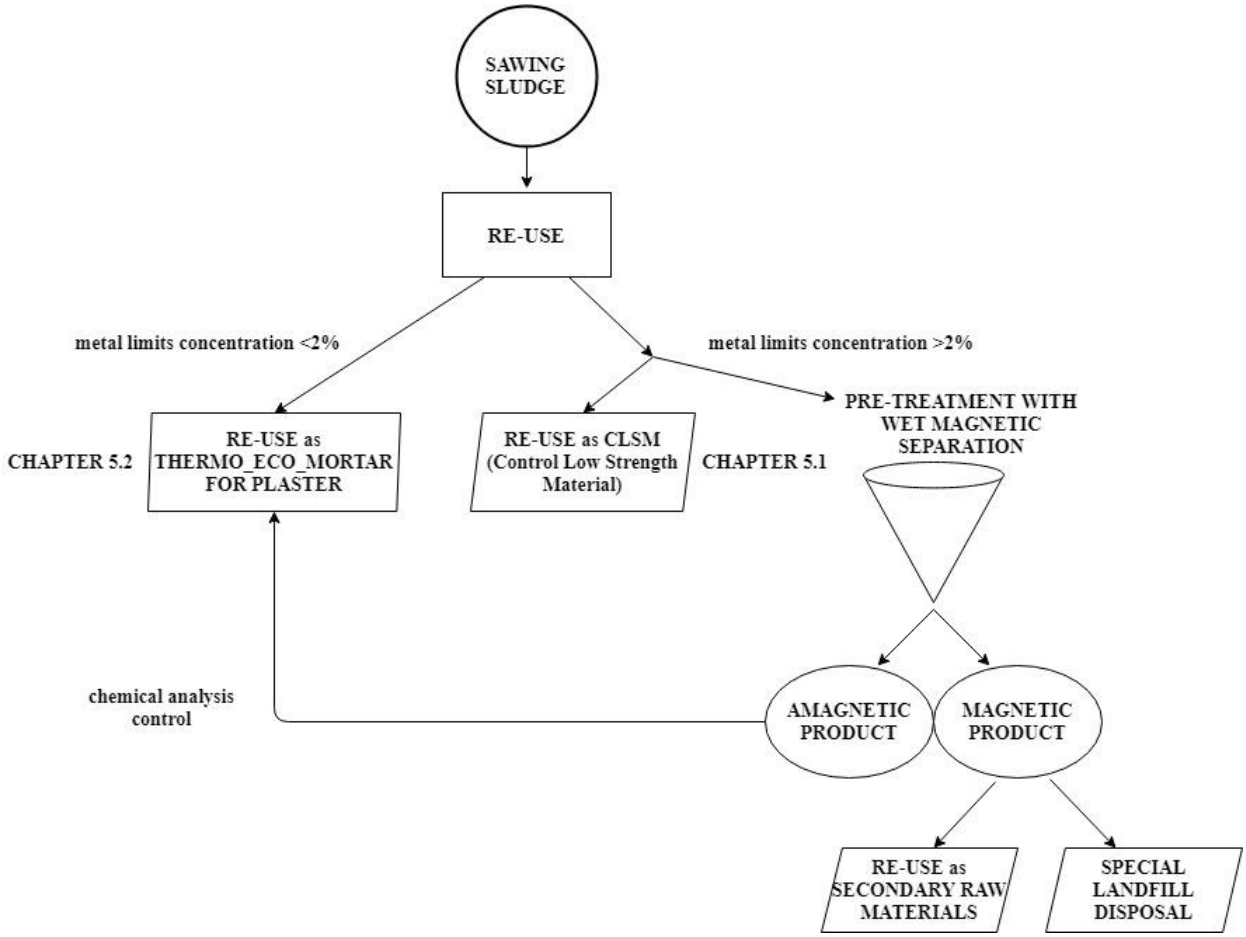


[9]

*Figure 87: Flowchart for reutilization process of sawing sludge, based on chemical-physical characteristics.*

The problem related to the reuse of sludge deriving from the cutting of ornamental stone is a relevant topic for many countries. The amount of material that can be recovered as a by-product for other processes is high and would be a considerable economic and environmental advantage. In literature many studies are carried out on the recovery of sludge resulting from cutting silicate rocks.

Dino et al., in 2006, carried out a study on the recovery of sawing sludge as loam. The sludge studied derived from Piedmont Region, in particular from Verbano Cusio Ossola district. Four different mixes were produced, introducing different quantities of sludge deriving from diamond technologies, from gangsaw

[9] It is specified that the recoveries were carried out on the following samples:
-for CLSM: MVG and GVM
-for thermo eco-mortar for plaster: MCD

technology, and a mix of both, added with green material, compost and natural loam. The mixes showed a decrease in the content of TPH compared to the sludge in the initial state and the concentration of metals is diluted and with a value below the Regulation limits. The result obtained showed good qualities of the substrate to be used in quarry remediation.

Husam D. Al-Hamaiedeh and Waleed H. Khushefati, in 2013, studied the effect of adding different amount of granite sludge powder in cement, mortar and concrete. They conducted two set of investigations: in the first they partially replace cement with the sludge with different mass ratio; in the second set they add granite sludge to cement with different mass ratio. They assert that the replacement of concrete cement by granite sludge not affect the mechanical properties of concrete and the adding of sludge to cement increase the compressive strenght of concrete.

S.V. Ribeiro et al, in 2014, studied the reuse of granite cutting sludge in soil cement bricks. They found that a replacement of soil with granite sawing sludge, in the range up to 30% wt., produce a soil-cement brick with good physical and mechanical properties.

Allam M. et al., in 2014, carried out a research on re-use of granite sludge for producing green concrete. They performed 6 mix, three replacing cement with sludge in different quantities and three replacing sand with sludge in different quantities. They concluded that granite sludge provides good cohesiveness of the mix due to the fineness particle size distribution of sludge. They also found that while the replacement of the sand with the sludge increases the mechanical properties of the concrete, the replacement of cement with the sludge produced a decrease of the mechanical properties.

Kamel Al Zboon and Jehad Al-Zou'by, in 2015, carried out a study for recycling stone cutting sludge in concrete mixes, substituting potable water with sawing sludge in slurry state. The results of replacement produced an increase of mechanical properties of concrete, but a reduction of slump value therefore a decrease of concrete workability.

In this Chapter we want to present different sawing sludge recovery possibilities on the basis of their physical-chemical characteristics. The choice of the type of recovery was carried out on the basis of chemical and magnetic separation analyzes carried out during the sludge characterization step.

A sludge recovery in the unaltered state is provided, to reduce any costs connected to a pre-treatment and to make the recovery economically advantageous for companies.

# 5.1 Control Low Strenght Material (CLSM)

The controlled resistance cement-based mortars are self-leveling cementitious materials mainly used as fillers as an alternative to traditional granular materials (ACI Committee 229R, 1994). They are indicated in the international literature by the term "Controlled Low-strength Materials CLSM", but are also recognized under different names such as flowable fill, controller density fill, flowable mortar and plastic soil cement. The technical documents ACI 229R-99, is a guidelines, that describe the requirements that a CLSM must possess in terms of resistance, permeability, constituent materials and their dosage ranges according to the objectives to be achieved; how it is transported and the pouring. The CLSM must satisfy specific properties that allow to distinguish it from other filling materials. These properties are as follows:

- *Flowability*: indicates the ability of a self-leveling material, without conventional self-compacting system, to easily flow and fill the voids. This parameter is determined by spreading tests on a plate, according to ASTM D 1603. The mixture must be fluid but at the same time without any segregation, fluid separation and the components must satisfy the requisites. Is necessary to find a good balance between the fluid and aggregate components of the mixture.
- *Time of hardening*: interval necessary for cement mortar to switch between plastic to solid state, reaching resistances capable of supporting a person's weight. Generally it takes 3-5 hours.
- *Pumping*: the equipment for the distribution of CLSM are the usual ones of ordinary concrete. The mixtures must have sufficient cohesion as they will be subjected to high pumping pressures. Furthermore, interruptions must be avoided and a constant flow must be maintained in order to not create segregation problems.
- *Resistance:* CLSM must ensure controlled mechanical strengths that do not increase over time, due to an easy removal without using demolition tools, thus saving time and costs. These resistance must be comparable with those of a traditional granular material used for trench filling.
- *Density:* higher compared with traditional compacting materials. The value are about 1840-2320 kg/m$^3$.
- *Thermal conductivity and insulation:* CLSM are not good insulators, but are characterized by high thermal conductivity due to high density. In this application, in which there are electric cables, a high density and a low porosity are required, for the heat dissipation produced by the cables. An increase of humidity and density, induce an increase of thermal

conductivity.

- *Permeability:* Typical values for CLSM are between $10^{-4}$ and $10^{-5}$ cm/s. Permeability increase as the cement materials decrease and the aggregate content increase. This value is similar to compacting materials value.
- *Retreat:* the values are between 0.002 and 0.05% and not affect the CLSM performance.
- *Excavability:* the limits of excavation may differ according to the constituents of the mix design. Mix with coarse aggregate are difficult to remove without mechanical tools despite low mechanical strength value. Mix with fine sand or fly ash have been excavated with mechanical tools with resistance up to 2.1 MPa.

CLSM is used as a fill instead of traditional compacting soils. Due to its characteristics of high fluidity and self-compaction it is ideal for use in tight and inaccessible areas where it is difficult to place and compress the material.

The main actual applications of the CLSM are sewage trenches, bridge shoulders, containment walls, road foundations, underground tanks, piping laying beds and thermal insulation with high-air-based cement mortar.

One of the most important aspects that has been considered in the following study is that concerning the effect of the thermal conductivity of the filling material on the performance of the transmission lines. Buried electrical cables at high voltage, driven by direct current, generates heat due to the electrical resistance and joule effect. Generally these cables reach high temperatures around 70°C and if the surrounding material is not able to dissipate heat, these increase and damage their functioning. The dissipation must maintain the operating temperature of the electric cable at safety levels compatible with the materials it is made of.

The factors that affect the temperature of the cable, listed by Sundberg, J., in 2016, are:

- Thermal properties of natural soil;
- Natural variations of temperature and temperature undisturbed in the ground;
- Thermal properties of a cable at different temperatures;
- Type of cable, wire size and number of cables;
- Depth of laying for cable;
- Distance between the cables;
- Sizing of electric power and its duration.

Generally the cable are placed in trench with depth 1.2 m. An example is reported in ***Figure 88.***

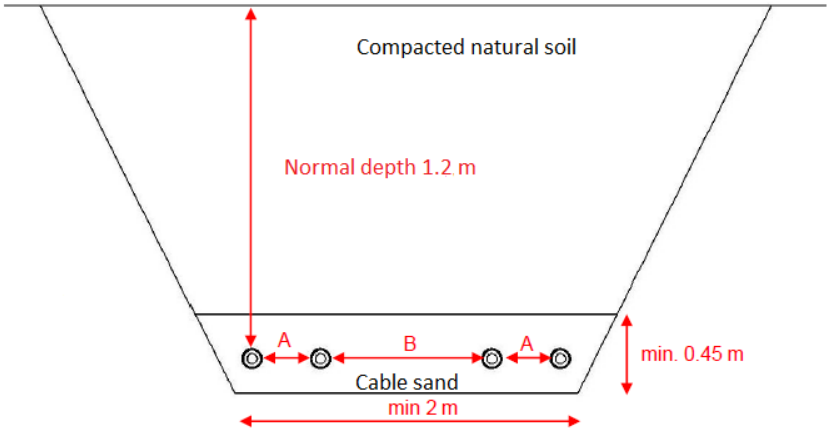


*Figure 88:Configuration example of electrical cable installation. (Source: Sundberg, J, 2016).*

The CEI 20-21of 2007 is the Italian technical regulation focused on the correct sizing of underground electric cables. The sizing and the depth of laying of the cables and the geometry of the excavation are established on the basis of the average thermal conductivity of the material used to cover them. Furthermore, the cable is designed for an electrical power (energy transport capacity) that generates a certain maximum temperature, related to the thermal conductivity of the filling material. Exceeding the design temperature may affect the service life of the cable. So the thermal conductivity value of the material used is of fundamental importance. The optimal material to be used must have a high thermal conductivity, to dissipate the heat quickly and a stable thermal conductivity, in the dry state, to guarantee the transmission performance of the cable throughout its life.

On the base on the requirements that the materials to be used in the CLSM must have, and following the results obtained during the sludge characterization step, two types of sludge was chosen for this application. Sludge sample derive: one from the cutting technology with gangsaw (MVG) and the other from mixed cutting technologies (GVM). These two sludge have an higher concentration of metals compared with those deriving from cutting with diamond tools and therefore could be more conductive.

In the following paragraphs the analyzes carried out on the sludge and on the aggregates used for the mix design of the CLSM are reported. Therefore the analyzes carried out on CLSM product to verify the correct performance of the sludge by comparing the two different typologies will be reported.

## 5.1.1 Sludge analyses for performance requirements on CLSM application.

The chemical-physical properties of MVG and GVM sludge, such as: particle size distribution, chemical analysis, leaching test and metal concentration are reported in Chapter 4 (Sludge characterization focus). In the following paragraphs the specific analyzes required for CLSM application are reported: quartz content and specific gravity.

### 5.1.1.1 Sludge quartz content.

Quartz is an excellent thermal conductor mineral, and for this reason it plays an important role for CLSM application. In plants MVG and GVM cut silicate stone such as gneiss, rich in quartz and feldspar. A calculation of the quartz content in the sludge is performed. For an easy identification of the quartz the analysis is carried out on each particle size distribution classes separately. The quantitative analysis was performed using the Image J software, already described in Chapter 4 paragraph 4.5.

On the particle size distribution classes lower than 0.106 mm (0.106 ÷ 0.075; 0.075 ÷ 0.038; <0.038 mm), 2 slides for each size class were performed for a total of 6 slides for sludge type. The slides were prepared by means of an oil with a refraction index of 1.550, perfect for the quartz identification. Each slide has been divided into 25 fields. Each field was photographed, through the Leika DMLP petrographic microscope, in two modalities: in phase contrast (PCOM) and in polarized light. In *Annex 5* are shown many photos used to performed quartz content analysis. The quartz grains were counted manually, while the diameter was measured using the ImageJ software (***Figure 90***). The identification of quartz through optical microscope is simple. In phase contrast quartz present a blue color with an orange halo and an irregular contour; in polarized light quartz present white color and an irregular contour. ***Figure 89*** shows an example of optical microscope quartz identification in the two modalities described above.

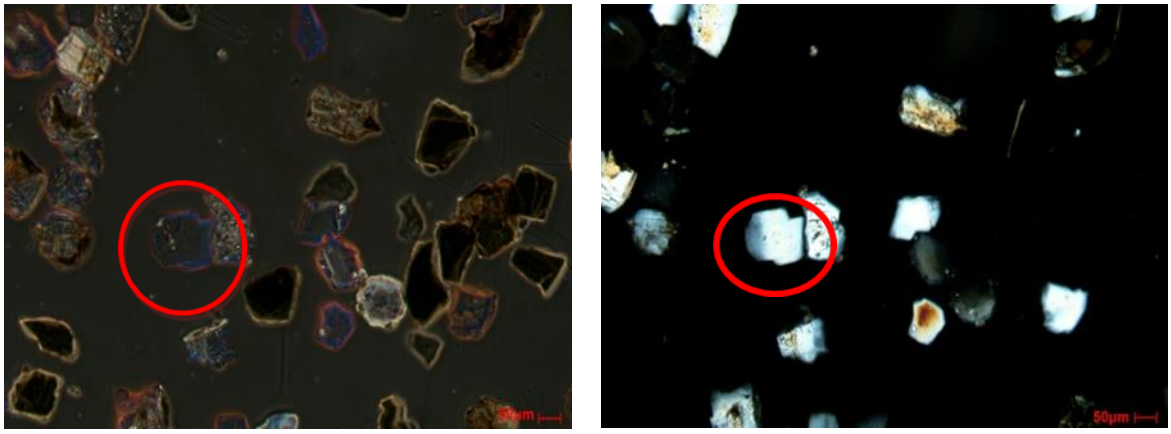


*Figure 89:Optical microscopic quartz identification. Sample GVM, particle size distribution class: 0.106÷0.075mm. Magnification 10X. Left: PCOM (phase contrast). Right: polarized light.*

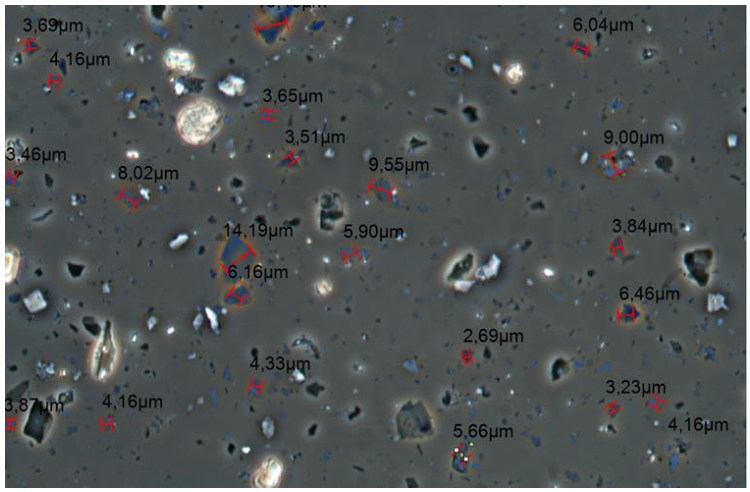


*Figure 90: Quartz diameter measurements, by means Image J software. MVG sludge sample – distribution particle size:<0.038mm – magnification 40X.*

On the particle size distribution classes >0.106 mm (>0.212; 0.212÷0.106), a macroscopic analysis was performed (***Figure 91*** and ***Figure 92***). 2 slides for size class were prepared, for a total of 4 slides for sludge type. Each slides have been divided in 25 fields, such as for the samples <0.106mm.

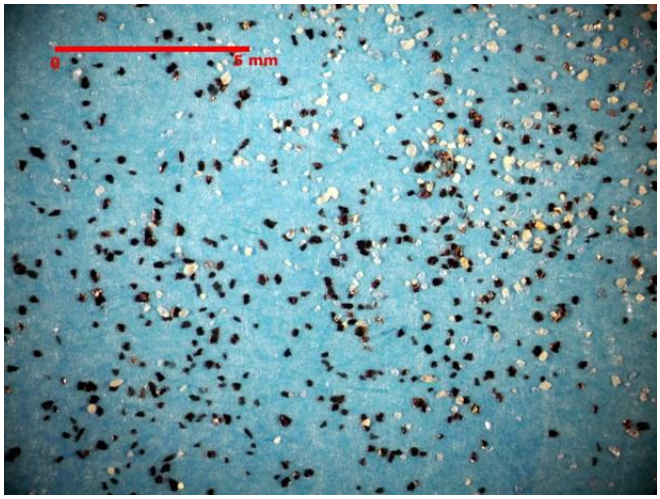


*Figure 91: MVG sludge sample macroscopic analysis. Distribution size class: 0.212÷0.106mm. Magnification 10X. Quartz grain in white colour.*

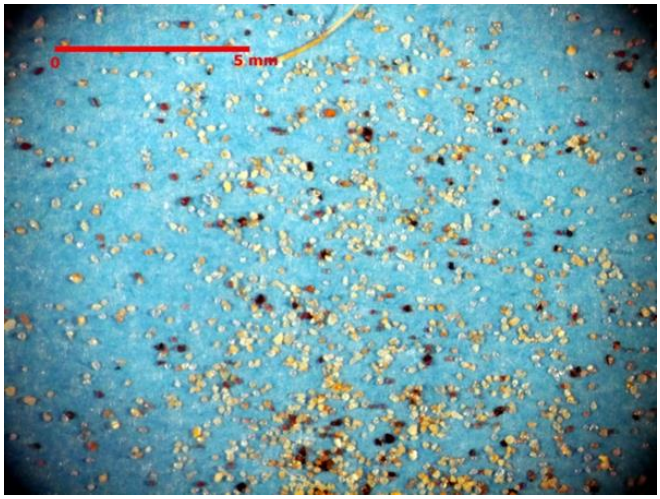


*Figure 92: GVM sludge sample macroscopic analysis. Distribution size class: 0.212÷0.106mm. Magnification 10X. Quartz grain in white colour.*

In order to quantify the weight percentage of quartz, respect to the other grains, the amount of initial powder deposited on each slide has been weighed and chosen based on the particle size distribution class and on the magnification used.

The parameters considered for the calculation of the percentage quartz content, in the sawing sludge, are the following:

- Weight of powder deposited on the slide [mg];
- Slide area occupied by powder [$mm^2$];
- magnification used;
- number of fields considered (25);
- area of 1 field [$mm^2$]
- diameter of the grains (calculated by means of Image J software) [mm];
- average density of quartz grains [2.6 $mg/mm^3$];
- volume of quartz grains (calculated by comparing quartz grain to a sphere);
- quartz grains mass [mg]

**Obtained results**:

***Figure 93*** and ***Figure 94*** shown the results of the quartz content calculation for GVM and MVG sample.

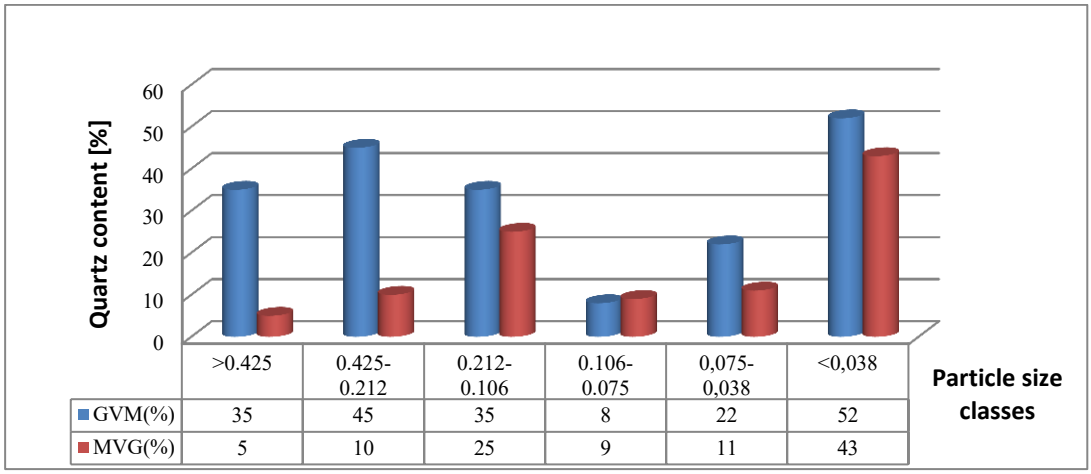


| | >0.425 | 0.425-0.212 | 0.212-0.106 | 0.106-0.075 | 0,075-0,038 | <0,038 |
|---|---|---|---|---|---|---|
| GVM(%) | 35 | 45 | 35 | 8 | 22 | 52 |
| MVG(%) | 5 | 10 | 25 | 9 | 11 | 43 |

*Figure 93:Quartz content of MVG and GVM samples divided for particle size distribution classes.*

GVM contains a greater amount of quartz as it cuts more silicate stones that have a quartz content ranging from 30 to 50%. MVG instead cuts only Serizzo which has a 30% quartz content. Observing the quartz content in the granulometric classes, an higher quantity is present in the finest class <0.038mm.

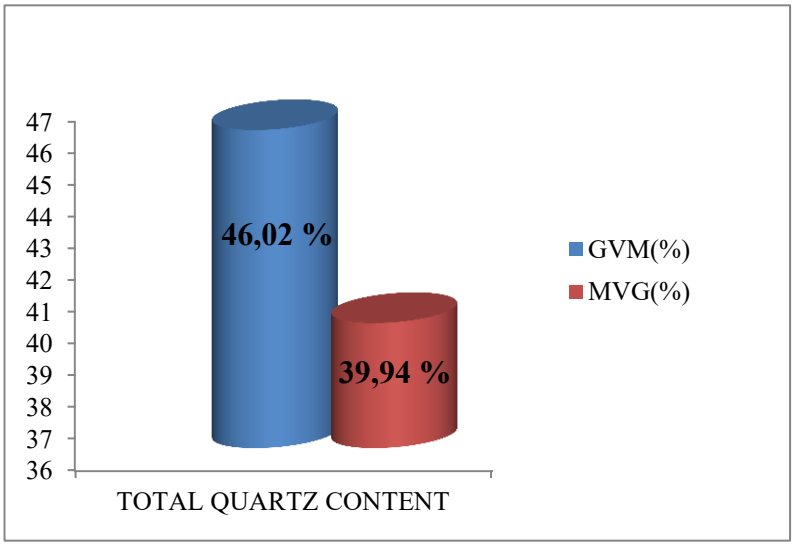


*Figure 94: Total quartz content in percentage for weight of MVG and GVM sample.*

### 5.1.1.2 Sludge specific gravity.

The specific gravity was measured using the Le Chatelier Flask method, as the sludge has a percentage of finer particle less than 0.075 mm, equal to 95.5% for MVG and 88.08% for GVM. Le Chatelier Flask is suitable for very fine material. The body holds about 250 ml and the bulb in the neck holds 17 ml. Graduations are 0-17 ml below the bulb and 18-24 ml above (***Figure 95***).

*Figure 95: Le Chatelier Flask according with standard EN 196-6 Methods of testing cement. Determination of fineness. (Source: http://multiserw-morek.pl/en/products,cement,le_chatelier_flask_en_196-6)*

**Obtained results**:

In ***Table 44*** are shown the results obtained from Le Chatelier Flask measures of specific gravity.

| Sample | Specific gravity [g/cm$^3$] |
|---|---|
| MVG | 2.67 |
| GVM | 2.74 |

*Table 44:MVG and GVM specific gravity results.*

## 5.1.2 Aggregates analyses for CLSM application.

The aggregates are the main materials that influence the performance of the CLSM. Its properties of strength, hardness, form, freezing, angulation are fundamental and must allow the concrete to achieve the best performance of both mechanical strength and durability, and workability and installation. The aggregates form the solid skeleton of the conglomerate. It is necessary to ensure that the aggregates and the fine particles are well matched, in order to fill all the interstitial voids formed between the coarse particles.

According to the legislation the fine aggregates are those with a diameter less than 4mm while the coarse ones are those with diameter higher than 4 mm.

The cement paste goes to occupy the remaining voids and once hardened it will transform the aggregate into a monolithic conglomerate.

For the construction of the mortars, aggregates were chosen with characteristics that increase the thermal conductivity and that allow a mechanical resistance comparable with that of traditional granular materials.

We opted to use quartzite with 90% pure quartz, to ensure a high thermal conductivity. Two are the distribution particle size classes chosen:

- quartzite with sizes 8-16 mm
- quartzite with sizes 0-8 mm.

The characterization of the aggregates (particle size distribution, specific gravity and water content) and the subsequent optimization of the parameters, are essential for the correct dosage to be considered in the mixture used to perform CLSM specimens.

In the following paragraphs particle size distribution, specific gravity and water content of the aggregates will be analyzed.

### 5.1.2.1 Aggregates particle size distribution.

Particle size distribution was carried out by means of sieves according to UNI EN 933-1. Two samples of quartzite were prepared:

-2 kg of quartzite with diameter 8-16mm;

-1.5 kg of quartzite with diameter 0-8mm.

Samples were first rinsed, in order to remove the fine particles, with a diameter less than 63 μm in order to know the percentage of fine particle required for the formulation of the mix-design. The material retained to sieve 63 μm was dried at 110 ° in the oven for 24 hours. The retained mass was measured and placed in a sieve column for the particle size distribution analysis. The cumulative percentage of passing mass of each class was determined to obtained the distribution particle size curve.

**Obtained results:**

***Figure 96*** shows the results obtained with the sieving analysis of quartz samples 0-8 mm and 8-16 mm.

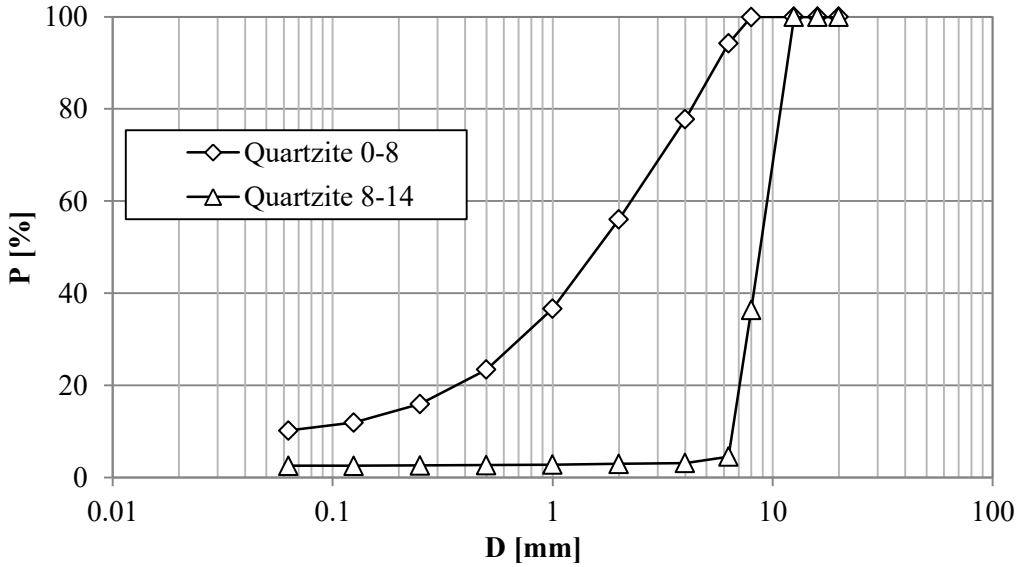


*Figure 96:Particle size distribution of Quartz aggregates (0-8 mm and 8-16mm).*

### 5.1.2.2 Aggregates specific gravity.

The specific gravity was performed using the pycnometer method, according with the UNI EN 1097-6: 2002 standard.

Two samples, with a mass of 600 g, were prepared for each class of quartzite. Following calibration of the vacuum pycnometer, the two quartzite samples were placed in and weighed with cap of pycnometer. Then air-free water was added up to a maximum of 30 mm below the cap joint. The instruments were placed under a vacuum pump for 4 hours, in order to remove all the air inside the instrument. Subsequently, distilled water was added to fill the entire volume of the instrument. The saturated tool with the aggregates is weighed again. Finally, the water temperature is measured with a suitable electric thermometer. The procedure was repeated twice for each sample of quartzite.

The formula applied for the determination of the specific gravity of the two quartzite is the following [16]:

$$specific\ gravity\ [\frac{g}{cm^3}] = \frac{(M2-M1)}{V-(M3-M2)/\ \rho_w} \text{.....[16]}$$

Where:

- M1 mass of pycnometer vaccum with cap;
- M2 mass of pycnometer+cap+aggregate;
- M3 mass of pycnometer+cap+aggregate+water;
- V pycnometer volume
- $P_w$ water density

**Obtained results:**

***Table 45*** show the results of the specific gravity analysis for the two samples tested.

| Material | $\rho_m$ [g/cm$^3$] |
|---|---|
| **Quartzite 0-8 mm** | 2.551 |
| **Quartzite 8-16 mm** | 2.662 |

*Table 45: Specific gravity of quartzite aggregate.*

The specific surface of two small grains is greater than the specific surface of a larger one. For this reason more air bubbles could be create around small grains than large grains. This could be the reason why the same material of different particle size distribution present difference in the specific density value.

### 5.1.2.3 Aggregates water content.

To determine the water content of quartzite aggregates, the samples under natural conditions were weighted. Subsequently they were placed in the oven at a

temperature of 110 °C for 48 hours. After drying they were weighed again. The difference between the two weighs after and before drying detects the water content.

**Obtained results:**

***Table 46*** show the results obtained with water content analysis for the two samples tested.

| Material | Water content [%] |
|---|---|
| **Quartzite 0-8** | 10 |
| **Quartzite 8-14** | 3 |

*Table 46:Water content of quartzite aggregate.*

# 5.1.3 CLSM mix design.

## 5.1.3.1 Mix design materials

Generally, CLSM contains water, Portland cement, fly ash, fine aggregates or coarse aggregates and additives. Some mixtures consist only of water, Portland cement and fly ash to avoid segregation.

The choice of mix design constituent materials is important because brings several advantages:

- fulfillment in terms of resistance and escavability:

- can be designed to achieve a 28-day compressive strength up to 8.27 MPa.

- can be easily excavated with conventional excavation equipment, maintaining its strength for filling needs.

- requires less inspection for its self-compaction feature.

- does not form voids during placing and does not stabilize or run under load (Smith A., 1991).

- versatility of the mix design:

- can be adjusted to meet specific filling requirements. Add more water to improve smoothness. Add more cement or fly ash to increase strength. Additives can be added to adjust setting times and other performance characteristics. Add foaming agents to produce a light insulating filling.

- cost reduction due to:

- use of by-products deriving from other processing waste, as in this context sawing sludge;

- easy retrieval of materials, using locally available by-products;

- the installation allows widen trenches due to self levelling requirements of CLSM (not require subsequent compaction).

- reduced equipment requirements as it can be installed without loaders or

rollers and does not require the storage of material (the trucks deliver the necessary quantities).

- can be placed quickly.

Materials used in this context are:

- Portland cement:

ASTM C150 standard suggests the use of Portland cement of type I or II. The purpose of the cement is to give cohesion and resistance to the mixtures. It influences the rheology of concrete, during preparation and installation, and mechanical strength.

For the following study, CEM I 42.5 R cement with a specific density of 3.15 g/cm$^3$ was chosen. That is Portland cement with a percentage of clinker of at least 95% and belonging to the 42.5 R resistance class.

- Additives:

Additive improving the performance of concrete. According to the UNI EN 934-2 standard, are defined as "a material to be added during concrete preparation in quantities no higher than 5% by mass on the cement content". Additives are composed of one or more chemical substances, of a polymeric and non-polymeric nature, for the most part of the cases dissolved and conveyed in water. They are classified according to properties that issue to concrete.

The additive used in this thesis work is called ADVA® Flow 455 and is a new generation superfluidifier, with a low effective dosage, to issue very high fluidity characteristics without segregation to cement mixtures. Generally this type of additives are composed of water-soluble polymeric substances with charged functional groups that have dispersing properties. Its fundamental properties are reduction of water content, avoids segregation and lump formation in the mix and increase in strength.

- Water:

Dosage and composition of water is crucial in order to ensure the required performance of the material. Water, with its chemical-physical properties, affect the concrete's life, ensures the hydration of cement, gives the concrete a certain plasticity and workability that allows an easy setting up. The main requirements that the water must have are: clarity and non-aggressive (free of salts such as chlorides and sulphates).

The water used is the tap water available at the laboratory. Suitable for preparing the mix due to the negligible content of dissolved salts and not compromise the hardening phase.

- Aggregates:

The literature prefers the use of fine aggregates compared to coarse ones. ASTM C33 standard define the aggregate requirements as follows:

- fine gravel with sand;
- aggregates with a maximum diameter of 19 mm;

- sandy soils, with a percentage of through-sieve opening 75μm greater than 10%;
- waste materials from quarries containing aggregates of a maximum size of less than 10 mm.

The aggregate used in this context are quartzite 0-8 mm and 8-16 mm for coarse aggregates; two different type of sludge: MVG and GVM for fine aggregates.

### 5.1.3.2 Mix Design dosage and flowability

The procedure for determining the mix is developed in three phases:

- optimization of the lithic skeleton starting from the particle size distribution of the aggregates through the reference curve Andreasen and Andersen equation model (1930), first adopted by Funk, J. E., & Dinger, D. R. ne 2013.;
- choice of the amount of cement, and additive dosage;
- dosage determination of the water/powder (w/p) ratio and mix design components.

*Lithic skeleton optimization:*

The optimization process purpose is to calculate the weight percentage of the aggregates to be included in the mix desing. The particle size distribution of each aggregate is applied with the project equations [17] and [18] and subsequently optimized in accordance with the modified Andreasen and Andersen reference curve [19] and [20]. The optimization process between the two curves is done using the solver tool command of Excel and is based on the least squares theory. In particular, the command calculates the value of the coefficients of the project equation that allows the associated curve to approach the reference curve.

The project equation are as follow [17] and [18]:

$$P_{P(Di)} = \alpha_{0-8} * P_{0-8} + \alpha_{8-16} * P_{8-16} + \alpha_{sludge} * P_{sludge} \quad [17]$$

$$\alpha_{0-8} + \alpha_{8-16} + \alpha_{sludge} = 1 \quad [18]$$

Where:

$P_i$ = material percentage passing through the diameter sieve;

$\alpha_i$ = coefficient of each aggregate used.

Andreasen and Andersen reference equation modified for self-covering concretes are as follow [19]:

$$P(D) = \frac{D^q - D_{min}^q}{D_{max}^q - D_{min}^q} \quad [19]$$

$$\sum [P(D) - P_P]^2 = \min \quad [20]$$

Where:

$P_i$ = material percentage passing through the diameter sieve D;

$\alpha_i$ = coefficient of each aggregate used;

$D_{min}$ = lithic skeleton minimum diameter;

$D_{max}$ = lithic skeleton maximum diameter;

q = adjustment coefficient.

In the modified A & A equation, the value of q depends on the workability condition that the CLSM must achieve. In particular the coefficient indicates the quantity of fine aggregates present and at an increase of q correspond a decrease of the fine aggregates. The value range of q is between 0-1 for very fluid mixtures. A value of 0.21 was chosen.

The smaller diameter of the particle that forms the lithic skeleton is 0.005 mm while the higher one is 12.5 mm, but the curves represented in figure 97 and 98 show particle size distribution from 0.063 mm because the optimization curves are determined starting from the particle size distribution of the aggregates (Reference UNI 933-1).

The value of the coefficients found, by means of SOLVER tools for each aggregate particle size distribution, is multiplied by one hundred to represent the percentage by weight of each aggregate in the mix design (***Figure 97*** - ***Table 47*** for GVM sludge and ***Figure 98*** - ***Table 48*** for MVG sludge).

*Obtained results*:

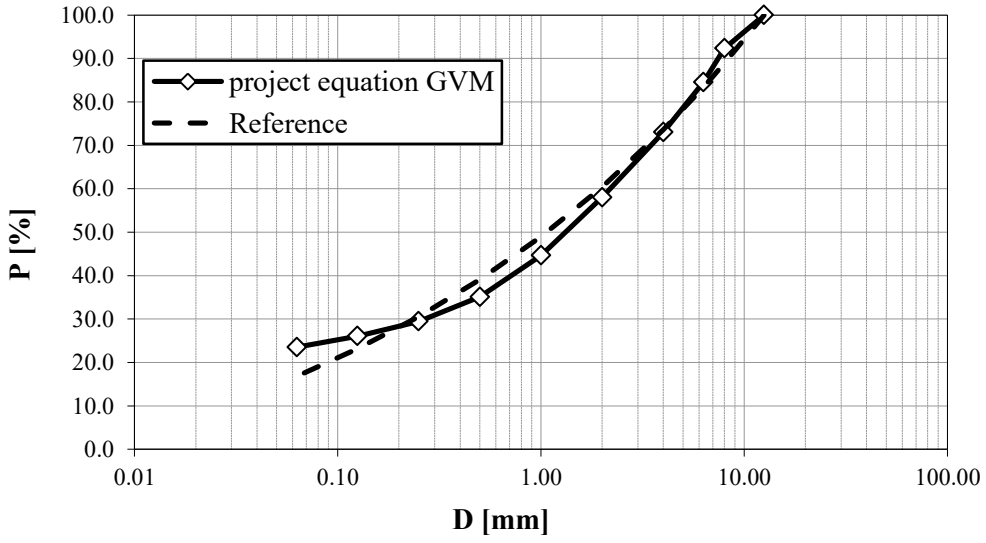


*Figure 97: GVM sludge project equation curve in comparison with reference curve by means of A & A equation.*

| Aggregates | % wt |
|---|---|
| **Quartzite 0-8 mm** | 69 |
| **Quartzite 8-16 mm** | 12 |
| **GVM sludge** | 19 |

*Table 47:Aggregates dosage calculated by means Excel Solver tool for GVM sludge.*

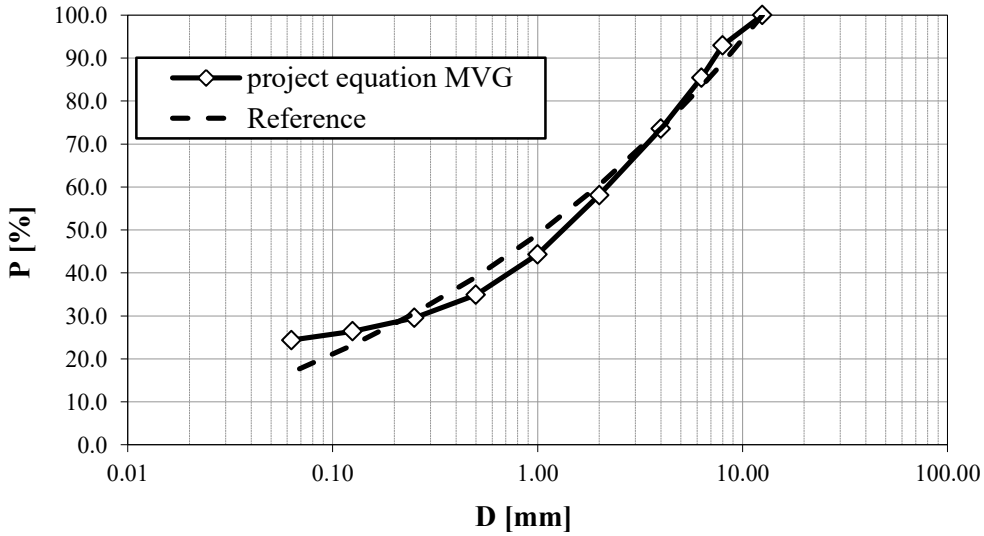


*Figure 98: MVG sludge project equation curve in comparison with reference curve by means of A & A equation.*

| Aggregates | % wt |
|---|---|
| **Quartzite 0-8 mm** | 71 |
| **Quartzite 8-16 mm** | 11 |
| **MVG sludge** | 18 |

*Table 48: Aggregates dosage calculated by means Excel Solver tool for MVG sludge.*

*Cement and additive dosage:*

The typical cement ratio value in the CLSM is equal to 30 – 120 [kg/m$^3$]. Generally a cement content of 50 kg/m$^3$ is fixed, but in this case it has been decided to proceed with both 50 kg/m$^3$ and 100 kg/m$^3$, to verify the influence of cement content on thermal conductivity.

The choice of the amount of additive depends on the aggregates characteristics. An additive value of 0.5 % respect cement dosage was adopted, according to Zisa G. et al., 2017 study.

*w/p ratio and mix design components dosage:*

In ***Table 49*** are reported the four mixes chosen with cement content 50 and 100 kg/m$^3$ for the two sawing sludge MVG and GVM.

| CLSM sample CODE | Cement content [kg/m$^3$] | Sawing sludge type | Additive [%] |
|---|---|---|---|
| **M50** | 50 | MVG | 0.25 |

| | | | |
|---|---|---|---|
| **M100** | 100 | MVG | 0.5 |
| **G50** | 50 | GVM | 0.25 |
| **G100** | 100 | GVM | 0.5 |

*Table 49:CLSM sample with cement content. Additive content and type of sludge used.*

The w/p (water and powder) ratio for each of the four mix was chosen by trial through the flowability test. The choice depends on the basis of easily workable mix, which self-expands and at the same time that there are no segregations between fluid and aggregates. For each of the four types of CLSM the following w/p ratios have been assumed: 0.6; 0.7; 0.75, 0.8, 0.85 and 0.9.

The mixes realized with the different w/p ratios are placed in molds to perform the flowability test. The mold consists of a cylinder with standardized dimensions (7.6 ± 0.3 cm of internal diameter and 15 ± 0.3 cm of height), anti-adherent, placed on a plastic plate measuring 40 x 40 cm (***Figure 99***). The cylinder is slowly lifted following a perpendicular movement respect the plate and the mix settle down on it with a circular shape. The average spreading diameter and disrupting effects are evaluated. The average diameter is the measure (cm) of the spreading diameter in the two direction that not exceed the 25 cm requirements.

*Figure 99: Standard cylindrical mold for the execution of the flowability test*

The flowability test is repeated with different w/p ratio until the requirement is met, according with the flowchart in ***Figure 100***.

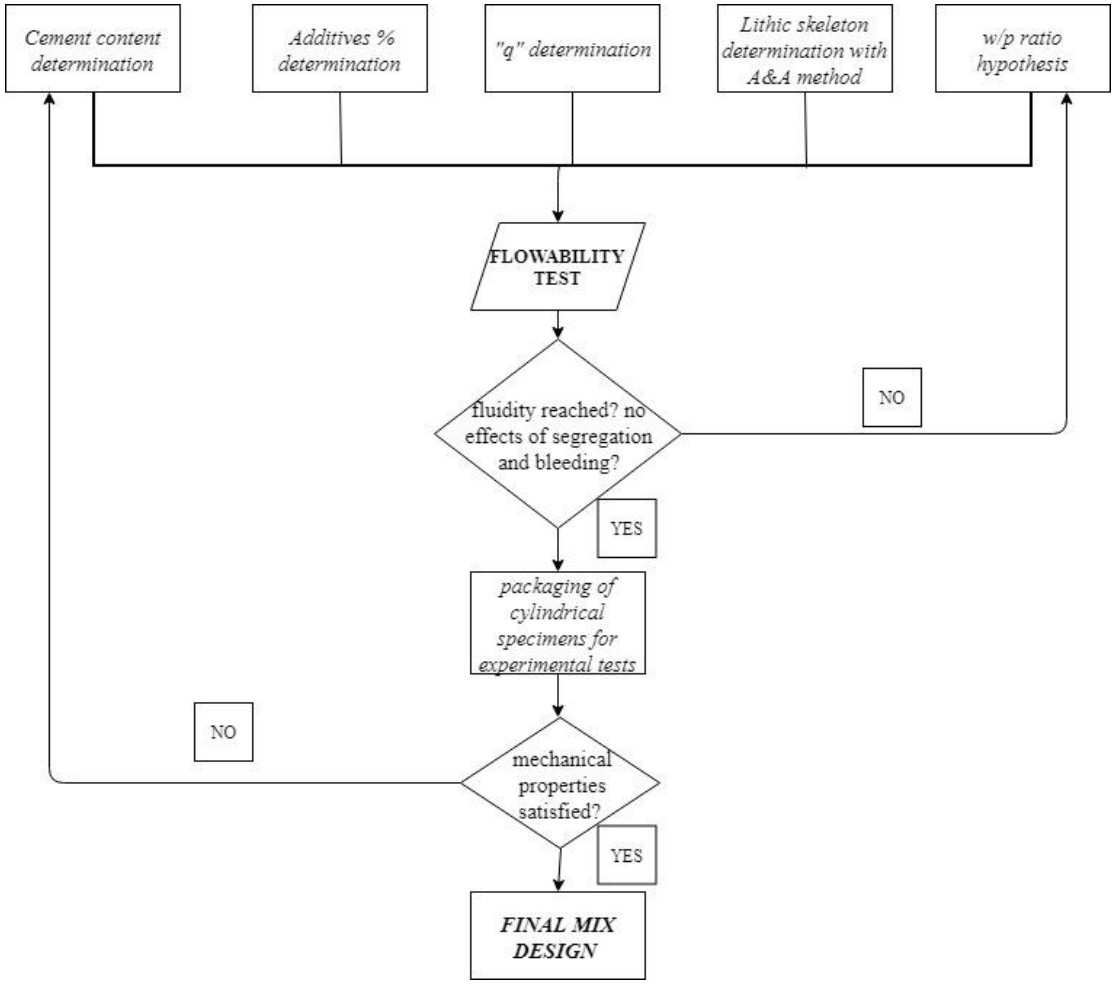


*Figure 100: Flowchart to perform mix design based on flowability test results.*

*Obtained results:*

***Table 50*** and ***Table 51*** shown the results of flowability test on MVG sawing sludge. M100 reports the optimal w/p ratio of 0.75, while for the M50 sample the best w/p ratio is 0.85. The optimal w/p ratio was chosen not only quantitatively but also qualitatively based on the segregation effect.

| **M_50** | | | | | | |
|---|---|---|---|---|---|---|
| **w/p** | 0.6 | 0.7 | 0.75 | 0.8 | **0.85** | 0.9 |
| **Flowability diameter [cm]** | 12 | 15 | / | 21 | **24** | 26 |

*Table 50:Flowability diameter of M 50 sample for the different w/p ratio. In bold the ratio choose for mix design.*

| **M_100** | | | | | | |
|---|---|---|---|---|---|---|
| **w/p** | 0.6 | 0.7 | **0.75** | 0.8 | 0.85 | 0.9 |
| **Flowability diameter [cm]** | 14 | 17.5 | **22** | 24 | / | / |

*Table 51: Flowability diameter of M 100 sample for the different w/p ratio. In bold the ratio choose for mix design.*

***Table 52*** and ***Table 53*** shown the results of flowability test on GVM sawing

sludge. Both sample G50 and G100 report the optimal w/p ratio equal to 0.75.

| G_50 | | | | | | |
|---|---|---|---|---|---|---|
| **w/p** | 0.6 | 0.7 | **0.75** | 0.8 | 0.85 | 0.9 |
| **Flowability diameter [cm]** | 12 | 19 | **25** | 27 | / | / |

*Table 52: Flowability diameter of G 50 sample for the different w/p ratio. In bold the ratio choose for mix design.*

| G_100 | | | | | | |
|---|---|---|---|---|---|---|
| **w/p** | 0.6 | 0.7 | **0.75** | 0.8 | 0.85 | 0.9 |
| **Flowability diameter [cm]** | 17 | 18.5 | **24** | 28 | / | / |

*Table 53: Flowability diameter of G 100 sample for the different w/p ratio. In bold the ratio choose for mix design.*

In ***Figure 101*** the influence of the cement content on the flowability test is shown. The mix design with cement content of 50 kg/m$^3$ show higher spread diameters than the design mix with a cement content of 100 kg/m$^3$. There is also a difference between the mixes performed with the MVG sludge compared to the GVM sludge. GVM sludge show higher value of diameter respect MVG sample.

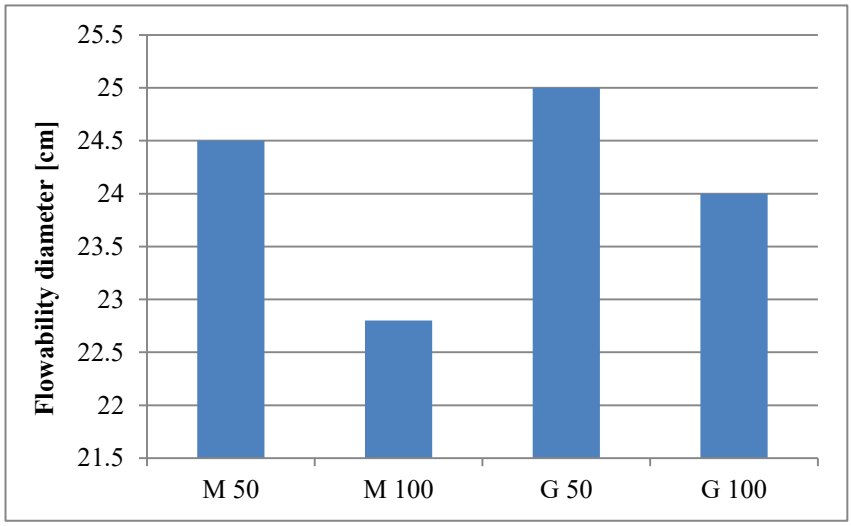


*Figure 101: Flowability diameter for all mix design in comparison.*

The calculation of the final dosage, of all the components of the mix, is determined through the corresponding density masses. For this calculation a reference model of 1 m$^3$ of mix composed by cement, aggregate, additive, water and zero voids was considered (***Table 54***, ***Table 55***, ***Table 56*** and ***Table 57***). Ratios w/p (water/powder), c/p (cement/powder) and w/c (water/cement) are reported.

| M 50 mix design | | |
|---|---|---|
| **Cement** | 50 | [kg/m$^3$] |
| **Quartzite 0-8** | 1236.3 | [kg/m$^3$] |
| **Quartzite 8-14** | 191.5 | [kg/m$^3$] |
| **MVG sludge** | 313.4 | [kg/m$^3$] |
| **Additive** | 0.25 | [kg/m$^3$] |
| **Water$_{tot}$** | 308.9 | [kg/m$^3$] |
| **W/P** | 0.85 | [%] |
| **C/P** | 0.14 | [%] |
| **W/C** | 6.18 | [%] |

*Table 54: Calculation of 1 m$^3$ sample for all component of M 50, with w/p ratio 0.85.*

| M 100 mix design | | |
|---|---|---|
| **Cement** | 100 | [kg/m$^3$] |
| **Quartzite 0-8** | 1212.8 | [kg/m$^3$] |
| **Quartzite 8-14** | 187.9 | [kg/m$^3$] |
| **MVG sludge** | 307.5 | [kg/m$^3$] |
| **Additive** | 0.5 | [kg/m$^3$] |
| **Water$_{tot}$** | 305.6 | [kg/m$^3$] |
| **W/P** | 0.75 | [%] |
| **C/P** | 0.25 | [%] |
| **W/C** | 3.06 | [%] |

*Table 55: Calculation of 1 m$^3$ sample for all component of M 100, with w/p ratio 0.75.*

| G 50 mix design | | |
|---|---|---|
| **Cement** | 50 | [kg/m$^3$] |
| **Quartzite 0-8** | 1236.9 | [kg/m$^3$] |
| **Quartzite 8-14** | 215.1 | [kg/m$^3$] |
| **GVM sludge** | 340.6 | [kg/m$^3$] |
| **Additive** | 0.25 | [kg/m$^3$] |
| **Water$_{tot}$** | 293.0 | [kg/m$^3$] |
| **W/P** | 0.75 | [%] |
| **C/P** | 0.13 | [%] |
| **W/C** | 5.86 | [%] |

*Table 56: Calculation of 1 m$^3$ sample for all component of G 50, with w/p ratio 0.75.*

| G 100 mix design | | |
|---|---|---|
| **Cement** | 100 | [kg/m$^3$] |
| **Quartzite 0-8** | 1166.7 | [kg/m$^3$] |
| **Quartzite 8-14** | 202.9 | [kg/m$^3$] |
| **GVM sludge** | 321.3 | [kg/m$^3$] |
| **Additive** | 0.5 | [kg/m$^3$] |
| **Water$_{tot}$** | 315.9 | [kg/m$^3$] |
| **W/P** | 0.75 | [%] |
| **C/P** | 0.24 | [%] |
| **W/C** | 3.16 | [%] |

*Table 57: Calculation of 1 m$^3$ sample for all component of G 100, with w/p ratio 0.75.*

## 5.1.4 CLSM final products analyses.

In the light of the results obtained with the flowability test and selected the mix design for the 4 samples M50, M100, G50 and G100 the specimens were prepared. Two cylindrical specimens per sample were prepared for a total of 12 specimens. The dimension of specimens is 200 mm by height and 100 mm by diameter. The aggregates were dried before their use in order to lose all the water contained. The ingredients are poured into a mixing device and after placed into the specimen holders (***Figure 102*** and ***Figure 103***).


*Figure 102:Left: mixing device used. Right: homogenous mix obtained.*

The procedure for preparing the mixes provides certain order of the components. First of all the cement is mixed with the sludge. After the aggregates and a quarter of the water with the additive already inside are mixed with cement

and sludge. After 5 minutes in which the mixing device is operated, is stopped to insert the remaining quantity of water. The mixing goes on for about 10 minutes until is homogeneous.

*Figure 103:Left: cylindrical specimens holder with dimension 200mm height and 100mm diameter. Right: specimens obtained after 24 hours of curing.*

The specimens produced have undergone two tests: the triaxial cell test and the thermal conductivity, described in the follow paragraphs.

### 5.1.4.1 Triaxial cell test with repeated load - Resilient modulus evaluation.

The "elastic" behavior of the CLSM, when subjected to repeated stresses due to the passage of vehicles, is important because affect the performance of the pavement. The Resilient Modulus ($M_r$) is an index that characterizes the elastic behavior of a material and is calculated using the triaxial repeated load test. The resilient modulus is a parameter required by the pavement layer thickness design equation.

The loads stresses, due to the passage of vehicles, induce vertical, horizontal and tangential tensions in the layers of the road foundations. These tensions change according to a law that can be assimilated to a sinusoid. The response of unbound materials, such as CLSM, under a generic load cycle, is shown in the ***Figure 104***.

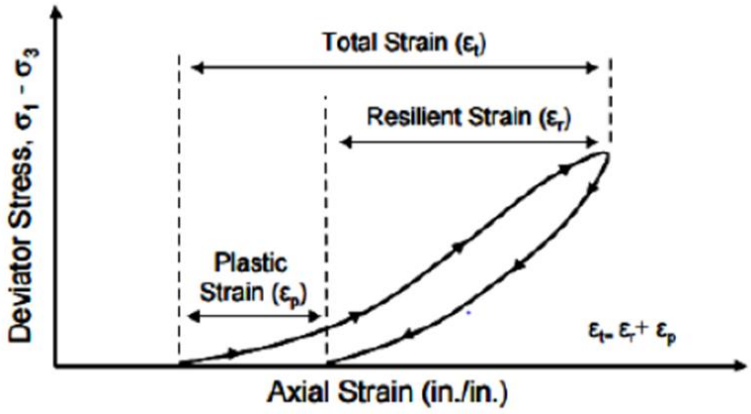


*Figure 104: Tension-strain graph of a non-binding material subjected to load stresses.*

During the loading phase the non linear behavior of the material is observed. The rigidity module is not constant but is a function of the stress state. In the unloading phase, not all the deformation is recovered. The deforming response, of unbound materials under cyclic loads, is characterized by a recoverable component (resilient strain) and a residual component (plastic strain). A soil subjected to several load cycles will provide a reduction of plastic deformation component and a settle of resilient deformation component.

The triaxial test with repeated loading is the best approximation of the stress-strain regimen. The test is performed in accordance with the AASHTO T307 standard. The standard provides that the specimens subjected to the test have a height twice the diameter and 28 days of curing. The device used for the test is shown in the ***Figure 105***.


*Figure 105: Triaxial cell with repeated load device used for the test.*

The device is composed of a cell where is placed the specimen, covered with an impermeable sheath and confined above and below by means of two porous stone disks (***Figure 106***).


*Figure 106:Specimen in the triaxial cell device.*

The cell transmits an isotropic constant pressure ($\sigma_3$) to the lateral surface of specimen, while the bases the specimen is subjected to a pulsating pressure $\sigma_1$.

$$\sigma 1 = \Theta + \sigma 3 \text{ …..[21]}$$

Where:

Θ is the deviatoric axial force due to a piston which generates cyclic pulses by means of compressed air.

The electronic load cell is designed to measure q force and is located between the actuator and the piston. To the left and right of the piston there are two LVDT transducers which convert the vertical movement into electrical signals and then measure the axial strain. According to the standard, load cycles consist in a load phase with a duration of 0.1 seconds (impulsive character), then there is a rest period of 0.9 seconds, then the $i^{th}$ cycle has a duration of 1 second.

The first phase is the specimen conditioning, that consist in 500 pulses generated to eliminate the contact imperfection between specimen-plates interface. Conditioning phase furthermore eliminate the effects generated in the time interval between compaction of specimen and the start of the test. Subsequently, the specimen is subjected to loads of 15 sequences of 100 pulses each and the average deformations recovered for each LVDT are recorded separately for the last five cycles. Load sequences are performed according to ***Table 58*** with subbase/base load sequence.

| Test Sequence | SUBGRADE | | | SUBBASE/BASE | | |
|---|---|---|---|---|---|---|
| | Confining Pressure (psi) | Deviator (Axial) Stress (psi) | Bulk Stress (psi) | Confining Pressure (psi) | Deviator (Axial) Stress (psi) | Bulk Stress (psi) |
| 0 | 6 | 4 | 22.0 | 15 | 15 | 60.0 |
| 1 | 6 | 2 | 20.0 | 3 | 3 | 12.0 |
| 2 | 6 | 4 | 22.0 | 3 | 6 | 15.0 |
| 3 | 6 | 6 | 24.0 | 3 | 9 | 18.0 |
| 4 | 6 | 8 | 26.0 | 5 | 5 | 20.0 |
| 5 | 6 | 10 | 28.0 | 5 | 10 | 25.0 |
| 6 | 4 | 2 | 14.0 | 5 | 15 | 30.0 |
| 7 | 4 | 4 | 16.0 | 10 | 10 | 40.0 |
| 8 | 4 | 6 | 18.0 | 10 | 20 | 50.0 |
| 9 | 4 | 8 | 20.0 | 10 | 30 | 60.0 |
| 10 | 4 | 10 | 22.0 | 15 | 10 | 55.0 |
| 11 | 2 | 2 | 8.0 | 15 | 15 | 60.0 |
| 12 | 2 | 4 | 10.0 | 15 | 30 | 75.0 |
| 13 | 2 | 6 | 12.0 | 20 | 15 | 75.0 |
| 14 | 2 | 8 | 14.0 | 20 | 20 | 80.0 |
| 15 | 2 | 10 | 16.0 | 20 | 40 | 100.0 |

*Table 58: load sequences for subgrade and subbase/base. The columns of subbase/base is that used for the test.*

Resilient deformations are calculated with the equation [22]:

$$\varepsilon_{1,r} = \frac{\Delta h_r}{h_i} \ldots [22]$$

Where:

$\Delta h_r$ = variation in height of the specimen, exhausted the plastic deformation component.

$h_i$ = initial height of the specimen, after 500 conditioning pulses.

The Resilient Modulus is calculated with the equation [23]:

$$M_r = \frac{\theta}{\varepsilon_{1,r}} \ldots [23]$$

Where:

$\Theta$ = deviatoric strain.

$\varepsilon_{1,r}$ = vertical elastic deformation.

In ***Table 59*** are reported the data registered from triaxial cell device.

| Parameters | Description |
|---|---|
| $\varepsilon_p$ | Permanent deformation |
| $\sigma_3$ | Confined voltage |
| $\sigma_v$ **max** | Maximum axial voltage |
| $P_v$ **max** | Maximum axial load |
| $P_v$ **cycle** | Cycle load |
| $P_v$ **contact** | Contact load |
| $\Delta h$ | Average resilient displacement |
| $\varepsilon_r$ | Resilient deformation |
| $M_r$ | Resilient Modulus |

*Table 59: Parameters registered by means of triaxial cell device.*

*Obtained results:*

In ***Figure 107*** are shown the results obtained by means of triaxial cell test, for the four specimens, after 28 days of curing. Specimens trends of resilient modula are shown together with the limit values related to the typical granular materials used for road foundation. The values obtained for each type of mixture follow approximately the same trend and all fall within the field delimited by the limits values. It can be asserted that the CLSM possess a behavior similar to that of granular materials not binding.

The graph show an increase of Θ associated an increase of $M_r$ of the mixes. This type of behavior is called "stress-stiffening" and is typical of granular soils.

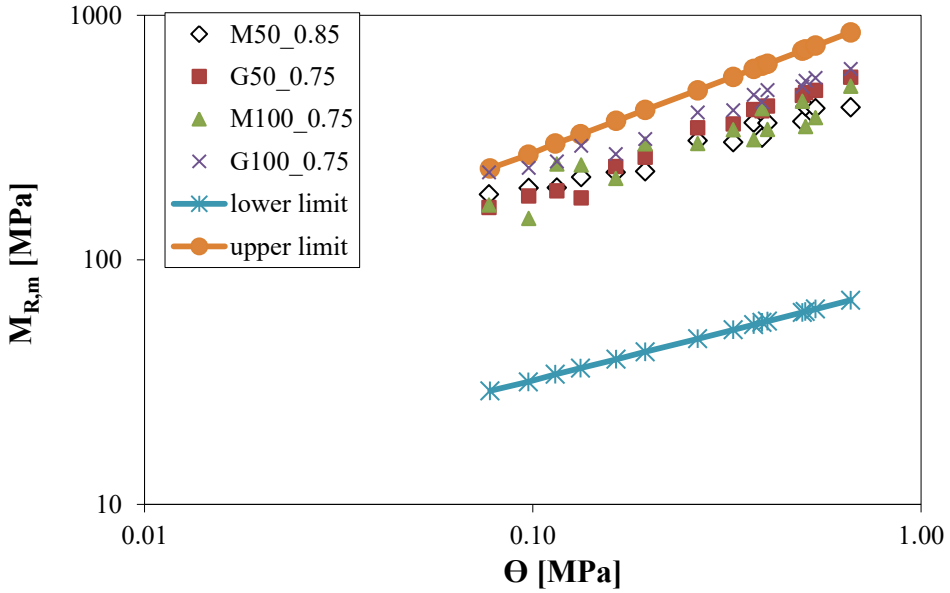


*Figure 107: Trend of the resilient modulus of the mixtures and the limit values referred to the typical granular soils used in road foundations.*

The amount of cement content in the mixes affects the results of the resilient modulus. Comparing the G50 and G100 specimens, higher resilient modulus values are observed for the mix with higher cement content (G100) (***Figure 108***).

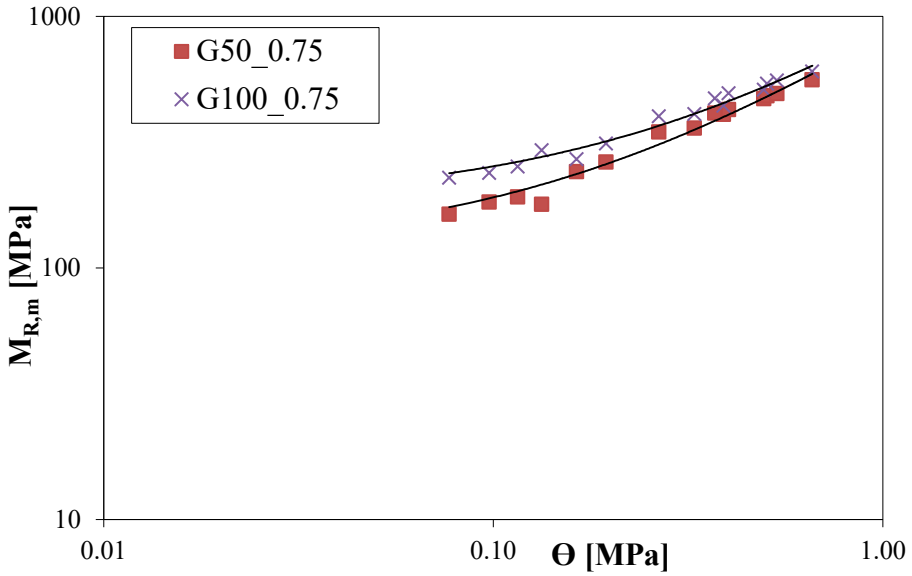


*Figure 108: Influence of the cement content in $M_r$ for 28 days of specimens curing. Comparison between G50 and G100.*

In ***Figure 108*** is shown an increase of stiffness of materials with an increase of cement content with the same type of sludge and same w/p ratio. It can also be observed for mix with 50 kg/m$^3$ of cement content a stress-stiffening behavior slightly more pronounced.

By comparing the type of sludge with the same cement content and w/p ratio, we observe higher value of $M_r$ for the specimen G100 with sludge type GVM. GVM offers higher mechanical resistance respect MVG sludge (***Figure 109***). This aspect may also be due to an higher quartz content of the GVM sludge.

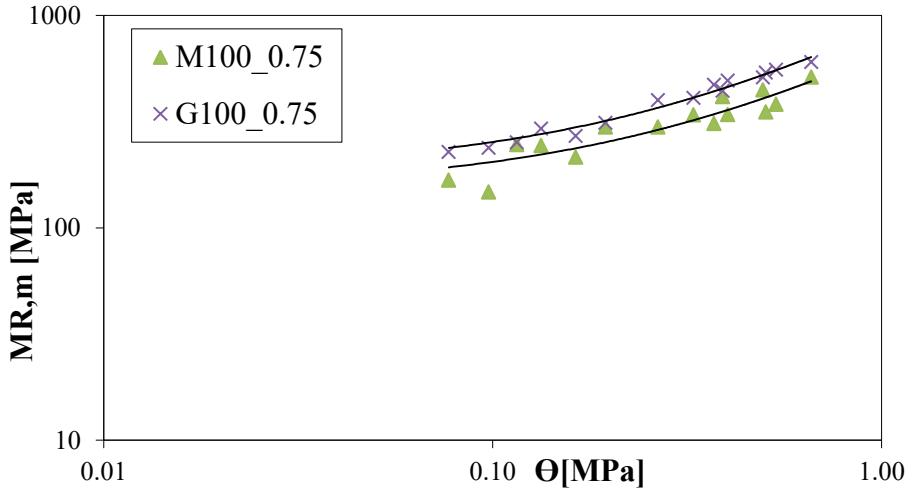


*Figure 109: Influence of the type of sludge in Mr trend for 28 days of specimens curing. Comparison between M100 and G100.*

Analyzing the influence of the w/p ratio keeping the cement content constant, it is observed that an increase of the w/p ratio, and therefore specimen humidity, correspond a slightly decrease of the resilient modulus (***Figure 110***). The material loses its stiffness in a not very sensitive way. This is due to the fact that a greater volume of water causes, as a result of the hardening of the material, a percentage of the largest voids. These pores are weaknesses in the material and contribute to the formation of cracks when the material is subjected to loads.

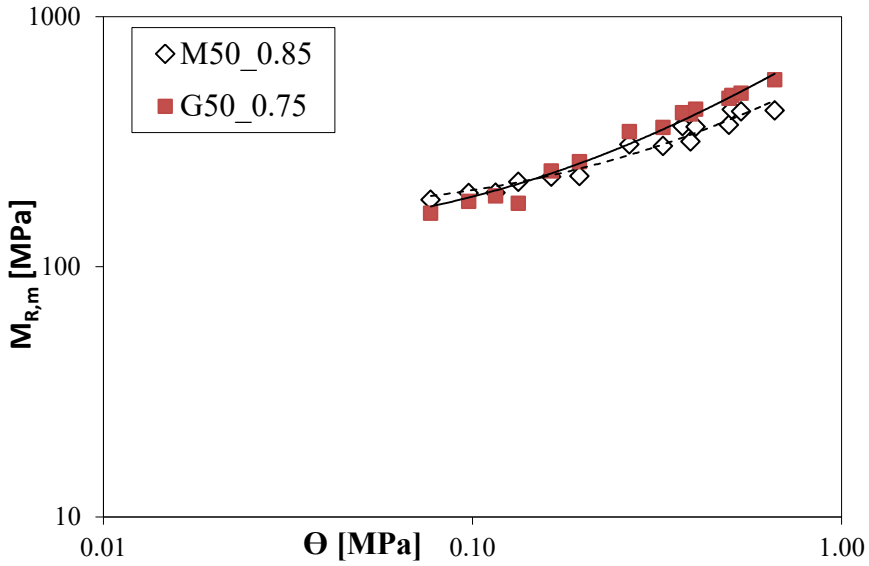


*Figure 110: Influence of w/p ratio in Mr trend for 28 days of specimens curing. Comparison between M50 and G50.*

Considering the five different confined pressure σ3, trends of resilient modula of the specimens tested are considered and compared. ***Figure 111***, ***Figure 112***, ***Figure 113***, ***Figure 114*** and ***Figure 115*** shown the results of resilient modula by means of σ3 equal to 0.020, 0.034, 0.068, 0.103 and 0.137 respectively. The resilient module increase with an increase of confined pressure. This behavior can be explained because the CLSM becomes increasingly rigid and strong increasing the confined pressure.

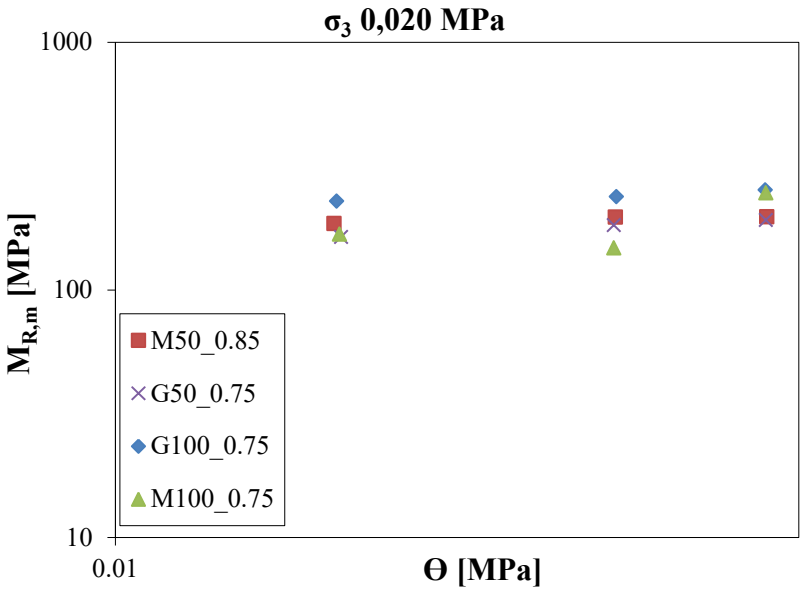


*Figure 111: Specimens resilient modula trend with confined pressure σ3 = 0,020 MPa.*

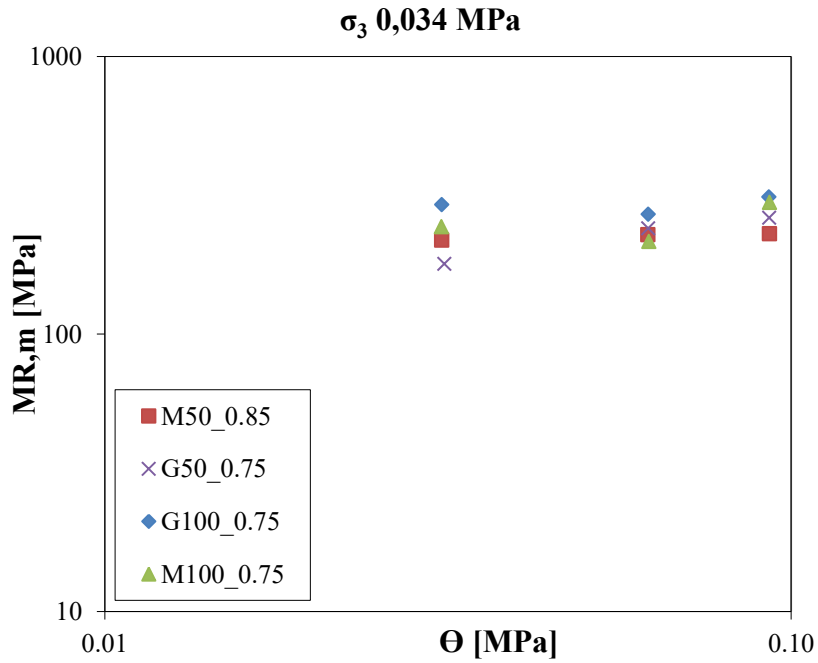


*Figure 112: Specimens resilient modula trend with confined pressure σ3 = 0,034 MPa.*

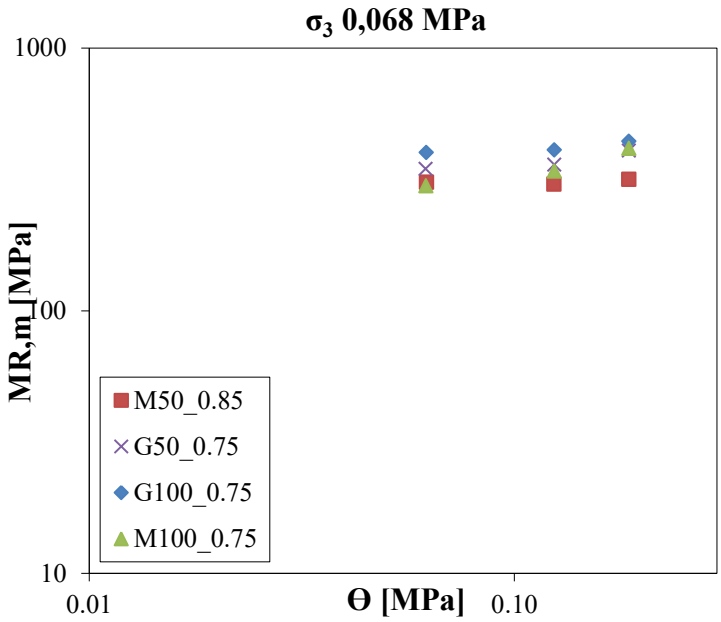


*Figure 113: Specimens resilient modula trend with confined pressure σ3 = 0,068 MPa.*

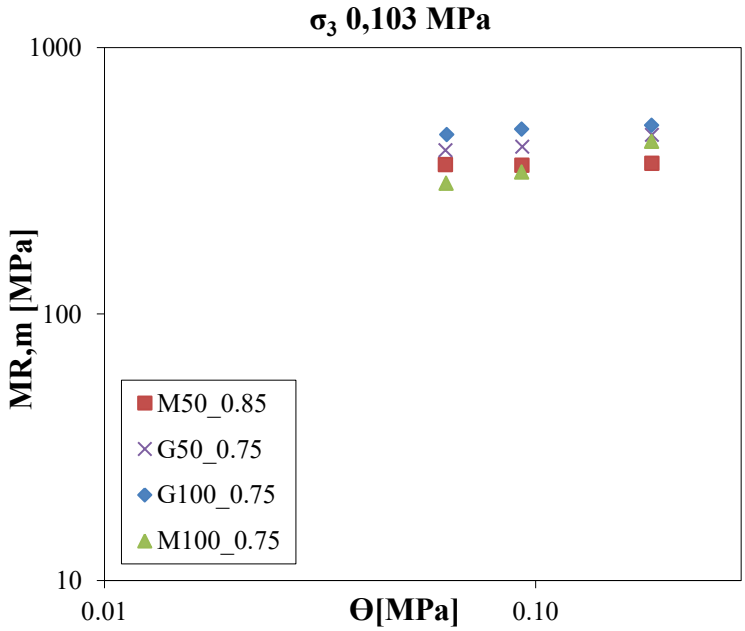


*Figure 114: Specimens resilient modula trend with confined pressure σ3 = 0,103 MPa.*

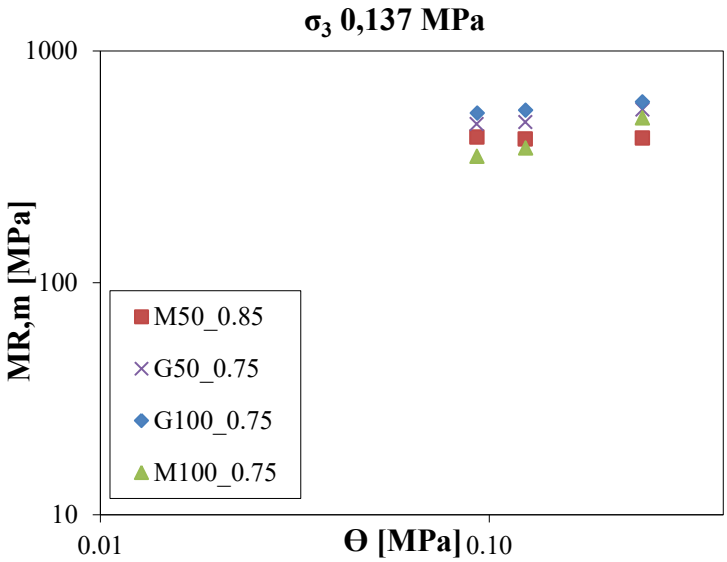


*Figure 115: Specimens resilient modula trend with confined pressure σ3 = 0,137 MPa.*

### 5.1.4.2 Thermal conductivity test

The thermal conductivity expresses the aptitude of a material to conduct the heat from the inside to the outside. The measurement of thermal conductivity was performed using a device called KD2 Pro. The instrument consists of a handheld that provides information on the value of thermal conductivity [W/m*K], the temperature of the specimen and the 'measurement error. To perform the measurement, a needle probe is used which is introduced into the cylindrical specimen by means of a special hole. The probe used is the RK-1 model, 6 cm long and 3.9 mm diameter (***Figure 116***).


*Figure 116: Device KD2 PRO used for thermal conductivity measurements.*

The probe consists of a heater and a temperature sensor. The current passes through the heater and the system monitors the temperature of the sensor over

time. Using algorithms that depend on the probe model used, it is possible to measure the value of thermal conductivity. The heat is fed into the specimen for ten minutes, the recorded temperatures are sixteen.

Two are the factor that can compromise the measurement: the contact between sensor and material, the migration of water from the region in which the heat is emitted and also the metal content in the sludge.

*Obtained results:*

The thermal conductivity of the four specimens was measured at 6 and 18 days of curing, repeating the measurements three times per specimen. On the eighteenth day, after the measurement, they were placed in the oven at 60 ° for 48h and the conductivity test was repeated in order to determine their thermal stability in dry conditions.

***Figure 117*** show the results of thermal conductivity at 6 days of curing of the specimens.

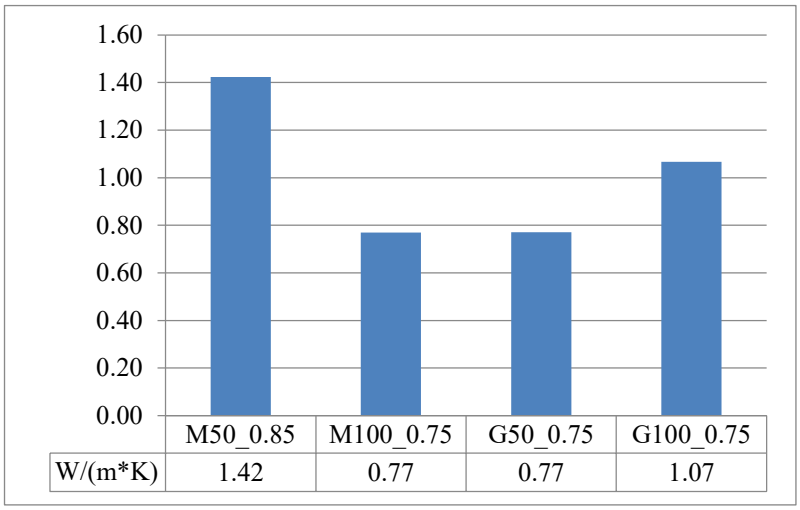


*Figure 117: Thermal conductivity results at 6 days of specimens curing.*

It can be observed that the specimen M50_0.85 is the one which has a higher thermal conductivity value. The result obtained depends on the water content greater than the other specimens, the w / p ratio established is 0.85, and the water behaves like a good conductor. In addition, the measurement was made on the sixth day of curing, so the water did not have enough time to free itself from the lithic skeleton of the specimens. Water is the factor that predominates on the thermal conductivity compared to the other components on the 6th day of curing.

Comparing the different type of sludge, keeping constant the cement content and the w/p ratio, the specimen G100, with GVM sludge, is more conductive respect the M100 specimen with MVG sludge (***Figure 118***). Sludge GVM is characterized by a higher quartz mineral content compared to MVG and is more conductive.

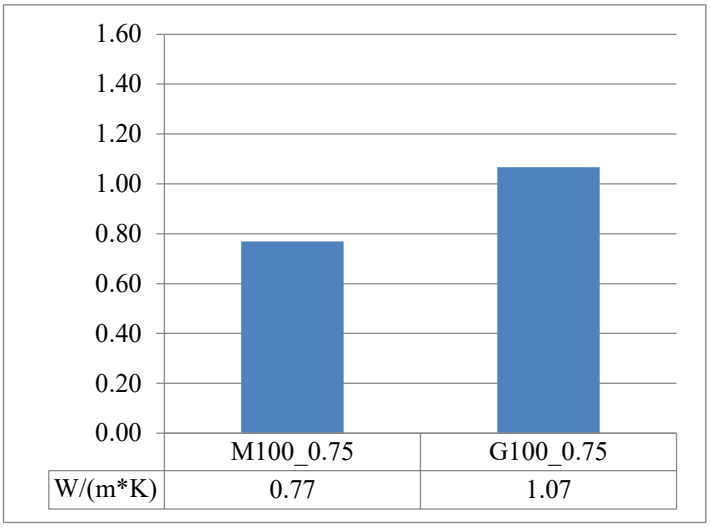


*Figure 118: Thermal conductivity comparison between M100 and G100 maintaining w/p ratio and cement content constant – 6 days of specimens curing.*

The specimens were tested on the 18th day of curing. The results obtained are shown in ***Figure 119.*** It can be observed that the samples containing the GVM sludge show higher thermal conductivity values than the samples with the MVG sludge. The motivation concerns the higher quartz content and a higher dosage of sludge in the mix design. The presence of quartz affect more the thermal conductivity.

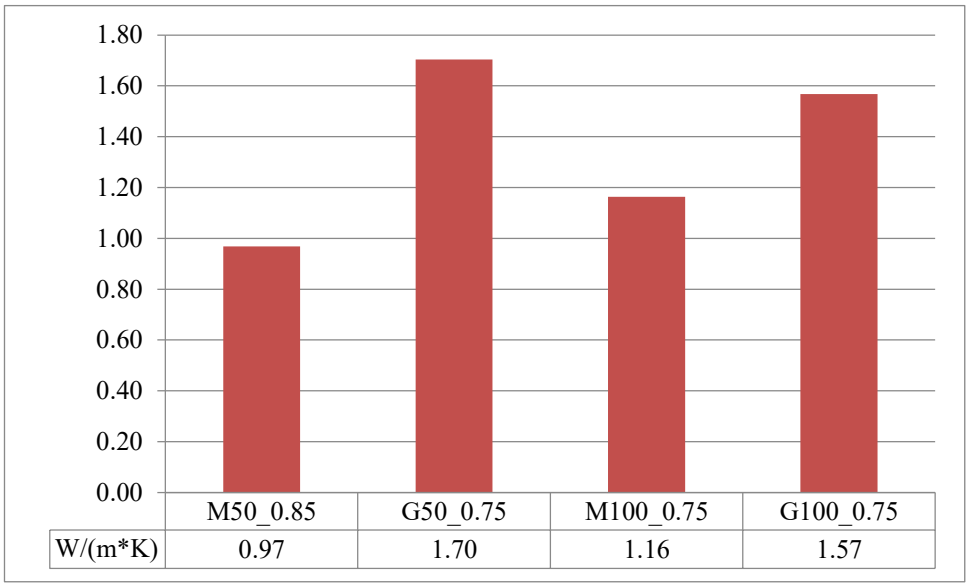


*Figure 119: Thermal conductivity results at 18 days of specimens curing.*

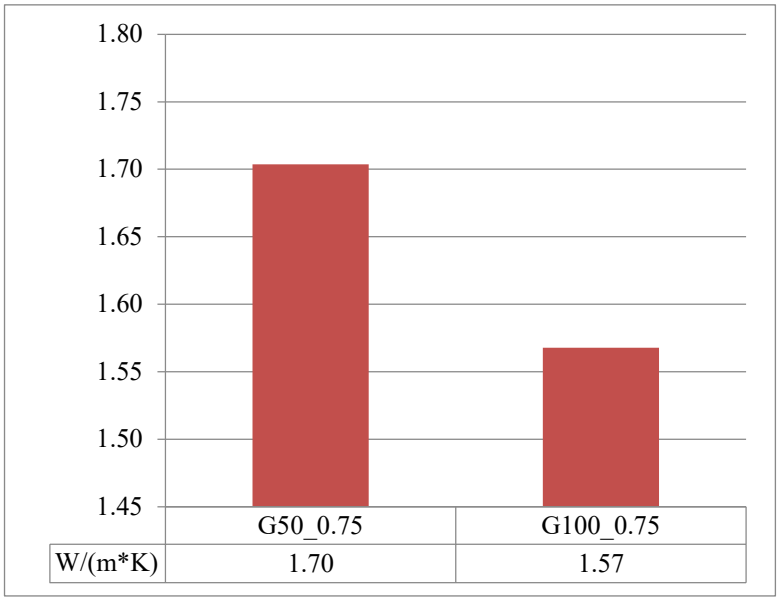


*Figure 120: Thermal conductivity at 18 days of specimens curing Comparison between G50 and G100. Cement content influence.*

By comparing the samples produced with the same sludge but with different cement content, we observe that on the 18th day of curing, the G50 sample had higher thermal conductivity results (***Figure 120***). On the 18th day the water content inside the specimens affect the measurement. The presence of the aggregates also influences the measurement. For this reason, the G50 sample obtain higher thermal conductivity. The cement content, in this case, does not slightly affect the measurements. In the specimens, water is still present at the eighteenth day of curing, and affect more the results. The G100 specimen contains more water and less aggregate than the G50 specimen.

To demonstrate the effective efficiency of CLSM, it is necessary to test it in dry conditions, ie in real condition. In fact, one of the objectives of the CLSM is to maintain a high conductivity regardless of the humidity values. It will have to be able to dissipate the heat generated by the cables in the dry conditions.

The same specimens of the eighteenth day, were placed in the oven for 48 h at 60 ° C and the results are shown in ***Figure 121***.

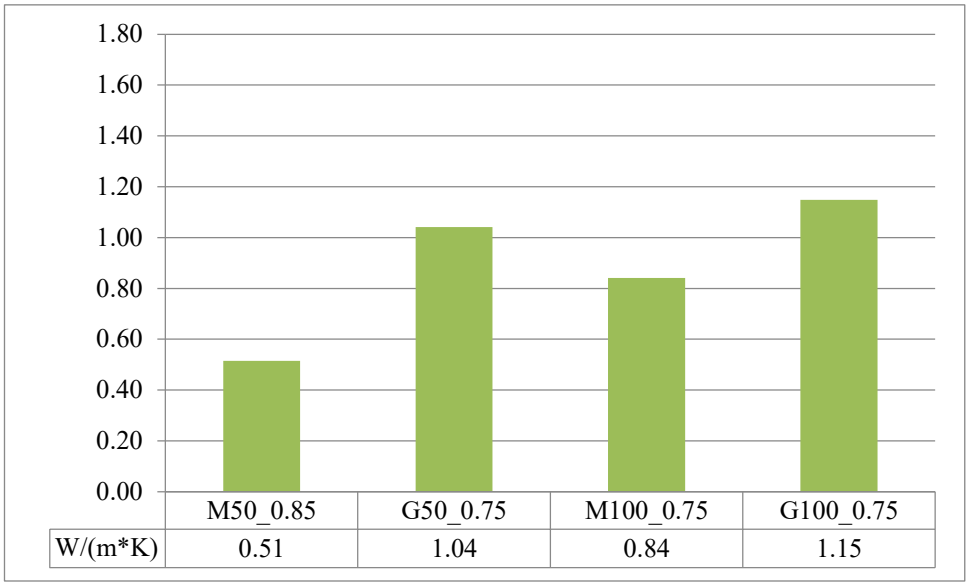


*Figure 121: Thermal conductivity in dry condition.*

As expected, the specimen with GVM sludge has higher conductivity values, but in dry conditions and therefore in absence of water, cement content is the component that predominates on conductivity results.

In ***Figure 122*** is shown the comparison between the sample at 18 days of curing and in dry condition. The trend is the same in both the condition. In Annex 6 are reported are the thermal conductivity values calculated.

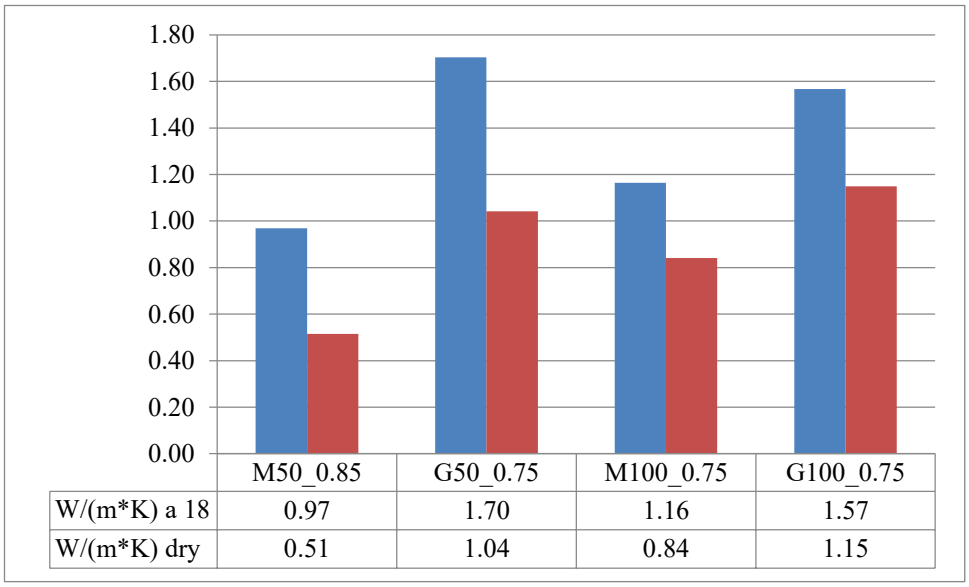


*Figure 122: Thermal conductivity comparison at 18 days of curing and in dry condition.*

The percentage of water lost during oven drying is shown in ***Table 60***, the sample M50 is the one that reaches the highest percentage.

| | **M50** | **G50** | **M100** | **G100** |
|---|---|---|---|---|
| **% lost water** | 9.5 | 6.2 | 7.3 | 6.2 |

*Table 60:water lost during oven dying process.*

### 5.1.4.3 Leaching test, chemical analysis and SEM analysis

Chemical analysis and leaching tests were performed on the finished product to verify the amount of metals present in the CLSM. When the sawing sludge is below the concentration limits, it can be considered a by-product to be used in other processes. In this case, concerning the leaching test, both sludge used in the CLSM, present metal concentration values below the standard limit. Regarding the chemical test, the MVG sludge present limits below column B, so its reuse in the CLSM can be allowed. On the other hand, GVM sludge showed a concentration of Cr of 1836 mg/kg over the concentration standard limits.

For the Italian legislation there are no controls on concentration limits on the CLSM, the results were then compared with the limits prescribed by Legislative Decree 152/2006 Annex 5, title V, part IV and Art. 8 of the D.M. 05/02/1998.

***Table 61*** show the results of chemical analysis test performed on CLSM specimens. All the value of metal concentration are below the limits provide by Italian law. Values of Cr concentration are lesser than the value of sawing sludge analysis due to dilution with other components of CLSM.

***Table 62*** show the results of leaching test on CLSM specimens. Cr concentration present in three cases value over the standard limit. This is an anomaly, since in the sludge leaching test both had limits below the standard limits. The presence of Cr could be justified by the release of this element from the mold with which the specimens were prepared.

| | Fe | Ba | Cu | Zn | Co | Ni | V | As | Cd | Cr | Pb | Be | Cr VI | Hg | Se |
|---|---|---|---|---|---|---|---|---|---|---|---|---|---|---|---|
| | mg/kg | mg/kg | mg/kg | mg/kg | mg/kg | mg/kg | mg/kg | mg/kg | mg/kg | mg/kg | mg/kg | mg/kg | mg/kg | mg/kg | mg/kg |
| **G50** | 4045 | 24 | 11 | 11 | 9 | 4 | 9 | <1 | <1 | 63 | 2 | <1 | <5 | <5 | <1 |
| **G100** | 3990 | 27 | 13 | 12 | 10 | 6 | 10 | 1 | <1 | 13 | 2 | <1 | <5 | <5 | <1 |
| **M50** | 5120 | 29 | 9 | 10 | 2 | 7 | 7 | <1 | <1 | 11 | 1 | <1 | <5 | <5 | <1 |
| **M100** | 6993 | 26 | 15 | 17 | 3 | 11 | 13 | 1 | <1 | 17 | 2 | <1 | <5 | <5 | <1 |
| **limit column B** | / | / | **600** | **1500** | **250** | **500** | / | **50** | **15** | **800** | **1000** | / | **15** | **5** | / |

*Table 61:Chemical analysis test on CLSM. Last row: Standard threshold limit concentration according to Lgs. D. 152/2006, Annex 5, title IV and Art. 8 of M.D. 05/02/1998.*

| | Fe | Ba | Cu | Zn | Co | Ni | V | As | Cd | Cr | Pb | Be | Cr VI | Hg | Se | NO3 | F | SO4 | Cl |
|---|---|---|---|---|---|---|---|---|---|---|---|---|---|---|---|---|---|---|---|
| | mg/l | mg/l | mg/l | mg/l | µg/l | µg/l | µg/l | µg/l | µg/l | µg/l | µg/l | mg/l | mg/l | mg/l | mg/l | mg/l | mg/l | mg/l | mg/l |
| **G50** | 0.03 | <0.01 | <0.001 | <0.001 | <1 | <1 | 7.5 | <1 | <1 | 49.57 | <1 | <0.001 | 0.04 | <0.0005 | <0.025 | 1.13 | 0.02 | 51.96 | 2.86 |
| **G100** | 0.08 | <0.01 | <0.001 | <0.001 | 4 | <1 | <1 | <1 | <1 | 62.18 | <1 | <0.001 | 0.05 | <0.0005 | <0.025 | 0.98 | 0.02 | 30.65 | 3.44 |
| **M50** | 0.03 | <0.01 | <0.001 | <0.001 | <1 | <1 | 2.28 | <1 | <1 | 94.91 | <1 | <0.001 | 0.08 | <0.0005 | <0.025 | 1.46 | 0.02 | 49.50 | 3.10 |
| **M100** | 0,1 | 0.03 | <0.001 | <0.001 | <1 | <1 | <1 | <1 | <1 | 84.94 | <1 | <0.001 | 0.06 | <0.0005 | <0.025 | 1.11 | 0.02 | 13.33 | 3.61 |
| **Limits** | / | **1** | **0,05** | **3** | **250** | **10** | **250** | **50** | **5** | **50** | **50** | **10** | / | **1** | **10** | **50** | **1,5** | **250** | **100** |

*Table 62:Leaching test on CLSM. Last row: Standard threshold limit concentration according to Lgs. D. 152/2006, Annex 5, title IV. In orange the values that exceed the standard limit.*

The SEM analysis was performed to verify both the contact surfaces between aggregates and cement paste and to verify the immobilization of heavy metals. Wang Q. and Yan P., in 2010, conducted a study on the immobilization of metals during the hydration of steel slag. The immobilization of heavy metals is a requirement for solidification/stabilization based on cement. This requirement reduces the possible dissolution of metals in landfills. The hydration of cement produces calcium-silicate-hydrate (CSH) which has a poorly crystalline structure. Hong S.Y. and Glasser F.P., in 2002, conducted a study on the binding affinity between CSH and metals. Choorackal E. et al, in 2018, confirmed the effectiveness of cement in controlling the immobilization of metals in the fluized thermal backfill (FTB).

The SEM analysis was conducted only on the G100 sample, for the difficulties on produce SEM sample with other specimens. The results of the analysis carried out are shown in the ***Figure 123*** and ***Figure 124***.

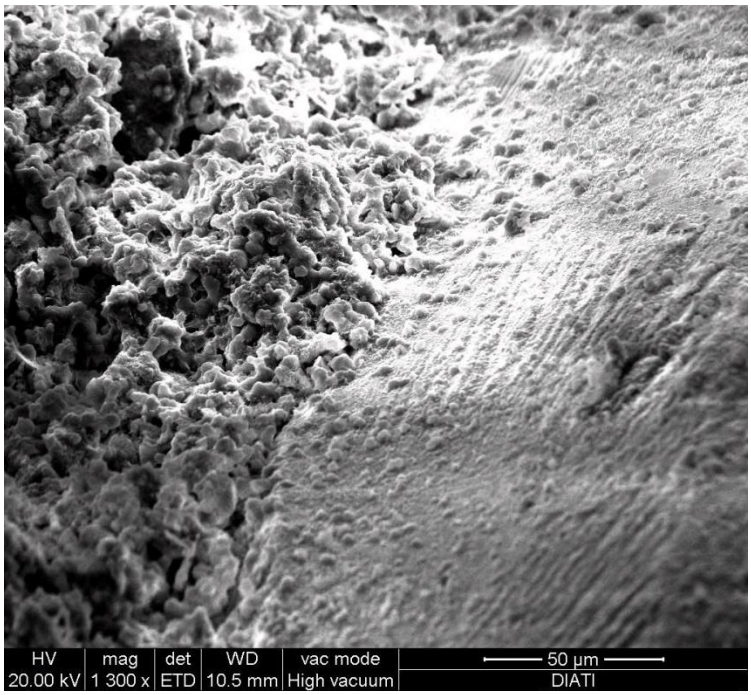


*Figure 123: SEM photo of G100 specimen. Interface between aggregate and cement paste.*

***Figure 123*** show a good contact between aggregate and cement paste. G100 specimen have a good proportion of the components. ***Figure 124*** show a good cement immobilization control of metals.

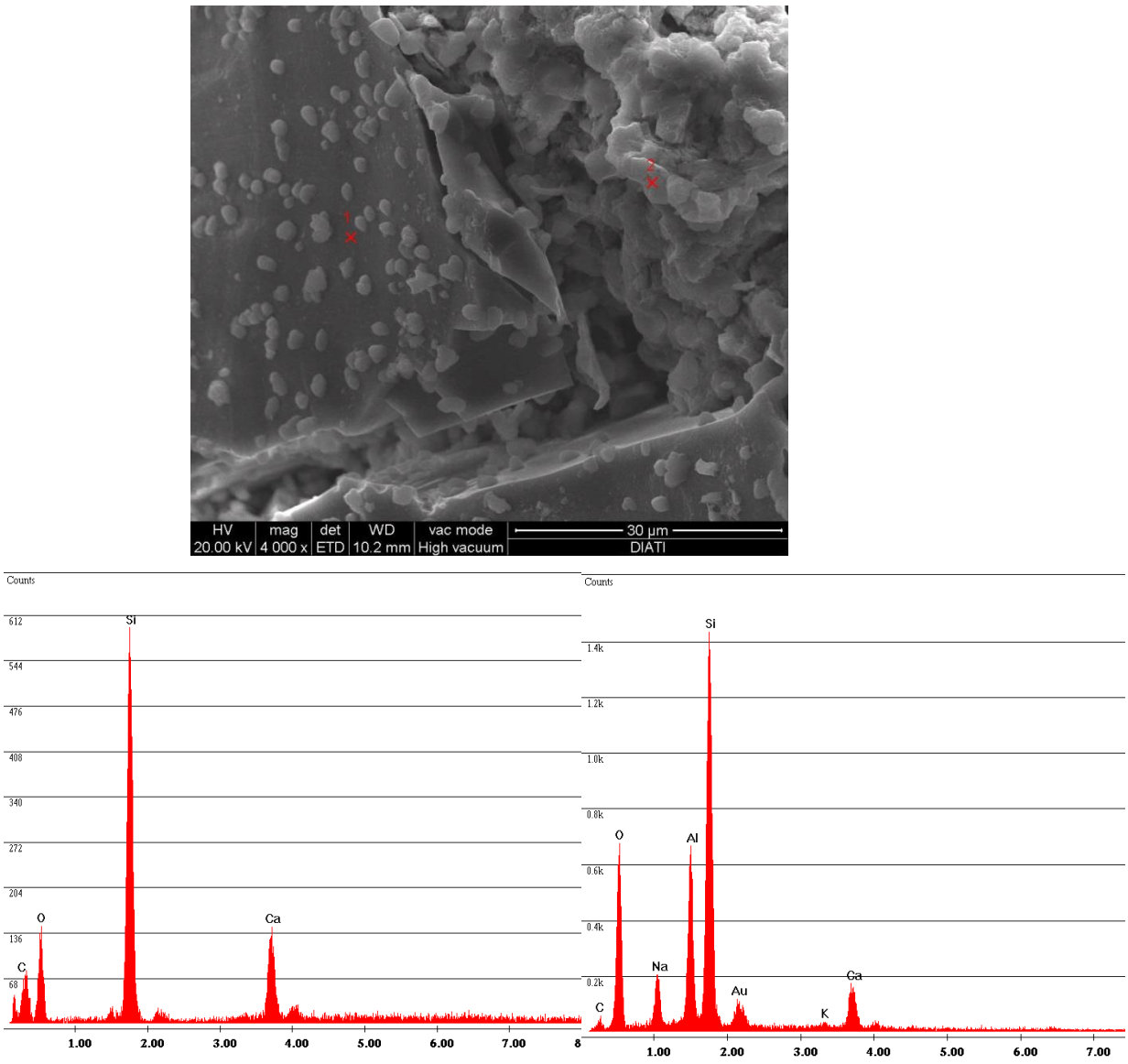


*Figure 124:G100 SEM analysis of metal immobilization by means of cement paste. Below on Left: analysis of point 1; Below on Right: analysis of point 2.*

# 5.2 Thermo-Eco Mortar for macroporous plaster .

The plaster has the function of regularizing the masonry surfaces and of constituting, where necessary, a protection against atmospheric agents. When no further coatings are planned on the plaster, it gives the wall surface its final aspect.

Basic features of the plaster, which they impose a careful choice of the mortars to be used are:

- good adherence and compatibility with the underlying support (of bricks, of stones, of concrete, etc.);
- meeting the requirements of impermeability, thermal and acoustic insulation and mechanical resistance;
- ability to allow transpiration processes through the walls perimeter;
- possibility of obtaining flat surfaces without defects (species in visible plaster) and straight edges.

The plaster is a mortar composed of a binding part (hardener) that incorporates sand with a selected particle size distribution. The maximum diameter of sand is not greater than 2 mm. It is possible to add additive substances such as cellulose, starch, silica smoke, plastics, etc., with the aim of modifying the physical-mechanical characteristics.

Plasters are classified according to the binder used:

- lime-based plaster, where the binder is lime (hydrated lime or hydraulic lime, in powder or greasy form);
- lime-cement plaster, where the binder is a mixture of hydrated lime and Portland cement, with a predominance of lime;
- cement-lime plaster, where the binder is a mixture of hydrated lime and Portland cement, with a predominance of cement;
- plaster based on gypsum, where the binder is exclusively gypsum;
- clay-based plaster, where the only binder is clay.

The sand used in the plaster can be clacareous or siliceous, of fluvial origin (natural) or deriving from grinding. The plaster forms a compact coating that covers the masonry with a thickness generally between 1.5 and 2 cm; in special cases the thickness can reach even 10 cm.

There are few studies in the literature concerning the reuse of sludge deriving from the cutting of ornamental stones as plaster. Husam D. Al- Hamaiedeh and Waleed H. Khushefati, in 2013, have studied the reuse of sludge deriving from the cutting of granites as an additive for mortars and concrete cement. Pierucci A. et al, in 2007, investigated the reuse of sludge deriving from the processing of

marble in mortars and plasters for the restoration of buildings. Marras G. et al, in 2017, studied the reuse of marble slurry for filler calcium carbonate application.

In this context the sludge deriving from the cutting of silicate rocks is to be reused in substitution of the sands and fine particle normally used to produce plasters. For this purpose the MCD sludge was chosen, which derives from the cutting of the Luserna Stone, with a low concentration of metals. What we want to achieve is a lightened thermal eco-plaster. In the following paragraphs the chosen mix design and the results of mechanical and chemical tests on the finished product will be reported. Please refer to Chapter 4 for the characterization of the sludge used for this application.

For the technical specifications and the requirements of the finished product, UNI EN 998-1 (Technical specifications for mortar for masonry work. Part 1: Mortars for internal and external plasters) has been taken as reference and to ornamental stone specification. The ***Table 63*** shows the tests performed with the normative references.

| TESTS CARRIED OUT | LEGISLATION REFERENCE |
|---|---|
| **Bulk density of fresh mortar** | UNI EN 1015-6:2007 |
| **Dry bulk density** | UNI EN 1015-10:2007 |
| **Flexural and compressive strength** | UNI EN 1015-11:2007 |
| **Flexural and compressive strength after freeze and thaw cycles** | UNI EN 12371:2010 |
| **Adhesive strength – pull out** | UNI EN 1015-12:2016 |
| **Compressive strength class** | UNI EN 998-2:2016 |
| **Compressive strength category** | UNI EN 998-1:2016 |
| **Spreading test** | ASTM D 6103:2017 |
| **Water absorption** | UNI EN 13755:2008 |
| **Thermal conductivity at 15 and 68 days of curing** | UNI EN 1745:2012 |
| **Thermal conductivity in dry condition** | UNI EN 1745:2012 |
| **Resistance to salts crystallization** | UNI EN 12370:2001 |
| **Chemical analysis and leaching test** | D.Lgs. 152/2006 Annex 5, Part IV and Art. 8 of D.M. 05/02/1998. |

*Table 63: Legislation reference of tests carried out on eco-plaster product.*

## 5.2.1 Thermo-Eco plaster mix design

The first step of preparation of plaster mix design was carried out at TEK.SP.ED.[10] Company in Casandrino of Naples, with the collaboration of ISIM[11] technologist Paolo Marone.

[10] TEK.SP.ED. s.r.l. Bunker. www.bunker-teksped.com Casandrino (NA)
[11] International Marble Institute. Confindustria Marmomacchine.

As a type of plaster, the cement plaster was chosen, where the binder is a mixture of hydrated lime and Portland cement, with a predominance of cement.

As mentioned in the previous paragraph the sawing sludge chosen for this application is the MCD, deriving from the cutting of the Luserna Stone (silicate gneiss). In addition, the Luserna stone sand, with particle size distribution of 0-3 mm, deriving from the flaming processes was also used. The mix design involves the presence of lime, cement, water, reinforcing fibers and foam. The foam has been used to give at the final material a certain lightness, while the fibers give greater mechanical resistance. ***Table 64*** shows the components of the mix design and the quantities used compared to 1 $m^3$. ***Table 65*** shows the mix design with the addition of Nola's Tufo powder, used only for the salts crystallization resistance test compared to specimens performed only with waste deriving from the Luserna stone.

| Mix design components | M.U. | Quantities for 1 $m^3$ |
|---|---|---|
| **Portland Cement 42,5R** | kg | 313.0 |
| **Lime NHL 3,5** | kg | 38.0 |
| **Luserna Flaming sand 0/3mm** | kg | 813.0 |
| **Filler MCD (*)** | kg | 187.0 |
| **Micro fiber (**)** | kg | 0.3 |
| **Natural Foam 72÷75 g/$m^3$** | $m^3$ | 0.37÷0.38 |

*Table 64:Eco-mortar for plaster mix design with MCD sludge. Components and quantities for 1 $m^3$. (*) filler from MCD sludge particle size distribution 0/300 µm- (**)polypropylene synthetic fibers = 6 ÷12 mm.*

| Mix design components | M.U. | Quantities for 1 $m^3$ |
|---|---|---|
| **Portland Cement 42,5R** | kg | 313.0 |
| **Lime NHL 3,5** | kg | 38.0 |
| **Luserna Flaming sand 0/3mm** | kg | 813.0 |
| **Nola's Tufo powder** | kg | 38 |
| **Filler MCD** | kg | 149.0 |
| **Micro fiber** | kg | 0.3 |
| **Natural Foam 72÷75 g/$m^3$** | $m^3$ | 0.37÷0.38 |

*Table 65:Eco-mortar for plaster mix design with addition of Nola's Tufo powder.*

The components were mixed with the S8 EVM machinery (***Figure 125***) of TEK.SP.ED. creation. The technical characteristics of the machine are shown in Annex 7. This machine is low power consumption, has a mixing system and a system for pumping plaster directly on site. This method allows to pouring the material on site very quickly.

*Figure 125: S8 EVM machinery creation of TEK.SP.ED s.r.l. used for eco-mortar for plaster mix design.*

Once the mix design was prepared, the material was pouring on a vertical panel to simulate normal work operations (***Figure 126***). To verify in this way both the adhesion of the material to the support and its behavior with hot summer temperatures and placed in front of sun. This critical weathering condition can cause cracks and fractures on normal plasters that can worsen over time.

*Figure 126: Left: Plaster pouring on vertical panel. Right: final results after pouring.*

After two days the results of plaster pouring is optimal. ***Figure 127*** shows the homogeneity of the product obtained and the absence of fractures and cracks.

*Figure 127: Pouring plaster results after two days from its application on panel.*

With the same mix design, specimens were prepared (***Figure 128***) for the physical-mechanical tests described in the following paragraphs. The number of specimens and their size is in accordance with the standards for each test reported in ***Table 63***.

*Figure 128: Plaster specimens prepared for physical- mechanical tests, according to standard UNI EN 998-1 and 2.*

## 5.2.2 Physical properties of plaster.

### 5.2.2.1 Bulk Density

*Fresh mortar condition:*

Bulk density of fresh mortar was performed according to UNI EN 1015-6 of 2007. The test involves weighing 1 $m^3$ of material in the fresh state (***Figure 129***). The result obtained is: 1380 $kg/m^3$.

*Figure 129: Bulk density of fresh mortar.*

*Dry condition:*

Bulk density in dry condition was performed, according to UNI EN 1015-10 of 2007, on 3 samples and the average of the values has been calculated.

The procedure involves an oven drying of the specimens at 105 °C. Then proceed with two weighing at a distance of 2 hours to verify that the mass is constant. The mass of the dry specimen is obtained ($M_{s,dry}$). The formula used to calculate the apparent bulk density for each specimen is as follows [24]:

$$Apparent\ bulk\ density\ [\frac{kg}{m^3}] = \frac{Ms,dry}{Vs} \quad [24]$$

Where:

Vs is the volume of the mold [$m^3$].

The average value of the 3 measurements is then calculated, approximate the result to 1 $kg/m^3$.

Each measurements and the average value obtained are shown below.

$V_s$=252*$10^{-6}$ [$m^3$] $M_{s,dry}$= 334.52 [g] *Apparent bulk density*: **1322 [kg/$m^3$];**

$V_s$= 262*$10^{-6}$ [$m^3$] $M_{s,dry}$= 321 [g] *Apparent bulk density*: **1222 [kg/$m^3$];**

$V_s$= 248*$10^{-6}$ [$m^3$] $M_{s,dry}$= 310 [g] *Apparent bulk density*: **1247 [kg/$m^3$];**

Apparent bulk density average value: **1264 [kg/m$^3$]**

From plaster regulations, it can be considered a lightened plaster if it has, as required, a dry density less than 1300 kg/m$^3$. The eco-plaster can therefore be defined as a light plaster.

### 5.2.2.2 Spreading test

Spreading test was performed in according with ASTM D 6103 of 2017. The Hargerman cone was used for the test. The cone has a chamfer of 45°, an upper diameter of 70 mm and a bottom diameter of 100 mm. ***Figure 130*** shows the spreading test with Hargerman cone. Once the cone has been removed, the plaster has not lost its shape.

*Figure 130: Spreading test on fresh mortar, with Hargerman cone.*

### 5.2.2.3 Thermal conductivity

Thermal conductivity was performed according to UNI EN 1745 of 2012. For this test was used the same device for CLSM sample, i.e. KD2 Pro with probe RK-1 model, 6 cm long and 3.9 mm diameter.

Thermal conductivity was carried out at 15 and 68 days of specimens curing and in dry condition (placed in the oven for 48 h at 60 °C).

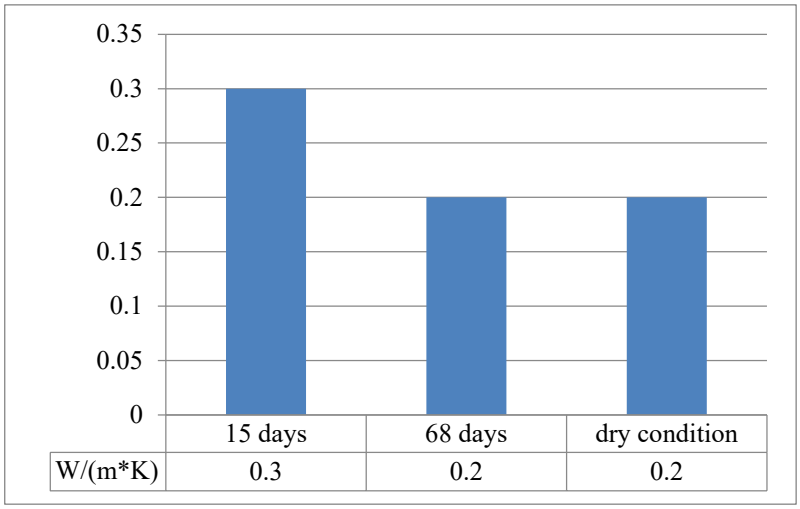


*Figure 131: Thermal conductivity results of eco-plaster. Comparison at 15 days, 68 days and in dry condition.*

The results of the thermal conductivity show excellent values that indicate a good thermal insulation of the plaster. Furthermore, the 68-day and dry values demonstrate the thermal stability of the mixture (***Figure 131***). In Annex 8 are reported all the results of thermal conductivity test.

## 5.2.3 Mechanical properties of plaster

### 5.2.3.1 Flexural strength before and after freeze and thaw cycle.

Flexural strength was performed on 3 samples, according to UNI EN 1015-11 of 2007. A constant speed load of 50 N/s was applied to obtain a break between 30s and 90s. Flexural strength after freeze and thaw cycle was performed according to UNI EN 12371 of 2010, related to natural stone, as it is not a test required by plaster standard. 25 freeze and thaw cycle were performed. 4 hours was the duration of each cycle, of which 2 hours at -15 °C (in saturated solution of sodium chloride) and 2 hours at 21 °C. The flexural test was performed 7 days after the last cycle, according to UNI EN 1015-11:2007.

The results obtained are reported in ***Table 66***.

| | [MPa] | Average value [MPa] |
|---|---|---|
| **flexural strength before cycle** | 1.26 | **1.03** |
| | 0.95 | |
| | 0.87 | |
| **flexural strenght after freeze and thaw cycle** | 1.38 | **0.93** |
| | 0.94 | |
| | 0.46 | |

*Table 66: Flexural test results before and after freeze and thaw cycle.*

There is no appreciably difference between flexural strength values before and

after freeze and thaw cycle.

### 5.2.3.2 Compressive strength

Compressive strength was performed on 6 samples, according to UNI EN 1015-11 of 2007. Freeze and thaw cycle was performed according to UNI EN 12371 of 2010, related to natural stone, as it is not a test required by plaster standard.

***Table 67*** show the results of compressive strength test. Value with * are abnormal and not included in the average value calculation. This anomaly is probably due to an incorrect size of the prepared specimens and then a cracking of the specimen similar to those caused by the flexural strength test.

| | [MPa] | Average value [MPa] |
|---|---|---|
| **compressive strength before cycle** | 12.01 | **11.97** |
| | 11.59 | |
| | 12.10 | |
| | 14.19 | |
| | 12.94 | |
| | 8.98 | |
| **compressive strenght after freeze and thaw cycle** | 14.22 | **10.76** |
| | 1.20* | |
| | 11.51 | |
| | 1.60* | |
| | 2.94 | |
| | 14.36 | |

*Table 67:Compressive strength results before and after freeze and thaw cycle. * abnormal values not included in the calculation of the average. Caused by a cracking of the specimen similar to those caused by the flexural strength test.*

The excellent results obtained, place the eco-plaster in M10 compressive strength class (in accordance with UNI EN 998-2) and in the category of compressive strength CS IV (in accordance with UNI EN 998-1).

### 5.2.3.3 Water absorption

Water absorption (according to UNI EN 13755:2008) was carried out on 12 samples, which 6 samples without freeze and thaw cycle and 6 after freeze and thaw cycle. The procedure involves placing specimens in oven at 60 °C to obtain a constant mass. Once the dry weight ($M_d$) of the specimens has been obtained, proceed in placing them in water until saturation. Subsequently, the specimens are weighed to obtain the saturated mass ($M_s$). The results are expressed as percentage of absorption obtained according to the equation [25]:

$$WA[\%] = \frac{M_s - M_d}{M_d} * 100 \quad [25]$$

Where

$M_s$ = saturated mass [g]

$M_d$ = dry mass [g]

The average values of the results obtained are shown in the ***Table 68***.

| SAMPLES | Water Absorption [%] – average values |
|---|---|
| **Plaster before freeze and thaw cycle** | 20 |
| **Plaster after freeze and thaw cycle** | 19 |

*Table 68:Water Absorption results on Plaster before and after freeze and thaw cycle.*

The results shown that there is no change in porosity of the specimens after the freeze and thaw cycles.

## 5.2.3.4 Pull out

Pull out test was carried out according to UNI EN 1015-12 of 2016 by TEK.SP.ED Company on plaster pouring directly on vertical panel after 28 days of curing.

***Figure 132*** show the modalities of performed test. ***Figure 133*** show the batched back test area and the good adhesion between plaster and panel support.

The results obtained is **1.55 MPa**.

*Figure 132:Left: Test plate mounted onto plaster; Right: Pull out test conducted.*

*Figure 133: Test area to be patched back.*

## 5.2.4 Chemical properties

### 5.2.4.1 Resistance to salt crystallization

Resistance to salts crystallization was carried out on 2 samples with Luserna stone mix design (L1 and L2) and 2 samples with mix performed adding Nola's Tufo Powder (T1 and T2), according to UNI EN 12370 of 2001, related to ornamental stone standard, as it is not a test required by plaster standard.

The test procedure includes the use of a 14% solution of sodium sulfate decahydrate. The solution should only be used for a test cycle. The specimens are dried up to constant mass and weighed. The total cycles are 15. Each cycle involves the immersion of the specimens in solution for 2 hours at a temperature of 20 °C and then a drying in the oven at 105 °C for a time ranging from 10 to 15 hours. After the 15th cycle, the specimens are placed in water for 24 hours at 23 °C and then rinsed in water. They are then weighed after drying to constant mass to evaluate the mass lost during the test. The results are expressed as a percentage and obtained with the following formula [26]:

$$\Delta M = \frac{M_f - M_d}{M_d} * 100 \quad [26]$$

Where:

$M_f$ is the final mass [g]

$M_d$ is the initial mass [g]

***Table 69*** show the results of the test for the four specimens L1, L2, T1 and T2.

| | $M_d$ [g] | $M_f$ [g] | ΔM [%] | Average value [%] |
|---|---|---|---|---|
| **L1** | 324.09 | 313.86 | **-3.16** | **-3.56** |
| **L2** | 351.09 | 337.2 | **-3.96** | |
| **T1** | 354.61 | 339.81 | **-4.17** | **-4.06** |
| **T2** | 355.8 | 341.72 | **-3.96** | |

*Table 69: Results obtained with resistance to salt crystallization test.*

After salt cycle specimens do not undergo big variations in weight or even aesthetic variations as shown by the ***Figure 134*** (before the cycles) and ***Figure 135*** (after cycles).

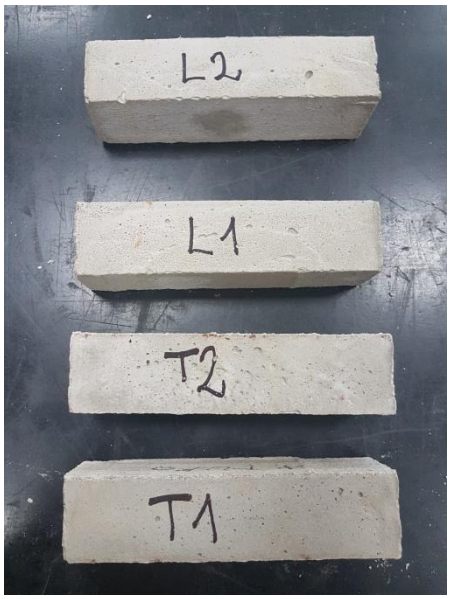


*Figure 134: Specimens before starting the test.*

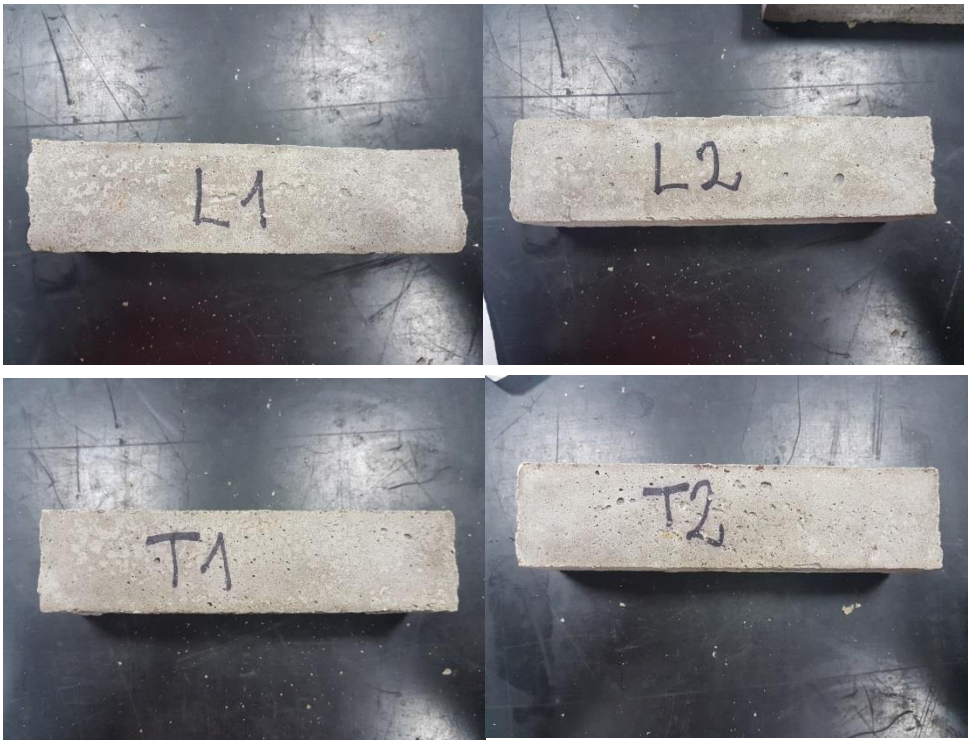


*Figure 135: Specimens after salt crystalization cycle.*

Upon verification of the physical and mechanical characteristics, on specimens L1, L2, T1 and T2 have been carried out water absorption and flexural strength.

Flexural strength test reported good values, higher than eco-plaster before salt

cycle results (***Table 70***). While water absorption test carried out after flexural strength caused the breaking of the specimens during the saturation step (***Figure 136***). This aspect is to be explored in the next studies.

| SAMPLES | FLEXURAL STRENGTH [MPa] |
|---|---|
| **L1 and L2** | 1.36 |
| **T1 and T2** | 1.99 |

*Table 70: Flexural strength results after salt crystallization cycle on specimens L1, L2, T1 and T2.*

*Figure 136: Water absorption of L1, L2, T1 and T2 specimens after salt crystallization cycle and flexural strength test. Specimens breakdown.*

## 5.2.4.2 Chemical analysis and leaching test

Chemical analysis and leaching test are performed according to D.Lgs. 152/2006. These tests are not required for plaster, but they were nevertheless performed to verify the dilution of the metals present in the sludge after the recovery. The results of the two tests are shown in the ***Table 71*** for chemical analysis and ***Table 72*** for leaching test.

| | Fe | Ba | Cu | Zn | Co | Ni | V | As | Cd | Cr | Pb | Be | Cr VI | Hg | Se |
|---|---|---|---|---|---|---|---|---|---|---|---|---|---|---|---|
| | mg/kg | mg/kg | mg/kg | mg/kg | mg/kg | mg/kg | mg/kg | mg/kg | mg/kg | mg/kg | mg/kg | mg/kg | mg/kg | mg/kg | mg/kg |
| **Plaster** | 7861 | 94 | 41 | 91 | 5 | 13 | 41 | 6 | <1 | 15 | 10 | 1 | <5 | <5 | <1 |
| **limit column B** | **/** | **/** | **600** | **1500** | **250** | **500** | **/** | **50** | **15** | **800** | **1000** | **/** | **15** | **5** | **/** |

*Table 71: Chemical analysis test on Eco-Plaster. Last row: Standard limit concentration according to Lgs.D. 152/2006, Annex 5, title IV and Art. 8 of M.D. 05/02/1998.*

| | Fe | Ba | Cu | Zn | Co | Ni | V | As | Cd | Cr | Pb | Be | Cr VI | Hg | Se |
|---|---|---|---|---|---|---|---|---|---|---|---|---|---|---|---|
| | mg/l | mg/l | mg/l | mg/l | µg/l | µg/l | µg/l | µg/l | µg/l | µg/l | µg/l | mg/l | mg/l | mg/l | mg/l |
| **Plaster** | 0.401 | 0.02 | 0.019 | <0.01 | <0.005 | <0.005 | <0.005 | <0.01 | <0.001 | 0.075 | <0.01 | <0.001 | 0.07 | <0.0005 | <0.025 |
| **Limits** | **/** | **1** | **0,05** | **3** | **250** | **10** | **250** | **50** | **5** | **50** | **50** | **10** | **/** | **1** | **10** |

*Table 72: Leaching test on Eco-Plaster. Last row: Standard limit concentration according to Lgs.D. 152/2006, Annex 5, title IV.*

All metal values are below the standard limits threshold.

# Chapter 6

# 6. Conclusions

The doctoral research project was conceived and implemented with the aim of providing guidelines for the recovery of silicate stone sludge as a secondary raw material. The main objective of the study was to create a methodology for the characterization of sawing sludge, in order to exploit its characteristics in the different foreseen re-use bringing economic and environmental benefits.

Many Legislative difficulties have emerged from the study of sawing sludge management. The sludge is still considered waste due to heavy metals concentration, deriving from the wear of cutting tools. This feature, which must be constantly checked by plant owners through chemical analyzes and leaching tests (according to Legislative Decree 152/2006), means that they are always disposed in specialized landfills. Only in some cases (limits of metals concentration below the threshold limits of the Law) the Local Administrations allow their use as filling of quarries voids. This reuse creates other environmental and structural problems. In accordance with European legislation and the concept of circular economy, it is necessary to find different solutions to recognize sludge as a by-product to be re-used in other production processes. The Legislation difficulty, at National level, is linked to "by-product" and "normal industrial practice" interpretation and application.

The analyzes carried out showed that most of the sludge from sawing processes could be reused in industrial and commercial areas (limits below column B of Legislative Decree 152/2006). Therefore, two recoveries were planned, based on the sludge metals content. The first recovery, as CLSM, provided the use of a filler that increased the capacity to dissipate thermal energy, due to the passage in the sub-road network of sub-services. The second recovery, as thermos-eco-mortar for plaster, provided the use of a filler that would allow a thermal insulation and at the same time a good mechanical resistance.

Results on the tests carried out for CLSM and Plaster recovery are resumed in ***Table 73*** and ***Table 74***.

| CLSM TESTS CARRIED OUT | M50 (MVG) | M100 (MVG) | G50 (GVM) | G100 (GVM) |
|---|---|---|---|---|
| **Sludge quartz content [%]** | 39.94 | | 46.02 | |
| **Sludge Specific gravity [g/cm$^3$]** | 2.67 | | 2.74 | |
| **Sludge Metal content [%]** | 2.96 | | 2.46 | |
| **Mix design W/P ratio** | 0.85 | 0.75 | 0.75 | 0.75 |
| **Mix design Thermal conductivity [W/m*K]** | 0.51 | 0.84 | 1.04 | 1.15 |
| **Flowability diameter [cm]** | 24.5 | 22.8 | 25 | 24 |
| **Triaxial cell test*** | / | / | / | / |

*Table 73: Technical data sheet of CLSM samples.*Triaxial cell test results reference Chapter 5.1.4.1.*

| TESTS CARRIED OUT | Plaster (MCD) |
|---|---|
| **Fresh condition – density [kg/m3]** | 1380 |
| **Dry condition – volumic mass [kg/m$^3$]** | 1264 |
| **Fresh condition – slump test - Hargerman cone diameter: 100mm** | No evident slump |
| **Thermal Conductivity - 15 days [W/m*K]** | 0.302 |
| **Thermal Conductivity - 68 days [W/m*K]** | 0.204 |
| **Thermal Conductivity – dry condition [W/m*K]** | 0.201 |
| **Pull off [MPa]** | 1.55 |
| **Compressive strenght [MPa]** | 11.97 |
| **Compressive strenght after freeze and thaw [MPa]** | 10.76 |
| **Compressive strength class (UNI EN998-2)** | M10 |
| **Compressive strength category (UNI EN 998-1)** | CS IV |

| | |
|---|---|
| **Flexural strenght[MPa]** | 1.03 |
| **Flexural strength after freeze and thaw [MPa]** | 0.93 |
| **Water absorption [%]** | 19÷20 |
| **Resistance salt crystallization cycle** | No evident decay. |
| **Flexural strength after salt crystallization cycle [MPa]** | 1.67 |
| **Water absorption after salt crystallization cycle** | Breakdown of sample during saturation step. |

*Table 74: Technical data sheet of plaster sample.*

Concerning CLSM products, it can be assert that all four mix design M50, M100, G50 and G100 meets the requirements for this application. Some observation can be supported, in particular:

- change of w/p ratio, achieve a significantly change on workability, fluidity and thermal conductivity properties, on the other side, affect not much the resilient response of the materials;
- an increase of cement content produce a worsening of fluidity properties, while in dry condition an improving of resistance and thermal conductivity;
- mix performed with MVG sludge present worse fluidity, strength and conductivity characteristics respect mix performed with GVM sludge;
- resilient response of each mixes is comparable to traditional unalloyed granular materials. Low long-term resistances are assured for easy removal in the case of maintenance of underground utilities;
- thermal conductivity values are better than CLSM with standard aggregates, due to the sawing sludge quartz and metals content.
- leaching test on CLSM samples shows that there is no release of metals, as the cement mortar well incorporates the sawing sludge metals.

Concerning Thermal-Eco-Mortar for plaster application, sawing sludge with low content of metals as MCD (Luserna stone cutting with diamond blade), improved the rheological, thermal and physical performance, conferring a light macroporous cellular structure by means adding organic foam. This characteristic facilitate plaster installation even for high thickness. The mechanical strength and thermal conductivity obtained exceed the values of standard plaster, making this ecofriendly plaster an excellent product, ideal for energy saving of buildings and in environments with high presence of humidity. Resistance to salt crystallization reported a breakdown of samples after water absorption test. This feature should be investigated by comparing the results of a normal production plaster.

Nowadays there is no market or regulation in favor of the recovery of silicate sawing sludge as CLSM or Plaster. This Thesis aims to give a contribution to allow the re-use of this “waste” as a “by-products”. The studied recoveries were foresees on sludge without any treatment for economic advantages and to avoid disposal in landfill. For those sludge with high metals concentration limits, a pre-treatment could be provided through a magnetic separation. Magnetic separation could be a good method to be applied at industrial level, which could be considered a treatment of normal industrial practice, as it does not change the state of the material. This method not added any substances, simply divided the sludge in two by-products (magnetic and amagnetic), with an high degree of purity. Magnetic product, rich in metals, can be reused in other productive sectors, or disposed in landfills (economic advantage due to a reduction of quantities dispose to landfill). Amagnetic product, mostly lithoids material, could be reused in building sector. The recovery of sludge as it is and/or after magnetic separation could turn a unidirectional system into a circular system.

# 6.1 Economic Evaluation

The costs related to the sawing sludge disposal depend on metals threshold concentration limits indicated by the legislation (Legislative Decree 152/2006 Annex 5, title V, part IV and DM 05_02_1998). If the limits are below the TRL the sludge can be disposed as inert waste and the cost remains around 13 €/t, otherwise it must be disposed as a special non-hazardous waste and the cost ranges from 70 to 80 €/t. In addition, it is necessary to consider the cost of transport to the landfill which depends on the distance between landfill and plant, which is hypothesized here of about 90 km.

The chemical analyzes provided by the considered plants show results below the TRL limits, especially if diamond wire and diamond blade technologies have been used. The waste produced by these plants can be considered as inert with low management costs. In the table 75 an evaluation of the costs related to the sawing sludge management is shown for small and medium companies, considering sludge as an inert or a non-hazardous special waste. As can be seen from the table below, the incidence of costs related to the management of sawing sludge from small to medium companies does not change. The percentage is 10% in the case of sludge disposed as an inert material, while it increases to 35% in the case of sludge disposed as non-hazardous special waste.

| | | small company | medium company |
|---|---|---|---|
| | sludge production [t/year] | 1,800 | 7,800 |
| **waste as inert** | landfill disposal cost [€/year] | 23,400 | 101,400 |
| | transport cost [€/year] | 21,600 | 93,600 |
| | total cost sludge management [€/year] | 45,000 | 195,000 |
| | company turnover [€/year] | 466,560 | 2,021.76 |
| | cost incidence of sludge management [%] | 10 | 10 |
| **waste as special non-hazardous waste** | landfill disposal cost [€/year] | 144,000 | 624,000 |
| | transport cost [€/year] | 21,600 | 93,600 |
| | total cost sludge management [€/year] | 165,600 | 717,600 |
| | company turnover [€/year] | 466,560 | 2,021.76 |
| | cost incidence of sludge management [%] | 35 | 35 |

*Table 75: evaluation of the costs related to the sawing sludge management is shown for small and medium company, considering sludge as an inert or a non-hazardous special waste*

The purpose of this doctoral thesis is to indicate the methodologies to obtain a zero waste recovering all the sludge according to the circular economy criteria. this obviously bring to an economic impact, reducing the costs related to sludge management.

# 6.2 Future Development

The first aim is to improve the mix design used for the plaster by increasing the amount of sludge used compared to the cement content. Furthermore, would be suitable the use of sludge obtained immediately after the filter press process, calculating the water content in this condition, so as to avoid a possible drying step in the oven which would lead to a high energy consumption. Pozzolan cement could be added to the mix design to avoid the disintegration of the plaster to the action of the salts.

The following PhD study led to the collaboration with I.S.I.M. Marmomacchine and TEK.SP.ED srl for the preparation of other building and environmental products for the reuse of sawing sludge. Among these new products we are developing the mix design for the production of pre-cast panels, blocks for walls, thermo cement mortar layer, self-leveling cellular cement and hydroseeding.

# References

AASHTO T 307. (2017). Standard Method of Test for Determining the Resilient Modulus of Soils and Aggregate Materials.

ACI Committee 229R, 1999. Controlled low-strength materials (CLSM) (ACI 229R-99). American Concrete Institute, Farmington Hills, MI, USA.

Agus, M., Bortolussi, A., Careddu, N., Ciccu, R., Grosso, B., & Massacci, G. (2003). Influence of stone properties on diamond wire performance. In Fourth international conference on computer applications in the minerals industries (CAMI 2003).

Allam, M.E., Bakhoum, E.S., Garas, G.L., (2014). Re-use of granite sludge in producing green concrete. Journal of Engineering and Applied Sciences, 9(12), 2731–2737. ISSN 1819-6608.

Al-Zboon, K., & Al-Zou'by, J. (2015). Recycling of stone cutting slurry in concrete mixes. Journal of Material Cycles and Waste Management, 17(2), 324-335.

Amaral, P., Cruz Fernandes, J., Frisa, A., Guerra Rosa, J., Manfredotti, L. & Marini, P. (2000). Evaluation of the workability by means of diamond tools of a series of portuguese commercial granites. Convegno su "Le cave di Pietre Ornamentali", *Associazione Georisorse e Ambiente*. November 2000, 323–329.

American Concrete Institute, Committee 229. Controlled low-strength materials (CLSM), ACI 229R-94 Report, 1994.

Andreasen, A. H. M. (1930). Über die Beziehung zwischen Kornabstufung und Zwischenraum in Produkten aus losen Körnern (mit einigen Experimenten). Kolloid-Zeitschrift, 50(3), 217-228.

Aydin, G., Karakurt, I. & Aydiner, K. (2013). Wear Performance of Saw Blades in Processing of Granitic Rocks and Development of Models for Wear Estimation. *Rock mechanics and rock engineering*, 46(6), 1559–1575. DOI 10.1007/s00603-013-0382-y.

ARPA Puglia.,(2016). Progetti di Gestione delle Cave di Materiali Lapidei nella RegionePuglia. http://93.63.84.69/ecologia/Documenti/GestioneDocumentale/Documenti/Attivita_Estrattive/09_Progetti_in_corso/AE_REP_PROG_02_Gestione_residui_cava.pdf.

ASTM C33 (2018). Standard Specification for Concrete Aggregates. American Society for Testing and Materials, Conshohocken, PA, USA.

ASTM C150 (2004). Standard Specification for Portland Cement. American Society for Testing and Materials, Conshohocken, PA, USA.

ASTM D 6103 (2017). Standard test method for flow consistency of controlled low strength material (CLSM). American Society for Testing and Materials, Conshohocken, PA, USA.

ASTM E384-11e1 (2011), Standard Test Method for Knoop and Vickers Hardness of Materials, ASTM International, West Conshohocken, PA, , www.astm.org.

Bellopede, R., Marini, P., Zichella, L., & Tori, A. (2015). Diamond wire cutting technology and workability of natural stones: validation of a new classification method (EASE R3). In International Conference on Stone and Concrete Machining (ICSCM) (Vol. 3, pp. 120-128).

Buyuksagis, I. S. (2007). Effect of cutting mode on the sawability of granites using segmented circular diamond sawblade. *Journal of Materials Processing Technology*, 183(2-3), 399-406.

Cardu, M., Morandini, A.F., Mancini, R. & Marini, P. (1996). Investigation research to define a standard laboratory test aimed to foresee the cuttability of ornamental stones by diamond tools. *Marmo Macchine International*,– pp. 206–222.

Careddu, N., Dino, G.A., (2016). Reuse of residual sludge from stone processing: differences and similarities between sludge coming from carbonate and silicate stones—Italian experiences. Environmental Earth Sciences, 75(14), 1075. https://doi.org/10.1007/s12665-016-5865-1.

Careddu, N., & Cai, O. (2014). Granite sawing by diamond wire: from Madrigali "bicycle" to modern multi-wires. Diamante – Applicazioni e Tecnologia, (79), Anno 20, pagg.33-50. Ed. G&M Associated Sas. Milano, Italy.

Careddu, N., Perra, E. S., & Masala, O. (2019). Diamond wire sawing in ornamental basalt quarries: technical, economic and environmental considerations. Bulletin of Engineering Geology and the Environment, 78(1), 557-568.

CEI 20-21/1-1 (2007). - Electric cables - Calculation of the current rating - Part 1-1: Current rating equations (100 % load factor) and calculation of losses - General

Chen L., 2011. Effect of magnetic field orientation on high gradient magnetic separation performance. *Minerals Engineering*. 24(1), 88-90. http://doi.org/10.1016/j.mineng.2010.09.019.

Chen L., Liao G., Qian Z., & Chen J., 2012. Vibrating high gradient magnetic separation for purification of iron impurities under dry condition. *International Journal of Mineral Processing*. 102, 136-140. http://doi.org/10.1016/j.minpro.2011.11.012.

Choorackal, E., Riviera, P. P., Dalmazzo, D., Santagata, E., Zichella, L., Marini, P. (2018). Reuse of reclaimed asphalt pavement and mineral sludges in fluidized thermal backfills. *Naxos Conference* 13-16 June 2018.

Citran G. (2000). La segagione del granito. Editors G. Zusi. ISBN 978-88-900067-2-2. URL https://books.google.it/books?id=YO4bnQAACAAJ.

Co.Fi.Plast. Wires. Diamond wires tools catalogue. http://issuu.com/ziosem/docs/cofiplast-catalogo-fili-bassa-risol?mode=window&backgroundColor=%23222222.

COM(2000). Commission Decision of 3 May 2000 replacing Decision 94/3/EC establishing a list of wastes pursuant to Article 1(a) of Council Directive 75/442/EEC on waste and Council Decision 94/904/EC establishing a list of hazardous waste pursuant to Article 1(4) of Council Directive 91/689/EEC on hazardous waste. *Official Journal of the European Communities,* L 226/3

COM (2005) 666 final. Taking sustainable use of resources forward: A Thematic Strategy on the prevention and recycling of waste. SEC(2005) 1681, SEC(2005) 1682. *European commission*.

COM(2011) 13 final. Report from the Commission to the European Parliament, the Council, the European economic and social committee and the committee of the Regions on the Thematic Strategy on the Prevention and Recycling of Waste. SEC(2011) 70 final. *European commission*

COM(2012) 82 final. Communication from the Commission to the European Parliament, the Council, The European economic and social Committee and the Committee of the Regions making Raw Materials available for Europe's future wellbeing proposal for a European Innovation Partnership on Raw Materials. SWD(2012) 27 final. *European commission.*

COM(2017) 490 final. Communication from the Commission to the European Parliament, the Council, The European economic and social Committee and the Committee of the Regions on the 2017 list of Critical Raw Materials for the EU. *European commission.*

Concu, G., De Nicolo, B. & Valdes, M. (2014). Prediction of building limestone physical and mechanical properties by means of ultrasonic P-wave velocity. *The Scientific World Journal*, p.8 http://dx.doi.org/10.1155/2014/508073.

Confindustria Marmomacchine Assomamarmomacchine. Cutting classes for natural stones in relation to tool performance on multi-wire machines rev. 2014. *Marmo Macchine International*. 86, p94

Dellas Spa. Diamond tools. Framesaw tools schedule. https://www.dellas.it/media/download/SUD0031_it.pdf

De Oliveira, L. J., Bobrovnitchii, G. S., & Filgueira, M. (2007). Processing and characterization of impregnated diamond cutting tools using a ferrous metal matrix. International *Journal of Refractory Metals and Hard Materials*, 25(4), 328-335. https://doi.org/10.1016/j.ijrmhm.2006.08.006.

Directive 1999/31/EC – Council Directive of 26 April 1999 on the landfill of waste. *Official Journal of the European Communities,* L 182/1.

Decision 2003/33/EC - Council Decision 2003/33/EC establishing criteria and procedures for the acceptance of waste at landfills pursuant to article 16 of and Annex II to Directive 1999/31/EC. *Official Journal of the European Communities.*

Directive 2006/21/EC – of the European Parliament and of the Council of 15 March 2006 on the management of waste from extractive industries.

*Official Journal of the European Communities,* L0021.

Directive 2008/98/EC - of the European Parliament and of the Council of 19 November 2008 on waste and repealing certain Directives. *Official Journal of the European Communities,* L 312/3.

Directive 75/442/EEC - Council Directive of 15 July 1975 on waste. *Official Journal of the European Communities,* No L 194/39.

Directive 91/156/EEC - Council Directive of 18 March 1991 amending Directive 75/442/EEC on waste. *Official Journal of the European Communities.* L 78/32.

DPR 616/1977 - Decree of the President of the Republic 24 July 1977, n. 616 Implementation of the delegation pursuant to art. 1 of the law of 22 July 1975, n. 382.

EIT Raw Materials. Supported by the EIT, a body of the European Union. *https://eitrawmaterials.eu/.*

Ersoy, A., Buyuksagic, S. & Atici, U. (2005). Wear characteristics of circular diamond saws in the cutting of different hard abrasive rocks. *Wear*. 258(9), 1422-1436. DOI:10.1016/j.wear.2004.09.060.

European Commission – Competition – List of NACE codes. *http://ec.europa.eu/competition/mergers/cases/index/nace_all.html.*

Falkenberg K. (2012). Guidance on the interpretation of key provisions of Directive 2008/98/EC on waste. *European Commission*.

Filgueira M. and Pinatti D. G. (2003) Processing of Diamond Composites for Cutting Tools by Powder Metallurgy and Rotary Forging. *Materials Science Forum*, Vols. 416-418, pp. 228-234. doi.org/10.4028/www.scientific.net/MSF.416-418.228.

Funk, J. E., & Dinger, D. R. (2013). Predictive process control of crowded particulate suspensions: applied to ceramic manufacturing. Springer Science & Business Media.

Gencel, O., Ozel, C., Koksal, F., Erdogmus, E., Martínez-Barrera, G., Brostow, W., (2012). Properties of concrete paving blocks made with waste marble. Journal of Cleaner Production, 21(1), 62–70. https://doi.org/10.1016/j.jclepro.2011.08.023.

Ghorbal, G. B., Tricoteaux, A., Thuault, A., Louis, G., & Chicot, D. (2017). Comparison of conventional Knoop and Vickers hardness of ceramic materials. *Journal of the European Ceramic Society*, 37(6), 2531-2535. https://doi.org/10.1016/j.jeurceramsoc.2017.02.014.

Goodman, R.E., 1989. Introduction to rock mechanics. 2nd edition, Wiley, New York.

Hong, S.Y., Glasser, F.P., (2002). Alkali sorption by C–S–H and C–A–S–H gels – part II. Role of alumina. *Cement and Concrete Research* 32 (7), 1101–1111.

Husam D. Al- Hamaiedeh and Waleed H. Khushefati. (2013). Granite Sludge Reuse in Mortar and Concrete. *Journal of Applied Sciences.* Volume 13

(3): 444-450. DOI: 10.3923/jas.2013.444.450. URL: https://scialert.net/abstract/?doi=jas.2013.444.450.

JRC – Raw Materials Information System (RMIS). EU SCIENCES HUB. *http://rmis.jrc.ec.europa.eu/*

Junca E., de Oliveira J. R., Espinosa D. C. R., & Tenório J. A. S., 2015. Iron recovery from the waste generated during the cutting of granite. *International Journal of Environmental Science and Technology*, 12(2), 465-472. DOI: 10.1007/s13762-013-0418-6.

Konstanty J. (2006) Production parameters and materials selection of powder metallurgy diamond tools, Powder Metallurgy, 49:4, 299-306, DOI: 10.1179/174329006X113508.

Kopač, J., & Kenda, J. (2009). Diamond tools for machining of granite and their wear. *Strojniški vestnik*, 12(55), 775-780.

Legambiente. (2017) Quarry report. The numbers and the economic and environmental impacts of mining activities in the Italian territory. Opportunities and challenges in the direction of the circular economy. *GF pubblicità - Grafiche Faioli - Pietracatella (CB)*

Legislative Decree 30 May 2008, n. 117. Implementation of Directive 2006/21 / EC on the management of waste from the extractive industries and amending Directive 2004/35 / EC. Published in the *Official Journal no. 157 of 7 July 2008.*

Legislative Decree 3 April 2006, n. 152. "Environmental regulations". Published in the Official Gazette n. 88 of April 14th 2006 - *Ordinary Supplement n. 96*

Legislative Decree December 3, 2010, n. 205. Provisions for the implementation of Directive 2008/98 / EC of the European Parliament and of the Council of 19 November 2008 on waste and repealing certain directives.

Mannella P. Estratto lame. Blades., 1-26. Marmilame S.r.l. https://ecitydoc.com/queue/la-lama-che-taglia-il-blocco-in-lastre-e-la-cosa-che-piu_pdf?queue_id=-1.

Marras, G., Careddu, N., & Siotto, G. (2017). Filler calcium carbonate industrial applications: the way for enhancing and reusing marble slurry. italian journal of engineering geology and environment, 63-77.

Ministerial Decree of 5_2_1998. “Identification of non-hazardous waste subject to simplified recovery procedures pursuant to of the articles 31 and 33 of the legislative decree 5 February 1997, n. 22”.

Ministerial Decree of 5 April 2006, n. 186.Regulation containing amendments to the ministerial decree of 5 February 1998. "Identification of non-hazardous waste subject to simplified recovery procedures, pursuant to articles 31 and 33 of the legislative decree 5 February 1997, n. 22 ". *Official Journal 19 May 2006, n. 115*.

Ministerial Decree 10th August 2012, n. 161 Regulations governing the use of excavated earth and rocks. (12G0182) . *GU General Series n.221 of 21-09-*

*2012*.

Newns A., & Pascoe R. D., 2002. Influence of path length and slurry velocity on the removal of iron from kaolin using a high gradient magnetic separator. *Minerals Engineering*, 15(6), 465-467. http://doi.org/10.1016/S0892-6875(02)00056-0.

Oberteuffer, J. (1974). Magnetic separation: A review of principles, devices, and applications. *IEEE Transactions on Magnetics*, 10(2), 223-238.

Ozcelik Y., Kulaksiz S., Cetin M. C. (2012). Assesment of the wear of diamond beads in the cutting of different rock types by the ridge regression. *Journal of material Processing Technology* 127 392-400 Department of mining Engineering, Hacettepe University 06532 Beytepe, Ankara, Turkey.

Ozcelik, Y., & Yilmazkaya, E. (2011). The effect of the rock anisotropy on the efficiency of diamond wire cutting machines. *International Journal of Rock Mechanics and Mining Sciences*, 48(4), 626-636.

Pierucci, A., De Tommasi, G., Calabrese, D., Petrella A. (2007). Reuse of limestone cutting waste in the production of mortars and plasters for building restoration. *VARIREI 2007*, Valorization and Recycling of Industrial Waste. VI International Congress.

Regional Law of 26 April 2000, n. 44. Regulatory provisions for the implementation of Legislative Decree 31 March 1998, n. 112 Conferral of functions and administrative tasks of the State to the Regions and Local Authorities, in implementation of Chapter I of the Law of 15 March 1997, n. 59. *Piedmont Regional Council*.

Regional Law n. 23 of 17 November 2016. Discipline of mining activities: provisions concerning quarries. *Piedmont Regional Council*.

Ribeiroa, S. V., & Holandaa, J. N. F. (2014). Soil-cement bricks incorporated with granite cutting sludge. Int J Eng Sci Innovative Technol, 3(2), 401-408.

Royal Decree of 29 July 1927, n. 1443. Rules of a legislative nature to regulate the research and cultivation of mines [in Kingdom]. This decree is updated and coordinated with Legislative Decree 4 August 1999, n.213. *In Gazz. Uff., 23 August 1927, No. 194*

Selçuk, L. & Nar, A. (2015). Prediction of uniaxial compressive strength of intact rocks using ultrasonic pulse velocity and rebound-hammer number. *Quarterly Journal of Engineering Geology and Hydrogeology*, 49, 67-75. doi:10.1144/qjegh2014-094.

Scanell, Y. (2012). The regulation of mining and mining waste in the European Union. *J. Energy Clim. Environ*., 177, pp. 177-268.

Smith A. (1991). Controlled low strength material. A cementitious backfill that flows like a liquid, supports like a solid, and self-levels without tamping or compacting. *The Aberdeen Group*. https://www.concreteconstruction.net/_view-object?id=00000153-8bb2-dbf3-a177-9fbbee2f0000.

Spriano S., Ferraris S., Bellopede R., Marini P., Zichella L., Tori A. (2015).

Diamond wire – stone interaction during the cutting process: mechanical, physical and chemical investigation. In *International Conference on Stone and Concrete Machining* (ICSCM). 2–03.11.2015 Ruhr-universitat Bochum Conference Proceedings (2015), pp. 112-119.

Sundberg, J. (2016). Evaluation of thermal transfer processes and back-fill material around buried high voltage power cables. Department of Civil and Environmental Engineering. Division of GeoEngineering. *Chalmers Publication Library (CPL)*. Gothenburg, Sweden 2015 Report 2016:5. http://publications.lib.chalmers.se/publication/238089. ISNN 1652-9162.

Tuğrul, A. & Zarif, I.H. (1999). Correlation of mineralogical and textural characteristics with engineering properties of selected granitic rocks from Turkey. *Engineering Geology*. 51, 303–317. DOI:10.1016/S0013-7952(98)00071-4.

UNI EN 1015-6: (2007). Test methods for mortar for masonry work - Part 6: Determination of the apparent density of fresh mortar.

UNI EN 1015-10: (2007). Test methods for mortar for masonry work - Part 10: Determination of the apparent density of the dried hardened mortar.

UNI EN 1015-11: (2007). Test methods for mortar for masonry work - Part 11: Determination of flexural and compressive strength of hardened mortar.

UNI EN 1015-12: (2016). Test methods for mortar for masonry work - Part 12: Determination of adherence to the support of external and internal plaster mortars.

UNI 10802: (2013). Waste - Manual sampling, sample preparation and eluate analysis.

UNI EN 12370: (2001). Test methods for natural stones - Determination of resistance to crystallization of salts.

UNI EN 12371: (2010). Test method for natural stones - Determination of frost resistance.

UNI EN 12457-2 (2004). Waste characterization - Leaching - Compliance test for leaching of granular and sludge waste - Part 2: Single stage test, with a liquid / solid ratio of 10 l / kg, for materials with particles smaller than 4 mm ( with or without size reduction).

UNI EN 13755:2008. Test methods for natural stones - Determination of water absorption at atmospheric pressure.

UNI EN 14205 (2003). Natural stone test methods - Determination of Knoop hardness. CEN-European Committee for Standardization.

UNI EN 1745: (2012). Masonry and masonry products - Methods for determining thermal properties.

UNI EN 933 part 1: (2012). Tests to determine the geometrical characteristics of the aggregates - Part 1: Determination of the particle size distribution - Particle size analysis by sieving.

UNI EN 934 part 2: (2012). Additives for concrete, mortar and mortar for injection - Part 2: Concrete additives - Definitions, requirements,

conformity, marking and labeling.

UNI EN 998-1: (2016). Specification for mortar for masonry work - Part 1: Mortars for internal and external plasters.

UNI EN 998-2: (2016). Specification for mortar for masonry work - Part 2: Masonry mortars.

Vasanelli, E., Colangiuli, D., Calia, A., Sileo, M., & Aiello, M. A. (2015). Ultrasonic pulse velocity for the evaluation of physical and mechanical properties of a highly porous building limestone. *Ultrasonics*, 60, 33-40. https://doi.org/10.1016/j.ultras.2015.02.010.

Vasconcelos, G., Lourenço, P. B., Alves, C. A. S. & Pamplona, J. (2008). Ultrasonic evaluation of the physical and mechanical properties of granites. *Ultrasonics*, 48(5), 453–466. DOI:10.1016/j.ultras.2008.03.008.

Wang, Q., Yan, P. (2010). Hydration properties of basic oxygen furnace steel slag. *Constr. Build. Mater.* 24, 1134–1140. doi:10.1016/J.CONBUILDMAT.2009.12.028.

Yilmazkaya, E. & Ozcelik, Y. (2015). Development of Cuttability chart for a marble cutting with monowire cutting machine. In *International Conference on Stone and Concrete Machining* (ICSCM)., 3 73–85.

Yurdakul, M., Gopalakrishnan, K., & Akdas, H. (2014). Prediction of specific cutting energy in natural stone cutting processes using the neuro-fuzzy methodology. *International Journal of Rock Mechanics and Mining Sciences*. 67, 127–135.

Zhang, H., Zhang, J., Wang, Z., Sun, Q., & Fang, J. (2016). A new frame saw machine by diamond segmented blade for cutting granite. *Diamond and Related Materials*, 69, 40-48. doi.org/10.1016/j.diamond.2016.07.003.

Zichella, L., Bellopede, R., Marini, P., Tori, A., & Stocco, A. (2017). Diamond wire cutting: A methodology to evaluate stone workability. *Materials and Manufacturing Processes*, 32(9), 1034-1040. https://doi.org/10.1080/10426914.2016.1269912.

Zichella, L., Bellopede, R., Spriano, S., & Marini, P. (2018). Preliminary investigations on stone cutting sludge processing for a future recovery. Journal of Cleaner Production, 178, 866-876. https://doi.org/10.1016/j.jclepro.2017.12.226.

Zisa, G., Santagata, E., Riviera, P., Choorackal Avirachan, E. (2017). The use of fluid cement mortars in the sites roads in the tunnel: mix design and field tests in true greatness. Master thesis in Civil Engineering. Polytechnic of Turin.

http://www.arpa.piemonte.it/reporting/indicatori-on_line/uso-delle-risorse/industria_cave-e-miniere-1

http://www.regione.piemonte.it/attivitaProduttive/web/attivita-estrattive/cave

https://www.youtube.com/channel/UC8ehvCplARHJ5ZI7rBue36w. Omec Distribuzione.

http://purvainternational.com/en_US/gangsaw-blades/.

http://stelcolimited.com/gang-saw-steel/ and Hard strips.

http://www.hardstrips.com/steel-grades-gang-saw/
http://www.pometon.com/materialsSteel_eng.php
http://it.pulitor.com/
http://www.pulvex.co.uk/technical-information/a-buyers-guide-to-diamond-blades/
http://www.minorsa.com/machines_55a.html
https://www.ec21.com/product-details/Monowire-Slab-Cutting-Machine--5005898.html
http://www.cofiplast.it/it
https://www.tyrolit.it/
http://www.pan-abrasives.com – Abrasive media guide.
https://digilander.libero.it/elan1972/cap6/images/fig6.htm.
http://multiserw-morek.pl/en/products,cement,le_chatelier_flask_en_196-6
https://www.diamant-boart.com/en-GB/product/processing-tools/gang-saw-blades/